MB 2026-03

U-Pb LA-ICPMS geochronology of samples collected in 2024 from Québec, Canada

Documents complémentaires

Additional Files

Licence

License

Ressources naturelles et Forêts
Québec

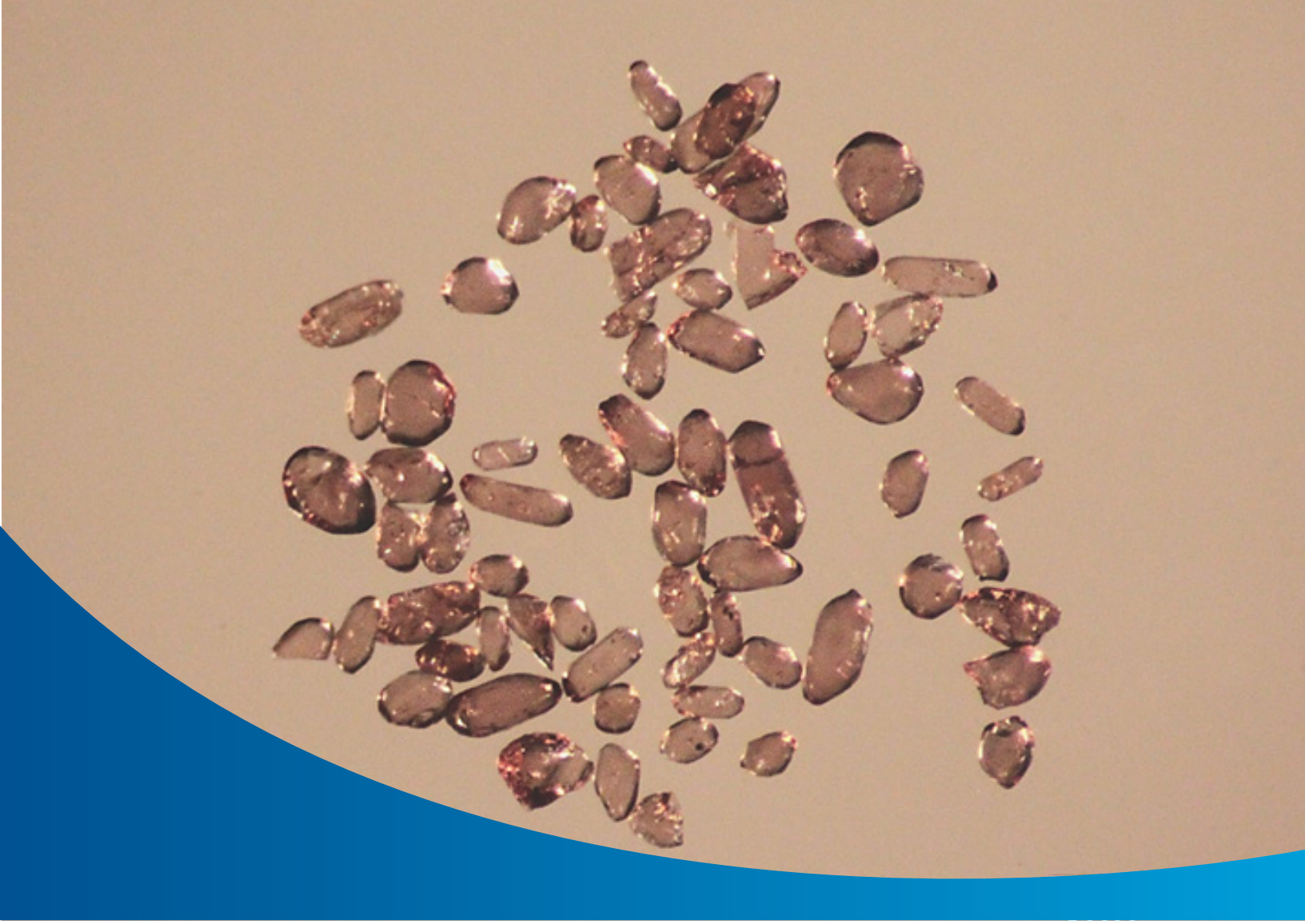

U-Pb LA-ICPMS geochronology of samples collected in 2024 from Québec, Canada

Heriberto Rochín-Bañaga and Donald W. Davis

MB 2026-03

Québec

U-Pb LA-ICPMS geochronology of samples collected in 2024 from Québec, Canada

Prepared for Ministère des Ressources naturelles et des Forêts

September 8, 2025

by
Heriberto Rochín-Bañaga and Donald W. Davis
Jack Satterly Geochronology Laboratory, Department of Earth Sciences, University of Toronto, 22 Ursula Franklin St., Toronto, ON, Canada M5S 3B1

SAMPLES

New U-Pb geochronological data are reported from 27 samples of Precambrian rocks from northern Quebec. U-Pb ages were determined on selected minerals such as zircon, monazite and/or titanite) using laser ablation - inductively coupled plasma mass spectrometry (LA-ICPMS). A sample list, grouped by project, is given below in Table 1 and in Table 2 (“Autres données numériques” folder). No datable minerals were found in samples 24-SL-4190A1, 24-AO-4029-A, 24-TD-2178-A, and 24-TD-2122-A. Analysis and image files are attached to this report.

Table 1. List of samples

	Numéro d’échantillon	Lithologie (unité stratigraphique indéterminée)	Résultats
	Supérieur (Eeyou Istchee Baie-James) - Lac Caulincourt		
1	24-CL-2166A	Tonalite gneissique à biotite-magnétite	Zircon: 2890 ± 9 Ma; Monazite: 2610-2650 Ma
2	24-CL-2113A	Tonalite gneissique à hornblende-biotite-magnétite	Zircon: 2689 ± 17 Ma; Monazite: 2677 ± 2 Ma
3	24-CL-2112A	Paragneiss	Zircon: 2706 ± 5 Ma; Monazite: 2693 ± 4 Ma
4	24-CL-2161B	Dacite	Zircon: 2696 ± 7 Ma
5	24-CL-2165A	Paragneiss	Zircon: 2691 ± 8 Ma; Monazite: 2693 ± 4 Ma

6	24-WM-1140A	Monzonite	Zircon: 2700 ± 2 Ma
7	24-WM-1161A	Tuf dacitique	Zircon: 2668 ± 3 Ma
	Supérieur (Eeyou Istchee Baie-James) - Lac Chamic		
8	24-DB-1021A1	Conglomérat	Zircon: 2706 ± 8 Ma
9	24-GS-2197A1	Conglomérat	Zircon: 2693 ± 12 Ma
10	24-DB-1110A1	Volcanoclastite andésitique	Zircon: 2707 ± 9 Ma
11	24-GS-2108A1	Gneiss tonalitique	Zircon: 2825 ± 4 Ma
12	24-GS-2205A1	Métatexite dérivée d'un gneiss tonalitique	Zircon: 2767 ± 3 Ma; Titanite: 2581 ± 3 Ma
13	24-GS-2205B1	Gneiss tonalitique rubané	Zircon: 2945 ± 8 Ma; Titanite: 2564 ± 20 Ma
14	24-GS-2204A1	Métatexite dérivée d'un gneiss tonalitique	Zircon: ca. 2840 Ma; Titanite: 2614 ± 5 Ma
	Churchill (Orogène de l'Ungava) - Lac Pingasulik		
15	24-MY-1037-B	Tuf de basalte andésitique	Zircon: 1894 ± 6 Ma
16	24-TD-2179-A	Wacke métamorphisé	Zircon: 1979 ± 13 Ma
17	24-TD-2182-A	Paragneiss	Zircon: 1879 ± 24 Ma; Monazite: 1876-1895 Ma
18	24-TD-2180-A	Tonalite	Zircon: 1876 ± 4 Ma
19	24-MY-1140-A	Granodiorite	Zircon: 1885 ± 4 Ma
20	24-AO-4150-A	Diorite	Zircon: 1856 ± 5 Ma
	Churchill (Orogène de l'Ungava) - Nuvujjuaq		
21	24-AM-5039-A	Paragneiss	Zircon: 1870 ± 6 Ma; Monazite: 1810 ± 8 Ma
22	24-AM-5140-A	Paragneiss migmatitisé	Zircon: ca. 2730 Ma; Monazite: 2808 ± 27 Ma
23	24-CB-2063-A	Gneiss granulitique de composition tonalitique	Zircon: 1839 ± 5 Ma
24	24-AM-5096-A	Granite	Zircon: 1817 ± 17 Ma; Monazite: 2672 ± 7 Ma
25	24-MV-1002-A	Granodiorite	Zircon: 2722 ± 6 Ma
26	24-MV-1024-A	Tonalite	Zircon: 2905 ± 5 Ma; Meta. zircon: 1791 ± 18 Ma; Rutile: 1774 ± 29 Ma
27	24-MV-1044-A	Monzogranite à magnétite	Zircon: 2527 ± 53 Ma Meta. zircon: 1817 ± 11 Ma; Titanite: ca. 1770 Ma

METHODS

Following crushing and pulverization, initial separation of heavy minerals was carried out on a Wilfley table. This was followed by paramagnetic separations with the Frantz isodynamic separator and density separations using methylene iodide. Final sample selection for geochronology was by hand picking under a microscope, choosing the freshest, least cracked grains of zircon, monazite and/or rutile. Grains were either mounted in epoxy and polished or fixed onto double-sided tape for ablation on natural surfaces. Polished grains were imaged with backscattered electrons (BSE) using a JEOL JSM6610-Lv scanning electron microscope in order to detect phases of growth that may have different ages.

U–Pb isotopic analyses were conducted at the Earth Sciences Dept., University of Toronto using an Agilent 7900 ICPMS and an NWR193 excimer laser system. Data were collected using spots analyses and were conducted with laser wavelength of 193 nm, fluence of about 4 J/cm^2 and frequency of 10 Hz at a rate of 20 microns/sec with typical beam diameter of 30 microns.

Data were collected on ^{88}Sr (10 ms), ^{206}Pb (30 ms), ^{207}Pb (70 ms), ^{232}Th (10 ms), and ^{238}U (20 ms). Prior to analyses, spots were pre-ablated with a larger beam diameter using 10 pulses to clean the surface. Following a 10 sec period of baseline accumulation, the sample was exposed to the laser beam and data were collected for 20 seconds followed by a washout (and laser warm-up) period of 10 seconds.

The zircon, monazite, titanite, and rutile standards used for LA-ICP-MS analyses were previously dated by ID-TIMS. For zircon, we used standard DD91-1 dated at 2682 ± 1 Ma (Davis, 2002). For monazite we used standard DD90-26A from Lac Lacroix granite from the Superior Province in Minnesota dated at 2671 +/- 2 Ma (D.W. Davis, unpublished report). The rutile standard is from the Great Zimbabwe Dyke dated at 2575 ± 1 Ma (Oberthur et al., 2002) whereas the titanite standard comes from the Heronry diorite in the Superior Province, Wabigoon Subprovince dated at 2699 ± 1 Ma (Davis and Edwards, 1986).

Data were edited and reduced using custom VBA software (UtilLAZ program) written by D. W. Davis. $^{207}Pb/^{206}Pb$ time resolved analytical (TRA) profiles are usually flat throughout the ablation whereas $^{206}Pb/^{238}U$ ratios show increasing fractionation for zircon caused by loss of refractory U with increasing penetration depth through the run. The degree of measured Pb/U fractionation depends on U zoning and radiation damage so is difficult to correct using standards. Accordingly, age estimates are based primarily on $^{207}Pb/^{206}Pb$ measurements. ^{88}Sr was monitored from zircon in order to detect intersection of the beam with zones of alteration or inclusions. Data showing high Sr signal accompanied by discordance or irregular time resolved profiles were either averaged over restricted time windows or rejected. In some cases, high Sr is due to ablation of small apatite inclusions, and does not significantly affect the U-Pb analysis or ages. No corrections were made for common Pb, since the ^{204}Pb peak is too small to be measured precisely in LA-ICPMS and common (crustal) Pb is usually insignificant for unaltered Precambrian zircon, monazite and rutile. Common Pb can be significant in titanite. On the Wetherhill Concordia plots used here, common Pb has the effect of pushing data to the right, along a shallow mixing line with slope determined by the isotopic composition of the common Pb component, which can be estimated using the Stacey and Kramers (1975) crustal Pb isotopic growth model. The concordia intercept of the mixing line depends strongly on measured 206Pb/238U values, which are poorly determined. This limits age interpretation of titanite data except where data are near-concordant and clustered. In high grade rocks, titanite and rutile ages are likely to represent closure to diffusion of Pb during cooling, whereas zircon and monazite tend to preserve ages unless metamorphism is of long duration when they may be partially reset.

The Th/U ratio of zircon can be a useful petrogenetic indicator and was also measured, although it is only a rough estimate because the ratio is not constant in the standard. For high Th minerals like monazite, ^{208}Pb is measured as a proxy for ^{232}Th and Th/U is calculated based on this and the $^{207}Pb/^{206}Pb$ age of the sample. Low Th/U (<0.1) is characteristic of metamorphic and hydrothermal zircon whereas most zircon crystallized from felsic melts has Th/U >0.1. Time resolved analytical (TRA) profiles can be used to assess the variability of Th/U within a grain. Large variability can indicate the

presence of different magmatic phases where small differences in ages are more difficult to assess from the U-Pb profiles.

RESULTS

Results of U-Pb isotopic analyses by LA-ICPMS are given in Table 3 ("Autres données numériques" folder) and data are plotted on Wetherill concordia or Tera-Wasserberg concordia plots. Average age errors in the text and error ellipses on figures are given at 2 sigma (2σ). These were calculated and plotted using the Isoplot program of Ludwig (1998, 2003). U decay constants are taken from Jaffey et al. (1971). For Paleoproterozoic and Archean samples, $^{207}Pb/^{206}Pb$ ages are more precise than $^{206}Pb/^{238}U$ ages and are also much less susceptible to fractionation biases between samples and standards. Therefore, ages are usually based on $^{207}Pb/^{206}Pb$ ratios. Representative images for individual samples are presented in the sections below.

1. 24-CL-2166A
Tonalite gneissique à biotite-magnétite, Complexe de Maingault (nAmng1)

This sample yielded a small amount of zircon with diverse morphologies (Fig. 1-1). BSE images show cracks, alteration zones with thin, slightly higher U overgrowths that are weakly zoned or unzoned (Fig. 1-2). $^{207}Pb/^{206}Pb$ ages for most U-Pb analyses are clustered but scatter outside of error with a mean of 2867 ± 5 Ma (MSWD – 6.7, Fig. 1-3). A single xenocrystic grain defines a concordant age of 3183 ± 8 Ma, suggesting an older age inherited from basement. A younger discordant analysis gives an age of 2766 ± 8 Ma but this is the youngest of two flat portions on the TRA profile, which correspond to different Th/U ratios. The older portion agrees in age with the main zircon cluster so the younger age may represent an overgrowth. A plot of probability density of $^{207}Pb/^{206}Pb$ ages shows 3 possible modes (Fig. 1-3). Applying the 'Unmix' program of Sambridge and Compston (1994) gives ages of 2890 ± 9 Ma, 2874 ± 4 Ma and 2857 ± 4 Ma for the modes. These ages may not be meaningful because of partial resetting but the oldest one should be closest to crystallization of the igneous protolith of the tonalite.

Monazite grains show distinctly younger Neoarchean ages with significant scatter (Fig 1-4). A probability density distribution (PDD plot) shows a possible tri-modal age population. Ages calculated from the 'Unmix' program of Sambridge and Compston (1994) are 2611 ± 3 (25%), 2630 ± 2 (63%) and 2650 ± 7 (12%) but these are based on a small number of analyses so may not be significant. There is no obvious correlation of U concentrations or Th/U ratios with age. The scatter in monazite ages suggests that the rock may have remained above the solidus for at least 40 Ma. Such long-term heating may have allowed some loss of Pb from the zircon and account for the scatter seen in the zircon ages.

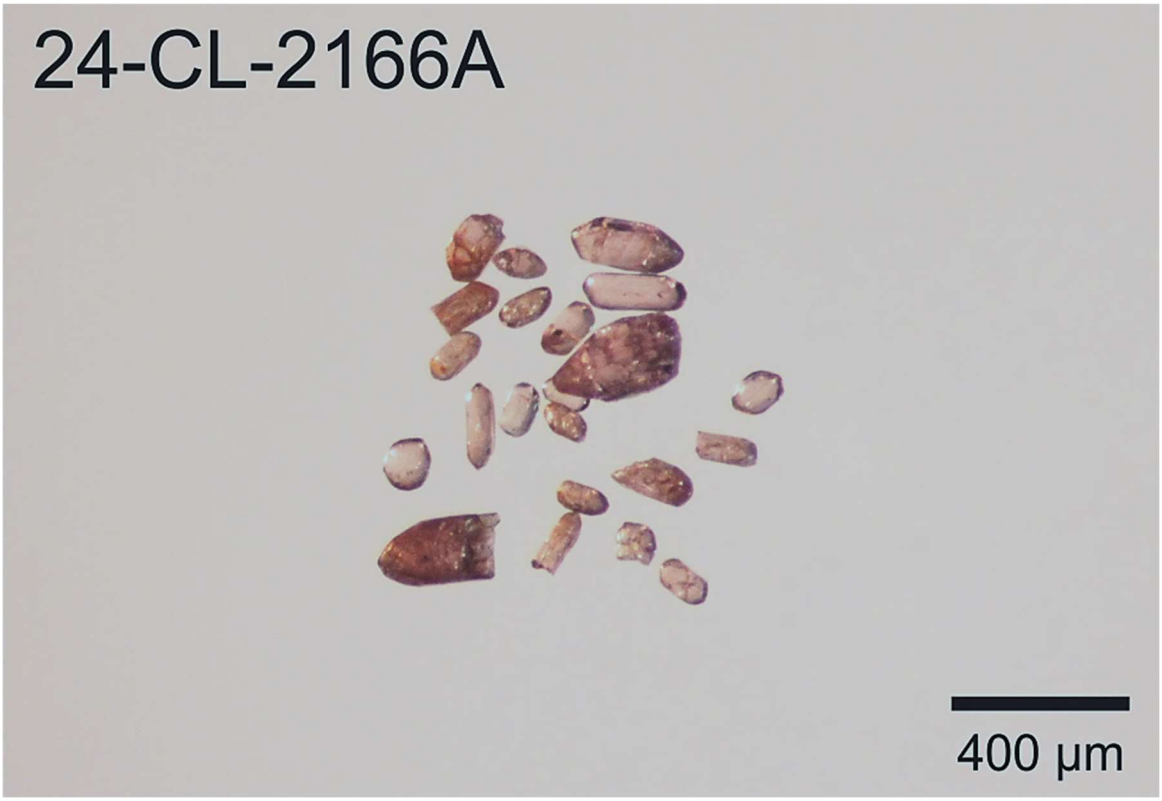

Figure 1-1. Picked zircon from tonalite sample 24-CL-2166A.

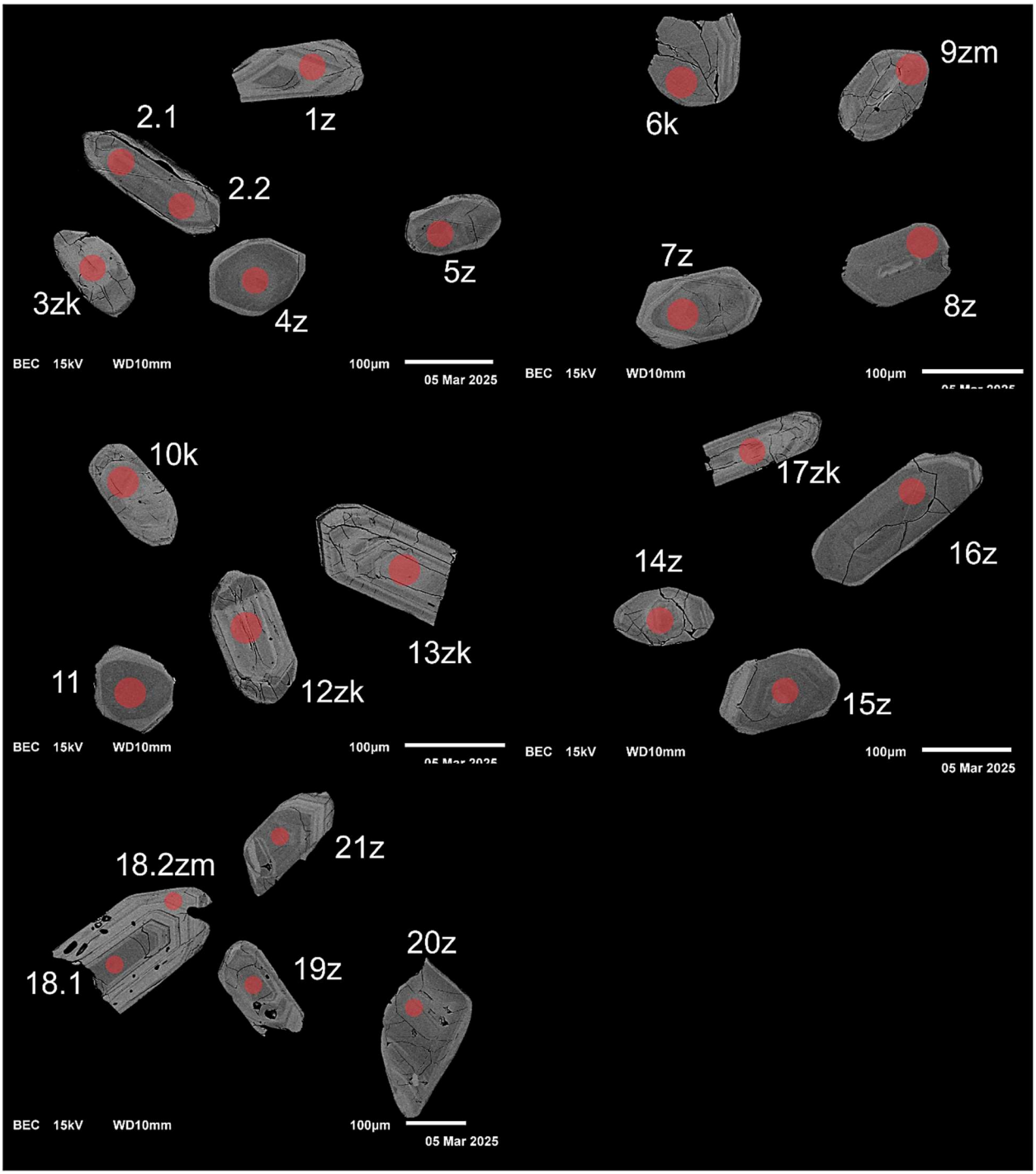

Figure 1-2. BSE images of selected grains from sample 24-CL-2166A. The red circles represent the approximate locations of laser ablation spots.

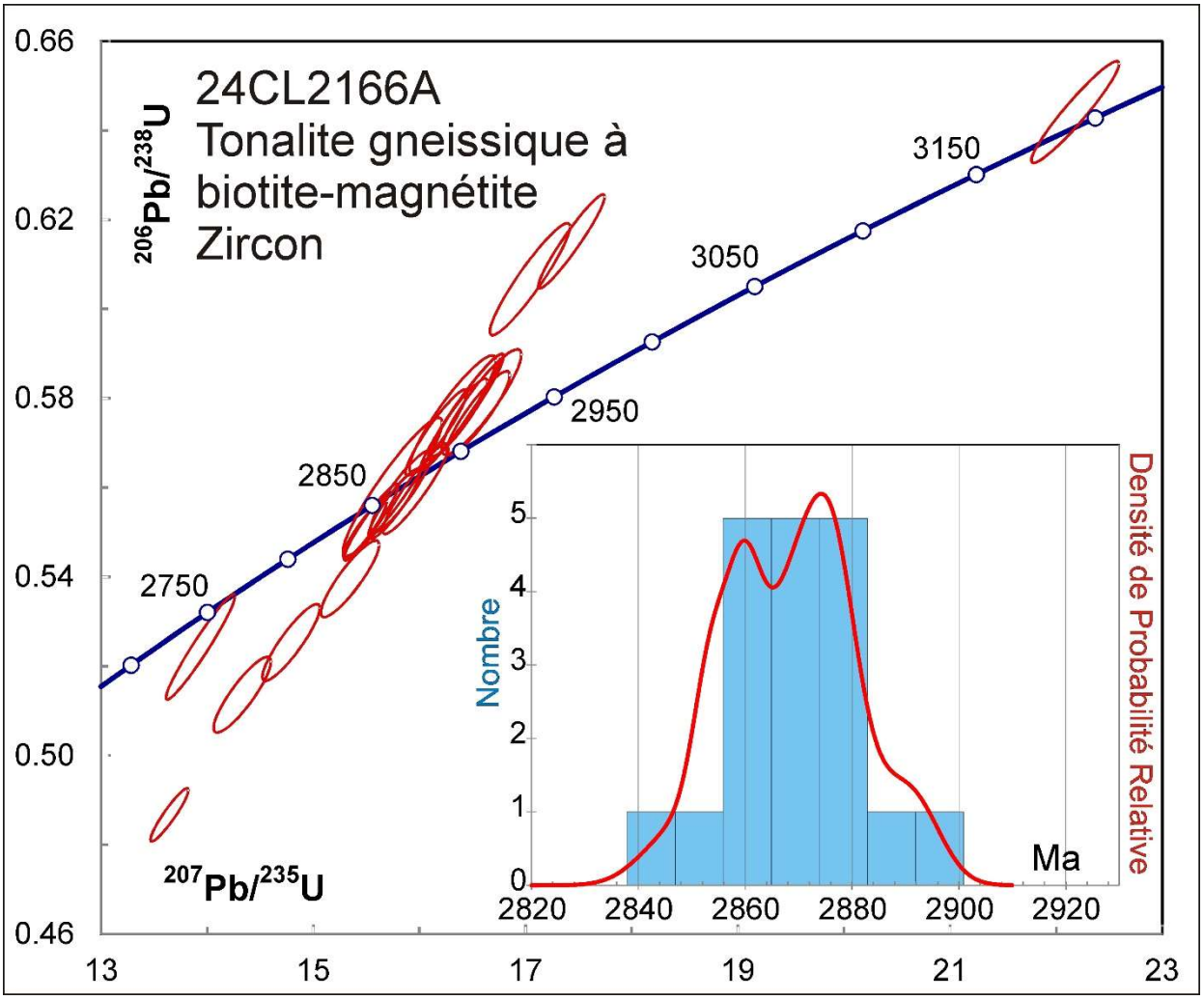

Figure 1-3. Concordia plot showing U-Pb isotopic data on polished zircon from tonalite sample 24-CL-2166A as well as a probability density plot of $^{207}Pb/^{206}Pb$ ages from the clustered data.

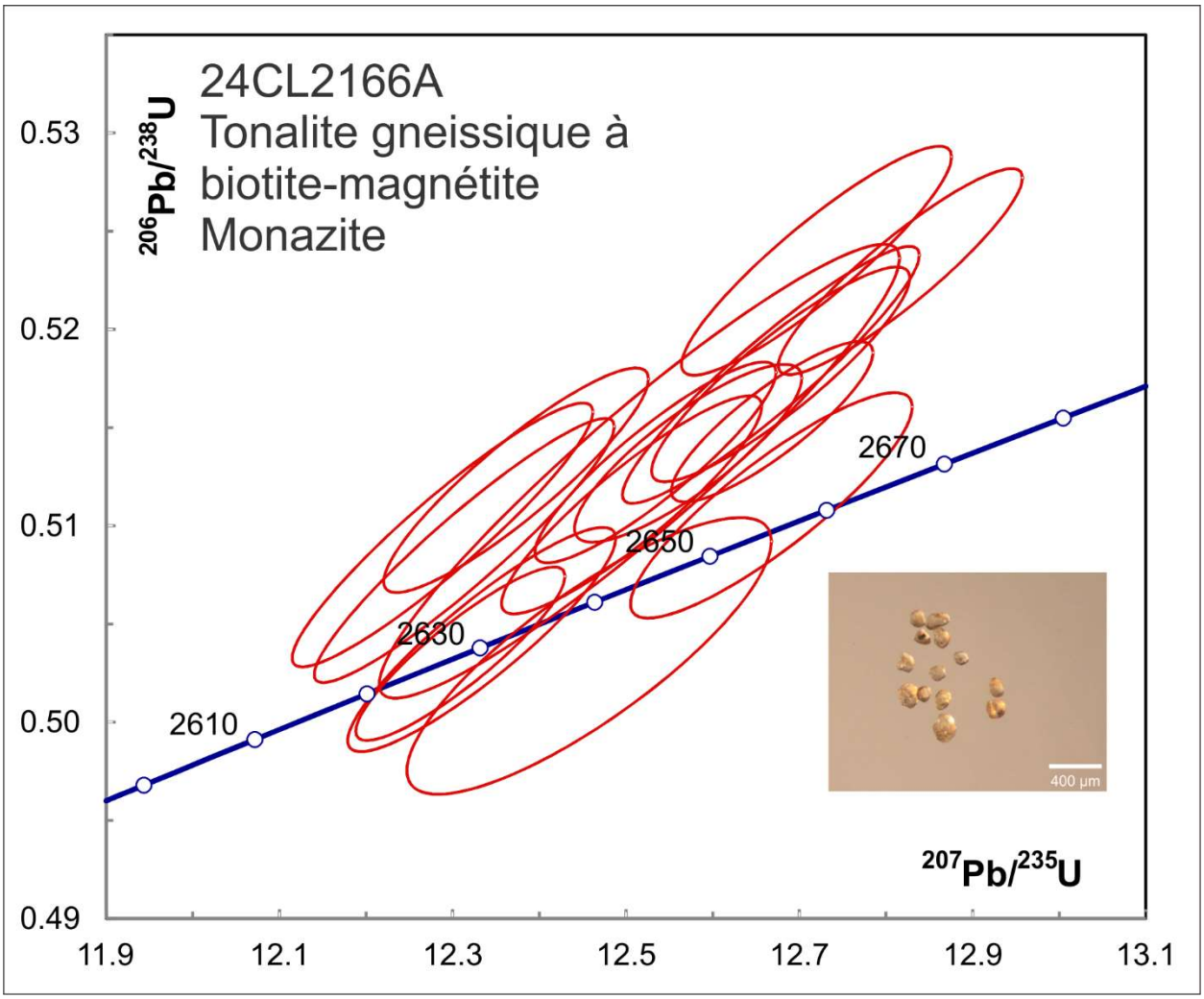

Figure 1-4. Concordia plot showing U-Pb isotopic data on polished monazite from tonalite sample 24-CL-2166A.

2. 24-CL-2113A
Tonalite gneissique à hornblende-biotite-magnétite, Suite de Travot (nAtvt)

This sample yielded a large amount of zircon with diverse morphologies from stubby to short-prismatic sub-rounded shapes (Fig. 2-1). BSE images show broad zoning with possible evidence for darker cores overgrown by lighter mantle. Some grains show thin higher U (brighter) rims (Fig 2-2). U-Pb analyses show Neoarchean $^{207}Pb/^{206}Pb$ ages that scatter outside of error (Fig. 2-3). The probability density distribution suggests the presence of 2 age components. Applying the 'Unmix' program gives 2670 ± 3 Ma (56%) and 2698 ± 3 Ma (44%) as the most likely ages of the components. Many time resolved analytical (TRA) profiles show relatively low Th/U at shallow levels followed by a higher ratio at deeper levels. This suggests the presence of relatively low Th/U overgrowths but all Th/U values are greater than 0.1, suggesting two magmatic phases. Ten other analyses were performed on apparent rim phases and gave an average age of 2689 ± 17 Ma, although these scatter somewhat outside of error (MSWD – 3.0, Fig. 2-4).

Analyses on monazite grains recovered from this sample are concordant and although two analyses appear to be slightly older, they are not chemically different and as a group they all scatter approximately within error with an average 207Pb/206Pb age of 2677 ± 2 Ma (MSWD – 1.3, Fig. 2-5). As with the previous sample, the presence of monazite suggests a peraluminous composition, which in turn suggests that the rock developed at least in part as a diatexite from a sedimentary protolith. In that case, the 2698 ± 3 Ma age may correspond to a detrital zircon component. It is likely that partial melting occurred over a period of several million years around 2670 Ma when the zircon overgrowths and monazite crystallized. The monazite shows order-of-magnitude higher Th/U ratios and lower U concentrations than the standard, which is from an S-type granite, suggesting that a U-rich mineral phase had previously crystallized. This is in contrast to monazite in the previous sample above, which has similar U and Th/U to the standard.

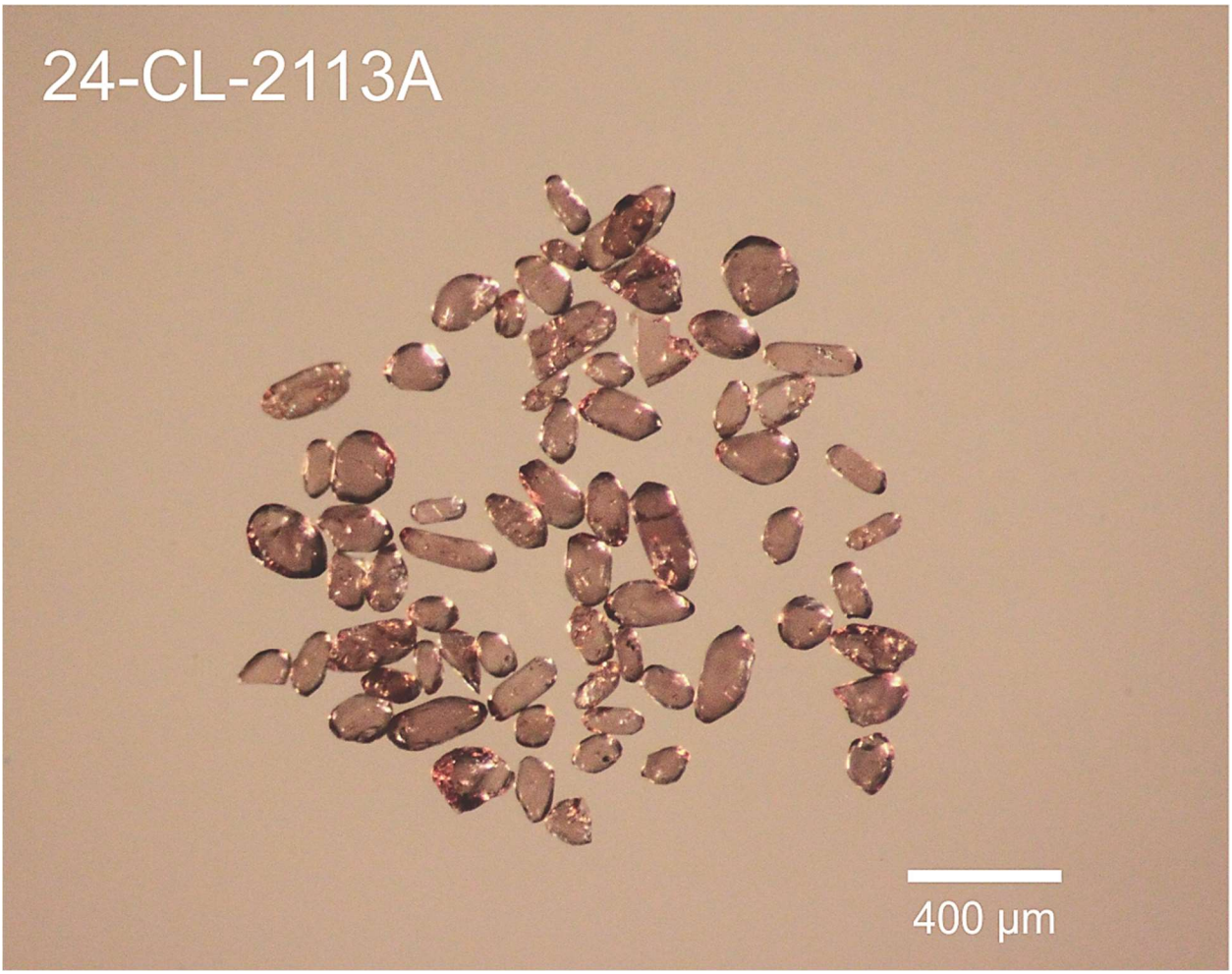

Figure 2-1. Picked zircon from tonalite sample 24-CL-2113A.

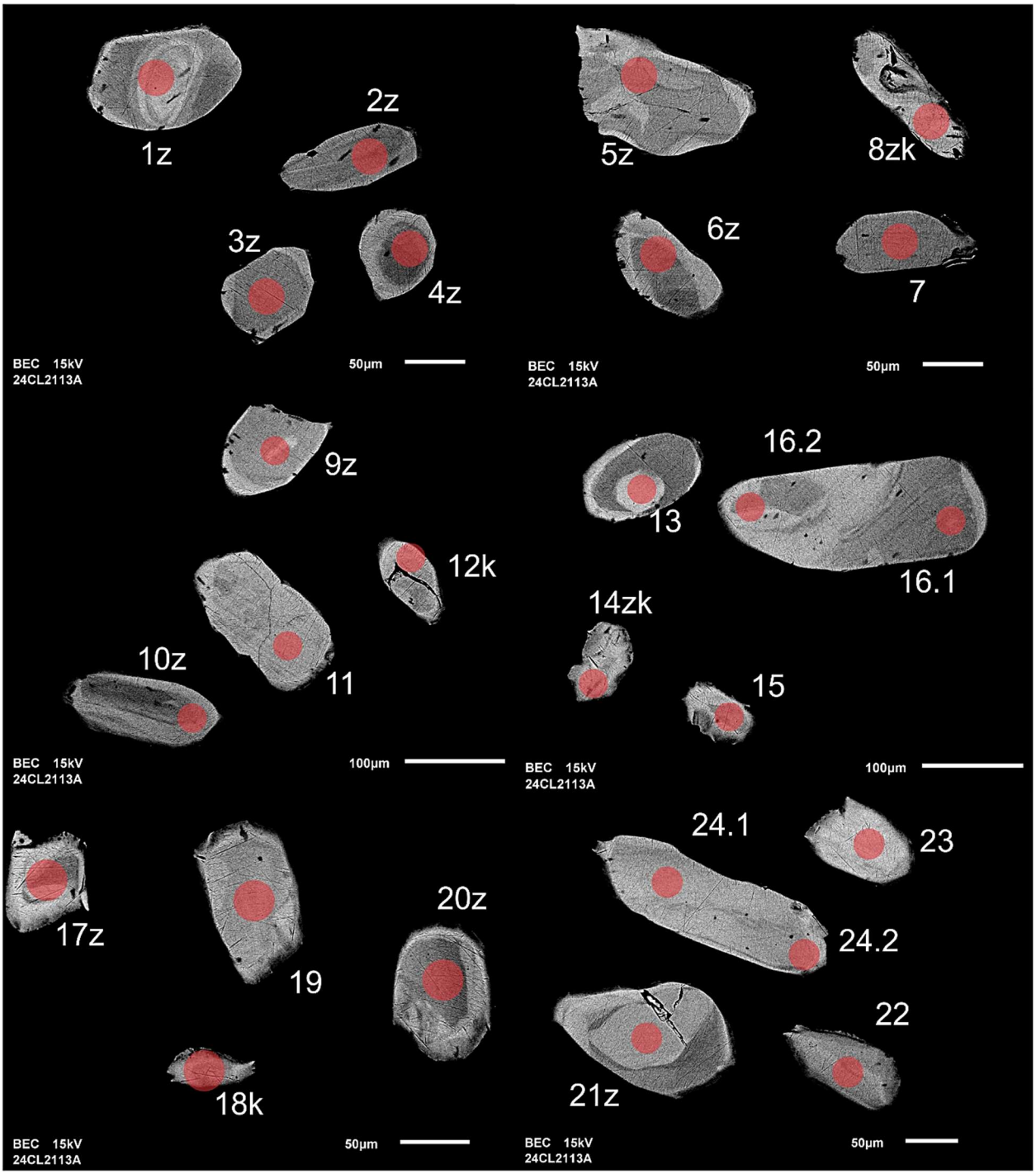

Figure 2-2-1. BSE images of selected grains from sample 24-CL-2113A. The red circles represent the approximate locations of laser ablation spots.

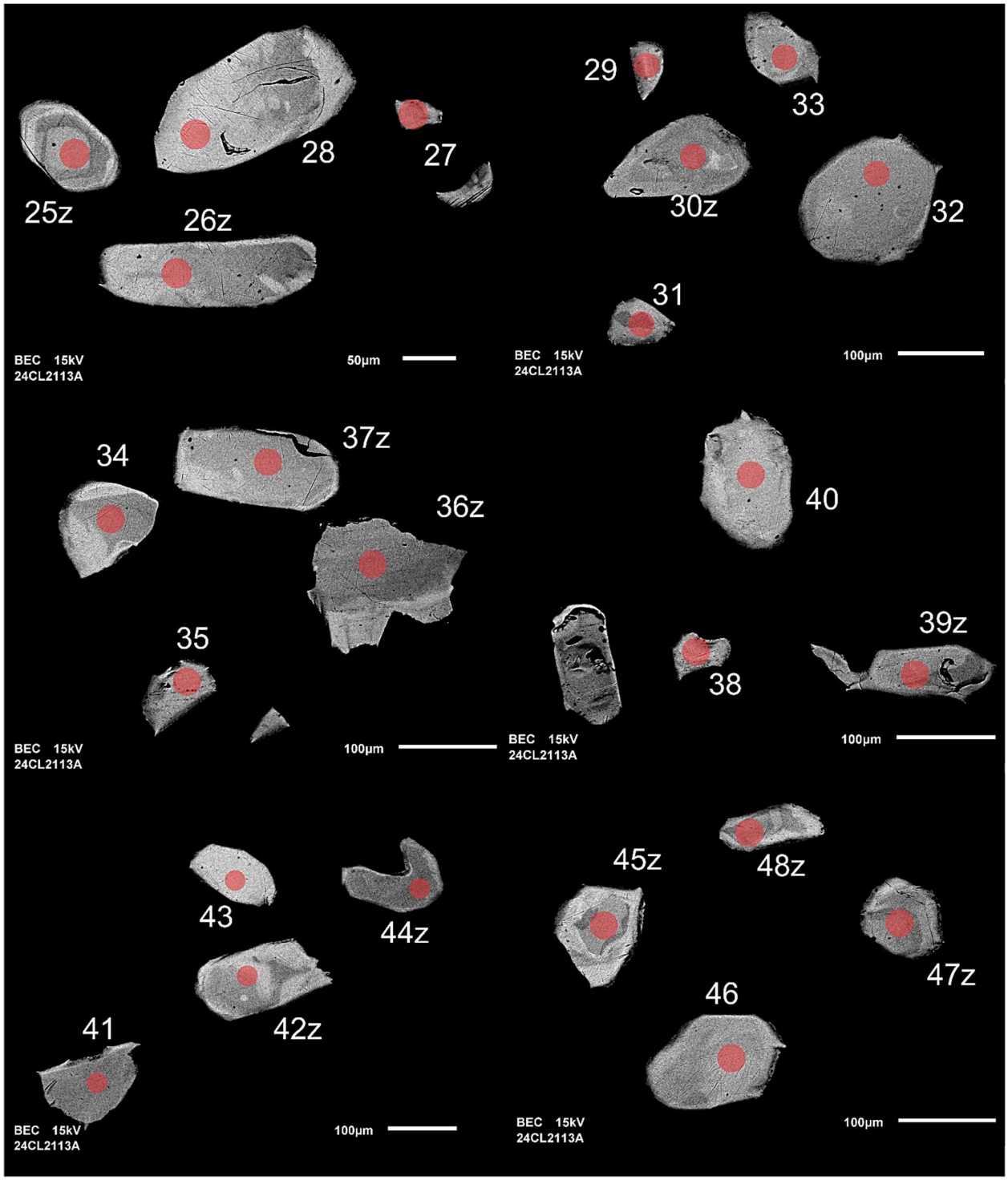

Figure 2-2-2. BSE images of selected grains from sample 24-CL-2113A. The red circles represent the approximate locations of laser ablation spots.

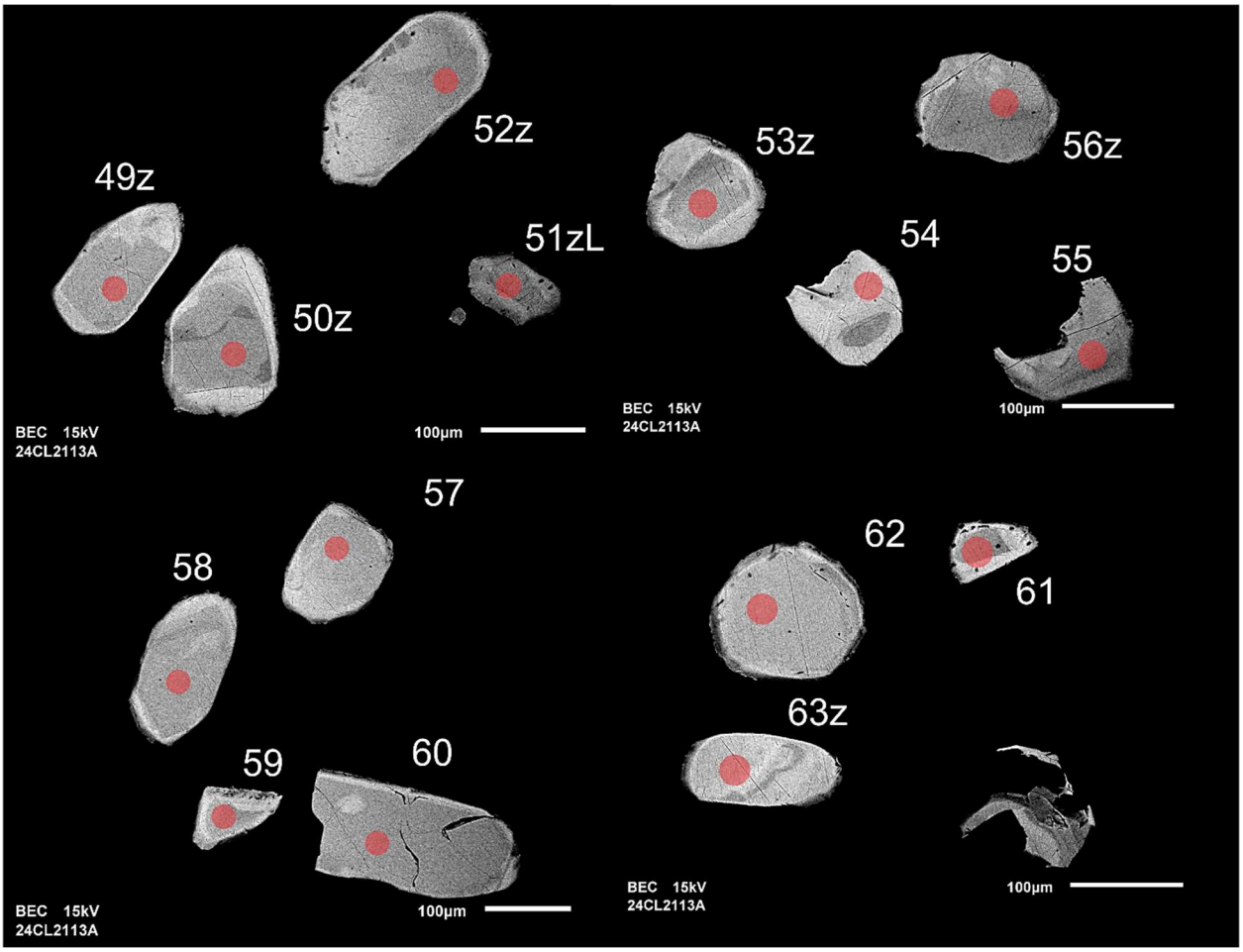

Figure 2-2-3. BSE images of selected grains from sample 24-CL-2113A. The red circles represent the approximate locations of laser ablation spots.

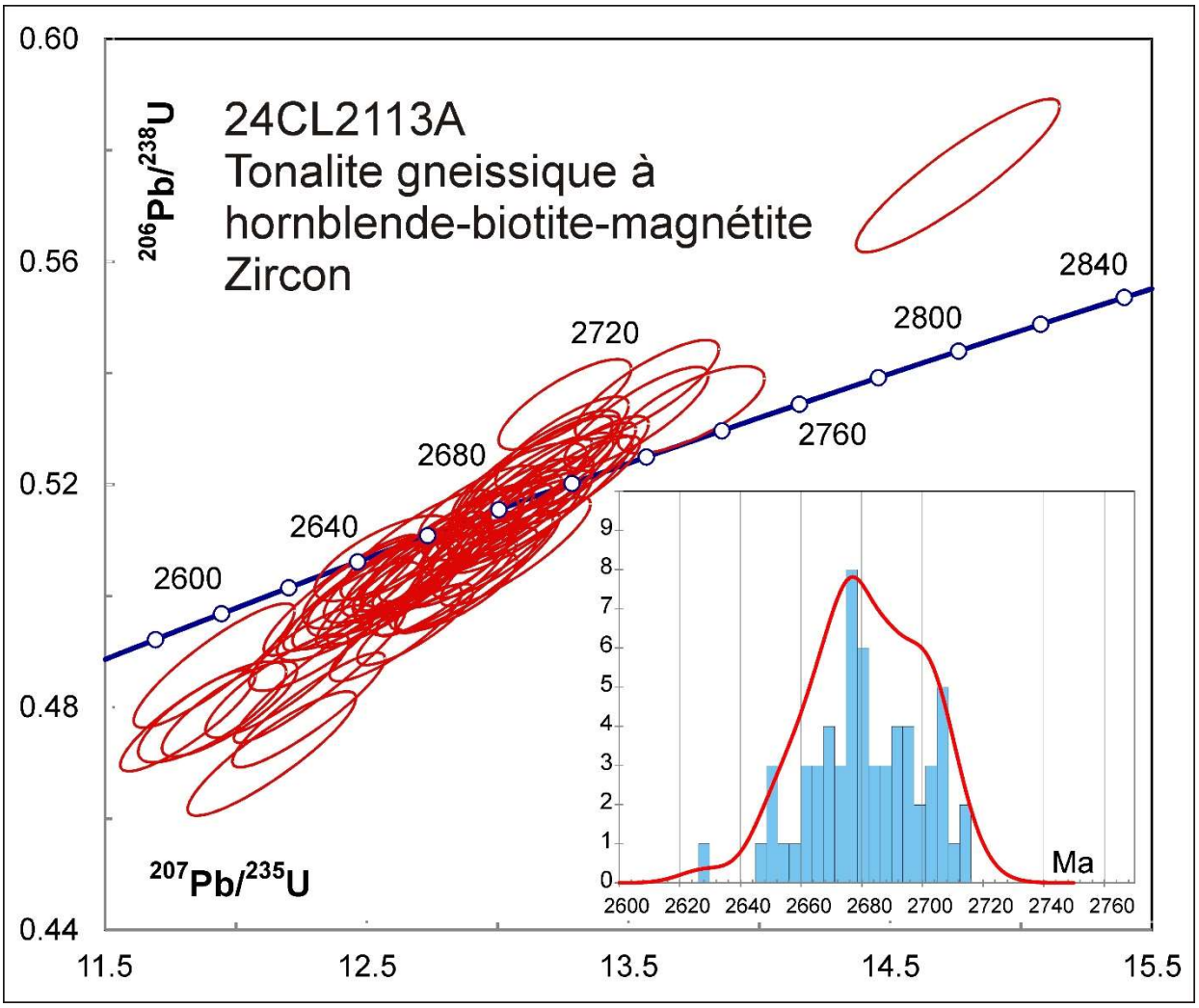

Figure 2-3. Concordia plot showing U-Pb isotopic data on polished zircon from sample 24-CL-2113A and a probability density plot of $^{207}Pb/^{206}Pb$ ages.

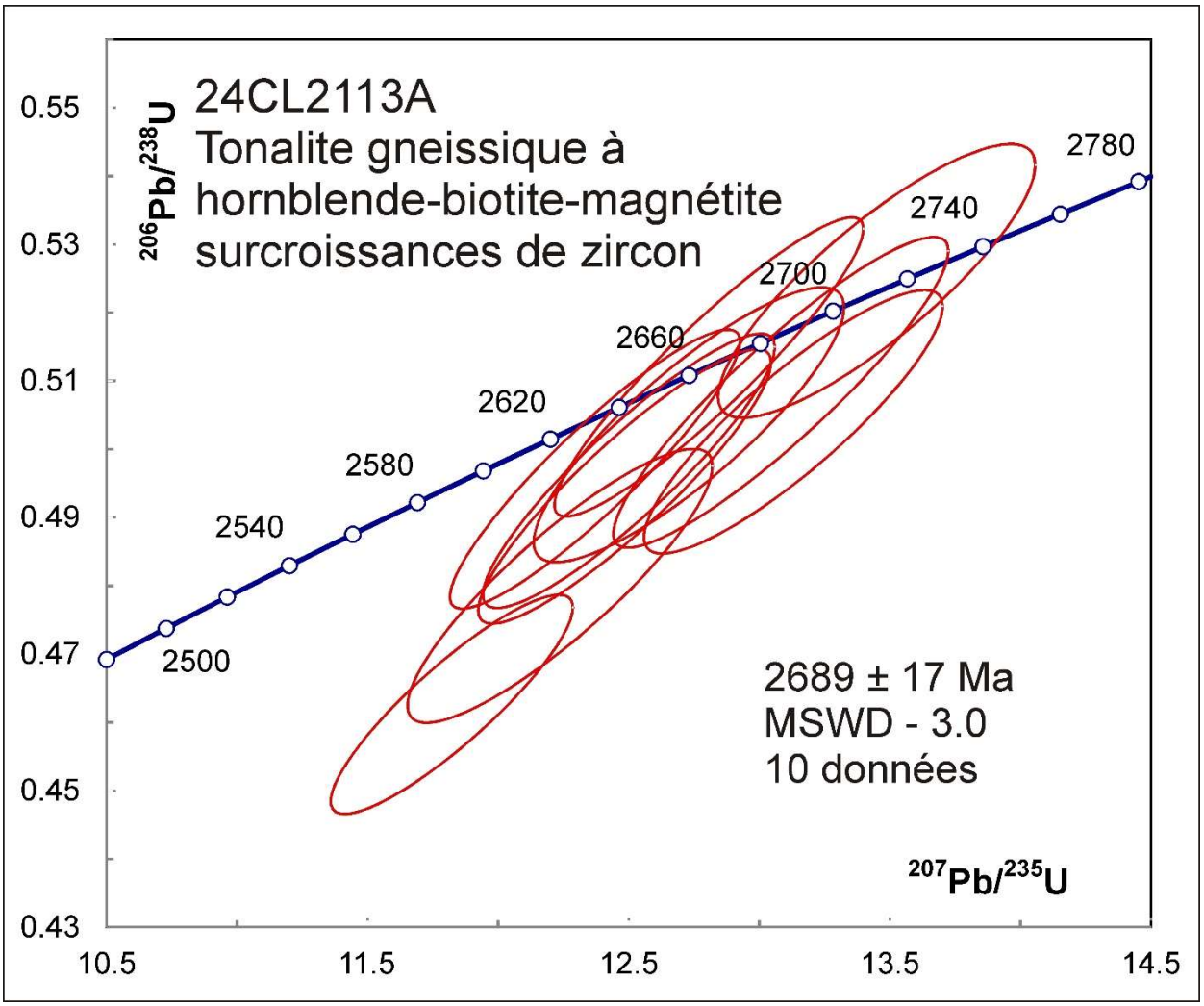

Figure 2-4. Concordia plot showing U-Pb isotopic data on polished zircon overgrowths from sample 24-CL-2113A.

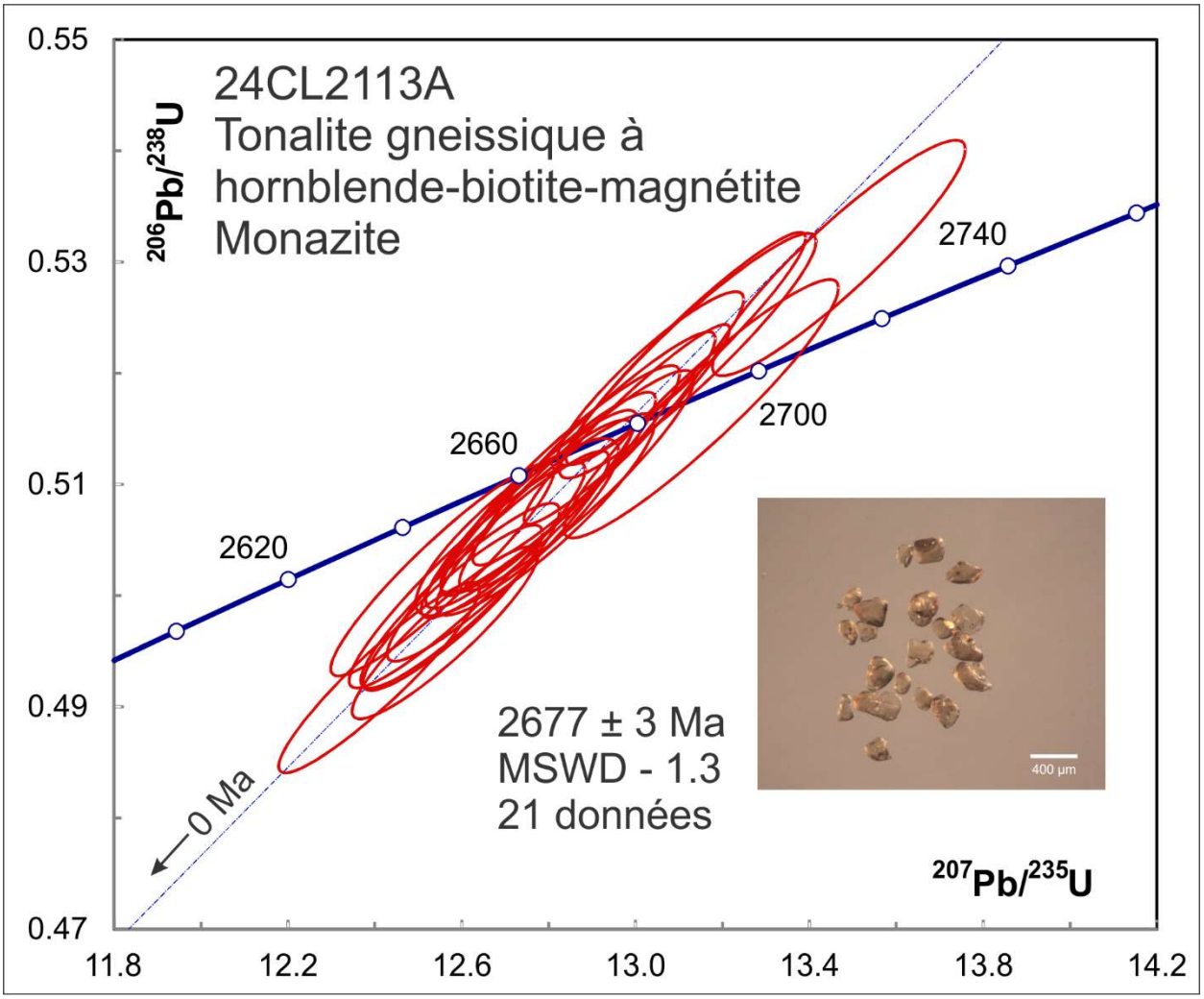

Figure 2-5. Concordia plot showing U-Pb isotopic data on monazite from sample 24-CL-2113A.

3. 24-CL-2112A
Paragneiss, Complexe de Laguiche (nAlgi2a)

This sample yielded a small amount zircon from stubby to short-prismatic sub-rounded shapes (Fig. 3-1). BSE images show broad and diffuse oscillatory zoning, with alteration zones, inclusions and with little evidence for older cores or younger rims (Fig 3-2). All analyses show magmatic Th/U > 0.1. Omitting problematic analyses with high Sr peaks and/or varying $^{207}Pb/^{206}Pb$ ages, U-Pb analyses show near-concordant data ranging from 2694 Ma to 2992 Ma (Fig. 3-3). A cluster of 14 youngest ages appears to be at least bimodal, in which case the 'Unmix' algorithm gives ages of 2706 ± 5 Ma (64%) and 2736 ± 6 Ma (36%). The broad age span of the zircon suggests that the older grains have a detrital origin.

Monazite grains were also recovered from this sample and appear to consist of 2 phases. Most analyses show high Th/U and relatively low U (Table 3) and scatter slightly outside of error with a mean age of 2719 ± 4 Ma (MSWD – 1.7, Fig. 3-4). Three analyses show relatively low Th/U and high U with the oldest at 2706 Ma and the youngest at 2656 ± 18 Ma. The youngest analysis shows a transition from high to low Th/U (the age was calculated over the low Th/U part). This suggests that the relatively younger low Th/U phase may have overgrown earlier monazite grains (analyses were done on polished grains so a core may have been exposed that transitioned to overgrowth with deeper penetration of the beam). The monazite results suggest that melting was a prolonged process that started at about 2720 Ma and may have extended to about 2660 Ma. In this case, the detrital zircon ages may have been partially reset. Alternatively, there may have been an early episode of metamorphic monazite formation in the sedimentary protolith with little U present (in a reduced state U should not be soluble in aqueous fluids) followed by melting and crystallization of a magmatic monazite phase.

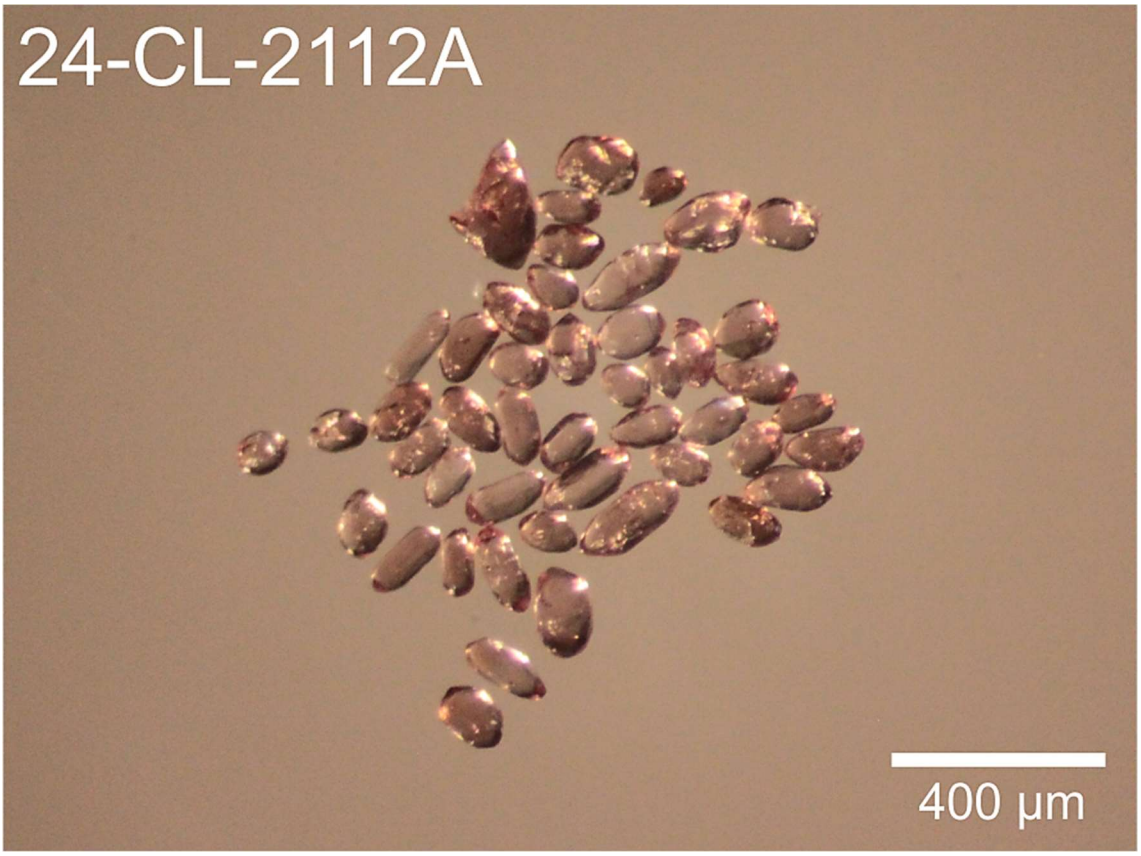

Figure 3-1. Picked zircon from granite sample 24-CL-2112A.

Figure 3-2-1. BSE images of selected grains from sample 24-CL-2112A. The red circles represent the approximate locations of laser ablation spots.

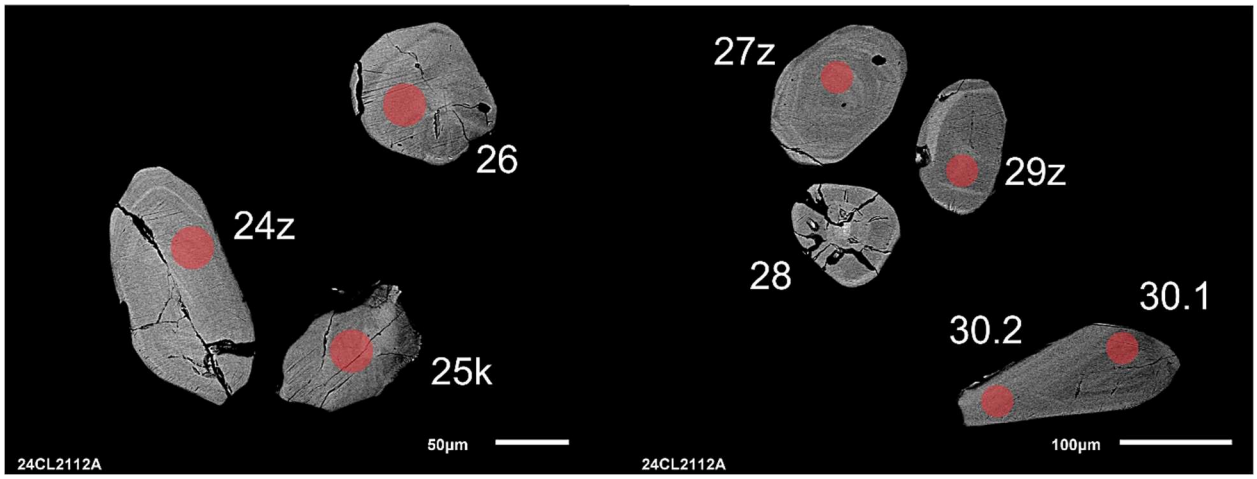

Figure 3-2-2. BSE images of selected grains from sample 24-CL-2112A. The red circles represent the approximate locations of laser ablation spots.

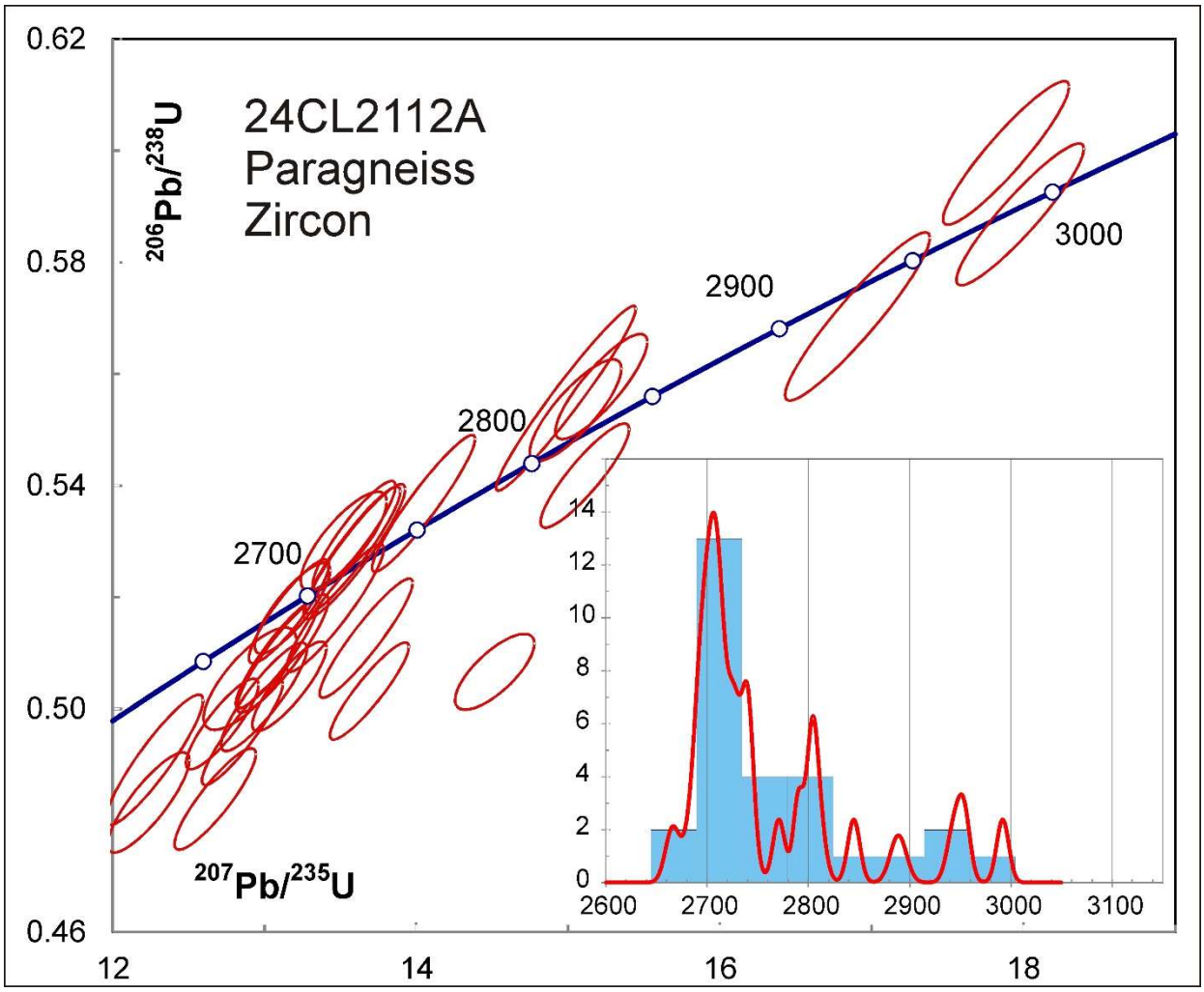

Figure 3-3. Concordia plot showing U-Pb isotopic data on zircon from sample 24-CL-2112A and a probability density plot of $^{207}Pb/^{206}Pb$ ages.

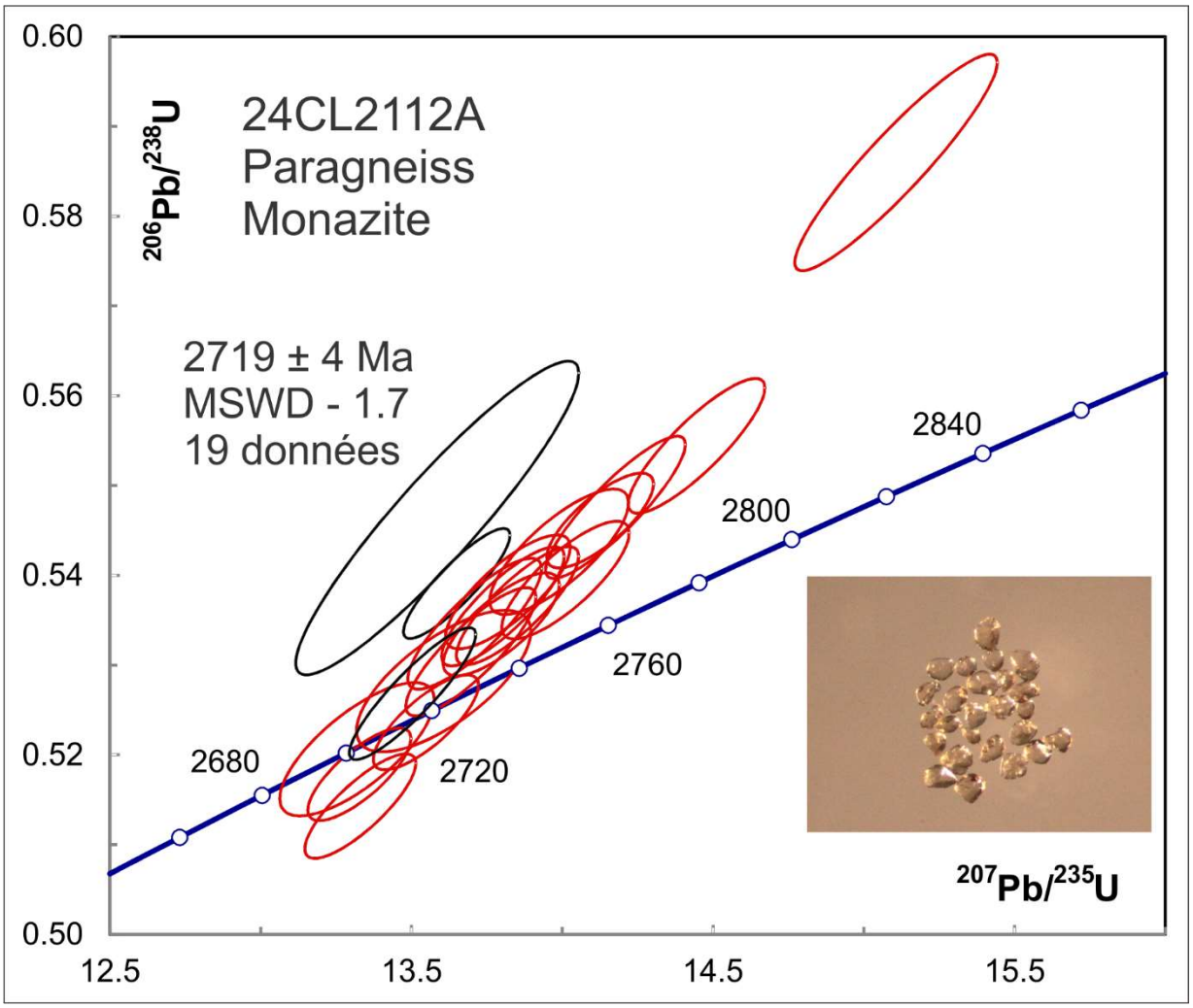

Figure 3-4. Concordia plot showing U-Pb isotopic data on monazite from sample 24-CL-2112A. Red ellipses correspond to spots considered in the age model whereas black ellipses correspond to omitted analyses.

4. 24-CL-2161B
Dacite, Groupe de Clauzel (nAclz2)

This sample yielded mostly small zircon grains from subhedral to well-rounded morphology (Fig. 4-1). BSE images (Fig 4-2) show broad zoning, with fractures, inclusions and with no evidence for older cores. All analyses show Th/U > 0.1 but some Th/U profiles (e.g. 23, 25, 32, 40) show an early increase over the range 0.1-1, accompanied by an order-of-magnitude decrease in U signal, suggesting the presence of metamorphic rims that are too thin to date. Many volcanic rocks are redeposited so can contain a detrital component, which seems to be the case here. Magmatic ages range from 2676 Ma to 3358 Ma but most are clustered around 2700 Ma (Fig. 4-3), and should contain any volcanic component. Applying the maximum likelihood algorithm in IsoplotR, which determines the most likely age of the youngest grain from an age distribution (Vermeesch, 2021) gives 2697 ± 8 Ma (Fig 4-4). This should represent the best age estimate for volcanism. It accords with the average of the 18 youngest grains (2696 ± 7 Ma, MSWD – 1.5, Fig 4-3).

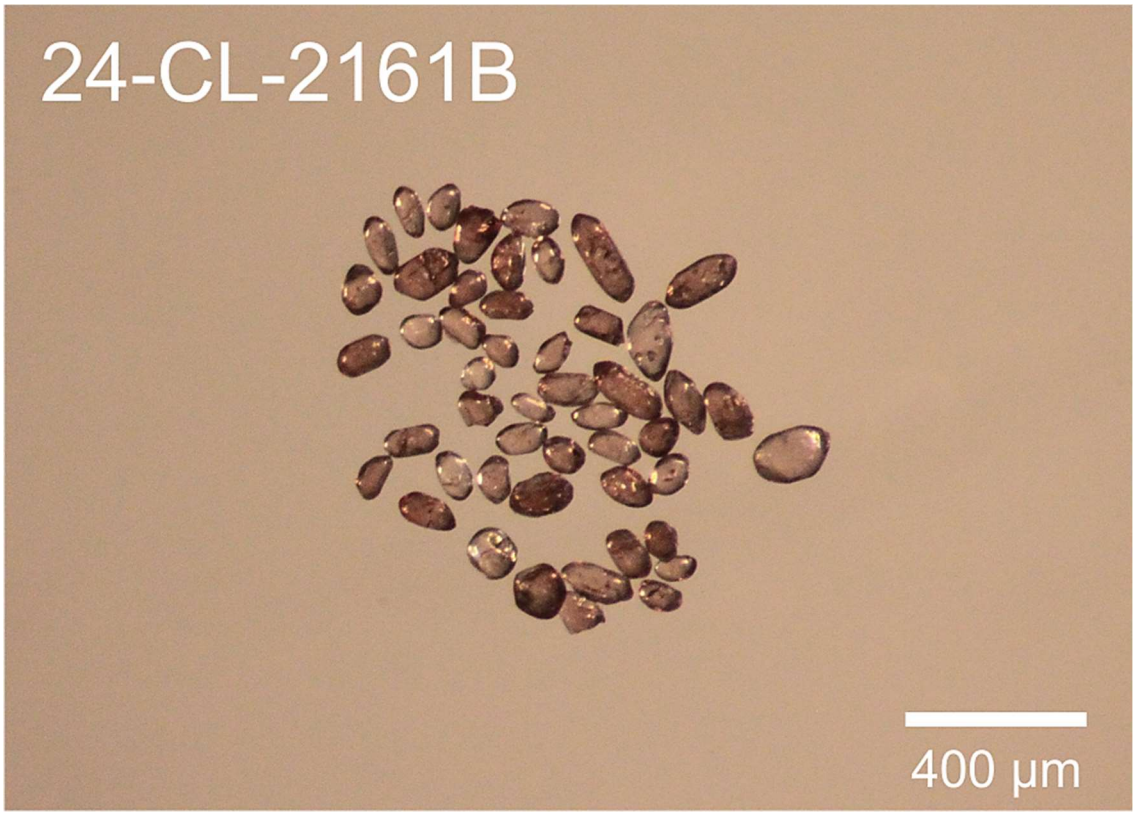

Figure 4-1. Picked zircon from dacite sample 24-CL-2161B.

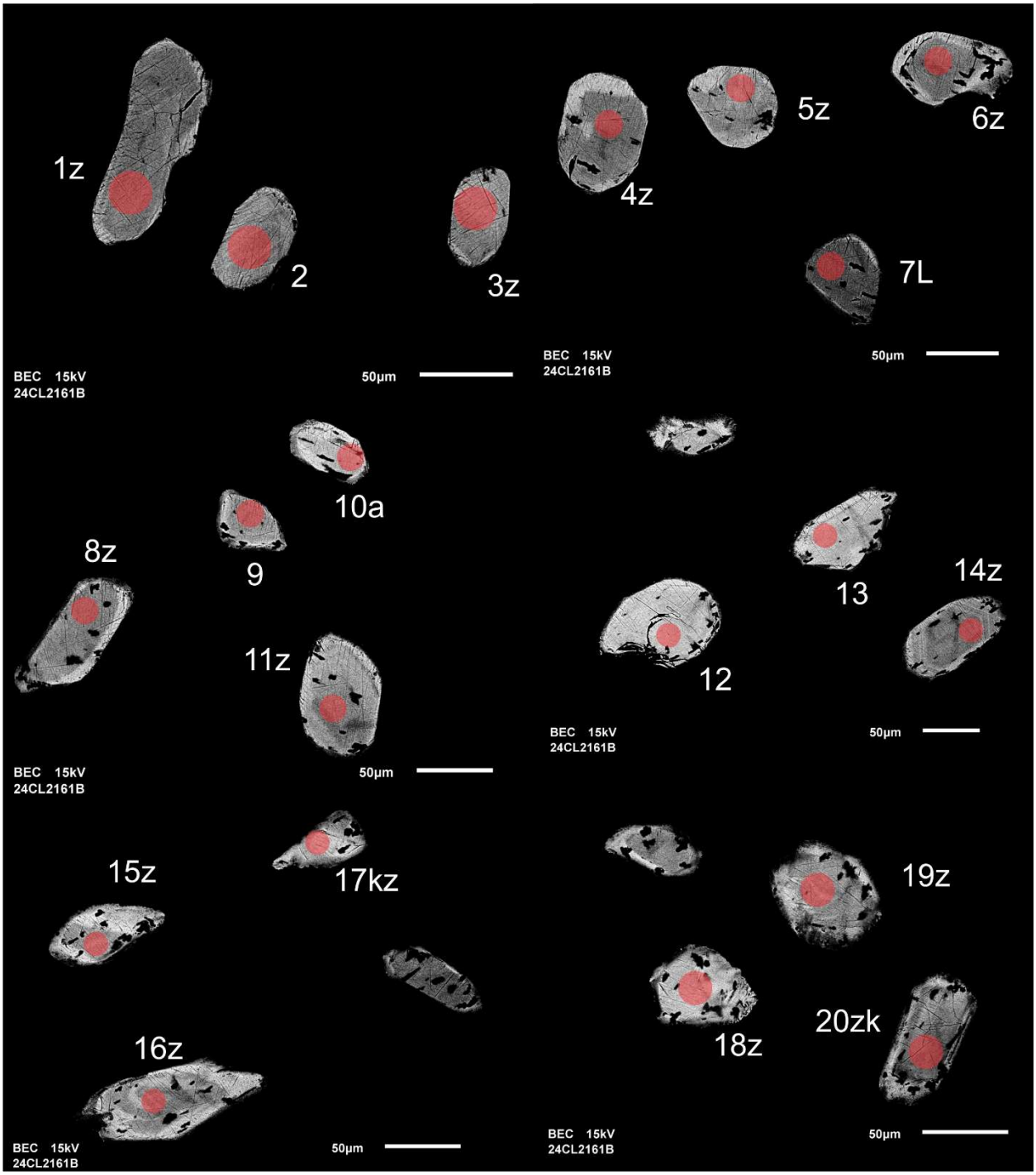

Figure 4-2-1. BSE images of selected grains from sample 24-CL-2161B. The red circles represent the approximate locations of laser ablation spots.

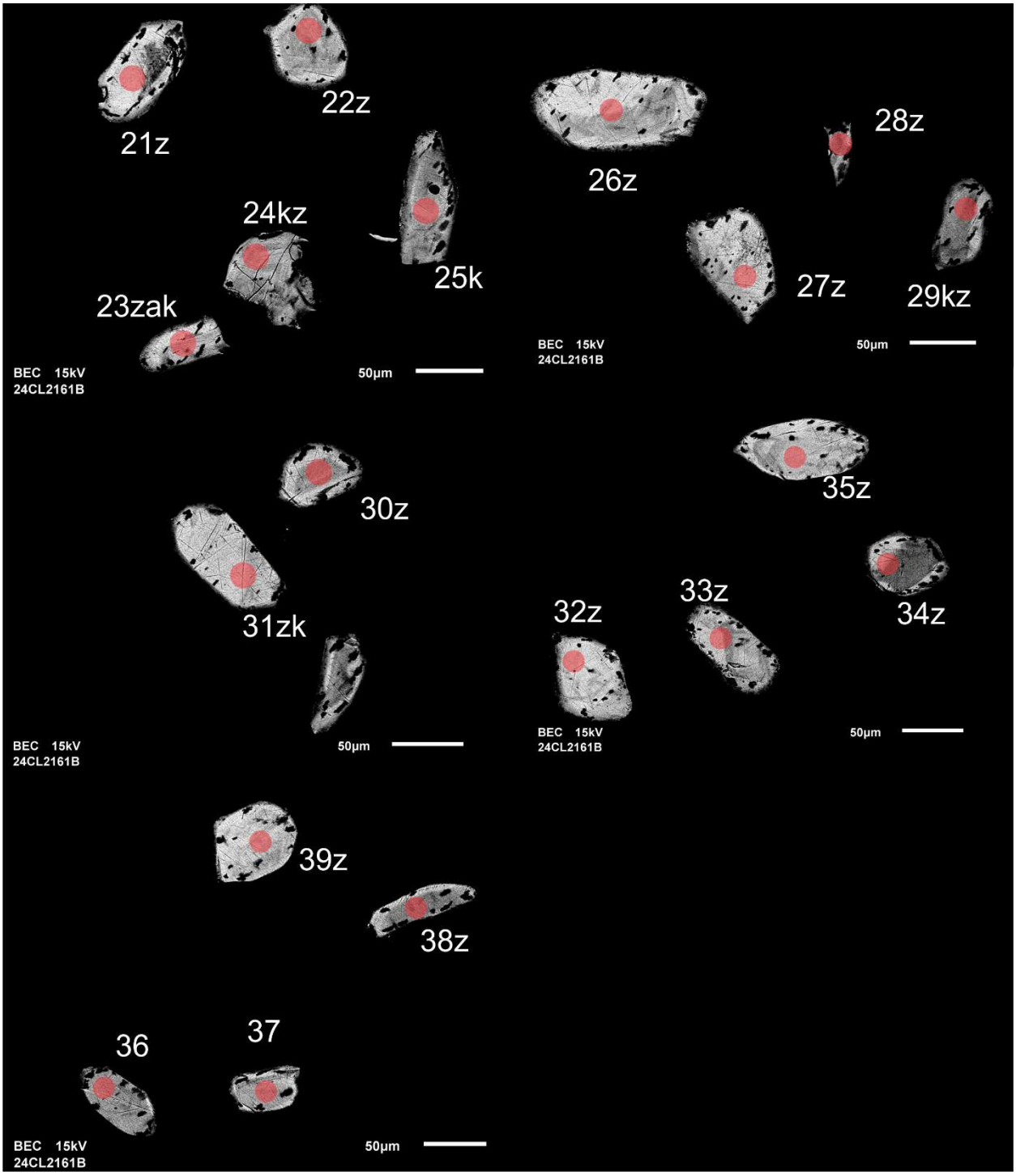

Figure 4-2-2. BSE images of selected grains from sample 24-CL-2161B. The red circles represent the approximate locations of laser ablation spots.

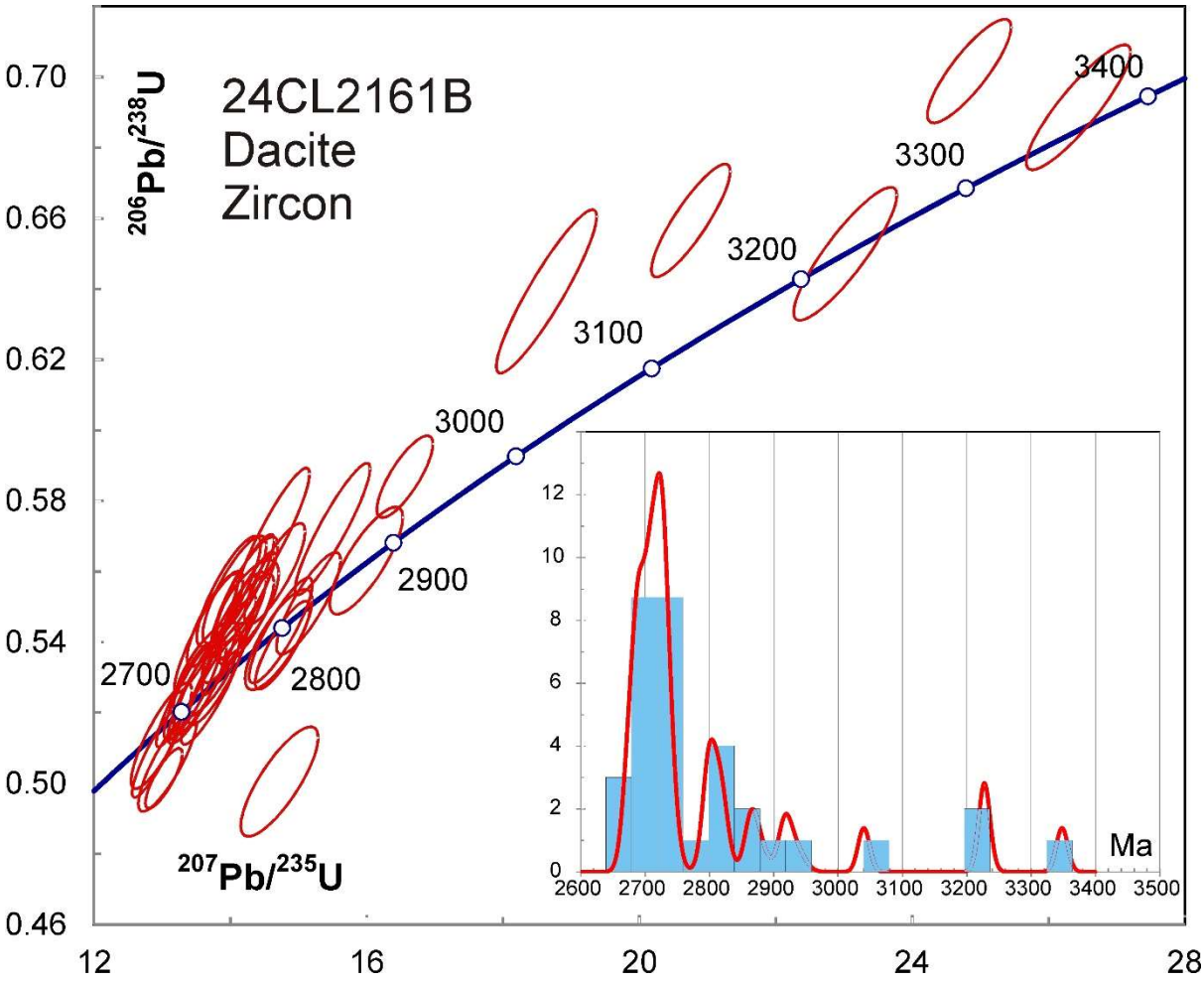

Figure 4-3. Concordia plot showing U-Pb isotopic data on zircon from dacite sample 24-CL-2161B and a probability density plot of $^{207}Pb/^{206}Pb$ ages.

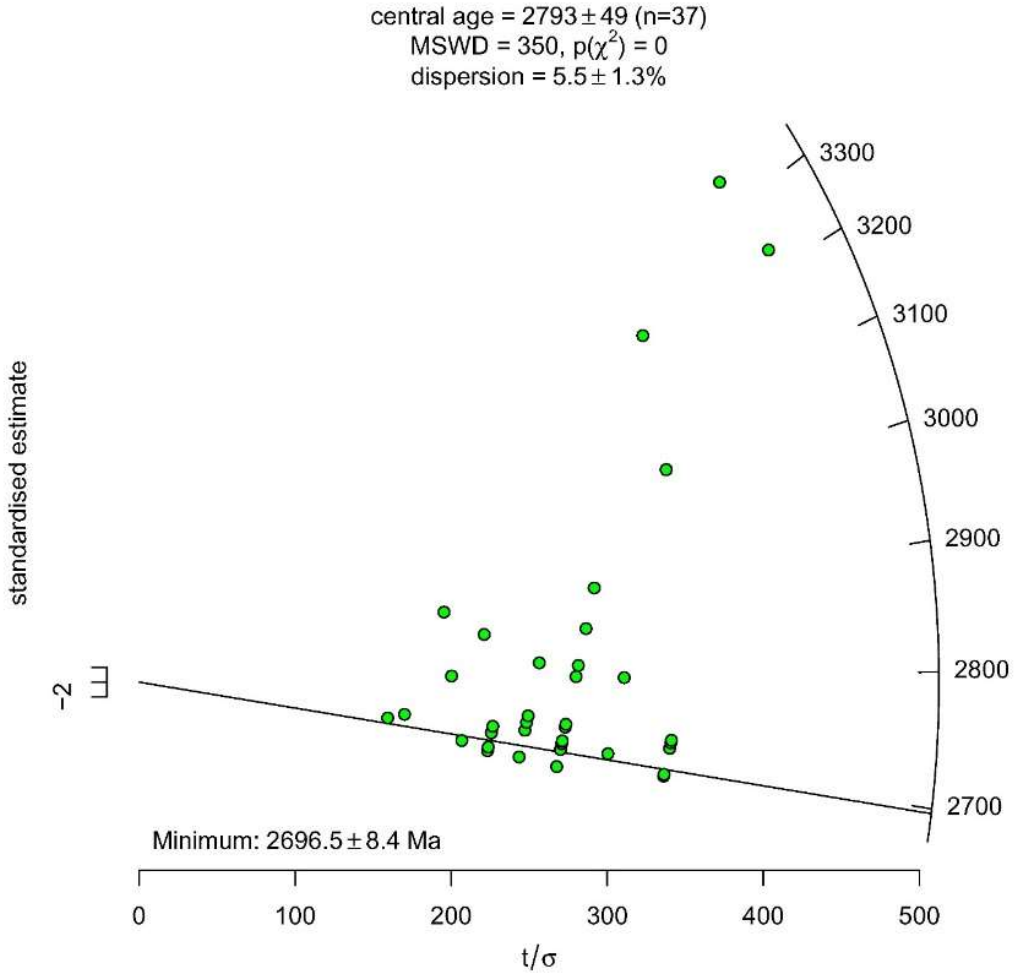

Figure 4-4. Radial plot showing the distribution of $^{207}Pb/^{206}Pb$ zircon ages from dacite sample 24-CL-2161B as well as the most probable estimate of the youngest age, which is an older estimate on volcanism/deposition.

5. 24-CL-2165A
Paragneiss, Formation de Prosper (nAprp1b)

This sample yielded zircon grains with a variety of brownish colouration from subhedral to rounded morphology (Fig. 5-1). BSE images show broad zoning, with fractures, inclusions but with no clear evidence for older cores, although some grains may have thin rims (Fig 5-2). U-Pb analyses show ages ranging from 2690 ± 6 Ma to 2995 ±14 Ma with two major peaks at ages around 2710 Ma and 2745 Ma (Figs. 5-3 and Fig. 5-4). Applying the maximum likelihood algorithm for detrital ages in IsoplotR gives a minimum age estimate of 2691 ± 8 Ma (Fig. 5-5), although this could have been updated by metamorphism. Analytical profiles for some analyses show low (<0.1) values of Th/U while others are variable. Care was taken to average results within a single phase within a profile. There is a general positive correlation between Th/U and U signals, which is unexpected, since low (metamorphic) Th/U zircon phases are usually seen to have high U. The low Th/U zircon phases are not the youngest but are spread throughout the age range. The diversity of ages suggests a detrital source for much of the zircon, which may include grains from older episodes of metamorphism.

Analyses on monazite again show the presence of high-U, low-Th/U and relatively low-U, high Th/U phases, which in some cases are present in the same grain. $^{207}Pb/^{206}Pb$ ages for each phase were determined separately by using appropriate windows. Unfortunately, this is less easily done for $^{206}Pb/^{238}U$ ages, which are only approximate. There are only four analyses from each phase. Ages scatter outside of error for both groups with mean values of 2693 ± 4 Ma (MSWD – 3.0) for the high-U phase and a scatter around 2650 Ma for the low-U phase (Fig. 5-6). The low-U phase ranges from about 2720-2690 Ma while the high-U phase ranges from about 2670-2600 Ma. As with previous samples, this phase is younger and may be magmatic while the other may have formed during prograde metamorphism that led to melting. The scatter of ages suggests that these episodes lasted for tens of Ma.

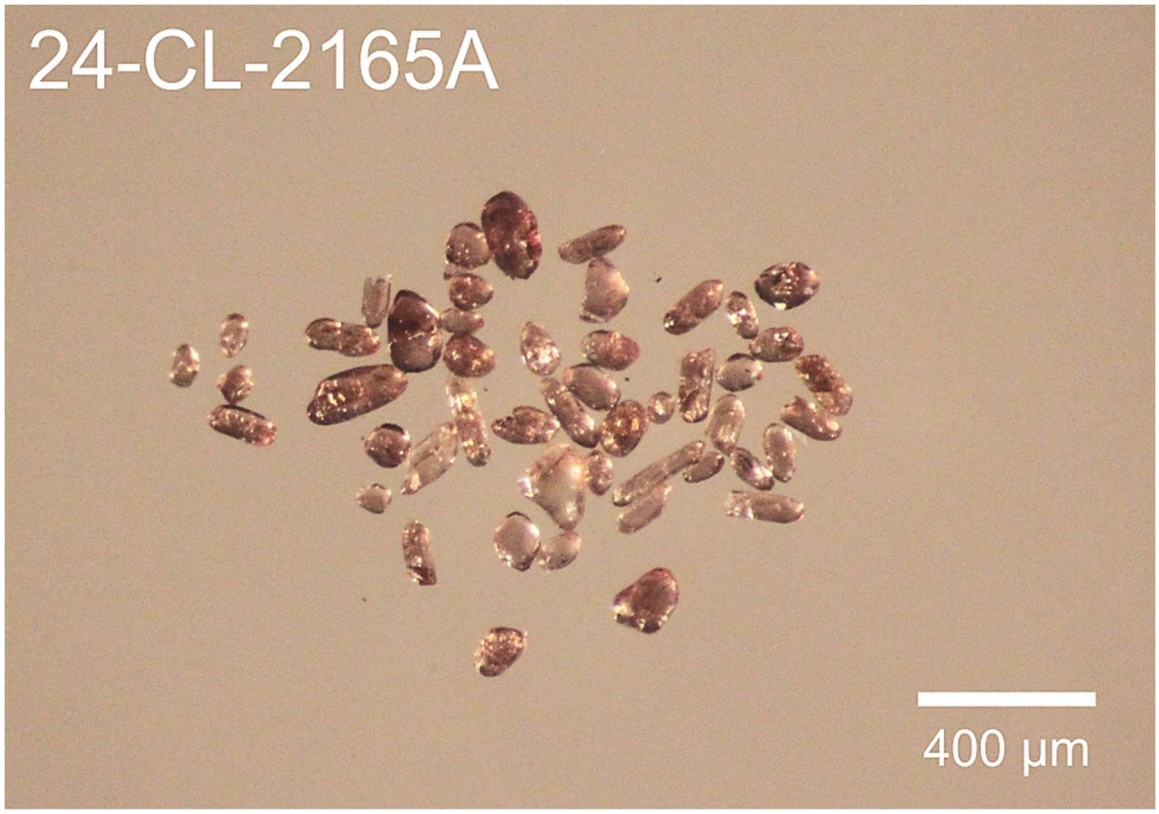

Figure 5-1. Picked zircon from paragneiss sample 24-CL-2165A.

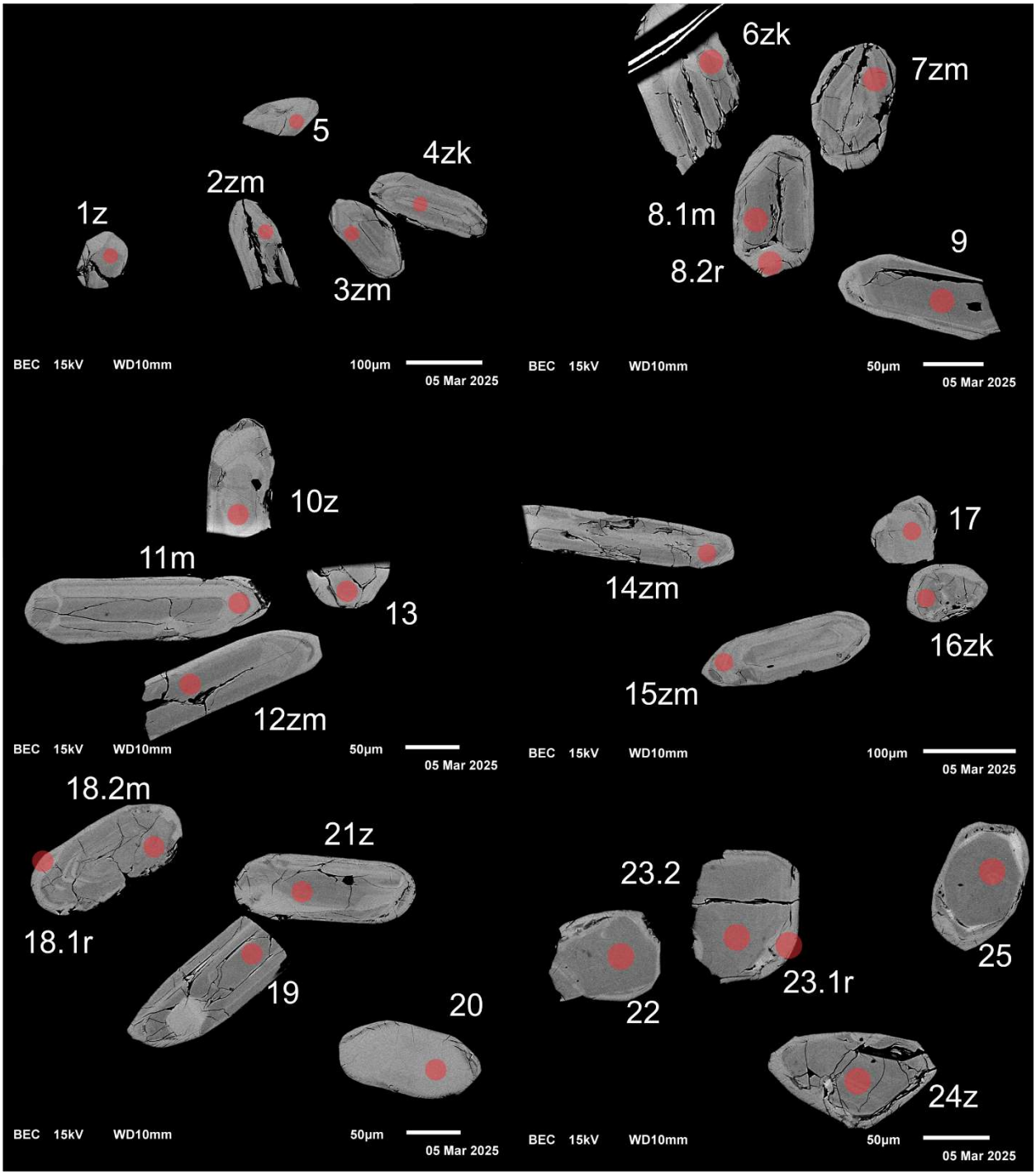

Figure 5-2-1. BSE images of selected grains from sample 24-CL-2165A. The red circles represent the approximate locations of laser ablation spots.

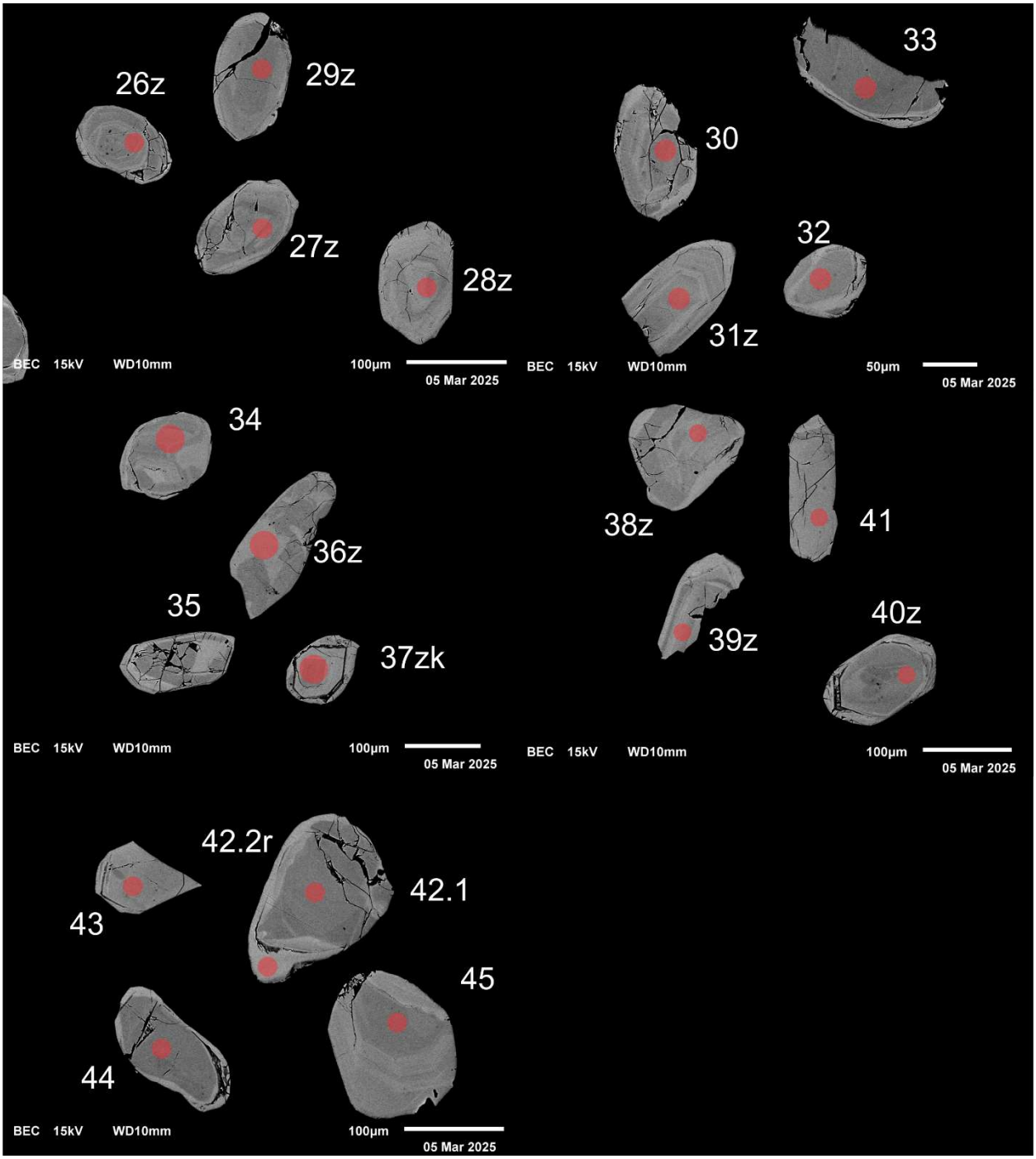

Figure 5-2-2. BSE images of selected grains from sample 24-CL-2165A. The red circles represent the approximate locations of laser ablation spots.

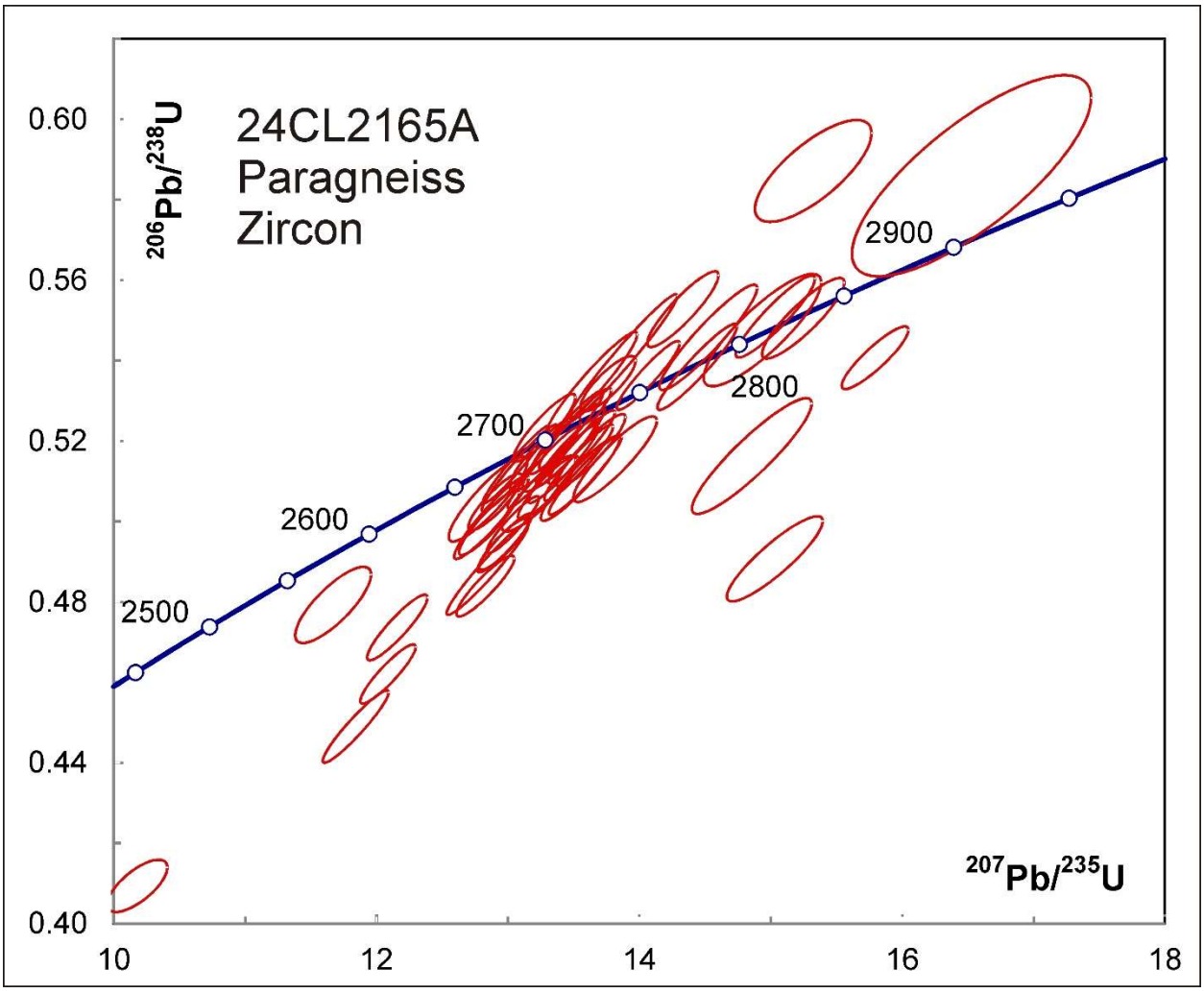

Figure 5-3. Concordia plot showing U-Pb isotopic data on zircon from sample 24-CL-2165A.

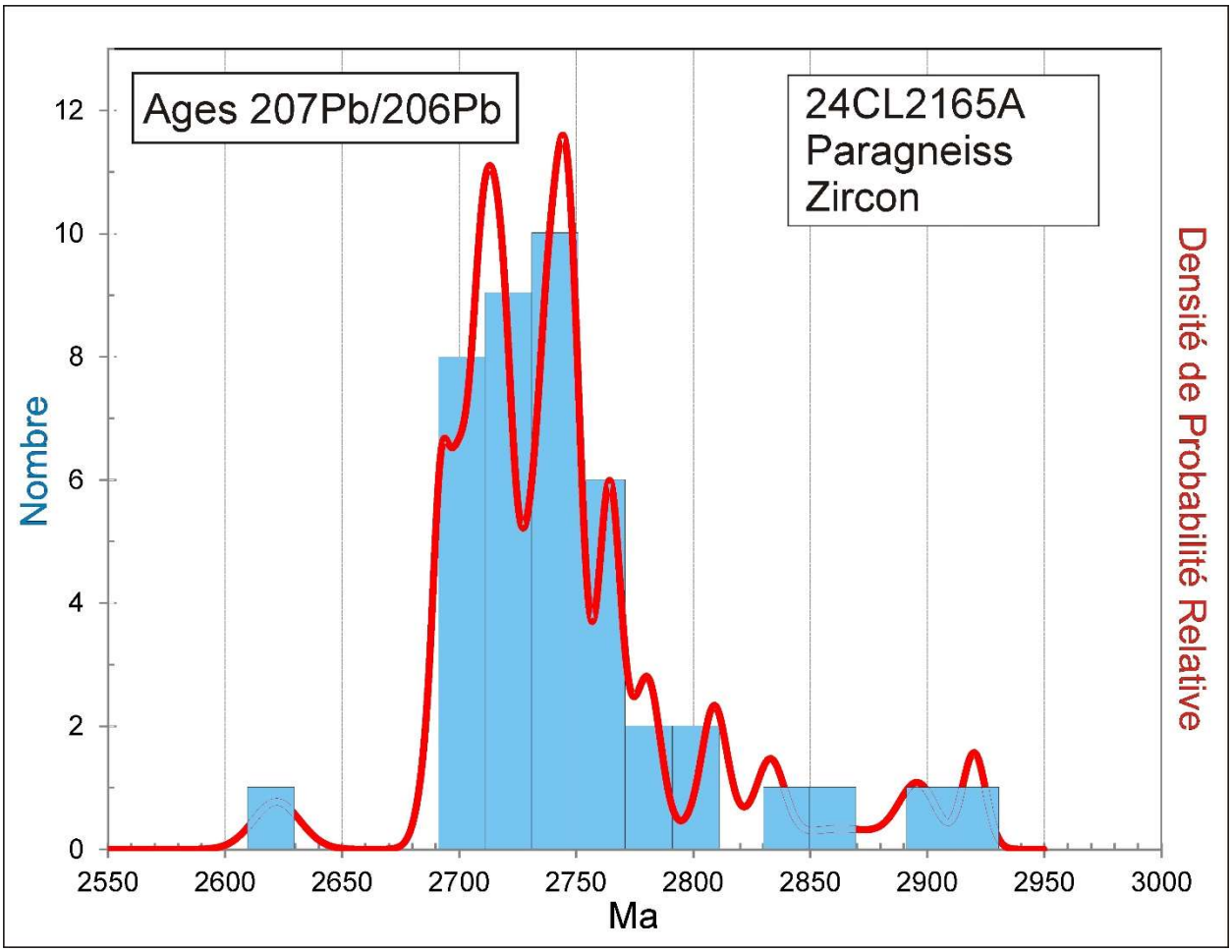

Figure 5-4. Combined probability density plot and histogram showing the distribution of $^{207}Pb/^{206}Pb$ ages on polished zircon from paragneiss sample 24-CL-2165A.

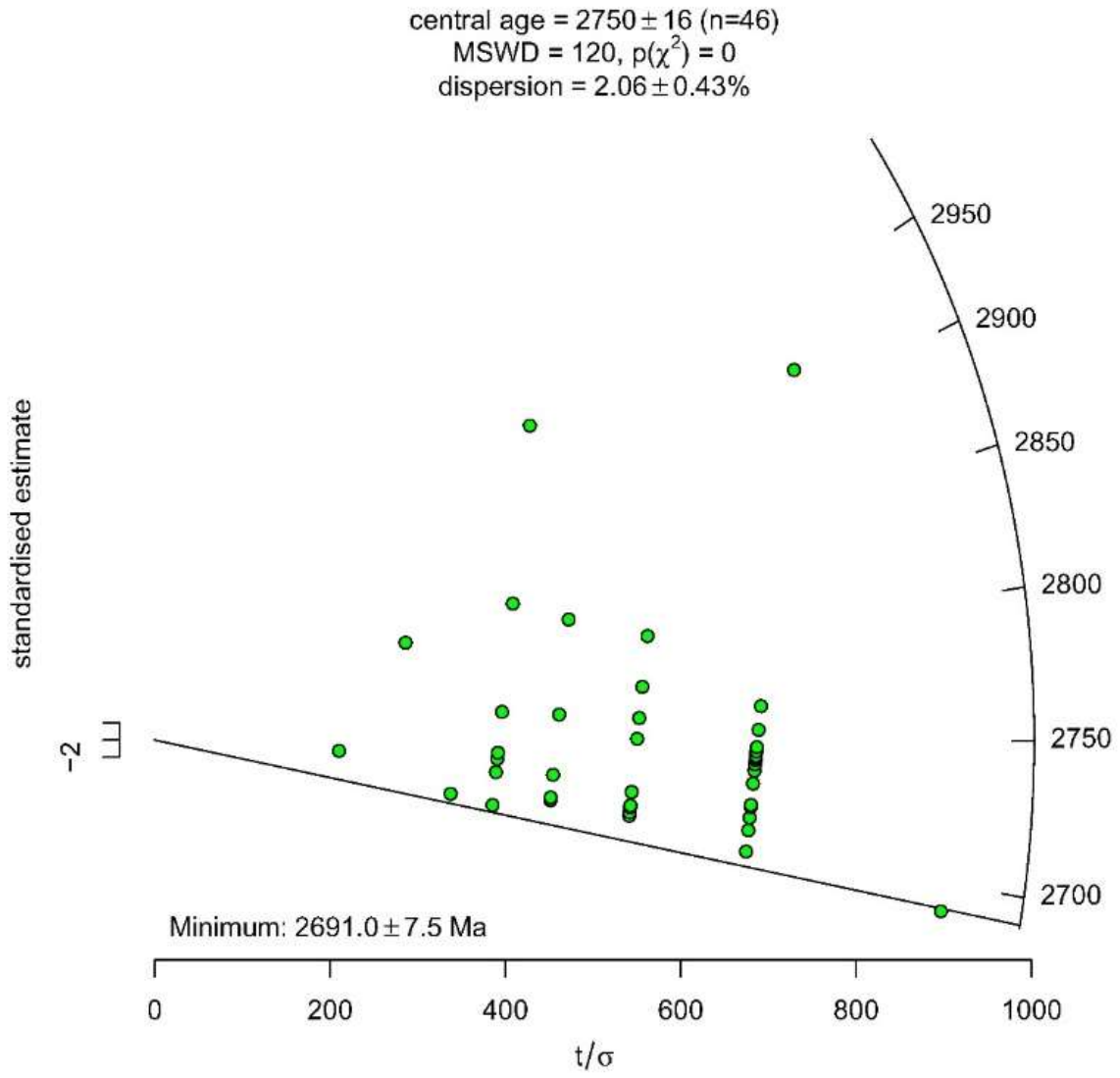

Figure 5-5. Radial plot showing the distribution of $^{207}Pb/^{206}Pb$ zircon ages from paragneiss sample 24-CL-2165A as well as the most probable estimate of the youngest age.

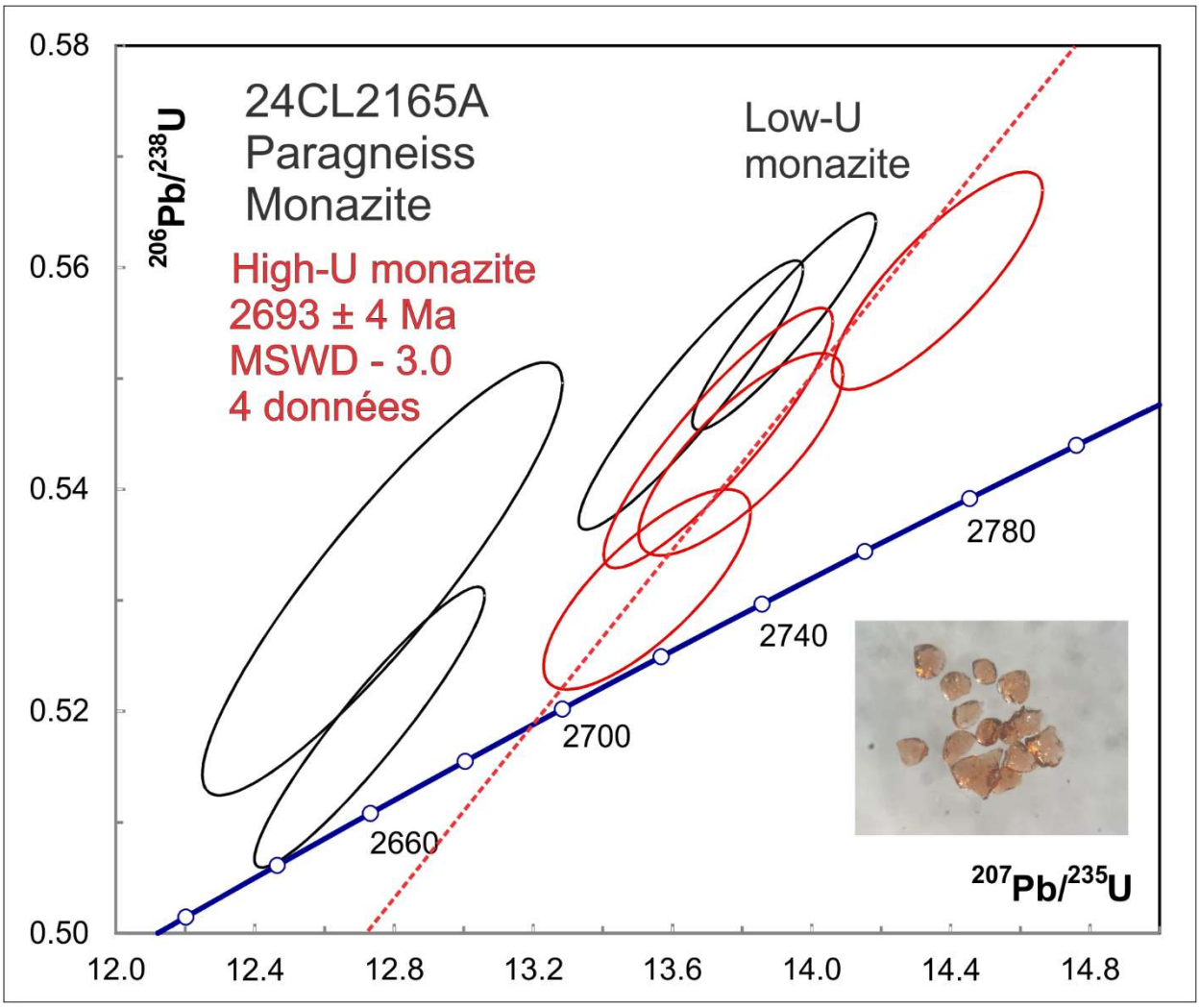

Figure 5-6. Concordia plot showing U-Pb isotopic data on monazite from sample 24-CL-2165A.

6. 24-WM-1140A
Monzonite, Suite de Féron (nAfer2)

This sample yielded a large amount of zircon with stubby to short-prismatic shapes (Fig. 6-1). BSE images show broad zoning, with alteration zones, inclusions and with no evidence for older cores (Fig 6-2). U-Pb analyses all show Th/U > 0.1 (magmatic) but ages scatter outside of error (Fig. 6-3) with 3 possible modes in the distribution (Fig. 6-4). Omitting the 3 youngest data, which are discordant and show significant Sr, as well as the 3 oldest, which may be inherited, the main peak of the distribution gives an age of 2700 ± 2 Ma. This is the best age estimate for magmatic emplacement. A small 2715 Ma component may result from inheritance. A younger peak at 2671 ± 5 Ma (13%) apparently consists of late magmatic zircon phases. Two of these spots were measured on tips of grains that also had spots giving ages in the main older cluster. This might suggest an extended period of crystallization or an episode of late reheating.

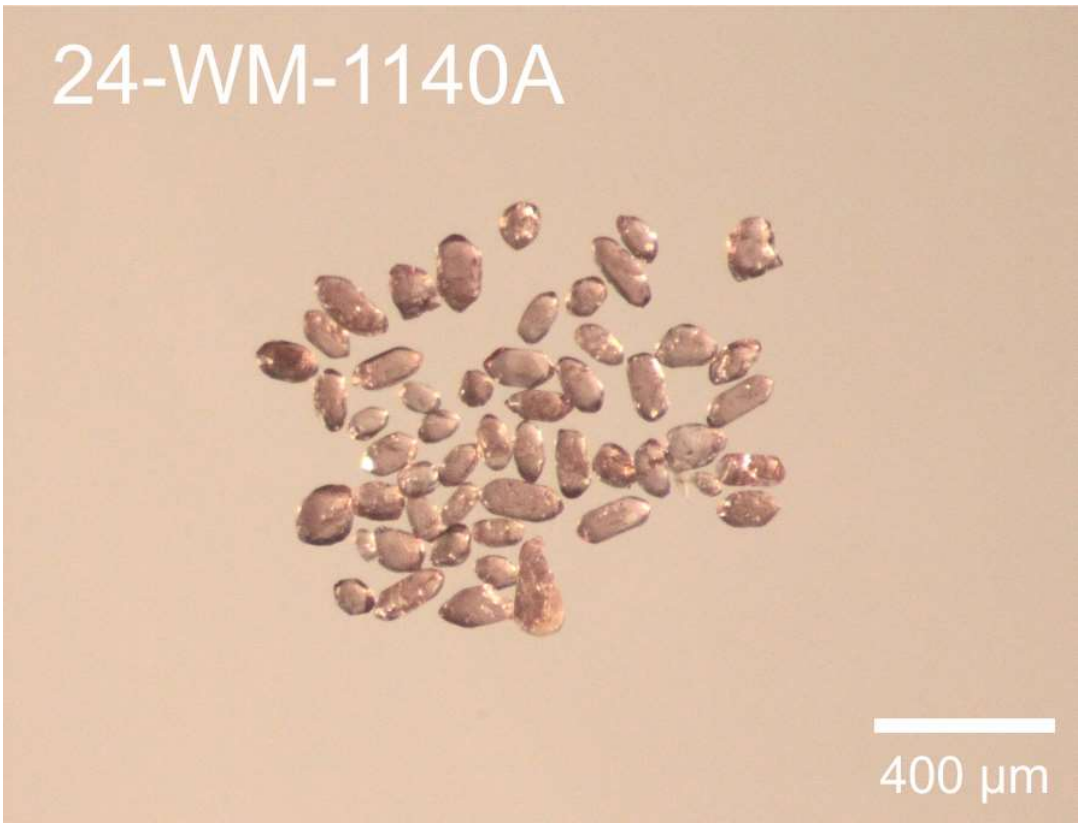

Figure 6-1. Picked zircon from monzonite sample 24-WM-1140A.

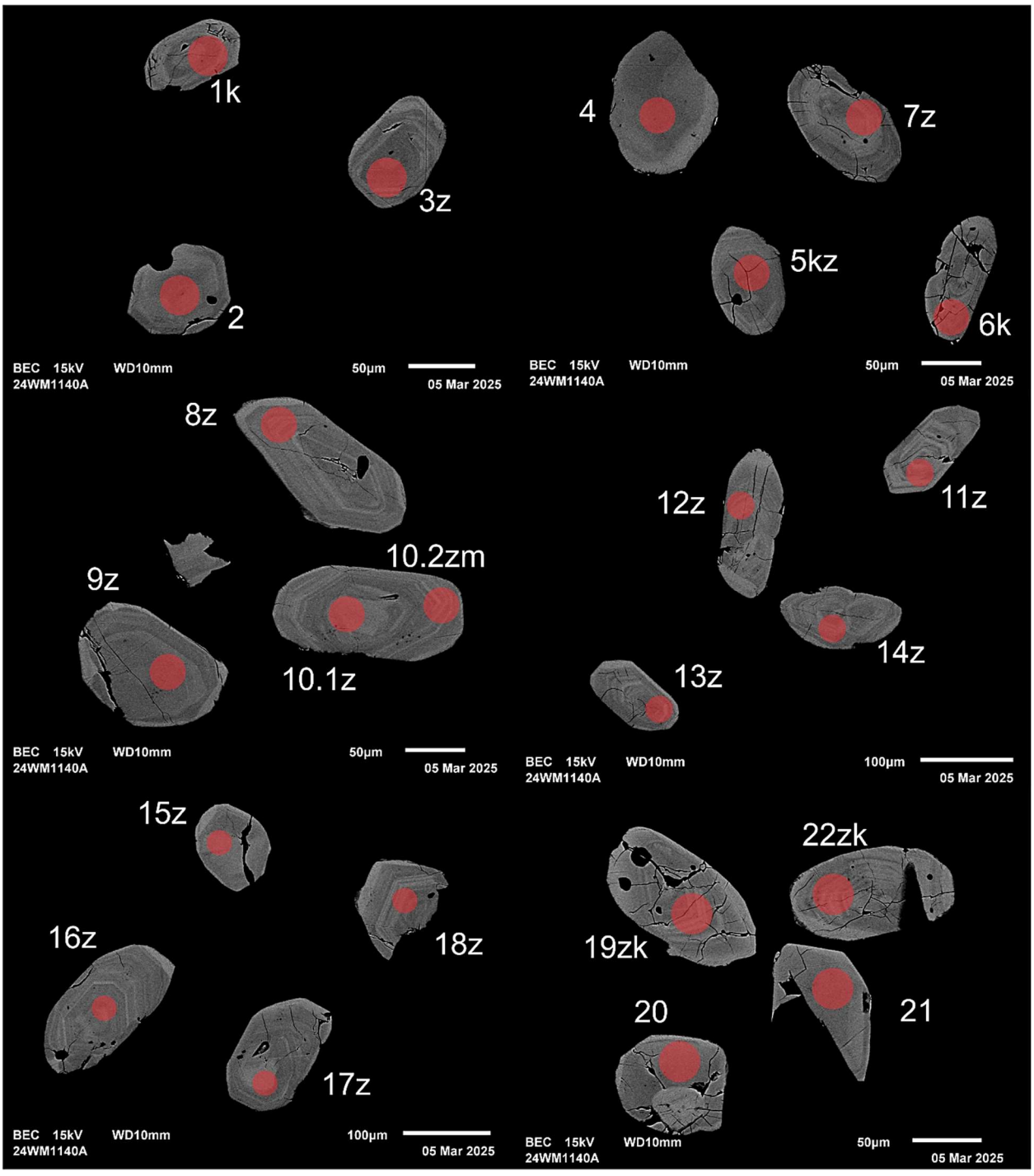

Figure 6-2-1. BSE images of selected grains from sample 24-WM-1140A. The red circles represent the approximate locations of laser ablation spots.

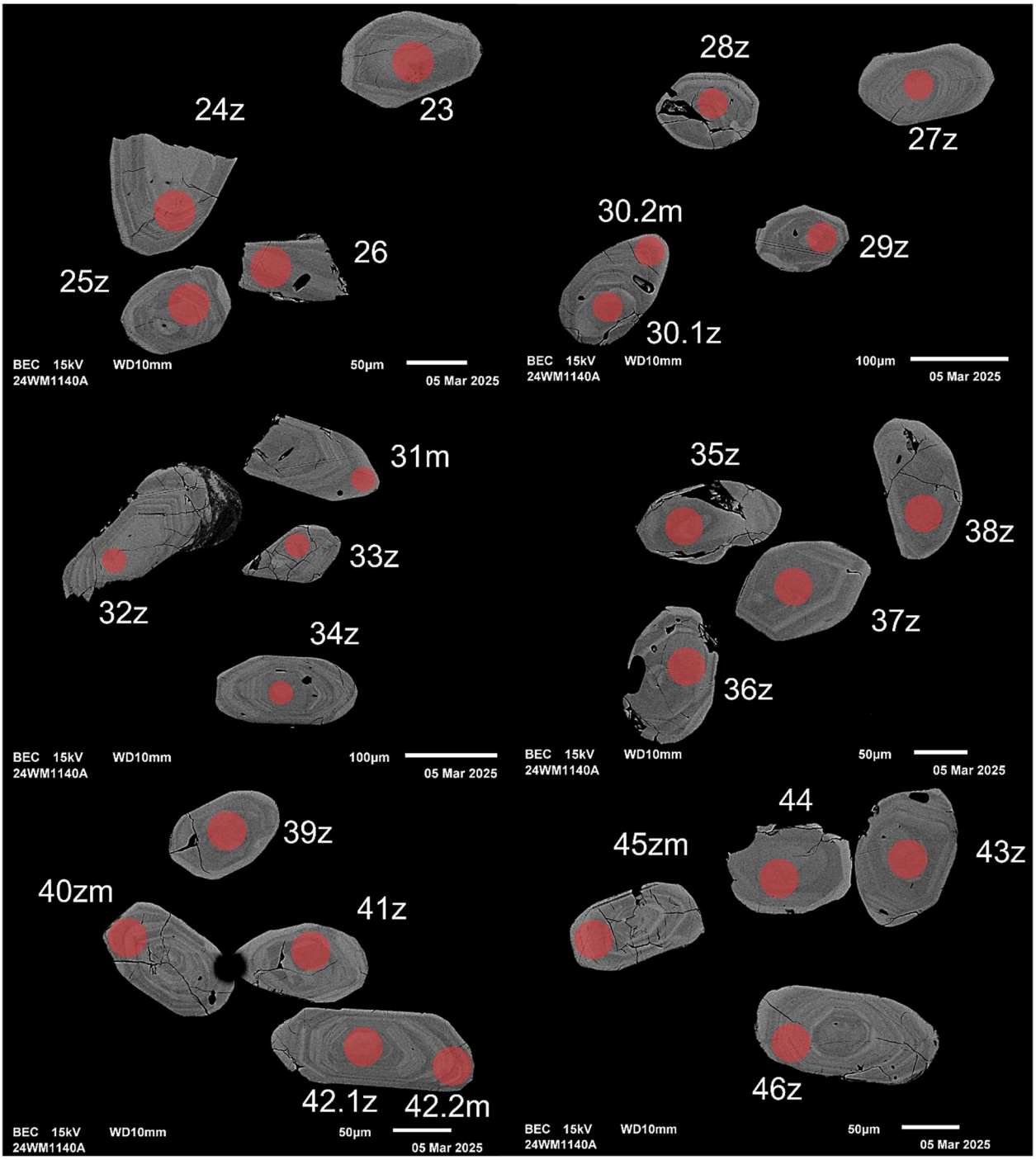

Figure 6-2-2. BSE images of selected grains from sample 24-WM-1140A. The red circles represent the approximate locations of laser ablation spots.

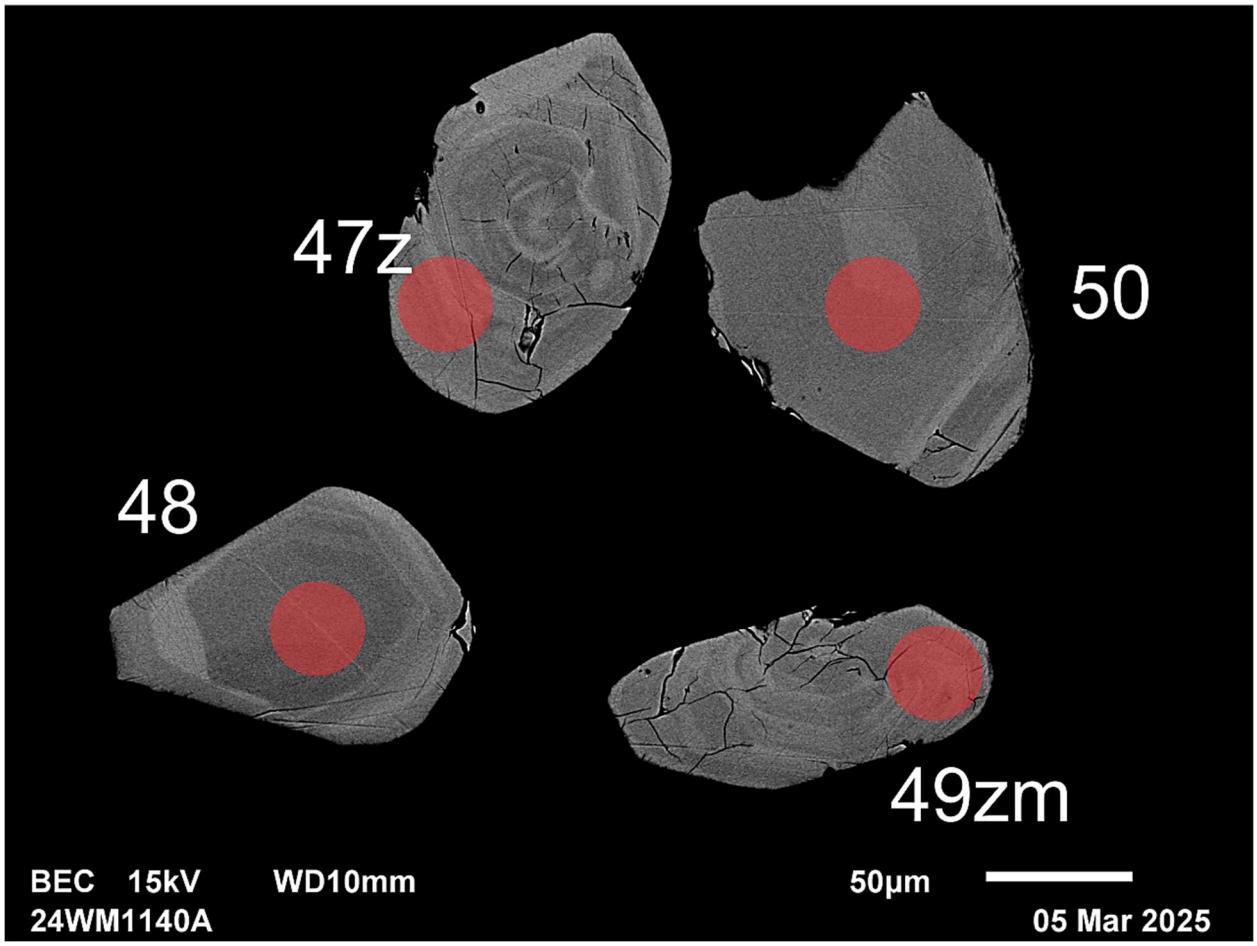

Figure 6-2-3. BSE images of selected grains from sample 24-WM-1140A. The red circles represent the approximate locations of laser ablation spots.

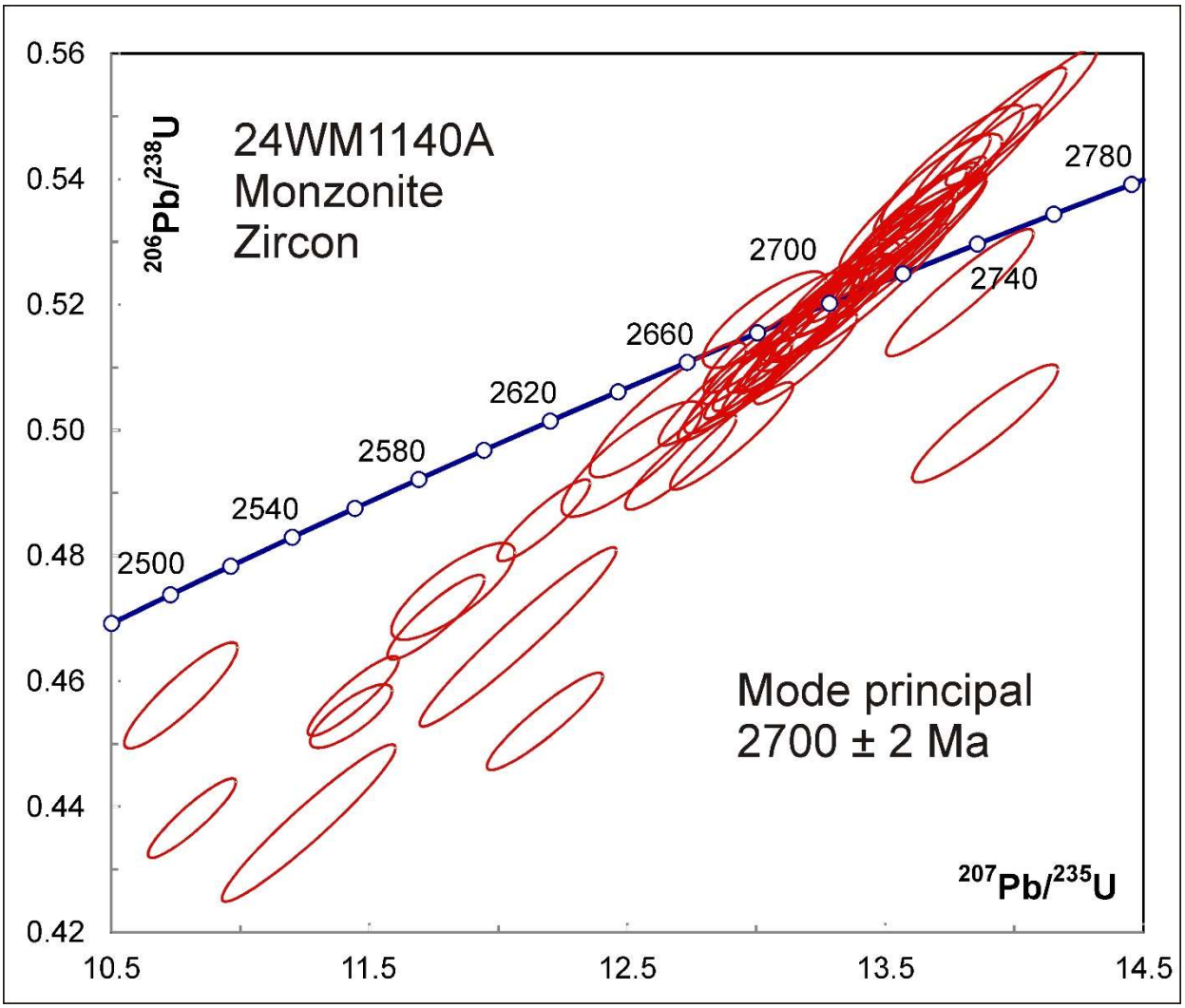

Figure 6-3. Concordia plot showing U-Pb isotopic data on zircon from sample 24-WM-1140A.

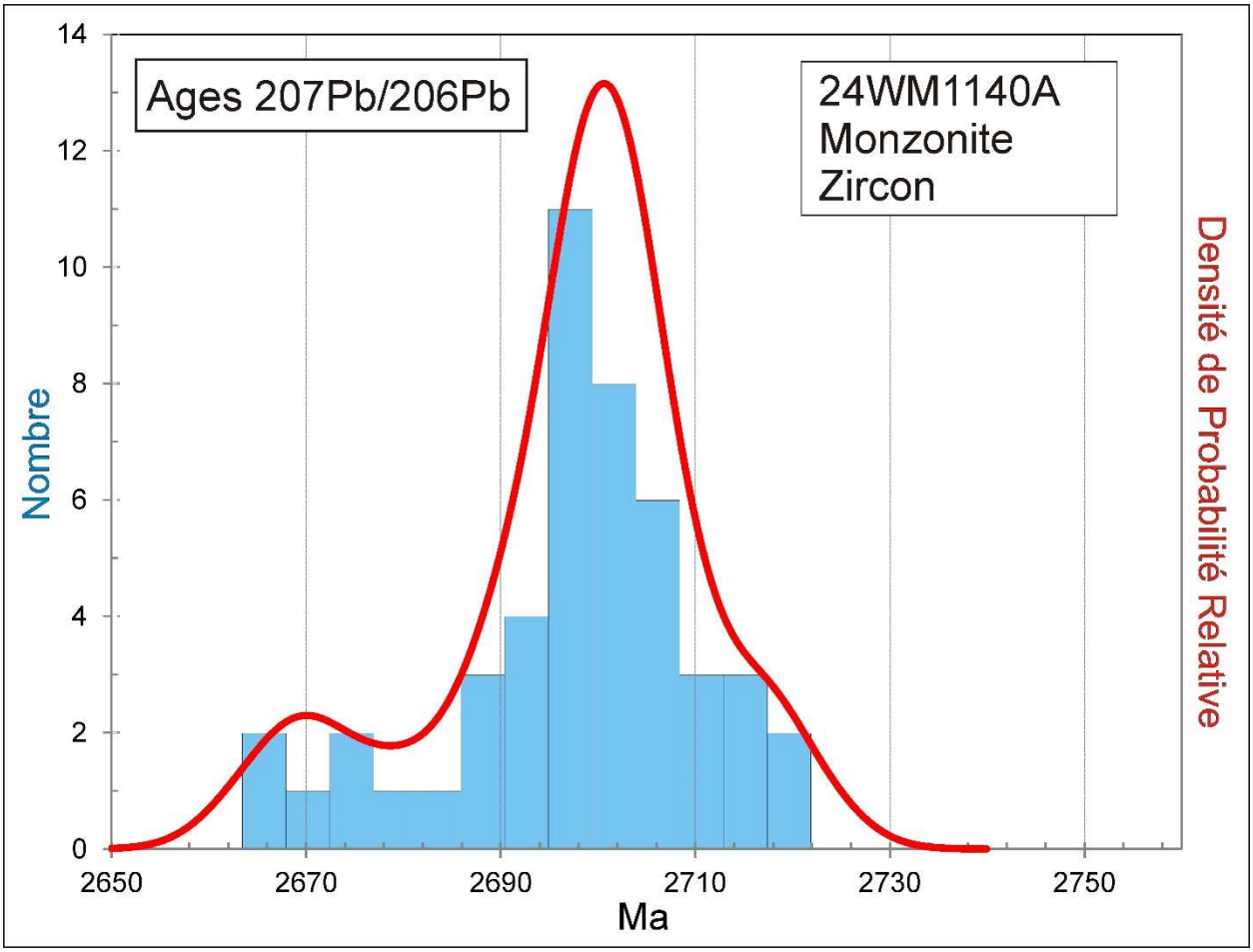

Figure 6-4. Combined probability density plot and histogram showing the distribution of $^{207}Pb/^{206}Pb$ ages on polished zircon from sample 24-WM-1140A.

7. 24-WM-1161A
Tuf dacitique, Formation de Caulincourt (nAclc2)

This sample yielded abundant zircon as tiny rounded grains (Fig. 7-1). Due to their size, the grains were mounted on double-sided tape and analyzed on natural surfaces. U-Pb analyses show ages ranging from 2651 Ma to 2687 Ma but most define an age of 2668 ± 3 Ma (MSWD – 3.4) (Fig. 7-2 and Fig. 7-3). All grains show Th/U ratios < 0.1, strongly suggesting that they are of metamorphic origin. 'Dacite' usually indicates a volcanic rock of intermediate composition. Metamorphic zircon can form by release of Zr from ilmenite (Bingen et al., 2001) and is usually found in mafic rocks. In this case, the rock has sustained metasomatic alteration and is enriched in garnets (in some beds up to 50%) which may have incorporated Zr during high P-T prograde processes. Some zircon growth could have happened during garnet breakdown when cooling. A relative probability density plot of $^{207}Pb/^{206}Pb$ ages (Fig. 7-3) reveals a probable bimodal population which is resolved by the 'Unmix' algorithm of Sambridge and Compston (1994) into a major population of age 2676 ± 2 Ma (62%) and a minor population of age 2658 ± 3 Ma (19%). These ages likely approximate the span of metamorphism.

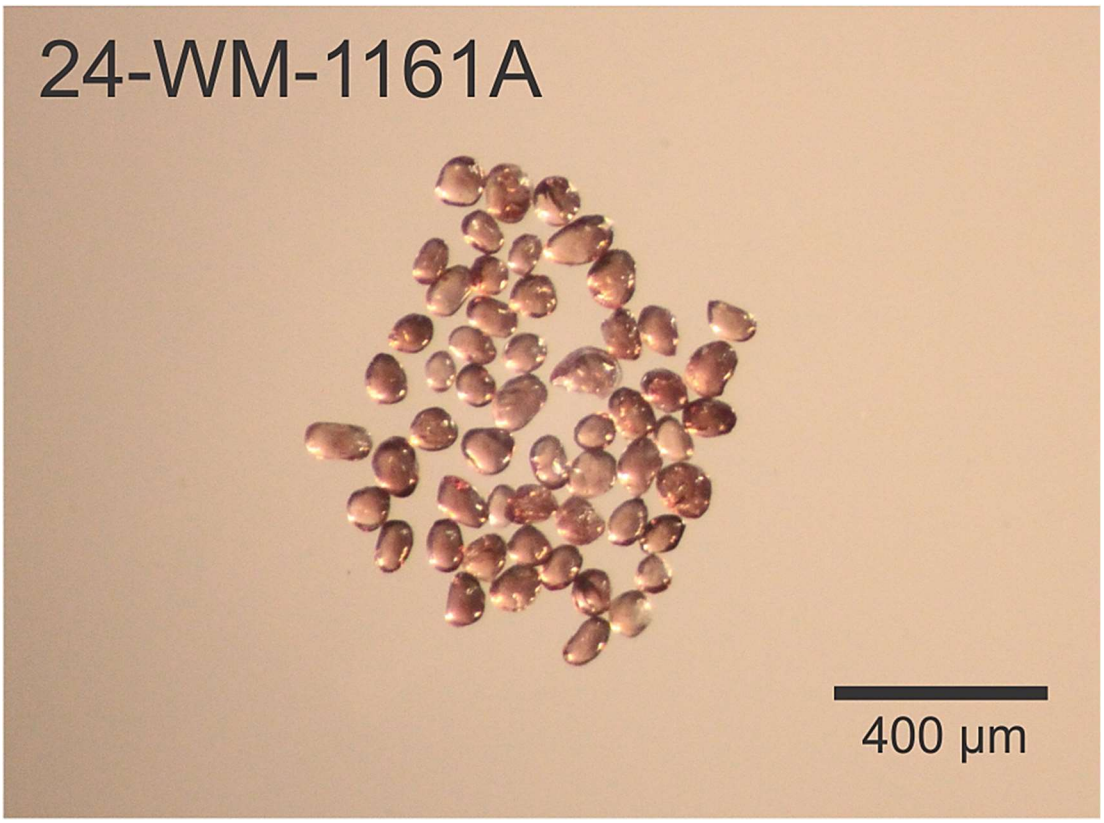

Figure 7-1. Picked zircon from dacite sample 24-WM-1161A.

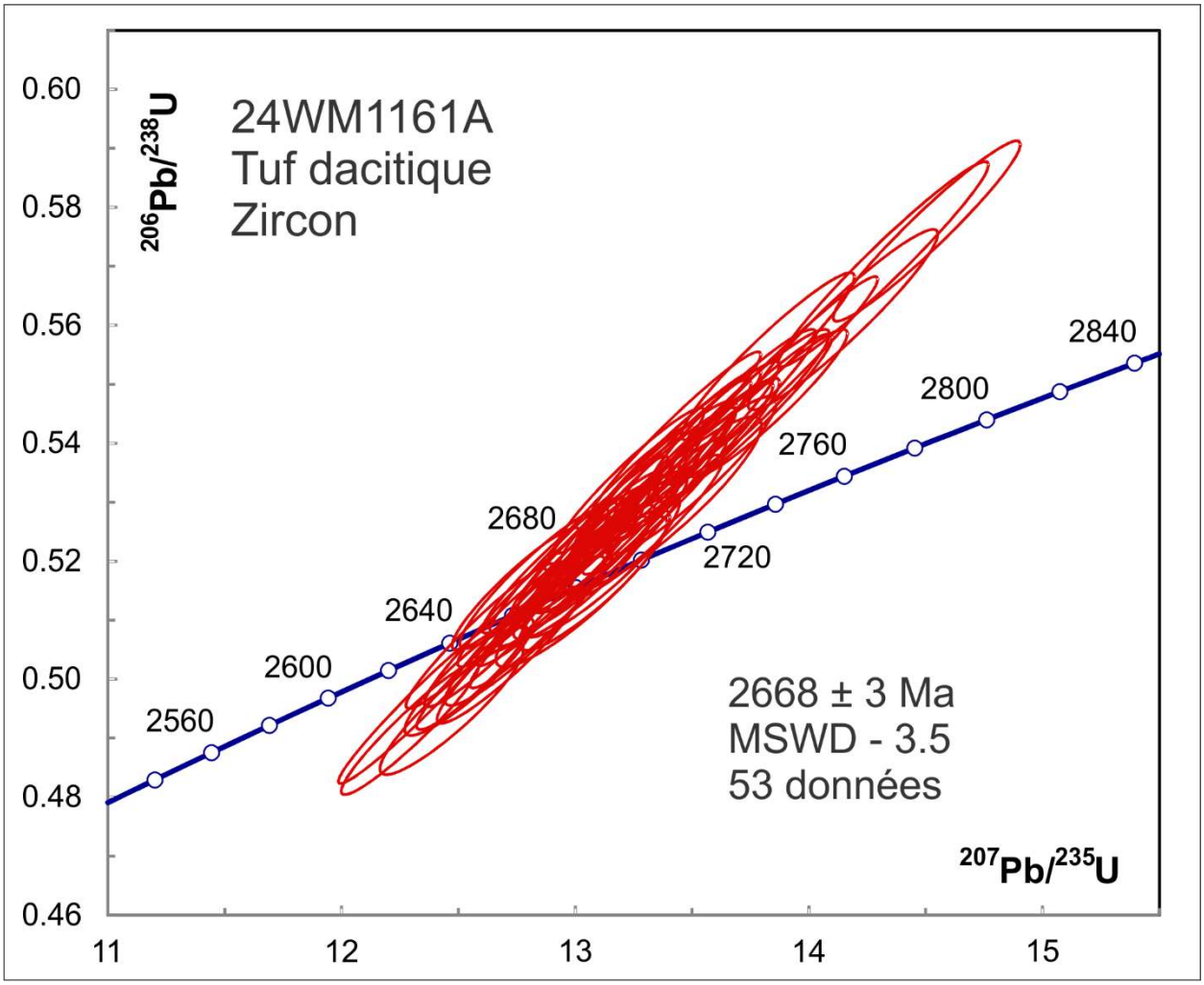

Figure 7-2. Concordia plot showing U-Pb isotopic data on zircon from dacite sample 24-WM-1161A.

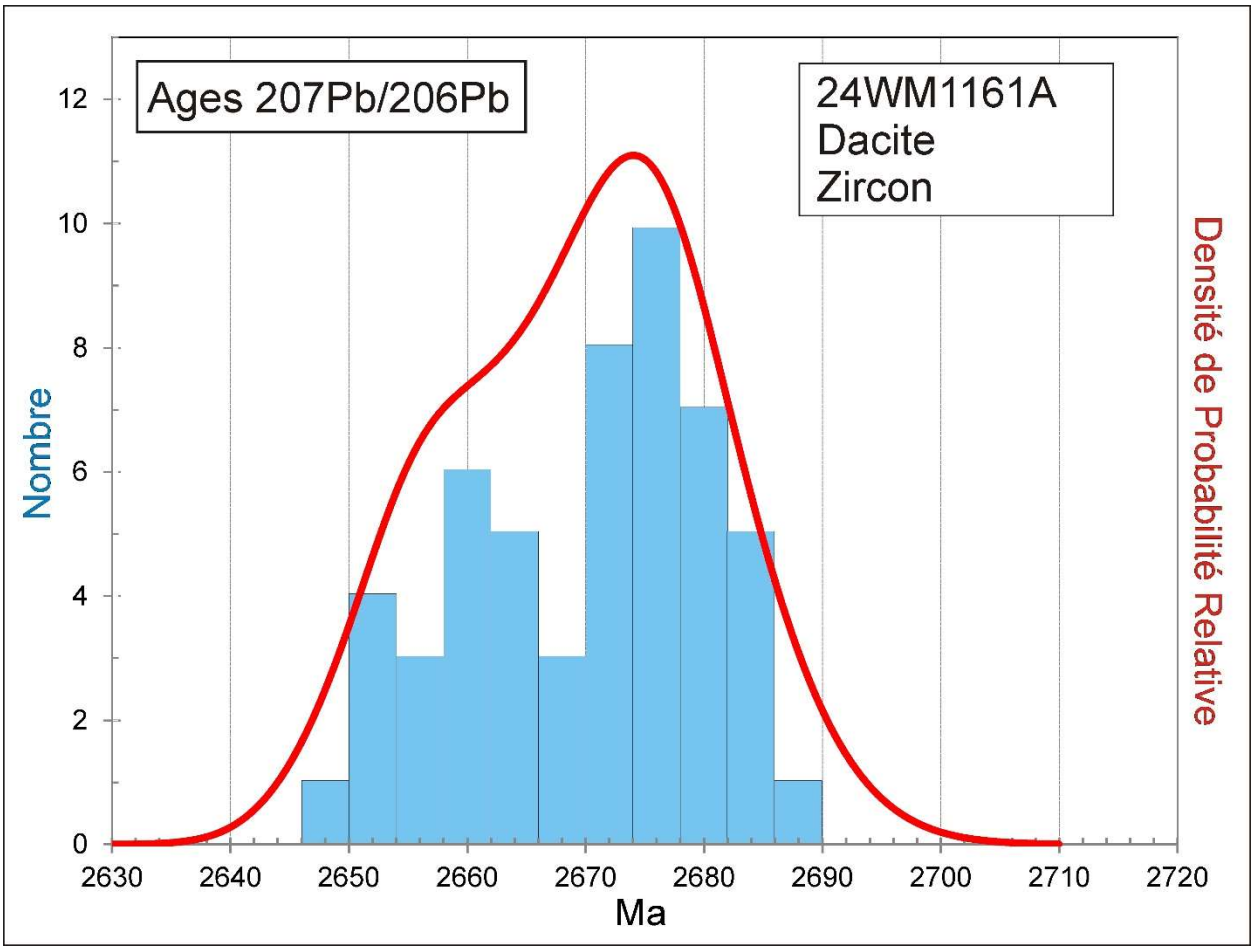

Figure 7-3. Combined probability density plot and histogram showing the distribution of $^{207}Pb/^{206}Pb$ ages on polished zircon from sample 24-WM-1161A.

Lac Chamic

8. 24-DB-1021A1
Conglomérat, Formation de Voirdye (nAvrd1)

This sample yielded a diverse population of zircon grains with variable brownish colouration and euhedral to rounded morphology (Fig. 8-1). BSE images show broad zoning, with alteration zones, inclusions and with no evidence of older cores or rims (Fig 8-2). U-Pb analyses show a multimodal detrital age distribution with the most significant peak around 2830 Ma but others around 2760-2780 Ma (Fig. 8-3 and Fig. 8-4). One 4% discordant analysis gives 3389 ±10 Ma. The two youngest spots from the same grain give a mean age of 2682 Ma although the 95% confidence error is very large because of the poor overlap and limited data set. A slightly older grain gives 2706 ± 8 Ma, which sets a probable older age estimate for deposition at around 2700 Ma.

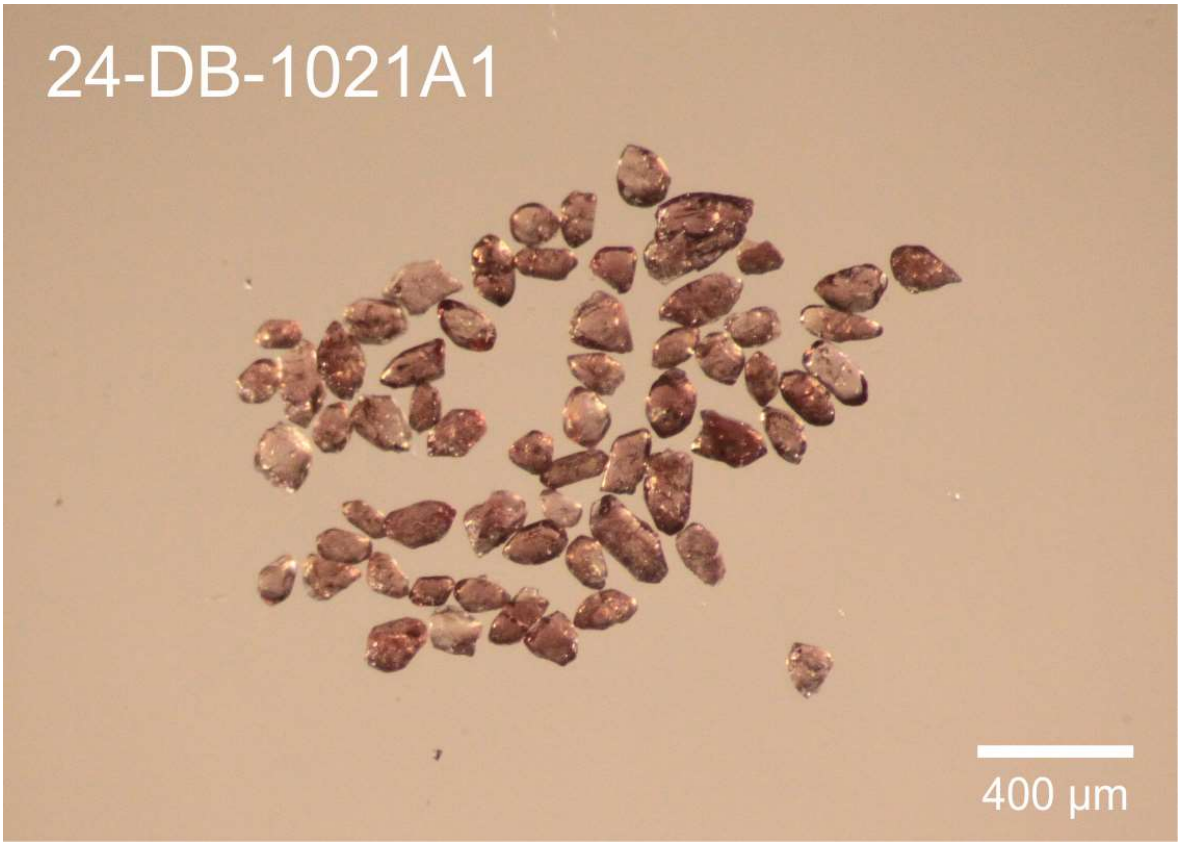

Figure 8-1. Picked zircon from conglomerate sample 24-DB-1021A1.

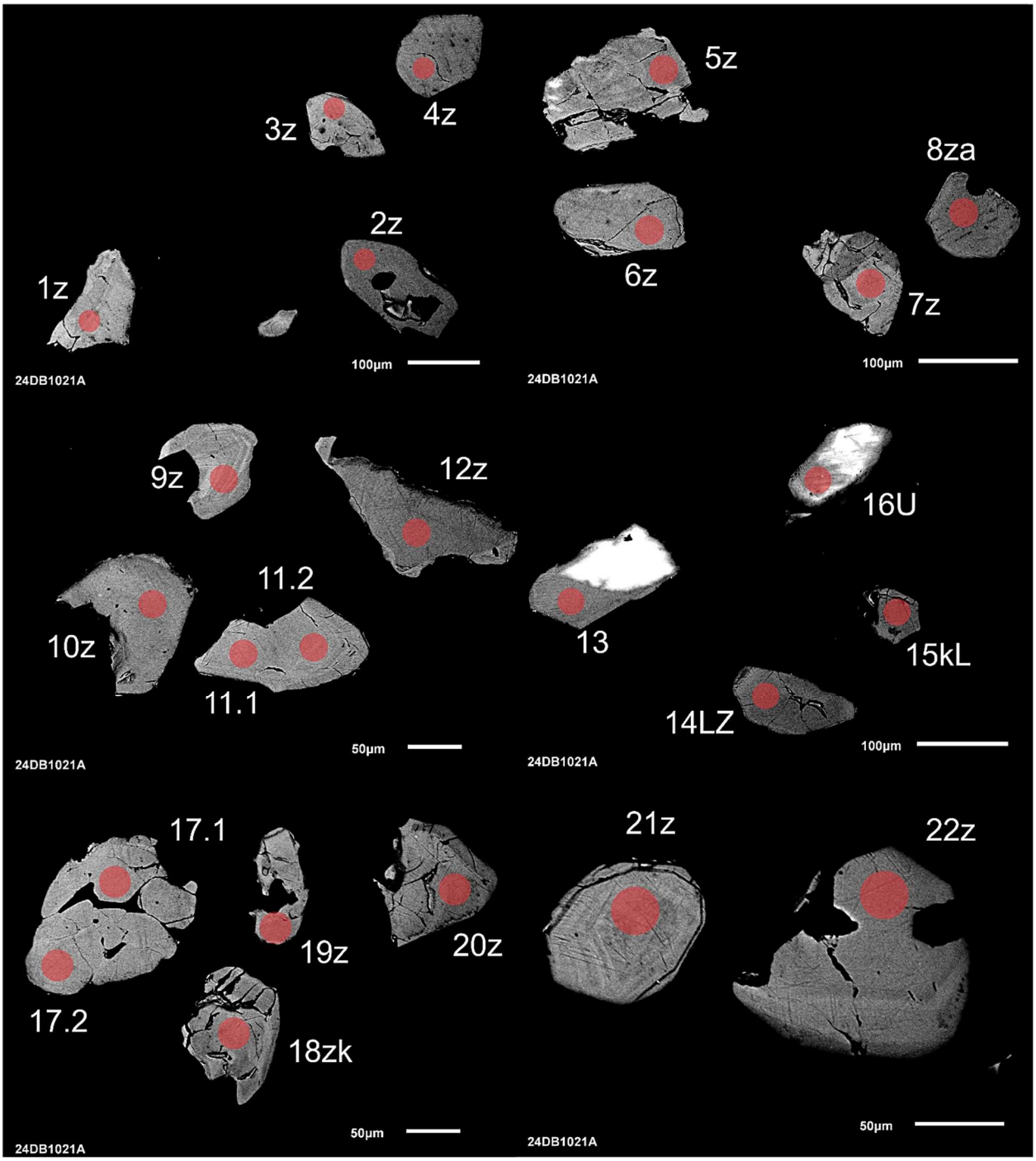

Figure 8-2-1. BSE images of selected grains from sample 24-DB-1021A1. The red circles represent the approximate locations of laser ablation spots.

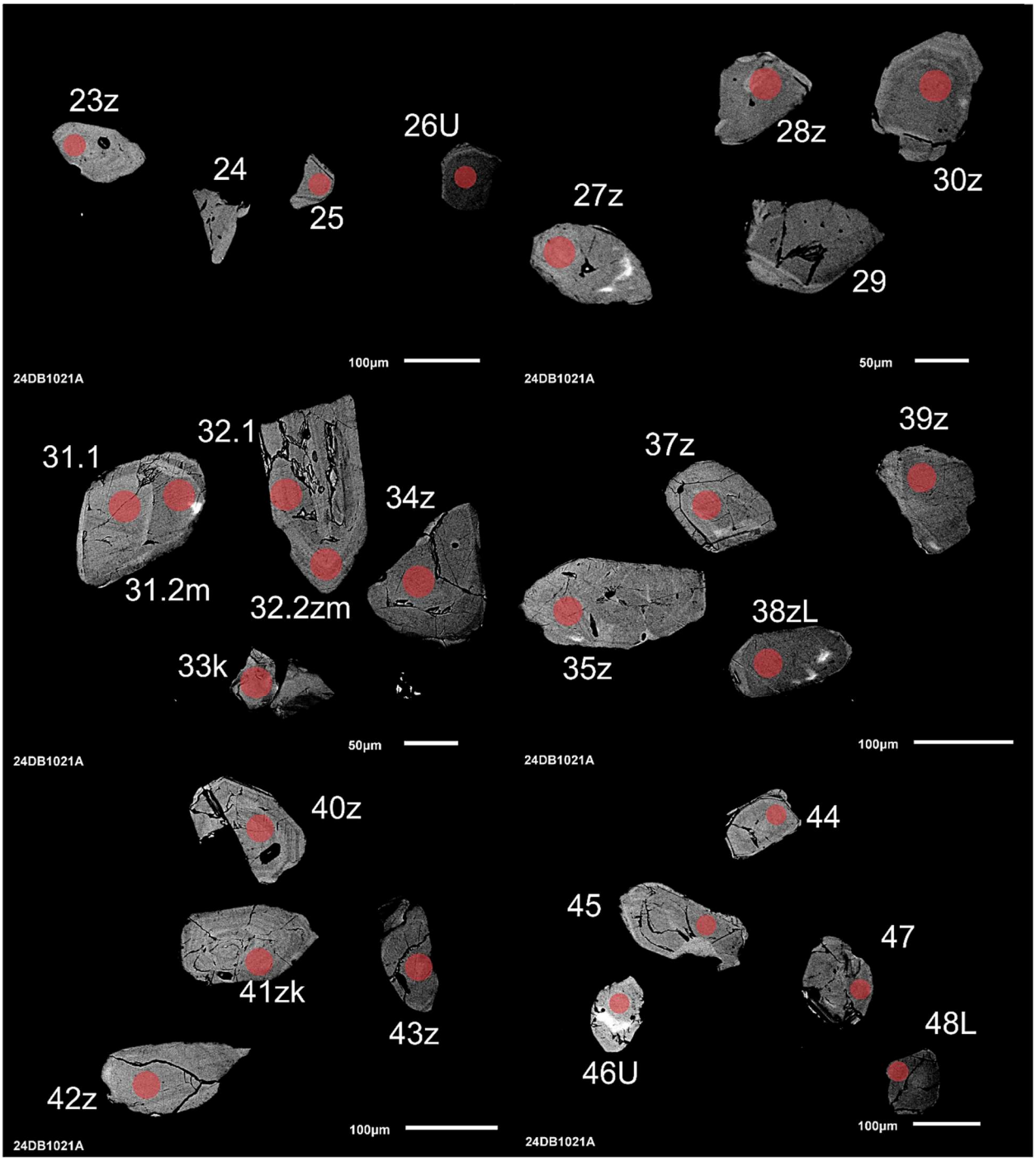

Figure 8-2-2. BSE images of selected grains from sample 24-DB-1021A1. The red circles represent the approximate locations of laser ablation spots.

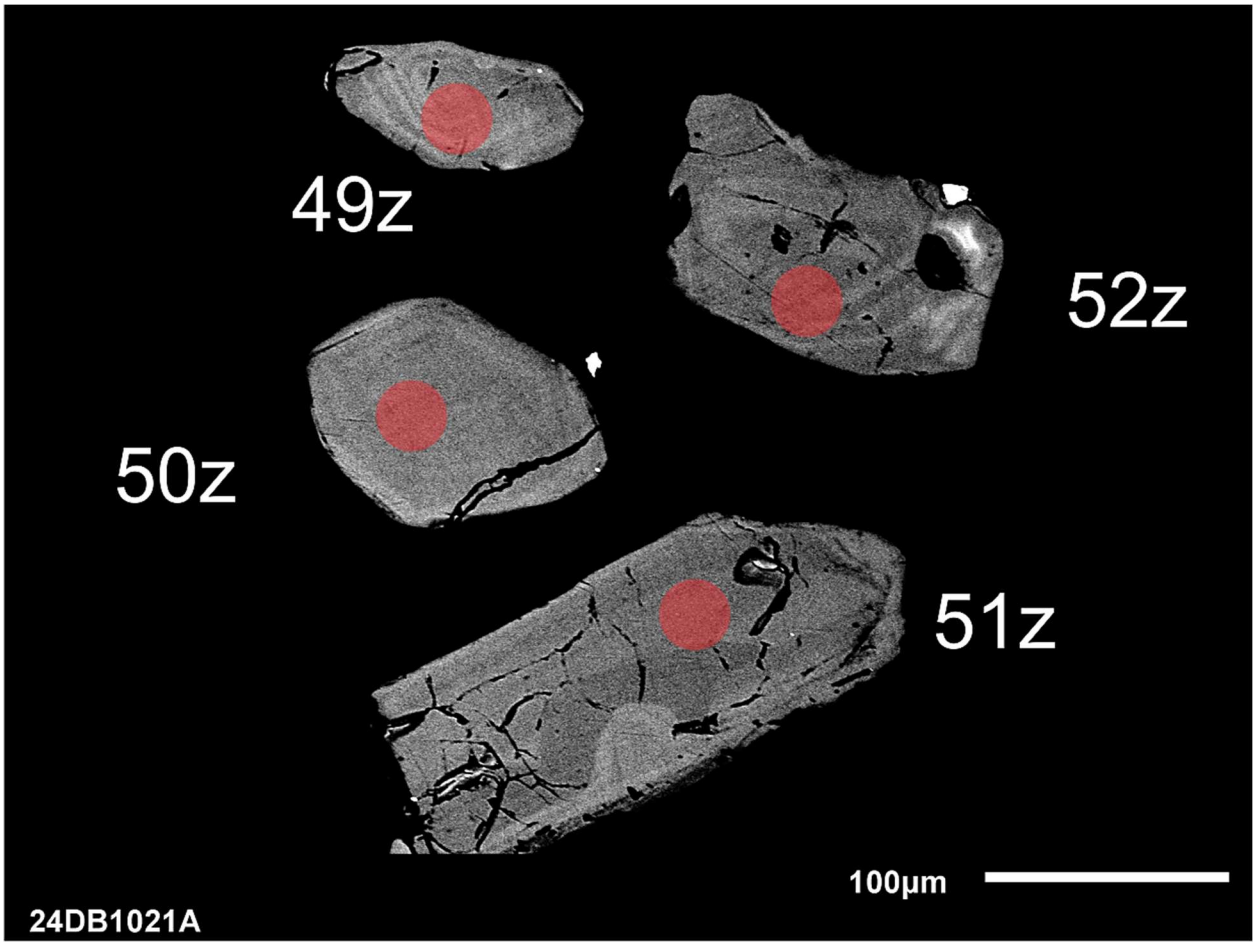

Figure 8-2-3. BSE images of selected grains from sample 24-DB-1021A1. The red circles represent the approximate locations of laser ablation spots.

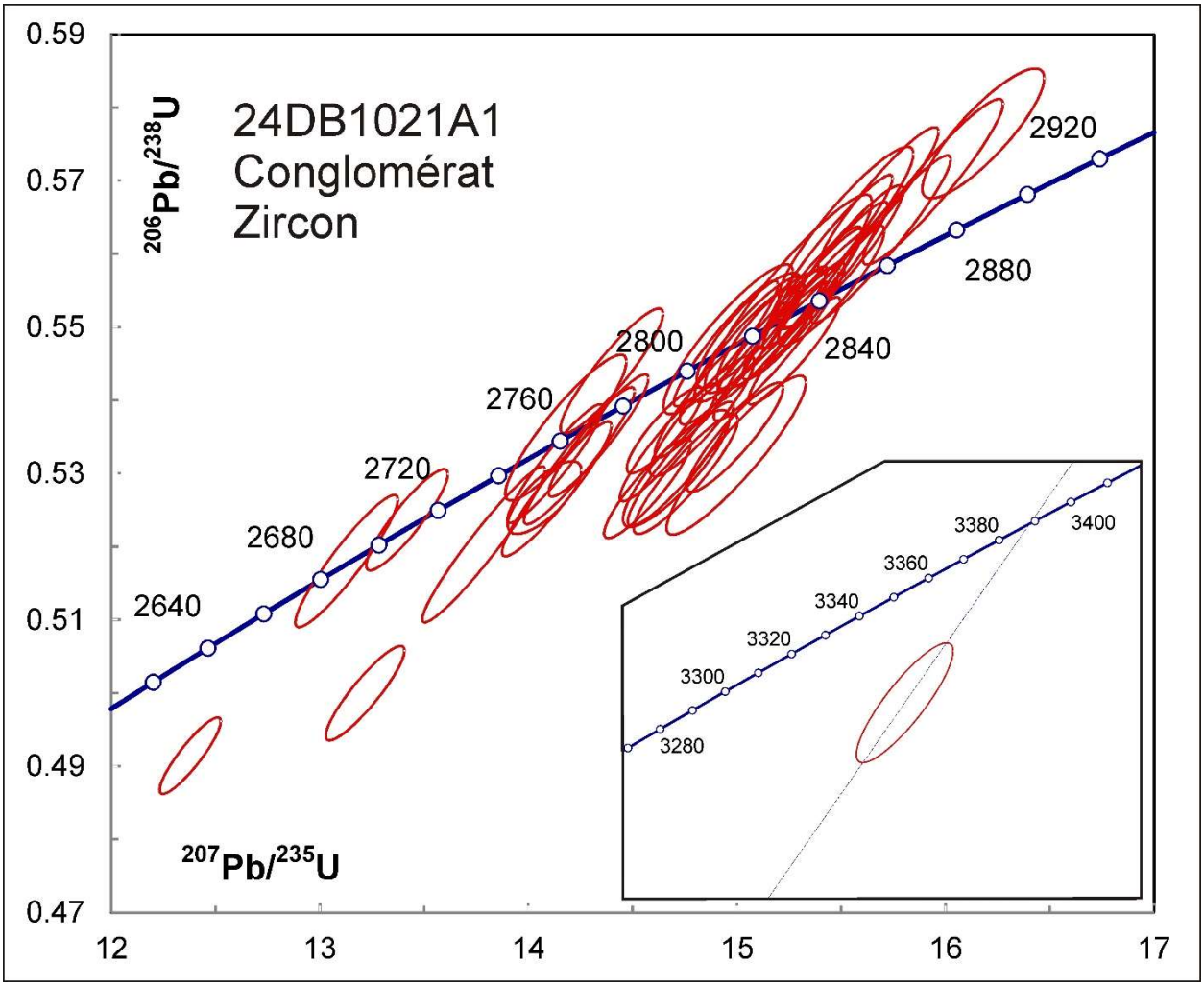

Figure 8-3. Concordia plot showing U-Pb isotopic data on zircon from conglomerate sample 24-DB-1021A1.

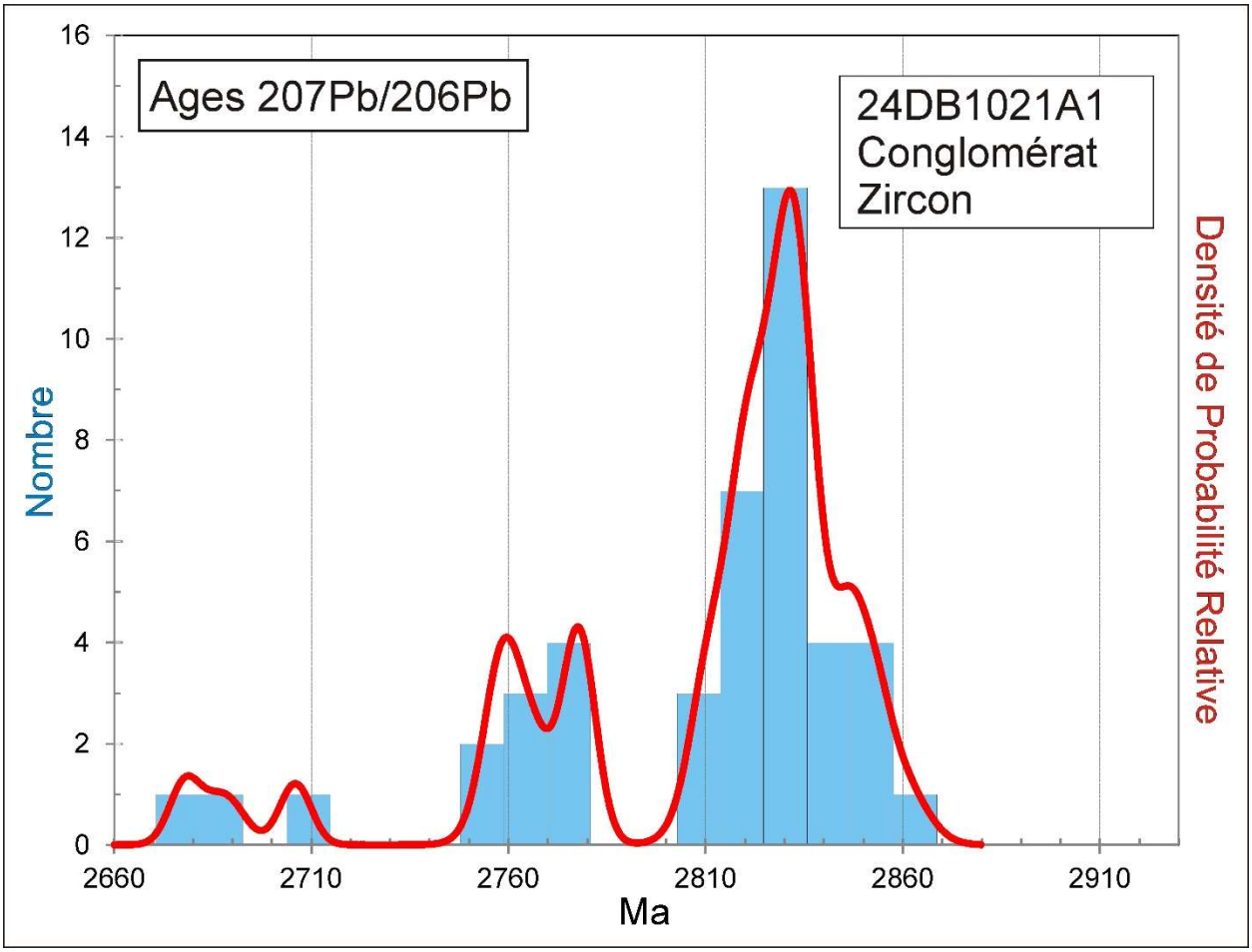

Figure 8-4. Combined probability density plot and histogram showing the distribution of $^{207}Pb/^{206}Pb$ ages on zircon from conglomerate sample 24-DB-1021A1.

9. 24-GS-2197A1
Conglomérat, Formation de Voirdye (nAvrd1)

This sample yielded a small amount of zircon consisting of subhedral grains and fragments (Fig. 9-1). BSE images show a variety of zoning patterns, fractures, and alteration zones (Fig. 9-2). All U-Pb analyses show Th/U > 0.1 and likely represent detrital ages. These range from 2693 ± 12 Ma to 2854 ± 10 Ma with the highest peak around 2760 Ma (Fig. 9-3 and Fig. 9-4).

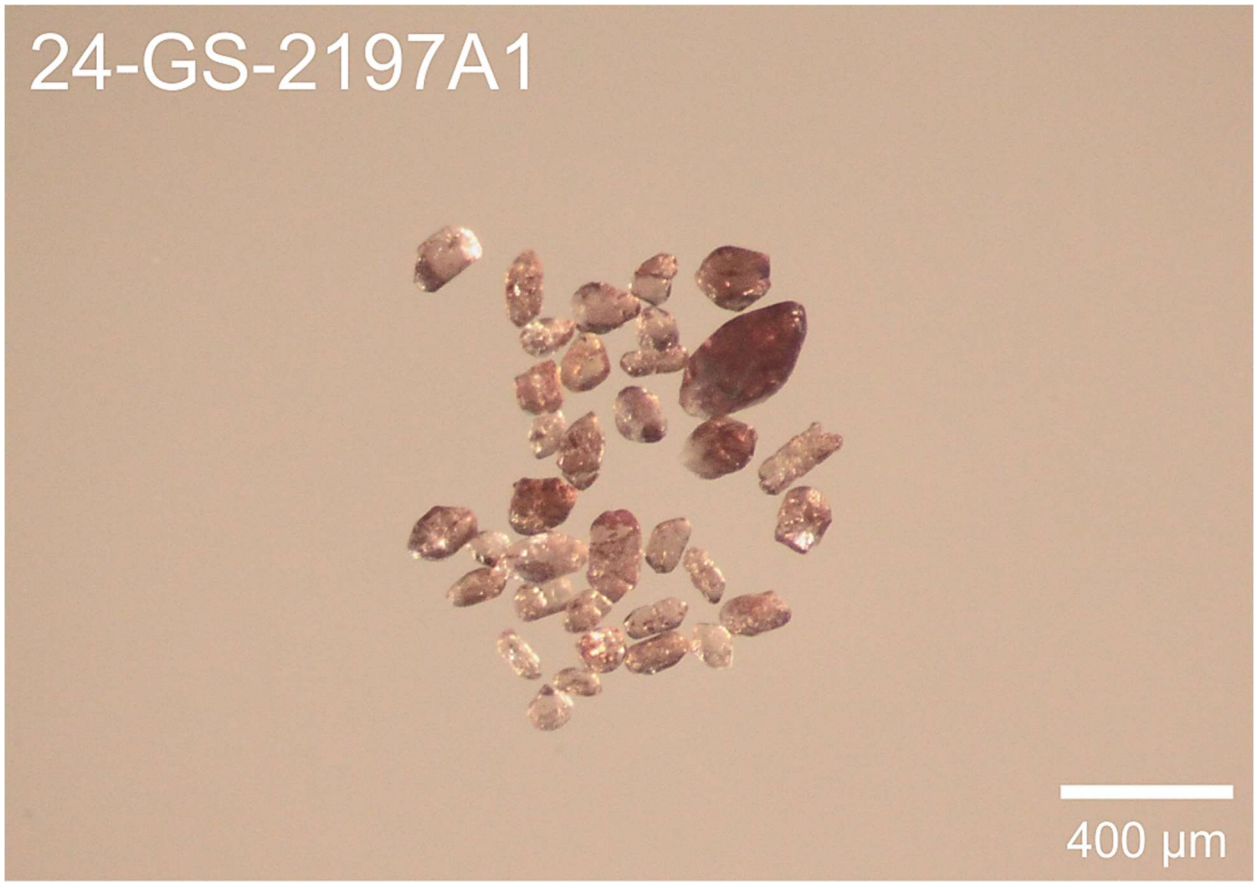

Figure 9-1. Picked zircon from conglomerate sample 24-GS-2197A1.

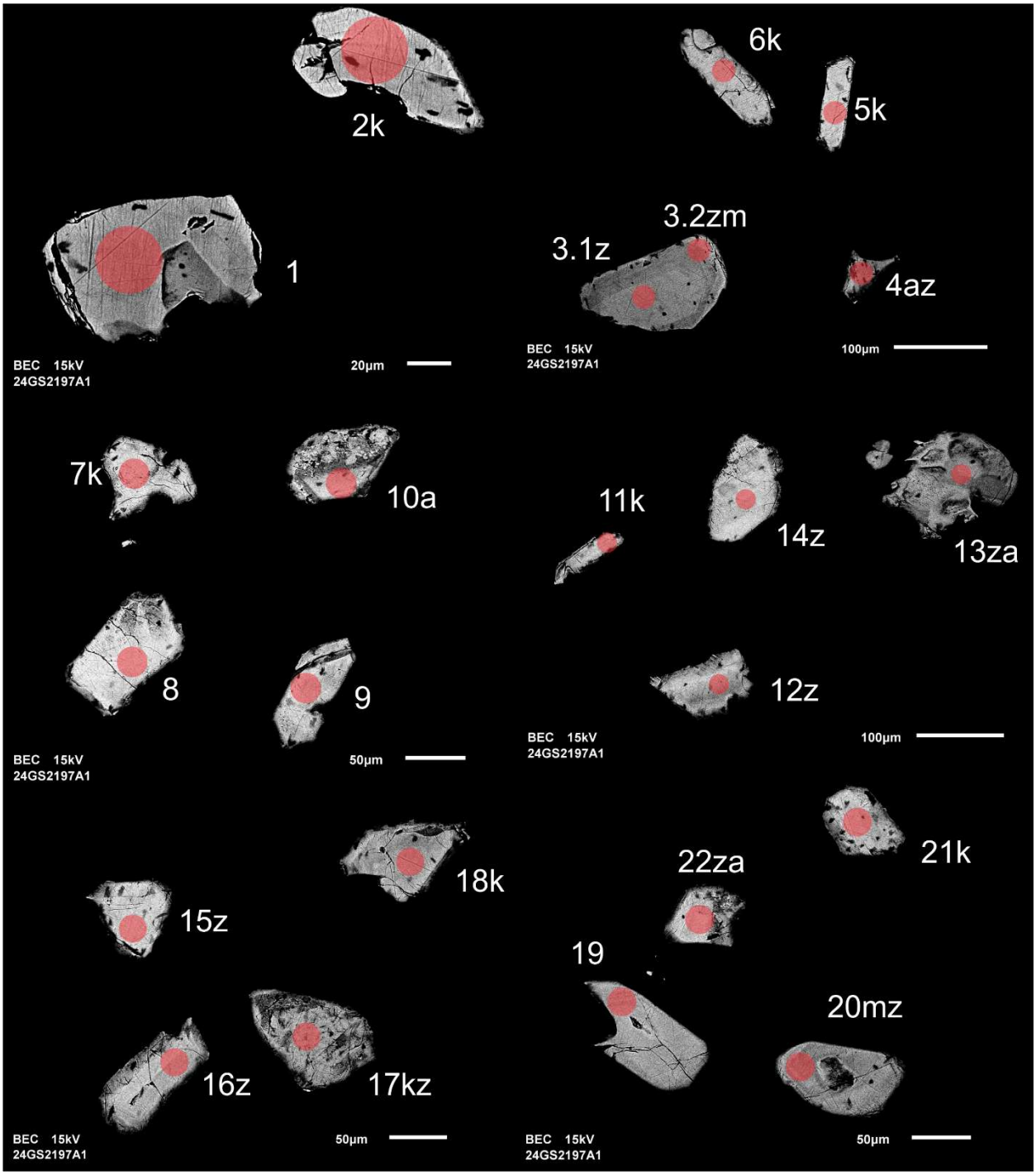

Figure 9-2-1. BSE images of selected grains from sample 24-GS-2197A1. The red circles represent the approximate locations of laser ablation spots.

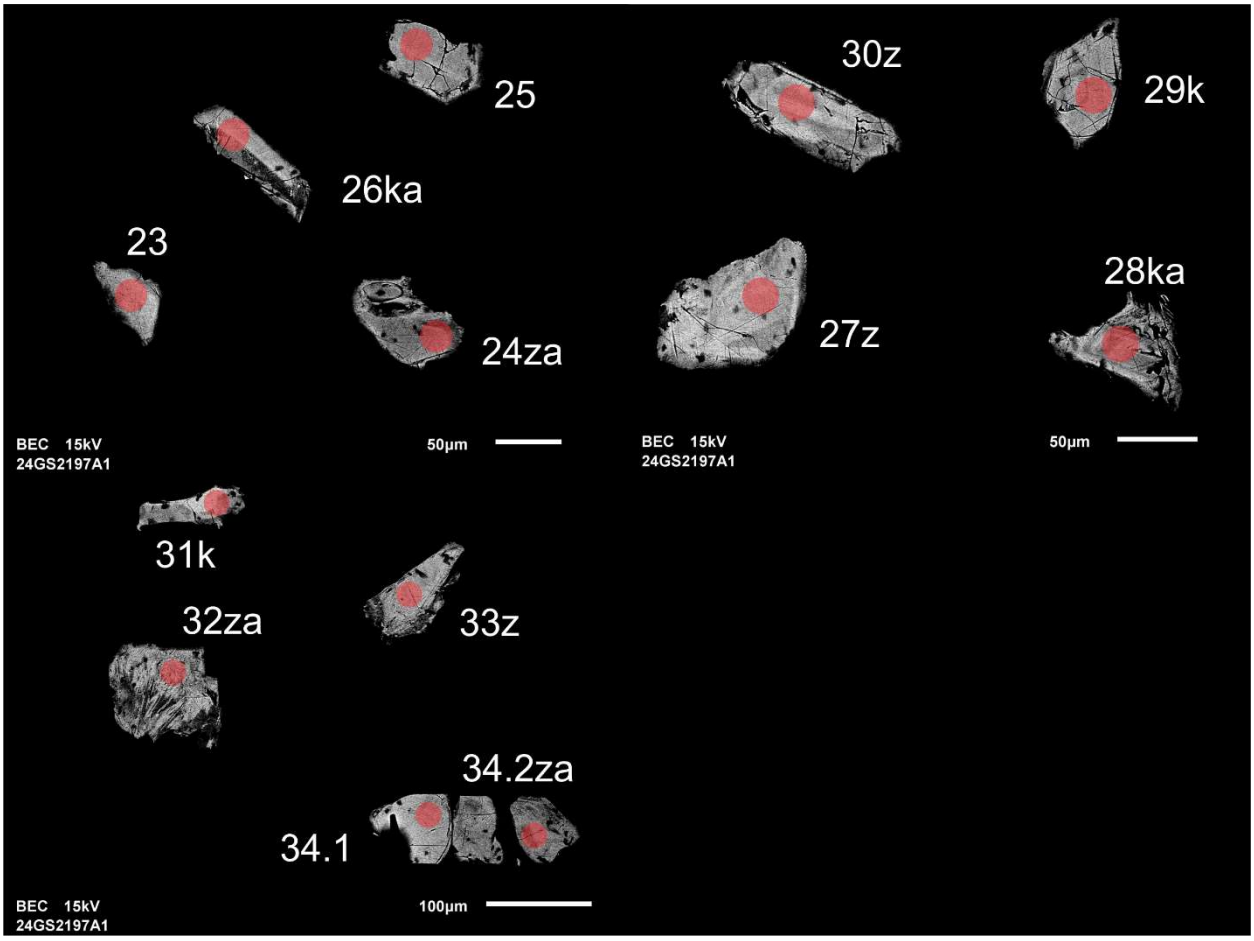

Figure 9-2-2. BSE images of selected grains from sample 24-GS-2197A1. The red circles represent the approximate locations of laser ablation spots.

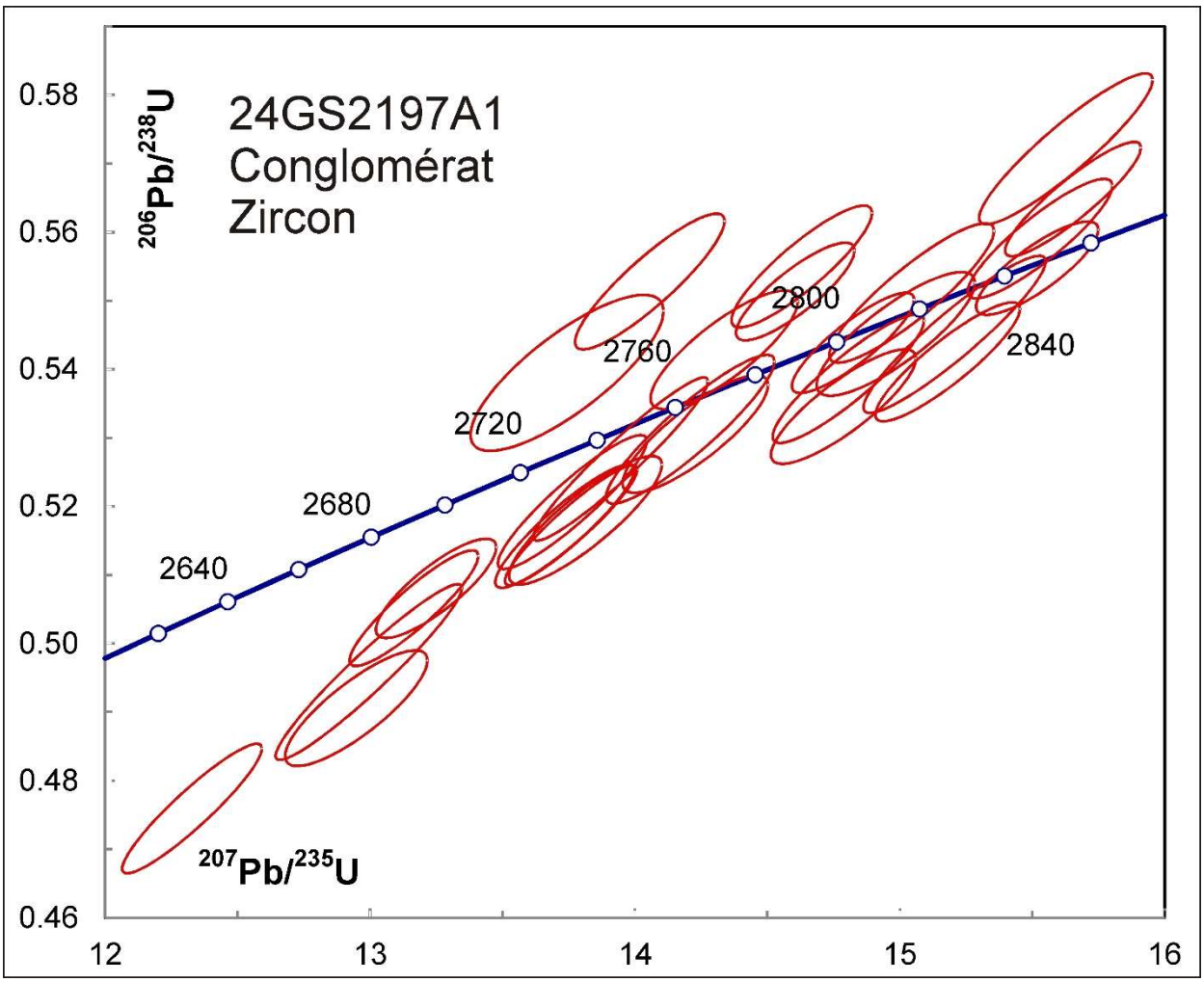

Figure 9-3. Concordia plot showing U-Pb isotopic data on zircon from conglomerate sample 24-GS-2197A1.

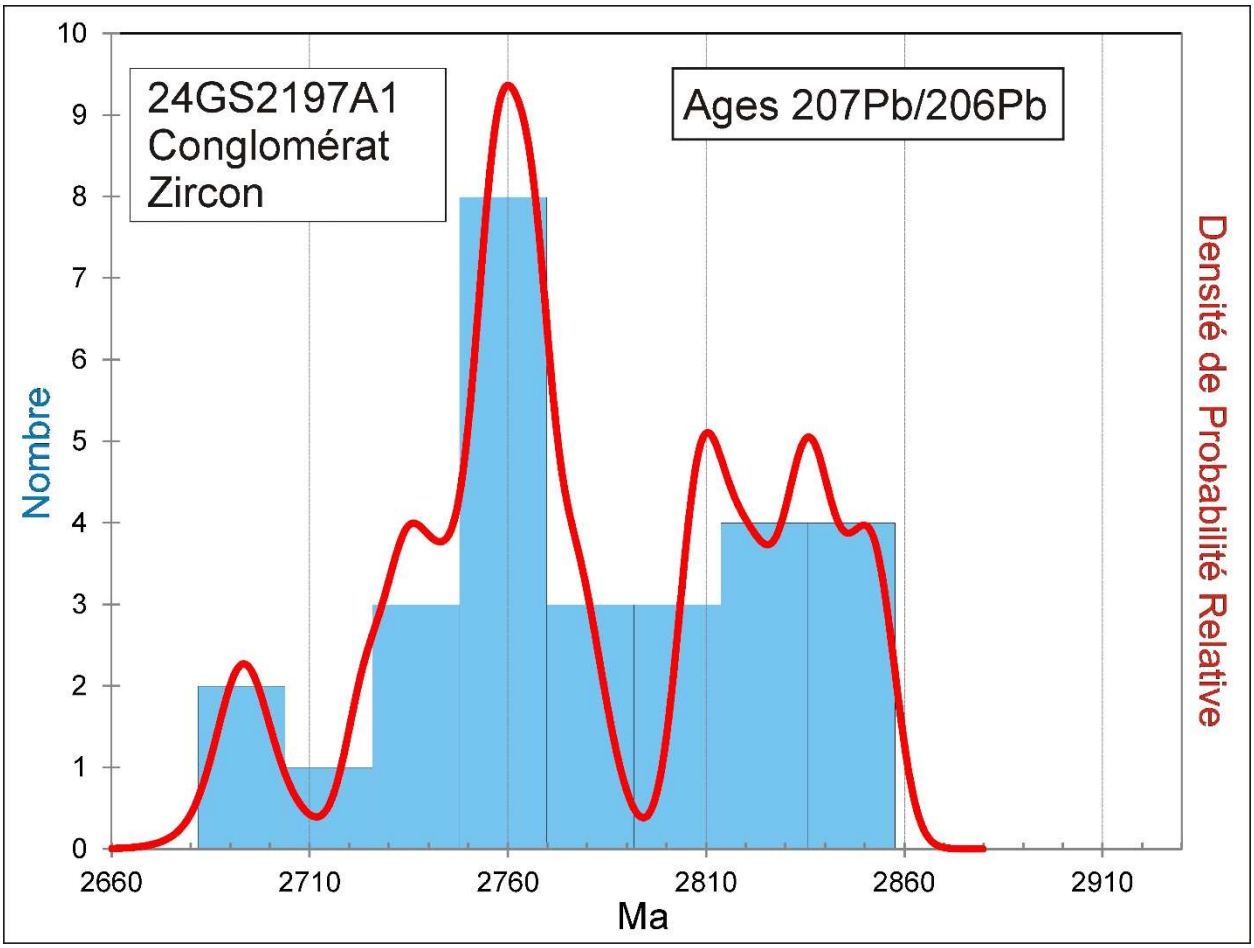

Figure 9-4. Combined probability density plot and histogram showing the distribution of $^{207}Pb/^{206}Pb$ ages on zircon from conglomerate sample 24-GS-2197A1.

10. 24-DB-1110A1
Volcanoclastite andésitique, Groupe de Tichégami (nAtg3)

This sample yielded small subhedral to well-rounded zircon grains (Fig. 10-1). Due to their small size, the zircon grains were mounted on double-sided tape and analyzed on natural surfaces. Reliable U-Pb analyses all show Th/U in the magmatic range (<0.1) with ages ranging from 2697 ± 18 Ma to 3395 ±12 Ma but most are Neoarchean with the highest and youngest peak at 2709 ± 4, which is the best estimate for volcanism (Fig. 10-2 and Fig. 10-3). Maximum likelihood analysis of the youngest grains using IsoplotR gives a best estimate of 2707 ± 9 Ma as the older limit on deposition (Fig. 10-4).

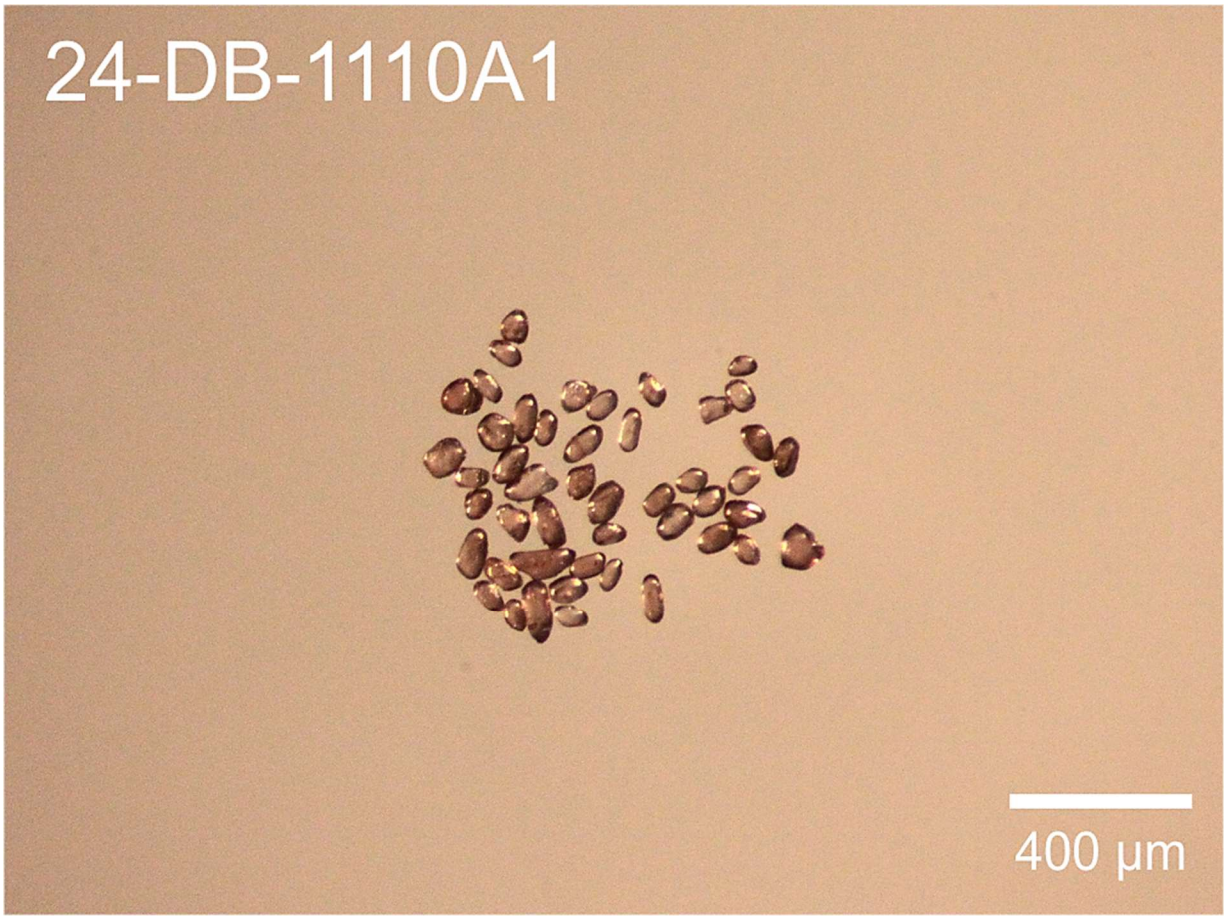

Figure 10-1. Picked zircon from volcanic sample 24-DB-1110A1.

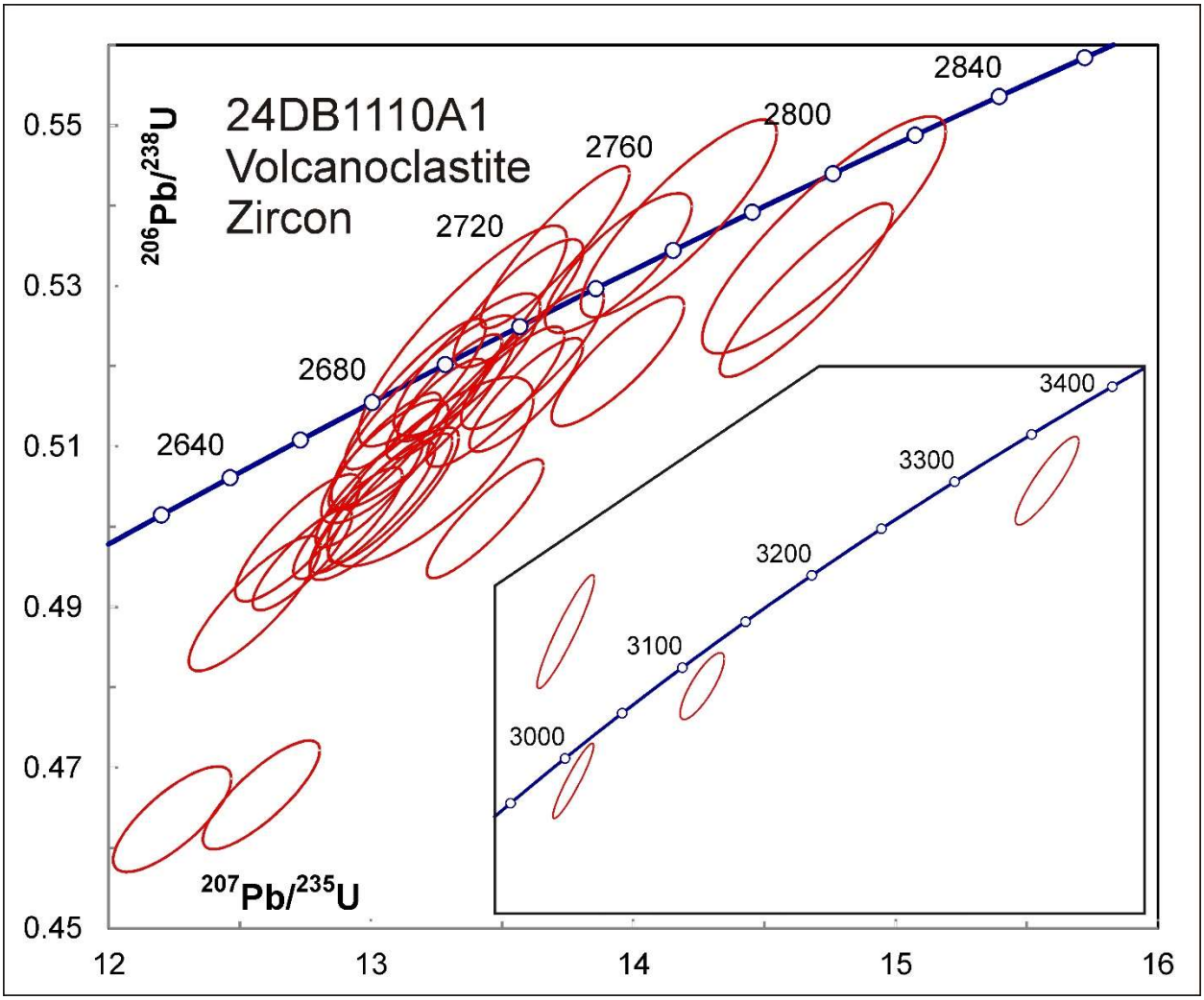

Figure 10-2. Concordia plot showing U-Pb isotopic data on zircon from sample 24-DB-1110A1. Older data are shown on the insert.

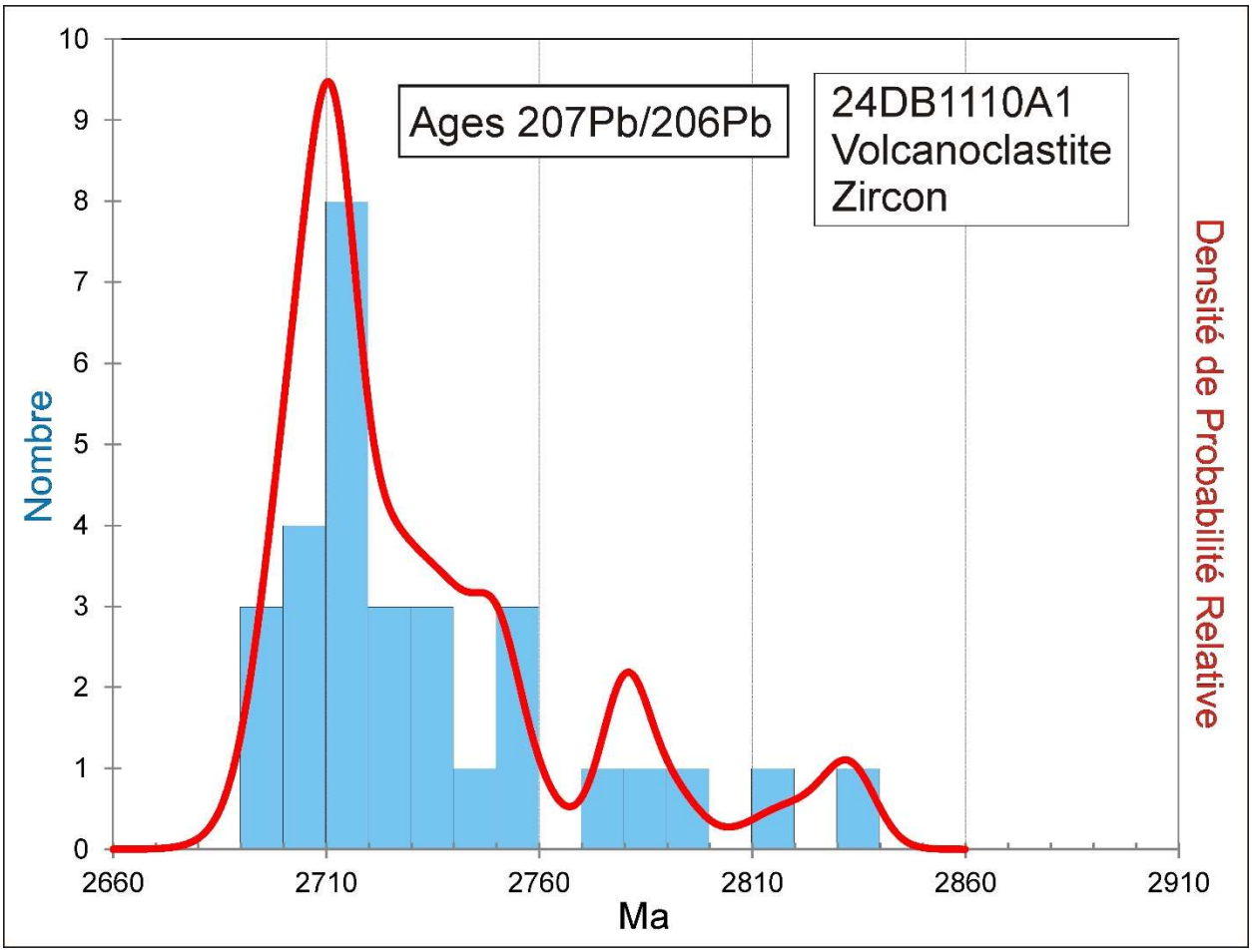

Figure 10-3. Combined probability density plot and histogram showing the distribution of $^{207}Pb/^{206}Pb$ ages on zircon from sample 24-DB-1110A1.

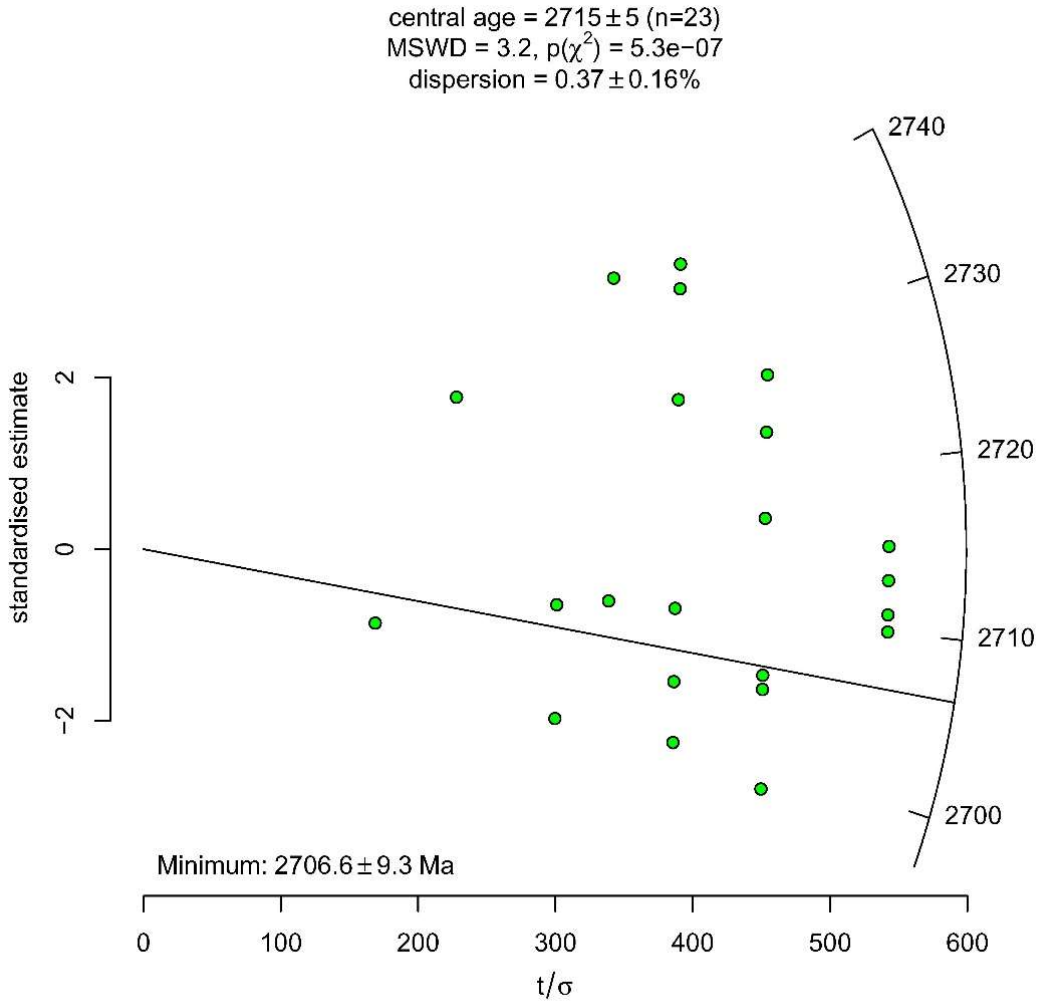

Figure 10-4. Radial plot showing the distribution of 207Pb/206Pb zircon ages from volcaniclastite sample 24-DB-1110A1 as well as the most probable estimate of the youngest (minimum) age, which is an older estimate on volcanism/deposition.

11. 24-GS-2108A1
Gneiss tonalitique, Complexe de Théodat (nAthe1)

This sample yielded a small amount of zircon consisting mostly of short-prismatic euhedral to rounded zircon grains (Fig. 11-1). Zircon grains were mounted on double sided tape and ablated on natural (unpolished) surfaces. Many TRA profiles show significant variation in Th/U suggesting the presence of different magmatic phases, although there is no obvious difference in $^{207}Pb/^{206}Pb$ ages. Acceptable U-Pb analyses on zircon show diverse ages ranging from 2759 Ma to 2853 Ma (Fig. 11-2 and Fig. 11-3). All analyses show Th/U > 0.1. Applying the Unmix program with the assumption of 6 components (the maximum allowed) gives age peaks from 2763 ±9 Ma (6%) to 2842 ± 5 Ma (18%). The largest peak is 2825 ± 4 Ma (43%). This is the best estimate for formation of the tonalite protolith. Younger ages may correspond to new zircon growth during partial melting and deformation.

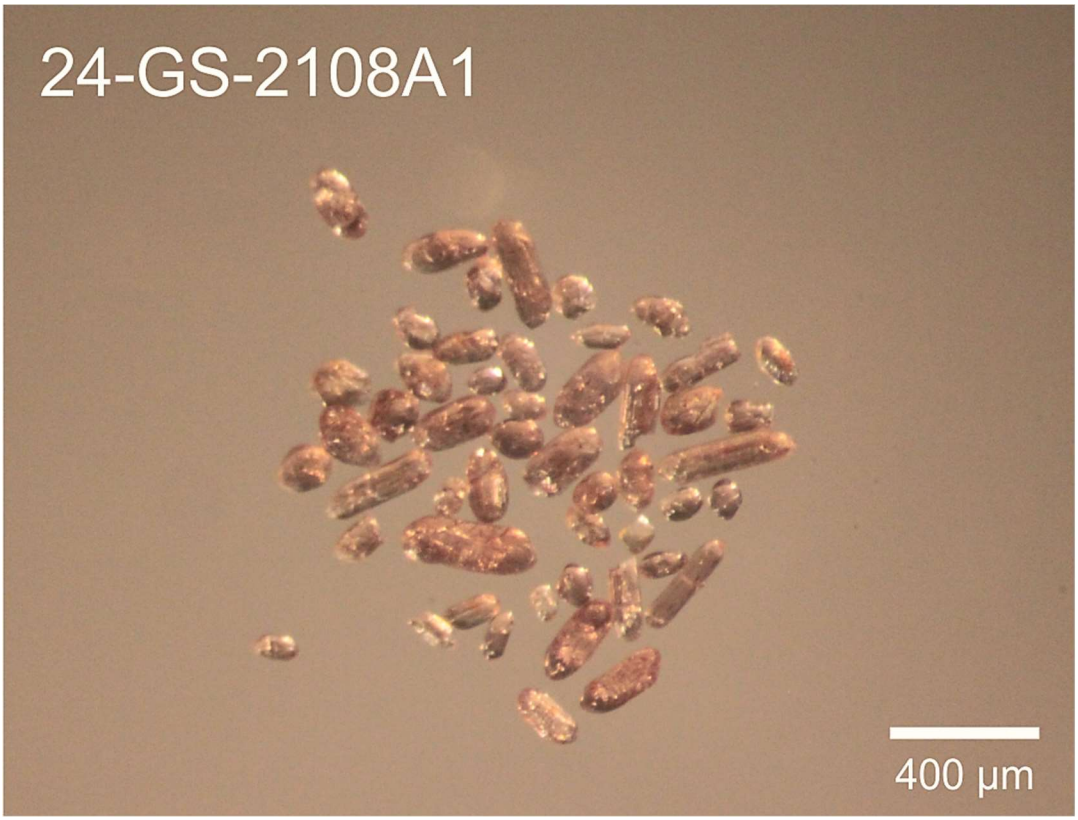

Figure 11-1. Picked zircon from gneiss sample 24-GS-2108A1.

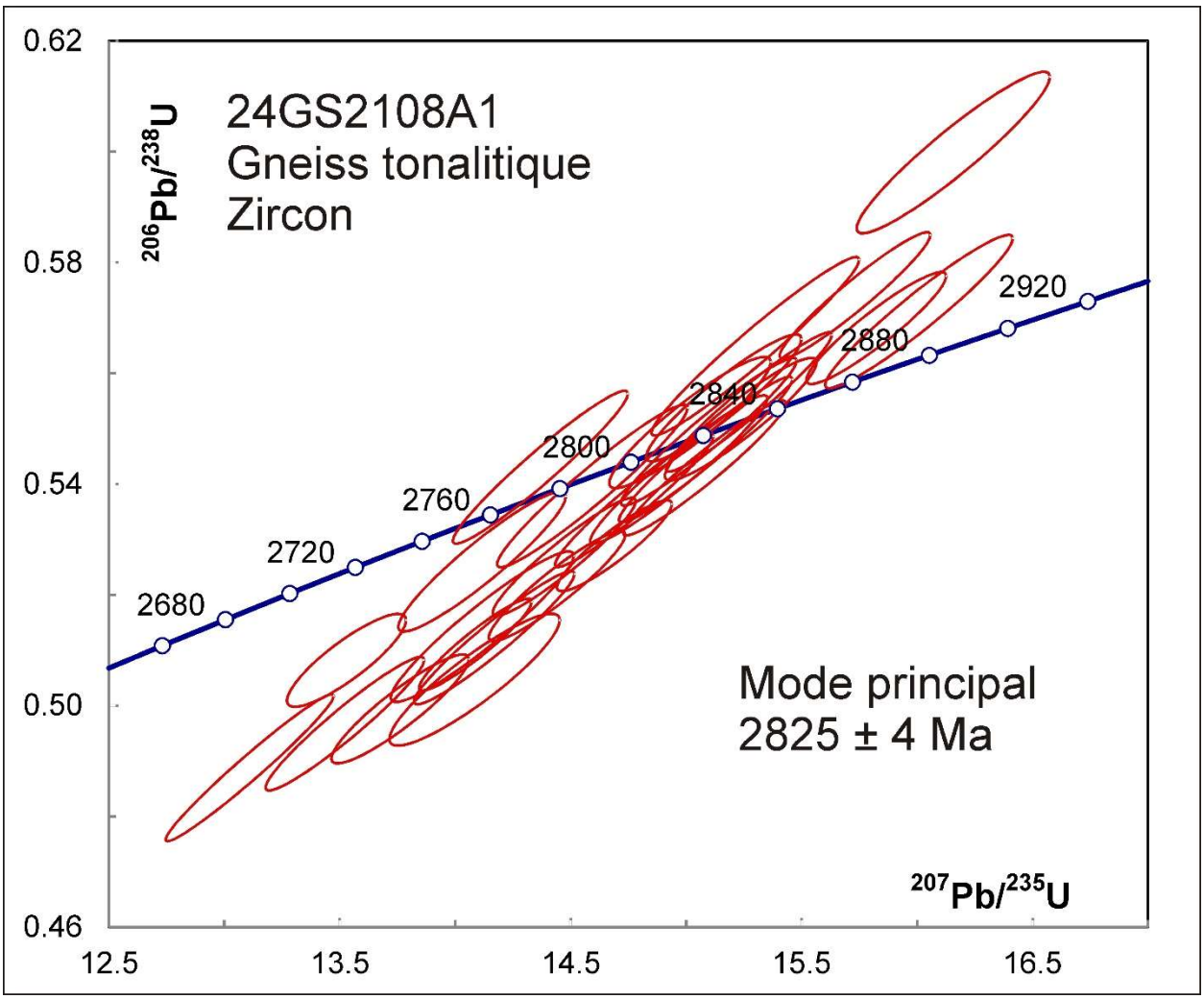

Figure 11-2. Concordia plot showing U-Pb isotopic data on zircon from sample 24-GS-2108A1.

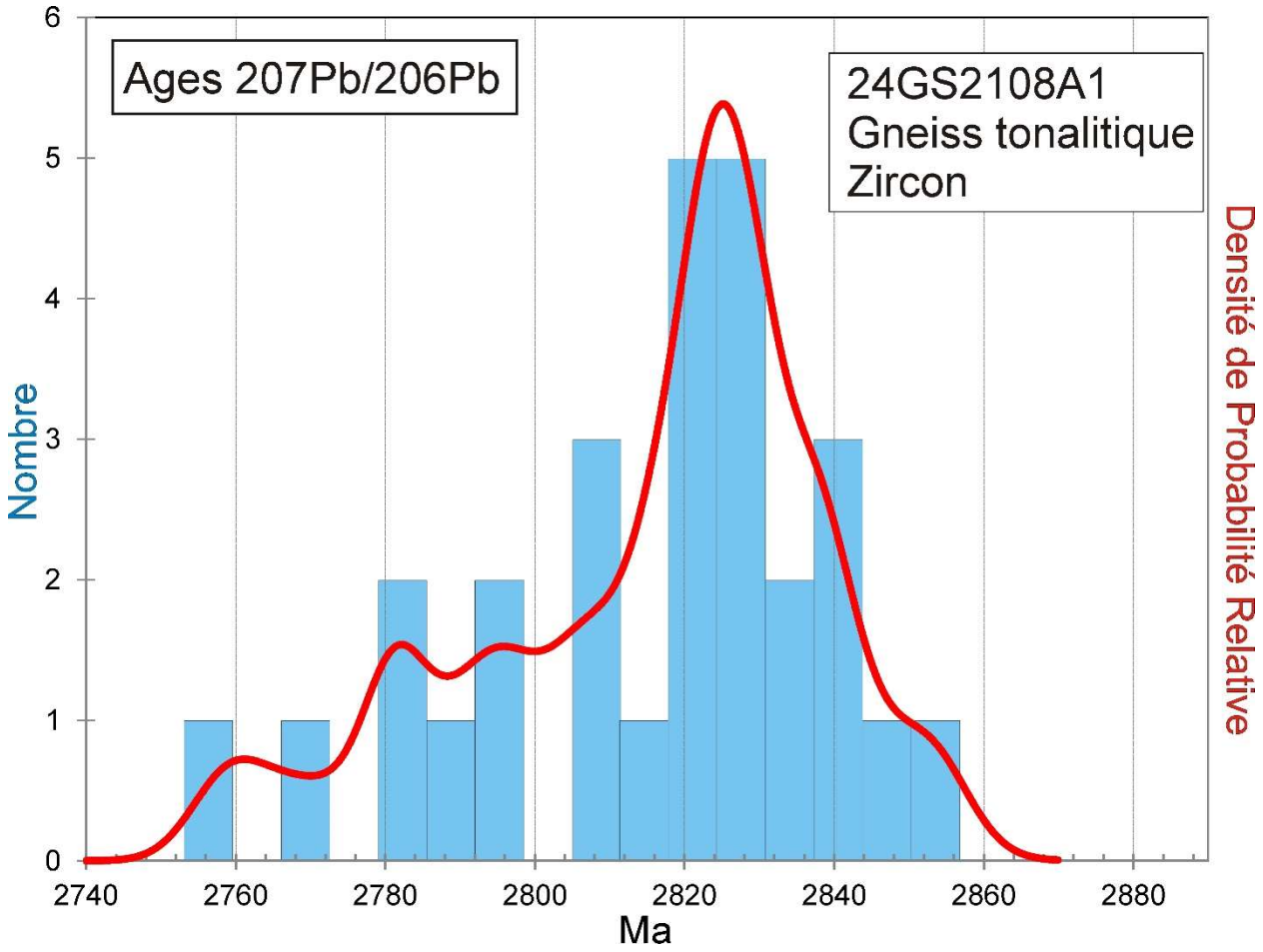

Figure 11-3. Combined age relative probability density plot and histogram showing the distribution of $^{207}Pb/^{206}Pb$ ages on zircon from sample 24-GS-2108A1.

12. 24-GS-2205A1
Métatexite dérivée d'un gneiss tonalitique, Complexe de la Hutte (Ahue1b)

This sample yielded a small amount of zircon consisting mostly of short-prismatic euhedral to well rounded zircon grains (Fig. 12-1). BSE images show zoning patterns, cracks, and alteration zones (Fig. 12-2). U-Pb analyses on zircon show diverse ages ranging from 2744 Ma to 2808 Ma (Fig. 12-3 and Fig. 12-4). The 'Unmix' age program gives 2750 ± 5 Ma (31%), and 2767 ± 3 Ma (69%) if one assumes 2 modes. All groups show Th/U > 0.1 and there is no consistent relationship between age and texture of the zircon. The major, older peak is probably the best estimate for emplacement of the tonalite while some zircon may have been slightly reset if metamorphism occurred over a protracted period.

Titanite grains were also found in this sample. Titanite tends to contain some proportion of common Pb, which has the effect of displacing data upward and to the right approximately parallel to the concordia curve. This is the pattern seen with the titanite analyses but the 13 data with the lowest apparent ages cluster on or near concordia with a mean $^{207}Pb/^{206}Pb$ age of 2581 ± 3 Ma (MSWD – 1.1). The titanite is likely metamorphic in origin but the age probably represents closure to diffusion following cooling down to 700°C (Moser et al. 2022). This may be evidence for protracted residence at high temperature.

Figure 12-1. Picked zircon from metatexite sample 24-GS-2205A1.

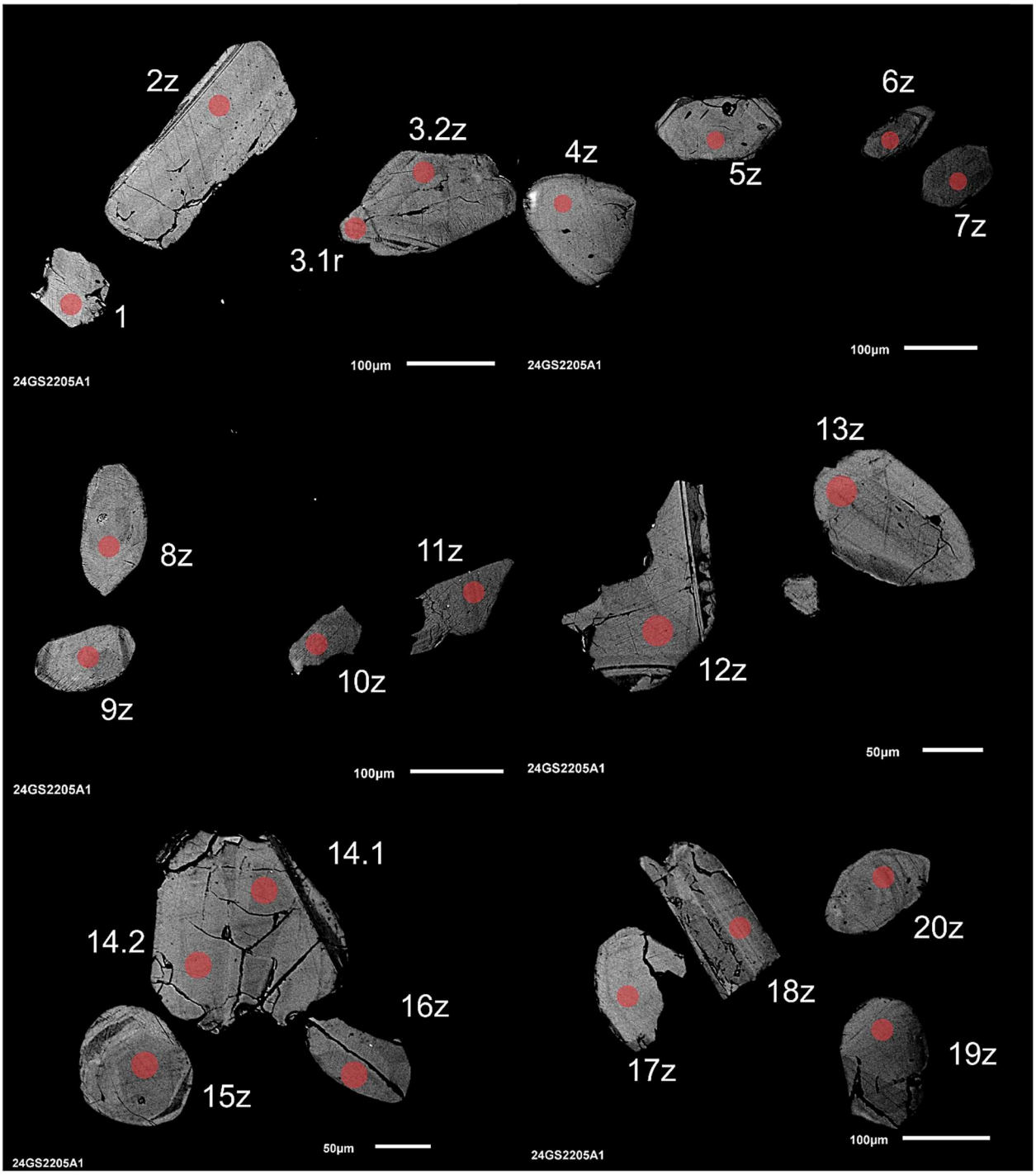

Figure 12-2-1. BSE images of selected grains from sample 24-GS-2205A1. The red circles represent the approximate locations of laser ablation spots.

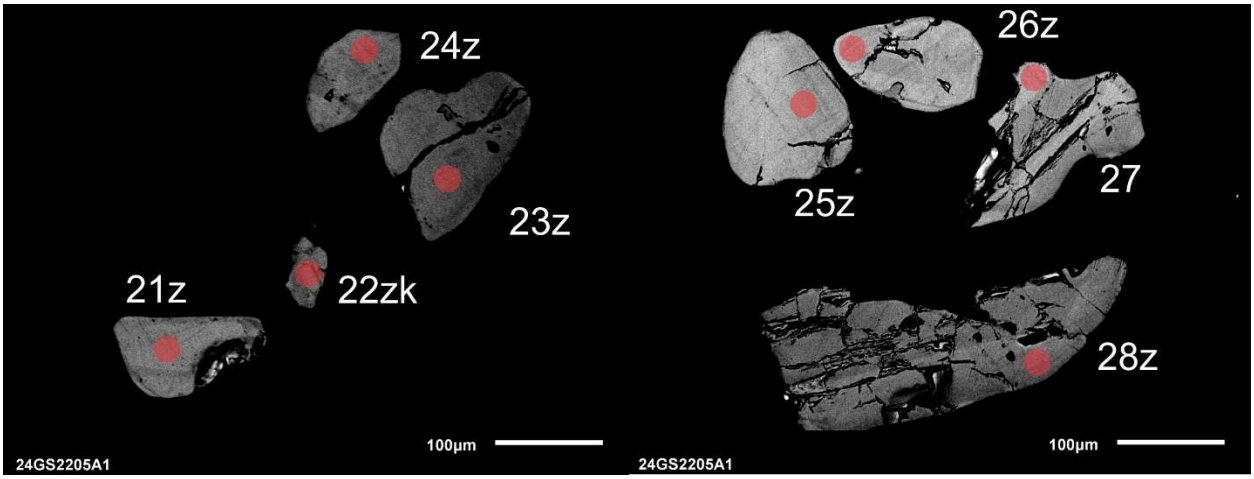

Figure 12-2-2. BSE images of selected grains from sample 24-GS-2205A1. The red circles represent the approximate locations of laser ablation spots.

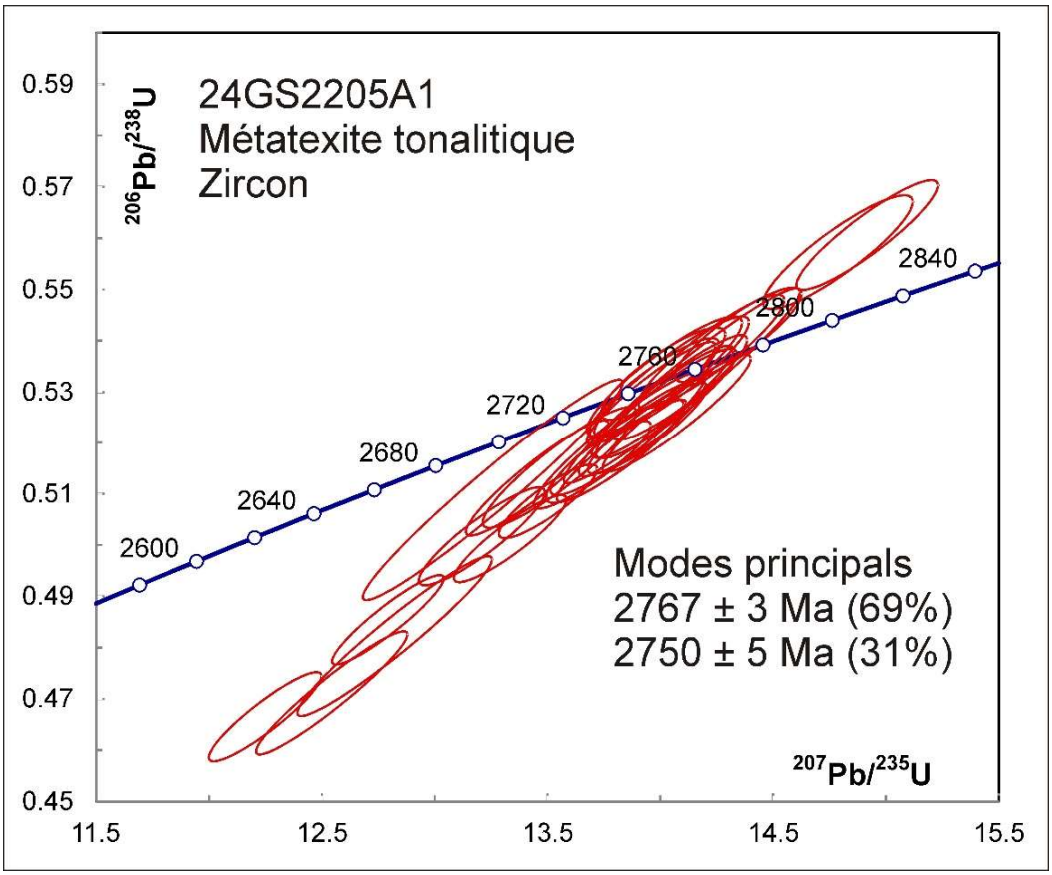

Figure 12-3. Concordia plot showing U-Pb isotopic data on zircon from sample 24-GS-2205A1.

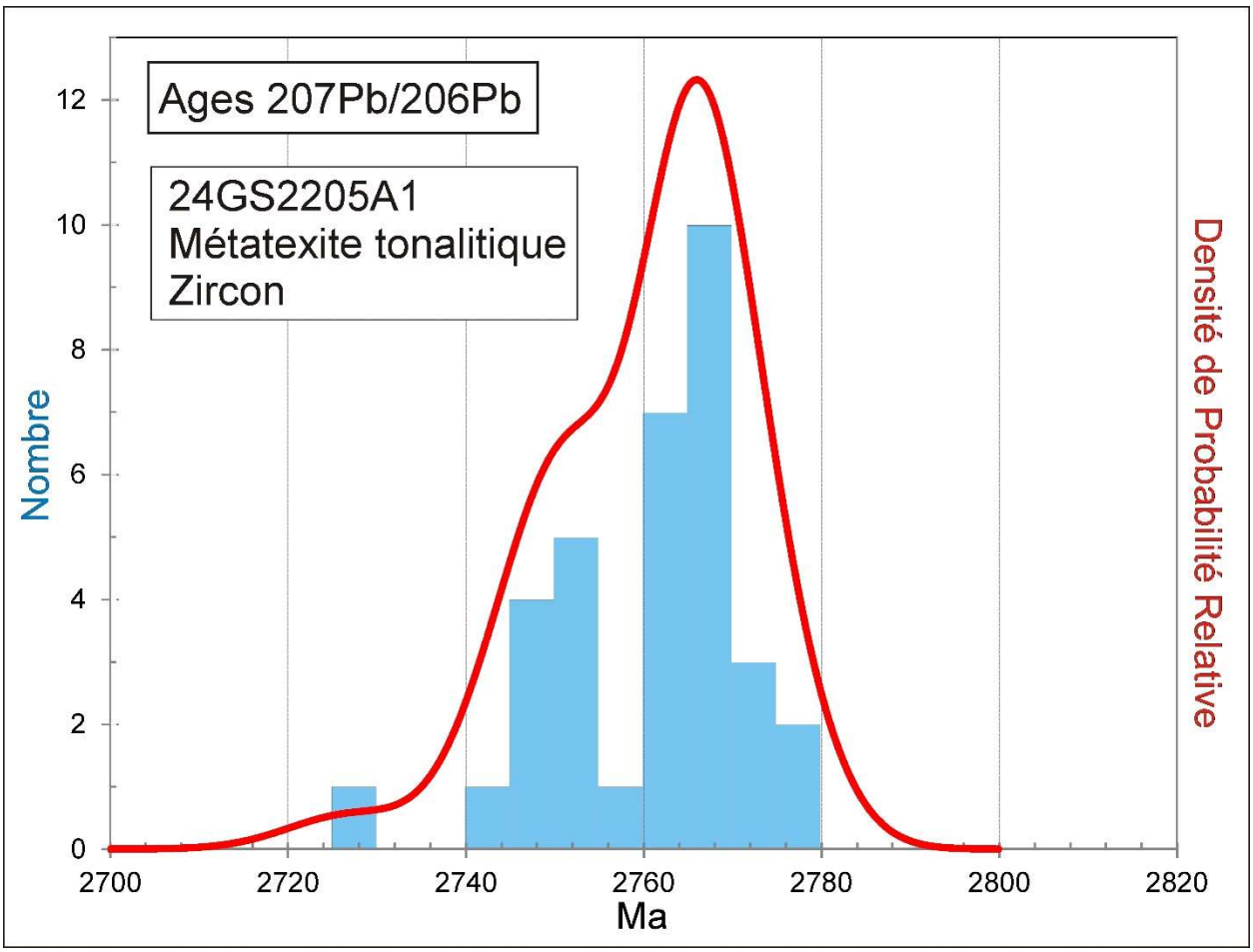

Figure 12-4. Combined age relative probability density plot and histogram showing the distribution of $^{207}Pb/^{206}Pb$ ages on zircon from sample 24-GS-2205A1.

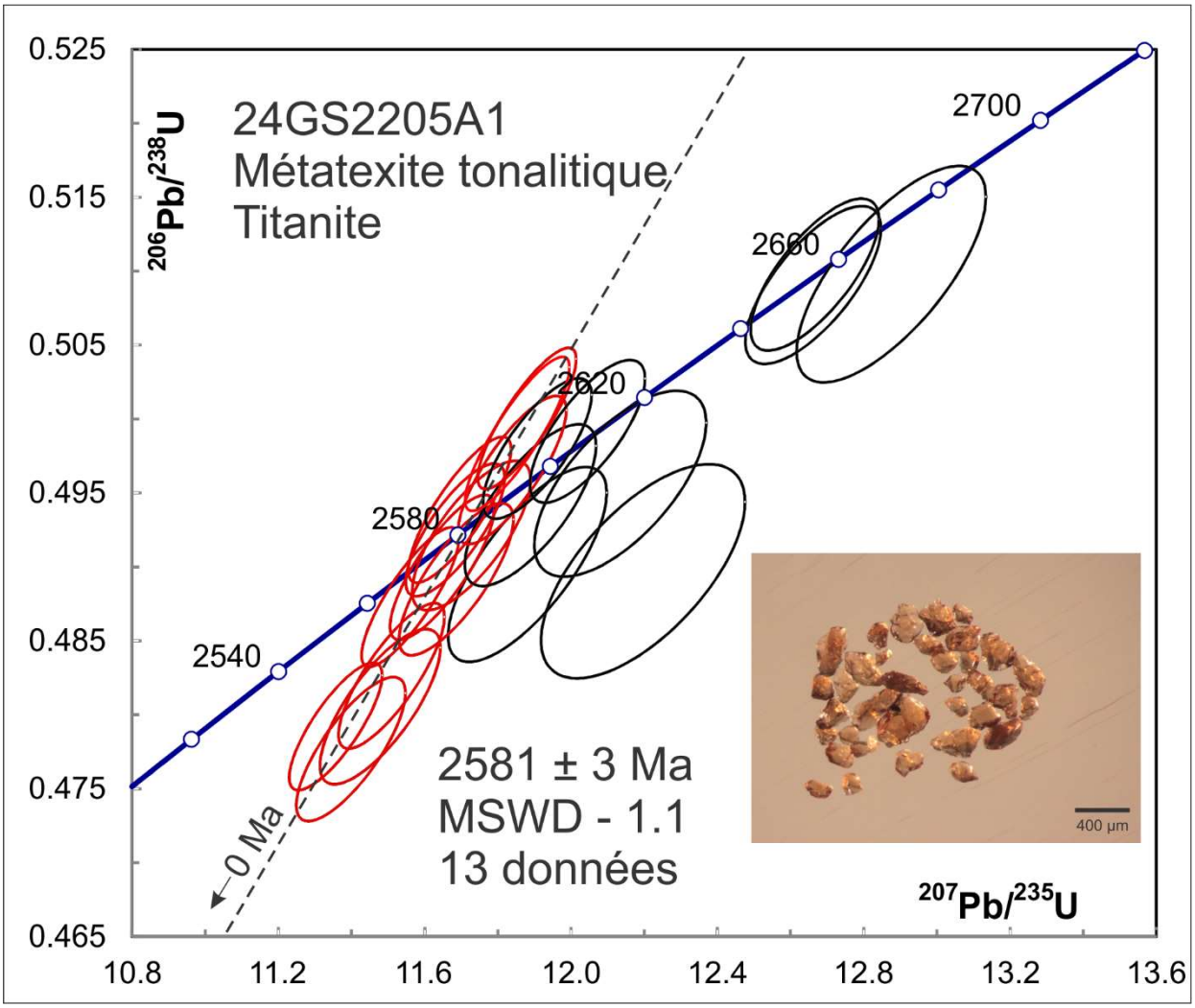

Figure 12-5. Concordia plot showing U-Pb isotopic data on titanite from sample 24-GS-2205A1. Red ellipses correspond to spots considered in the age model.

13. 24-GS-2205B1
Gneiss tonalitique rubané, Complexe de la Hutte (Ahue1)

This sample yielded a small amount of zircon consisting mostly of fragments (Fig. 13-1). Zircon grains were mounted on double-sided tape and analyzed on natural surfaces. Some of the zircon has undergone late low temperature Pb loss (discordance) probably due to alteration. Analyses >10% discordant have been rejected from age calculations. U-Pb analyses on zircon show diverse ages ranging from 2941 Ma to 2968 Ma (Fig. 13-2). All grains show magmatic Th/U ratios > 0.1 but Th/U ratios vary widely within a single analysis with the highest values approaching 4, which is unusually high for magmatic zircon from felsic rocks. These regions in the grain generally show very young $^{206}Pb/^{238}U$ ages although $^{207}Pb/^{206}Pb$ ratios may be unaffected. This may be due to alteration associated with crystallization of high-Th HREE-oxide or xenotime phases which are not high in Sr. U-Pb isotopic analyses of spots on 14 grains with relatively normal Th/U give $^{207}Pb/^{206}Pb$ ages that scatter somewhat outside of error with an age of 2945 ± 8 Ma (MSWD – 2.9, Fig 13-2). This Mesoarchean age is the best estimate for the primary magmatic age of the gneiss, which appears to have been derived from a uniform source.

Titanite grains were also analyzed from this sample. BSE images on titanite grains show broad zoning (Fig 13-3). Near-concordant analyses are spread along the concordia curve (Fig 13-4). This is likely not the result of variable proportions of common Pb, which would produce a trend of lower slope, but may result from variable degrees of diffusive resetting during prolonged metamorphism, which is grain-size dependent. The youngest datum should be closest to the time of cooling through the presumed closure temperature of about 700ºC (Moser et al., 2022). This gives a model age of 2564 ± 20 Ma, which is consistent with titanite from the previous sample.

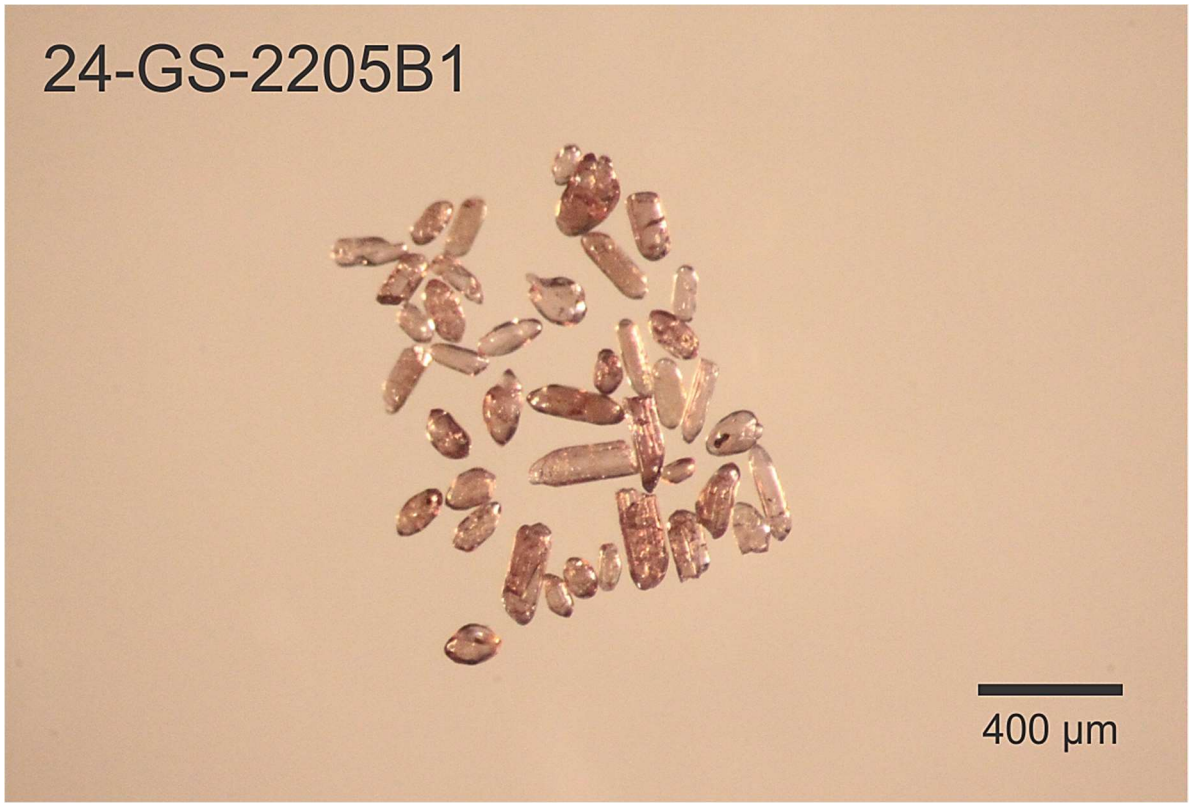

Figure 13-1. Picked zircon from gneiss sample 24-GS-2205B1.

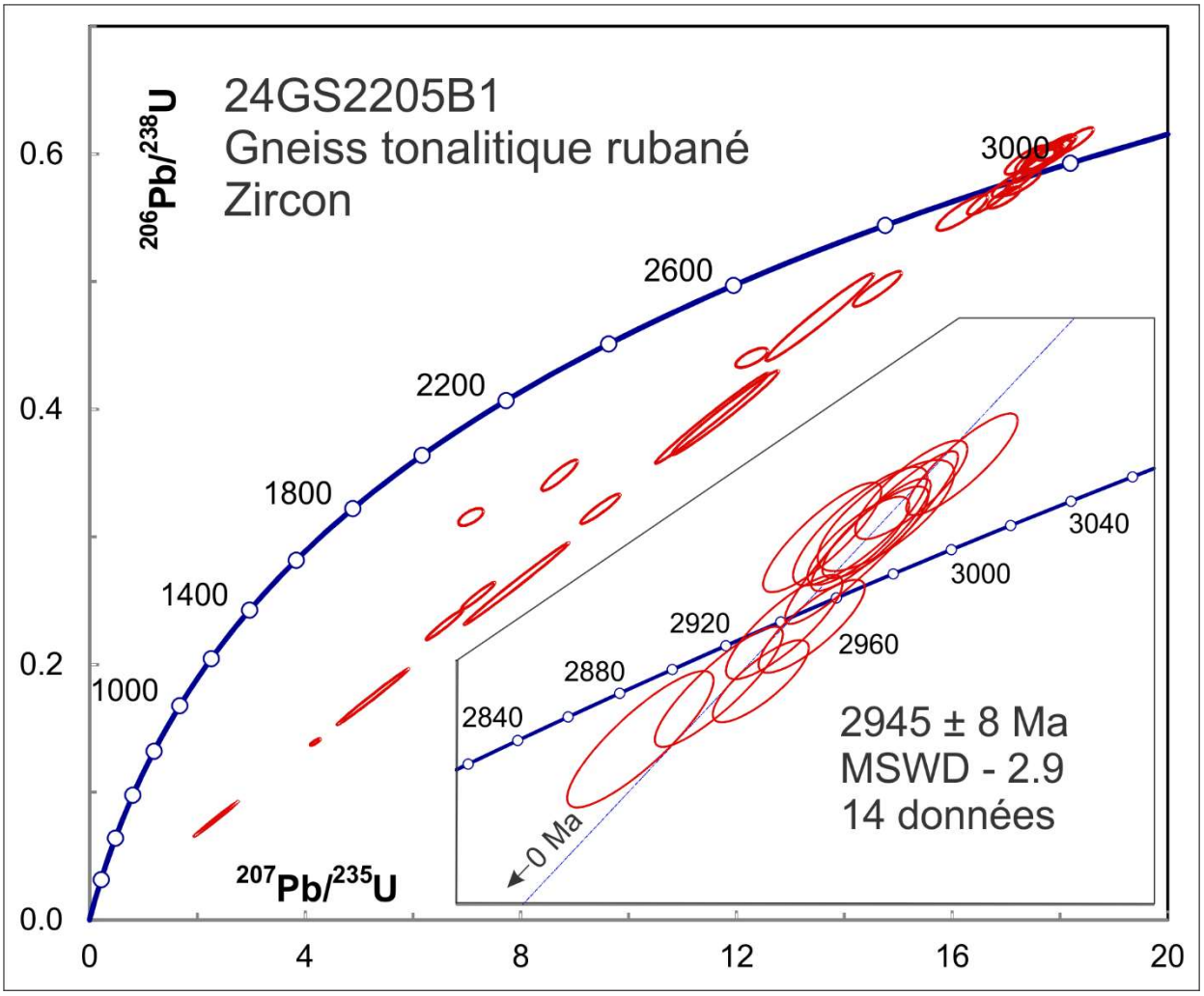

Figure 13-2. Concordia plot showing U-Pb isotopic data on zircon from sample 24-GS-2205B1.

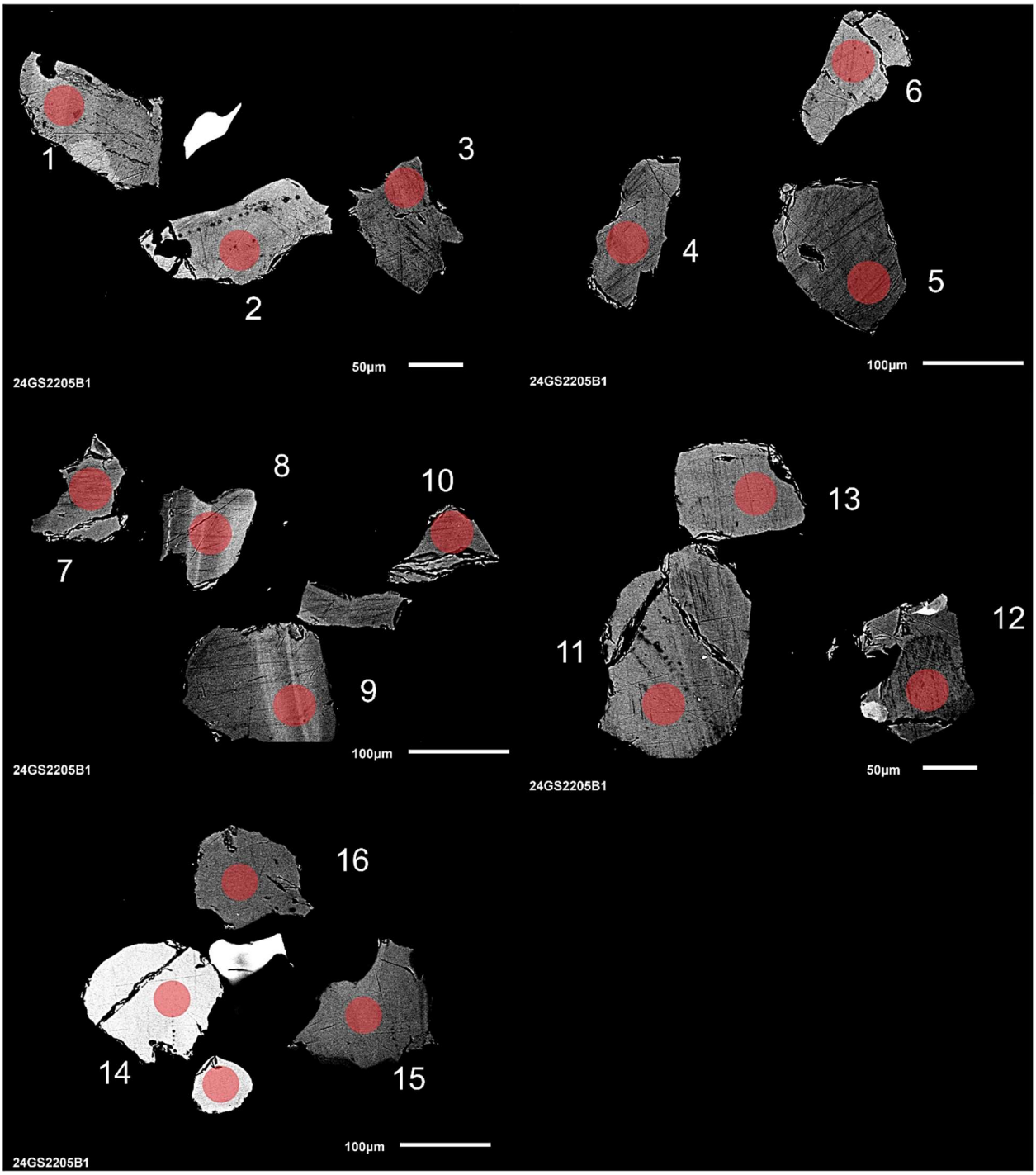

Figure 13-3. BSE images of selected titanite grains from sample 24-GS-2205B1. The red circles represent the approximate locations of laser ablation spots.

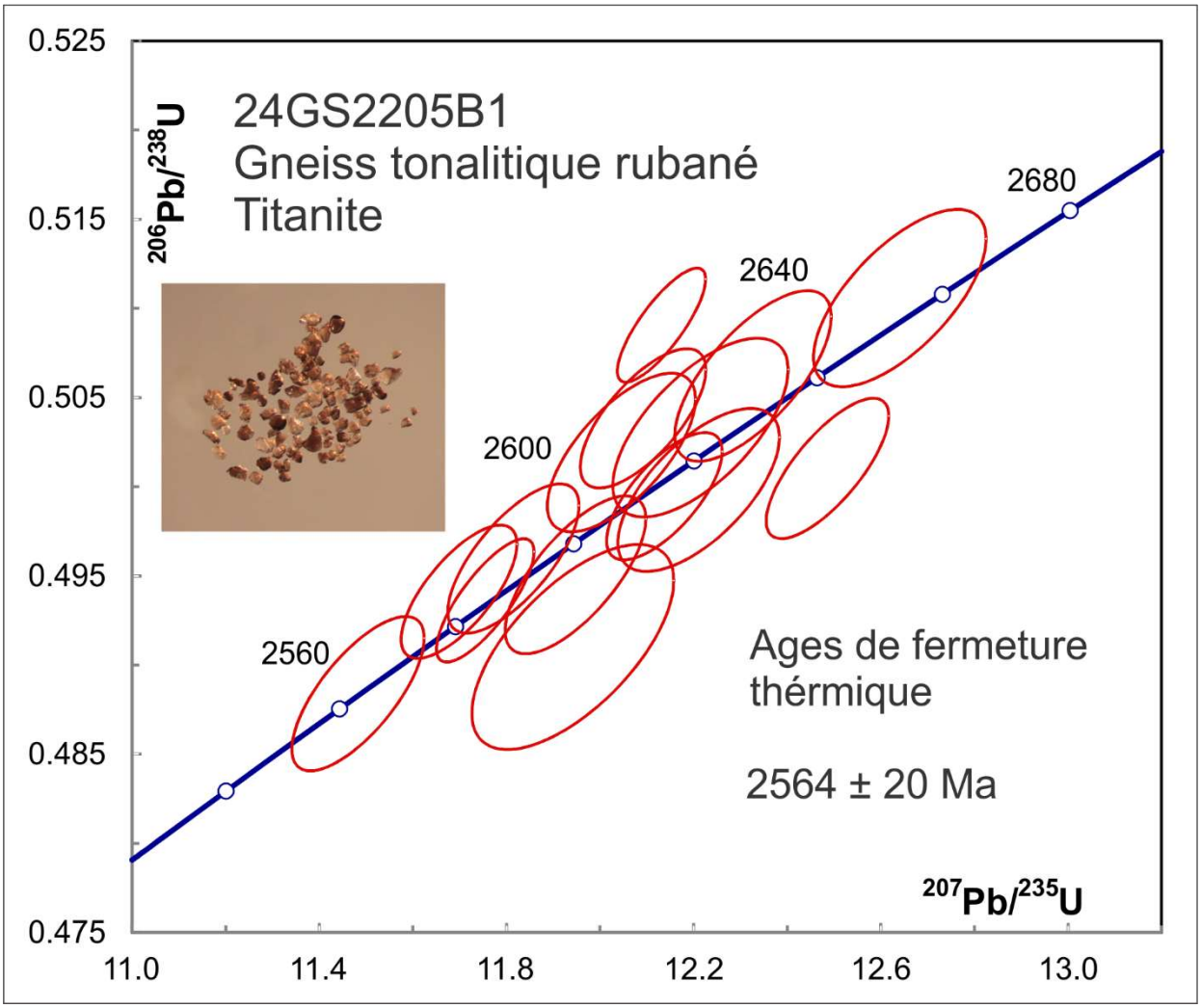

Figure 13-4. Concordia plot showing U-Pb isotopic data on titanite from sample 24-GS-2205B1.

14. 24-GS-2204A1
Métatexite dérivée d'un gneiss tonalitique, Complexe de Théodat (Athe2a)

This sample yielded a diverse population of small, short to long-prismatic sub-rounded zircon grains (Fig. 14-1). Due to their small size, the grains were mounted on double-sided tape and analyzed on natural surfaces. U-Pb analyses on zircon show diverse ages ranging from 2629 Ma to 2869 Ma (Fig. 14-2 and Fig. 14-3), as well as diverse Th/U ratios, which are seen to vary from around 0.1 to 1.0 in some grains (Table 3), but there is no correlation with $^{207}Pb/^{206}Pb$ age. The age-probability density plot shows multiple potential modes but the three largest peaks are around 2750 Ma, 2810 Ma and 2840 Ma. The <2700 Ma ages appear to be from near-concordant reliable analyses but are difficult to interpret. We conclude that the best estimate for the igneous protolith is around 2840 Ma and subsequent partial melting may have occurred around 2630 Ma or later and partially reset the older zircon population.

This sample also contains titanite grains. The youngest 10 out of 24 analyses cluster near concordia with a mean age of 2614 ± 5 Ma (MSWD – 2.0, Fig. 14-4), while the other analyses spread to the right as expected from the effect of common Pb. This is the best estimate for either formation or closure age through about 700°C of the titanite.

Figure 14-1. Picked zircon from Metatexite sample 24-GS-2204A1.

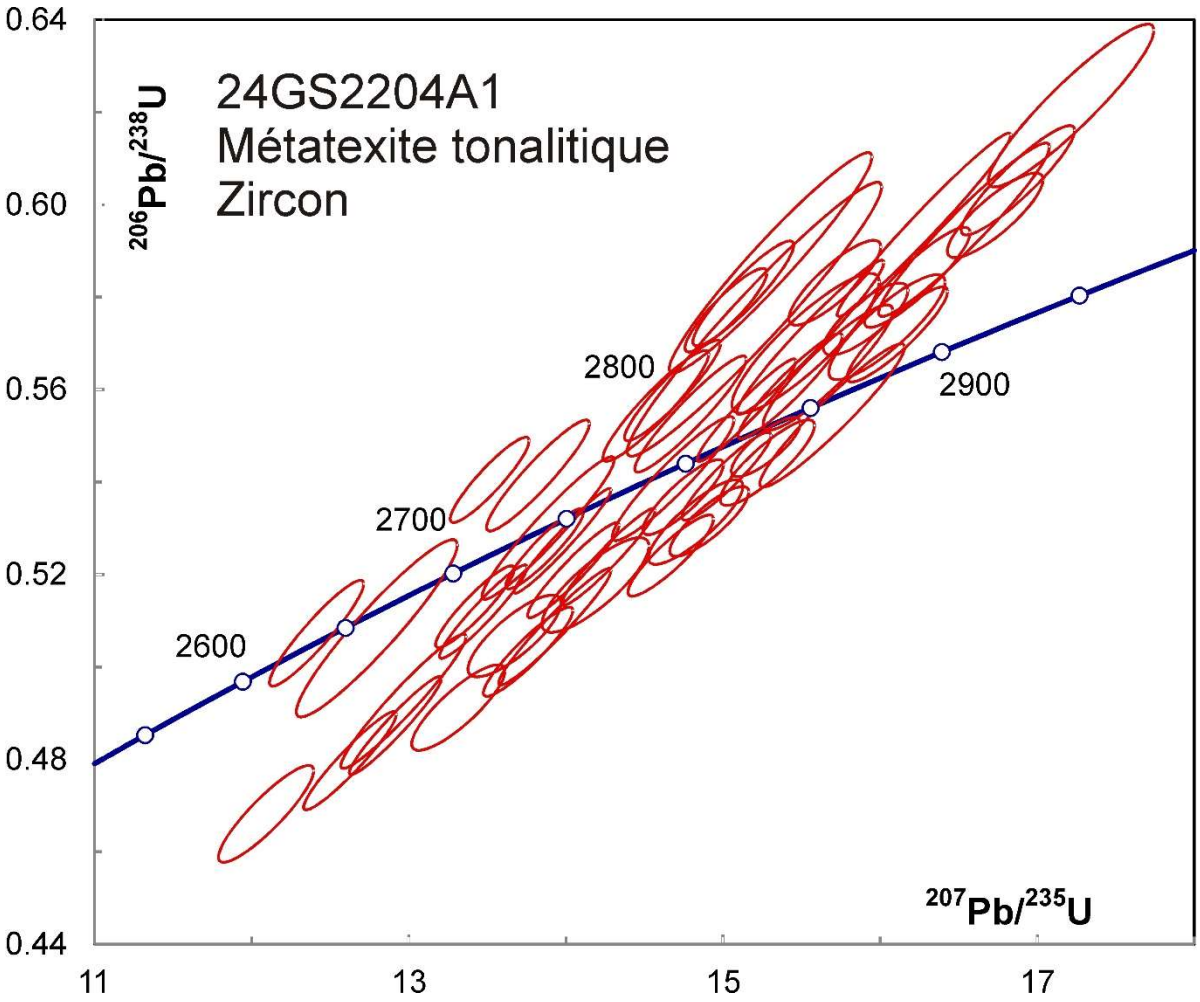

Figure 14-2. Concordia plot showing U-Pb isotopic data on zircon from sample 24-GS-2204A1.

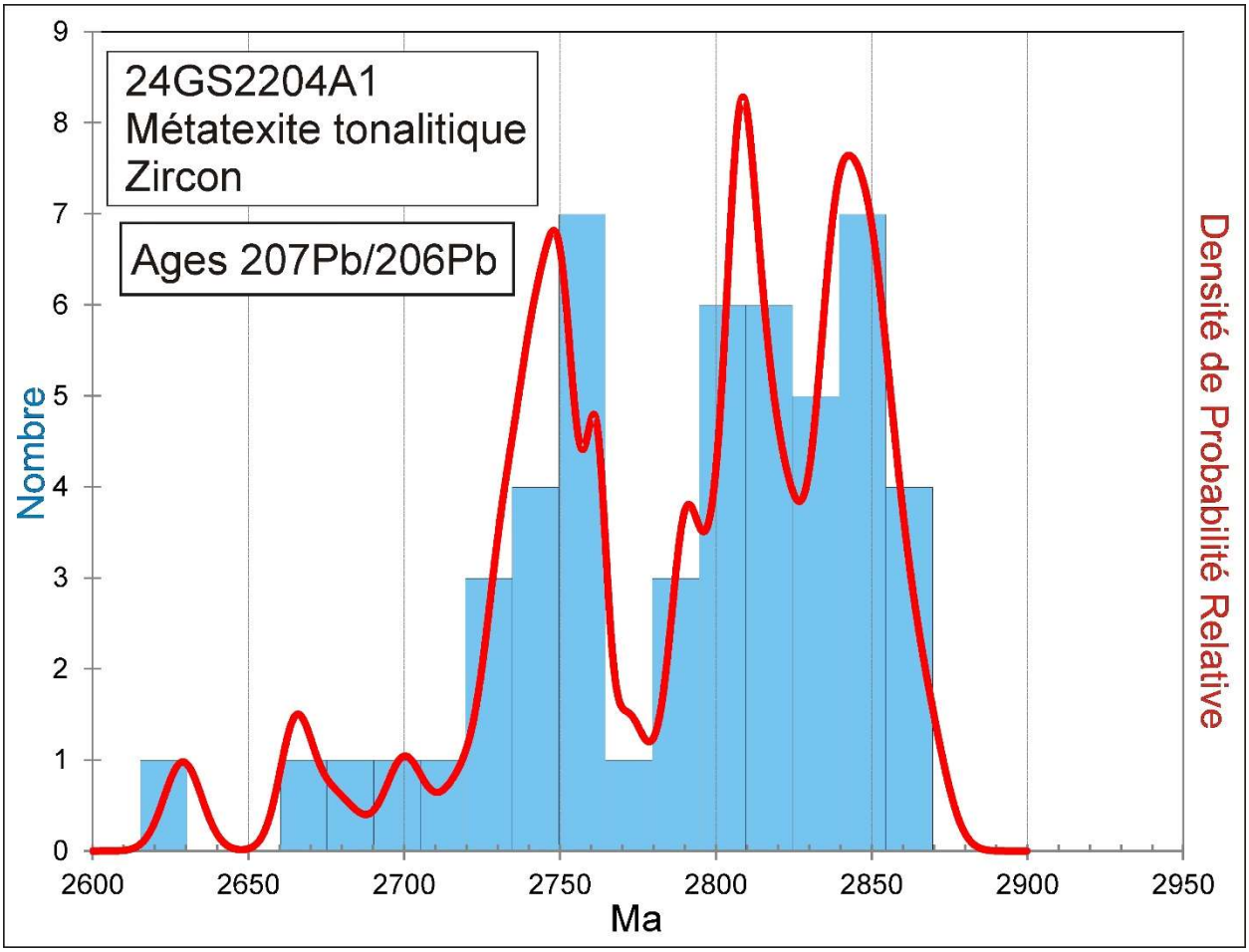

Figure 14-3. Combined age relative probability density plot and histogram showing the distribution of $^{207}Pb/^{206}Pb$ ages on zircon from sample 24-GS-2204A1.

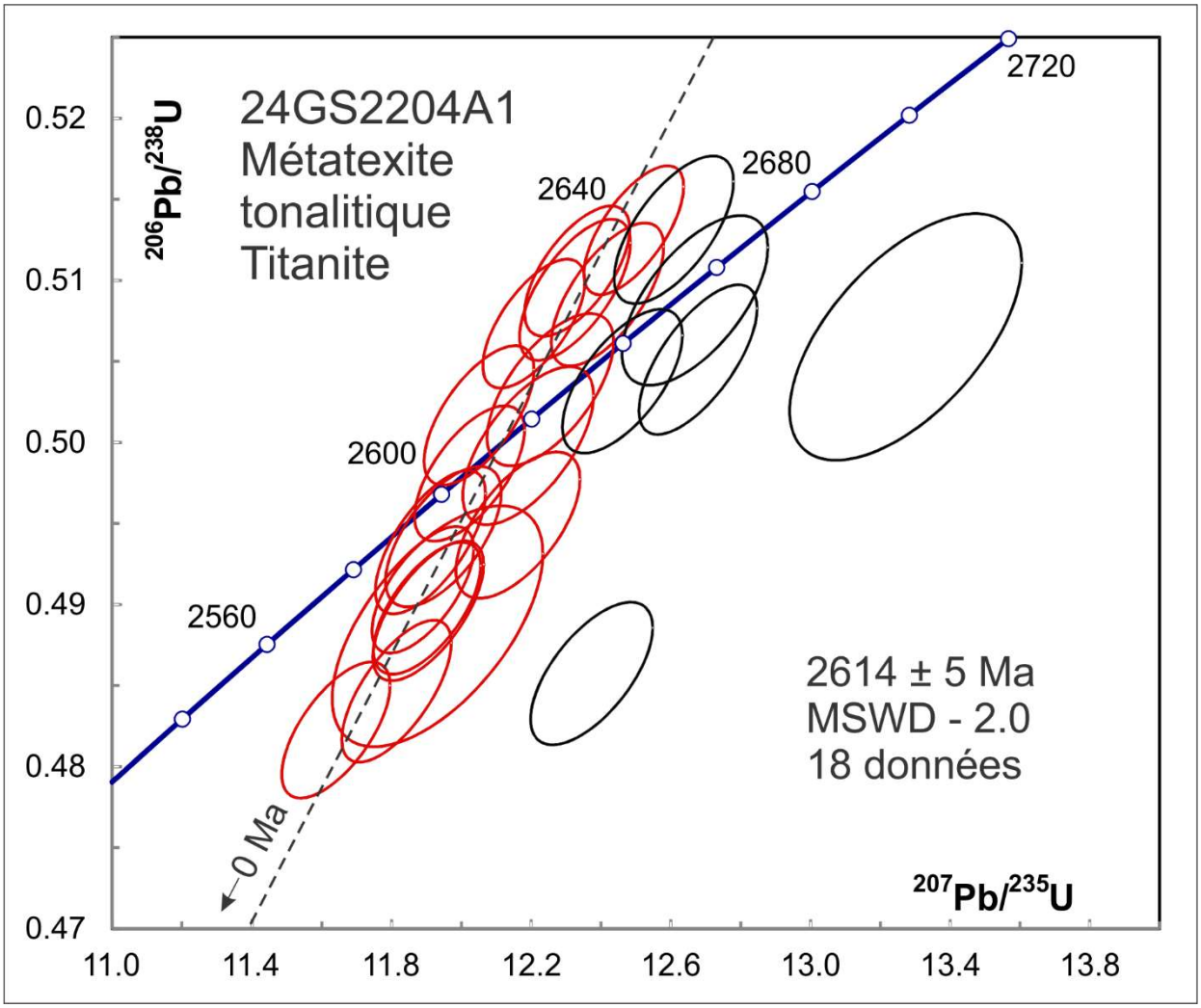

Figure 14-4. Concordia plot showing U-Pb isotopic data on titanite from sample 24-GS-2204A1. Red ellipses correspond to spots considered in the age model.

Pingasulik

15. 24-MY-1037-B
Tuf de basalte andésitique, Groupe de Parent (pPpa12)

This sample yielded just a few fragments of zircon grains (Fig 15-1). Because of the small size and number of grains, it was decided to mount them on double sided tape and ablate on natural (unpolished) surfaces. Twelve U-Pb analyses are all near-concordant with ages that scatter slightly outside of error giving a mean of 1894 ± 6 Ma (MSWD – 1.5, Fig. 15-2). This is the best age estimate for volcanism. The probability density plot (Fig. 15-3) suggests that 3 analyses may have been from a slightly older eruption. Omitting these defines an average age of 1890 ± 5 Ma (MSWD – 0.6).

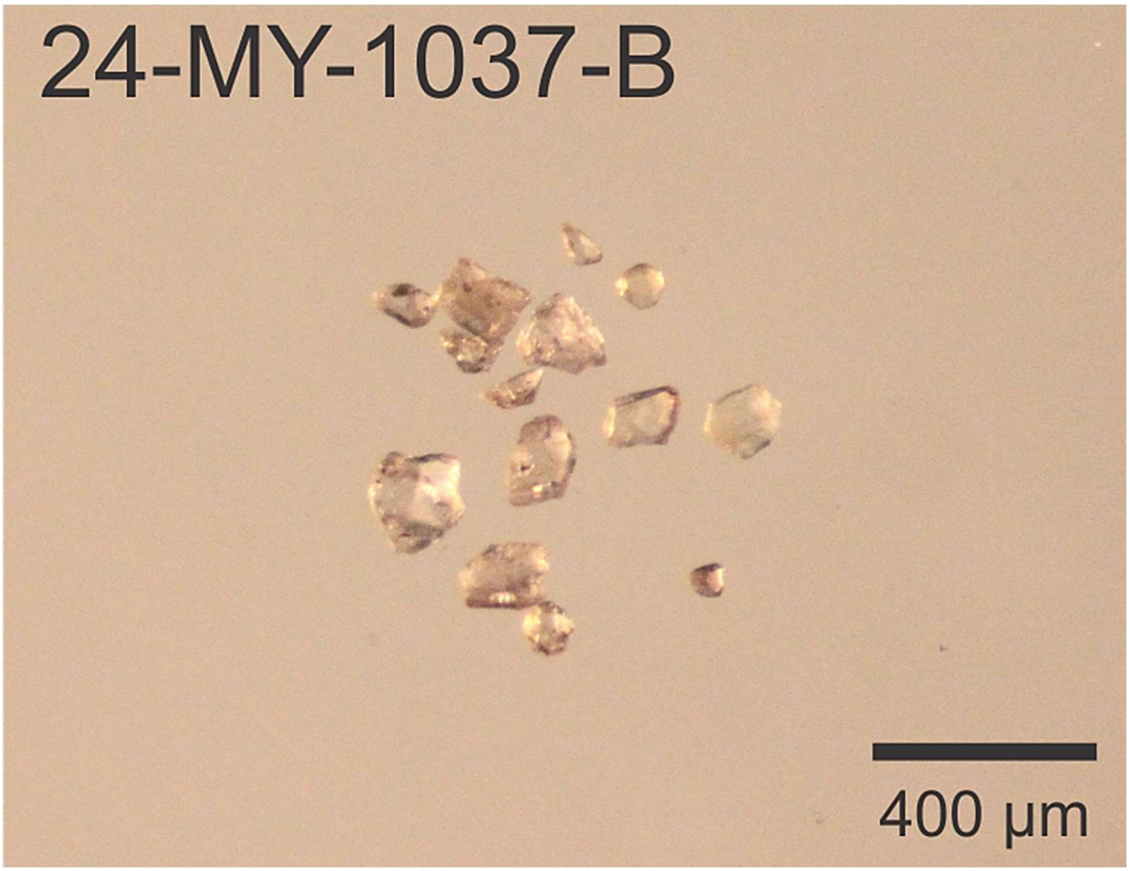

Figure 15-1. Picked zircon from tuff sample 24-MY-1037-B.

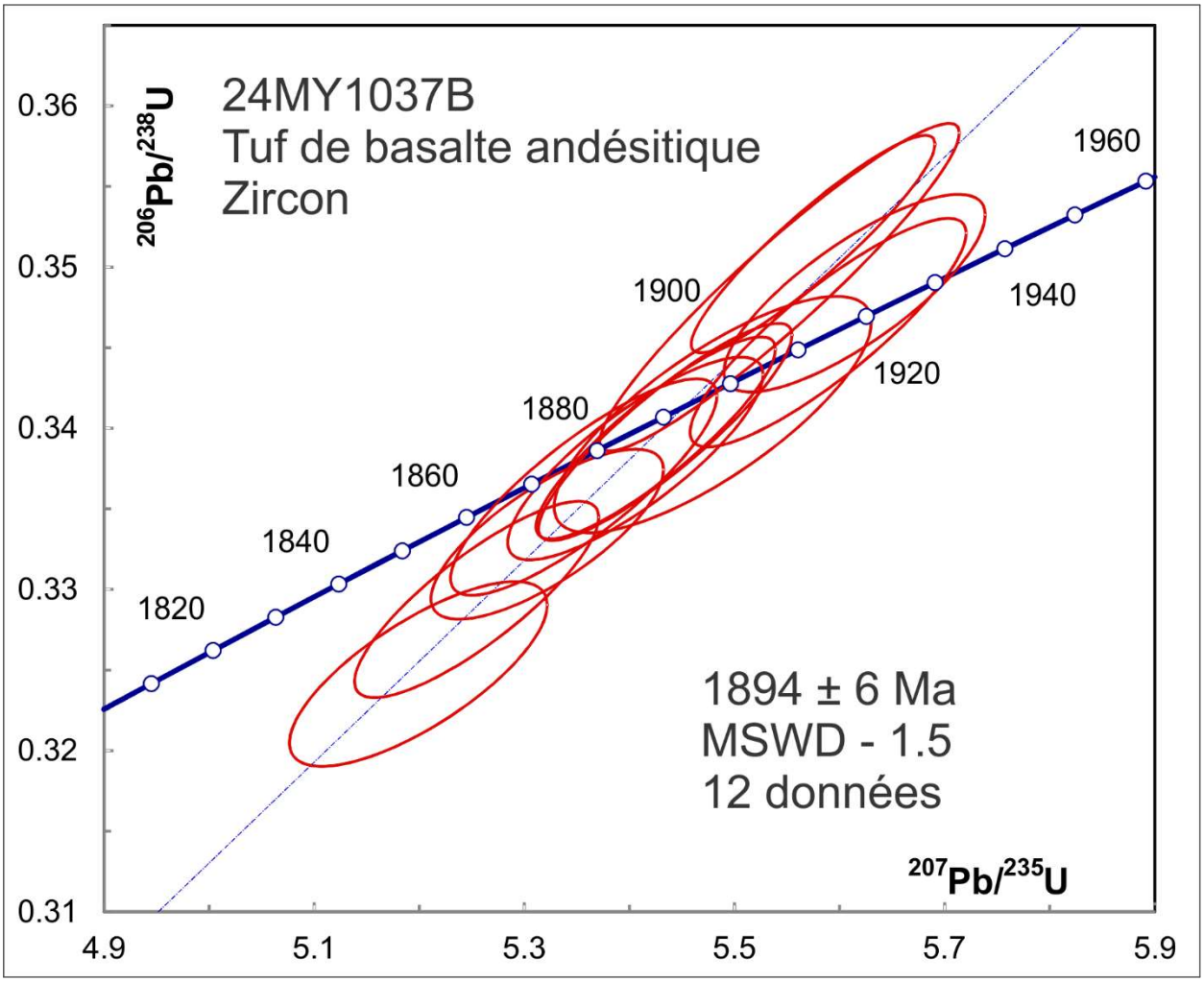

Figure 15-2. Concordia plot showing U-Pb isotopic data on zircon from tuff sample 24-MY-1037-B.

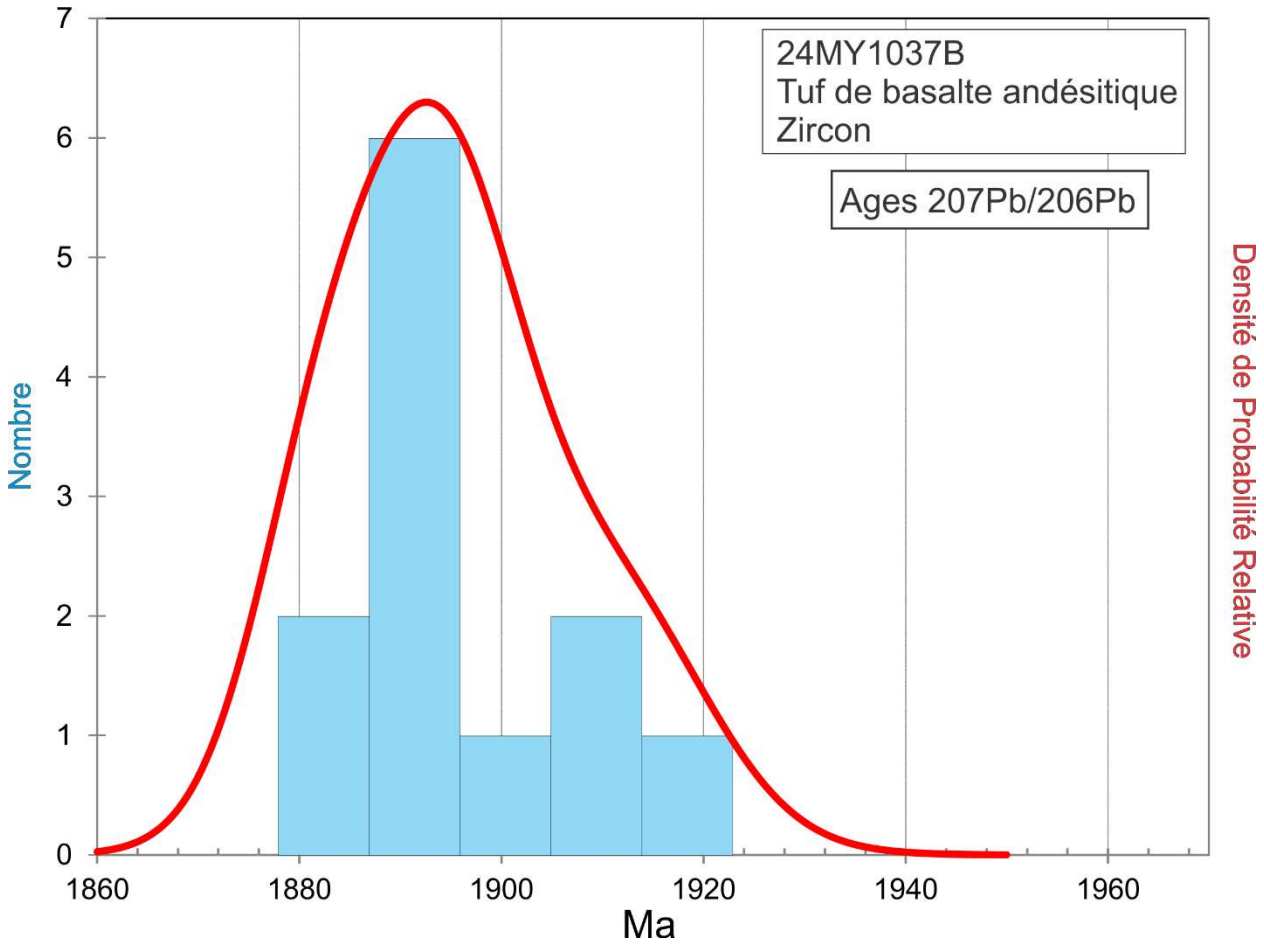

Figure 15-3. Probability density plot of 207Pb/206Pb ages on polished zircon from tuff sample 24-MY-1037-B.

16. 24-TD-2179-A
Wacke métamorphisé, Complexe de Qaaneq (pPqaa1)

This sample yielded a diverse population of zircon grains with variable brownish colouration and euhedral to well-rounded morphology (Fig. 16-1). BSE images show a range of oscillatory to indistinct zoning patterns with some evidence for cores (Fig. 16-2). Only U-Pb analyses that are <10% discordant are considered. These show diverse ages ranging from 1944 ± 32 Ma to 2704 ±12 Ma (Fig. 16-3). A few analyses show Th/U ratios <0.1, so may be from metamorphic zircon but these ages are also diverse and are likely derived from detrital grains. The probability density plot of $^{207}Pb/^{206}Pb$ ages (Fig. 16-4) shows a concentration of provenance ages in the approximate range of 2200-2500 Ma, while there is a near absence of ages older than 2700 Ma. This provenance is not characteristic for Laurentia and may therefore originate in an exotic terrane. A youngest cluster of 5 grains gives a mean age of 1979 ± 13 Ma (MSWD – 1.7) and is the best estimate for a maximum age of deposition.

Figure 16-1. Picked zircon from wacke sample 24-TD-2179-A.

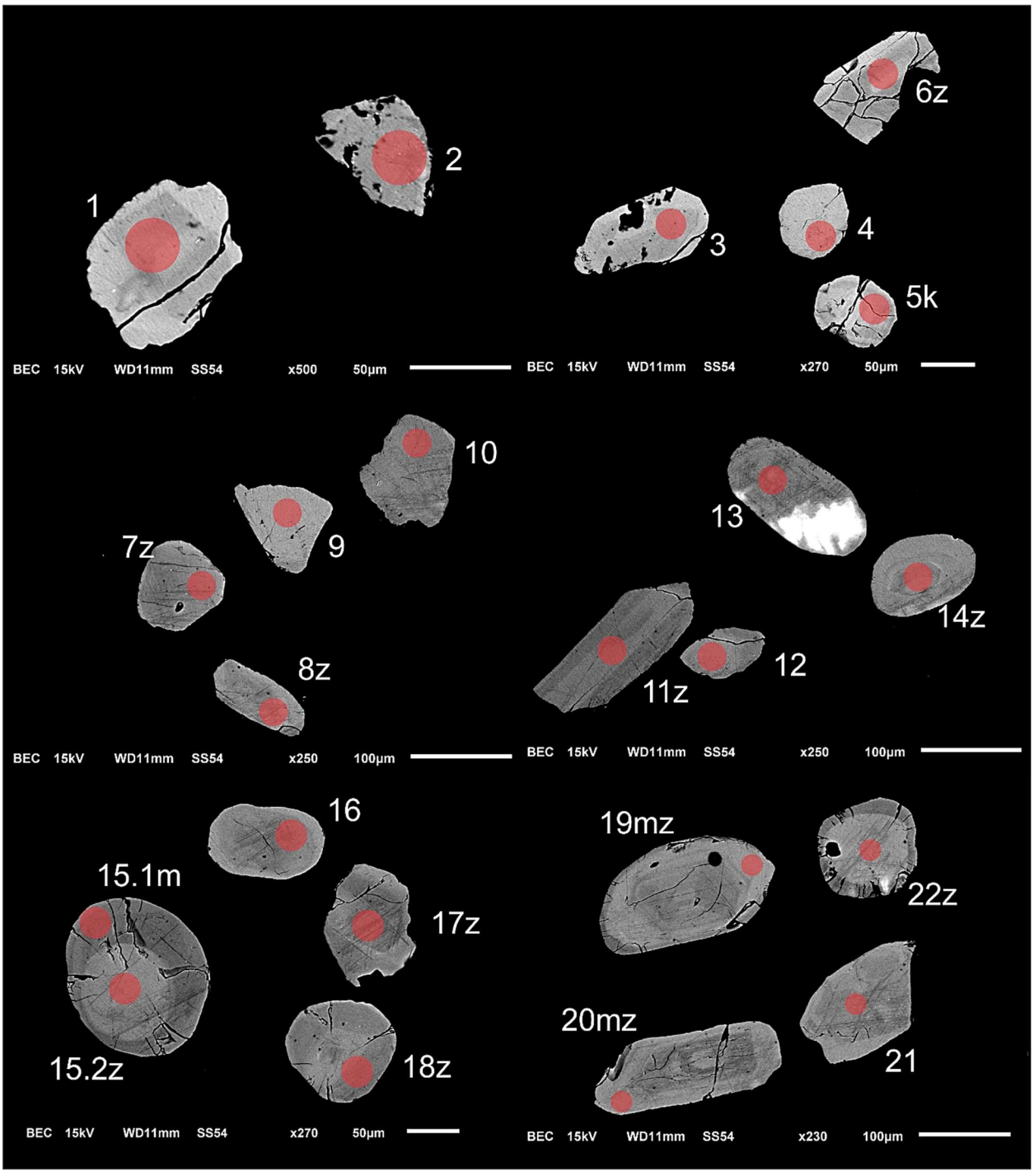

Figure 16-2-1. BSE images of selected grains from sample 24-TD-2179-A. The red circles represent the approximate locations of laser ablation spots.

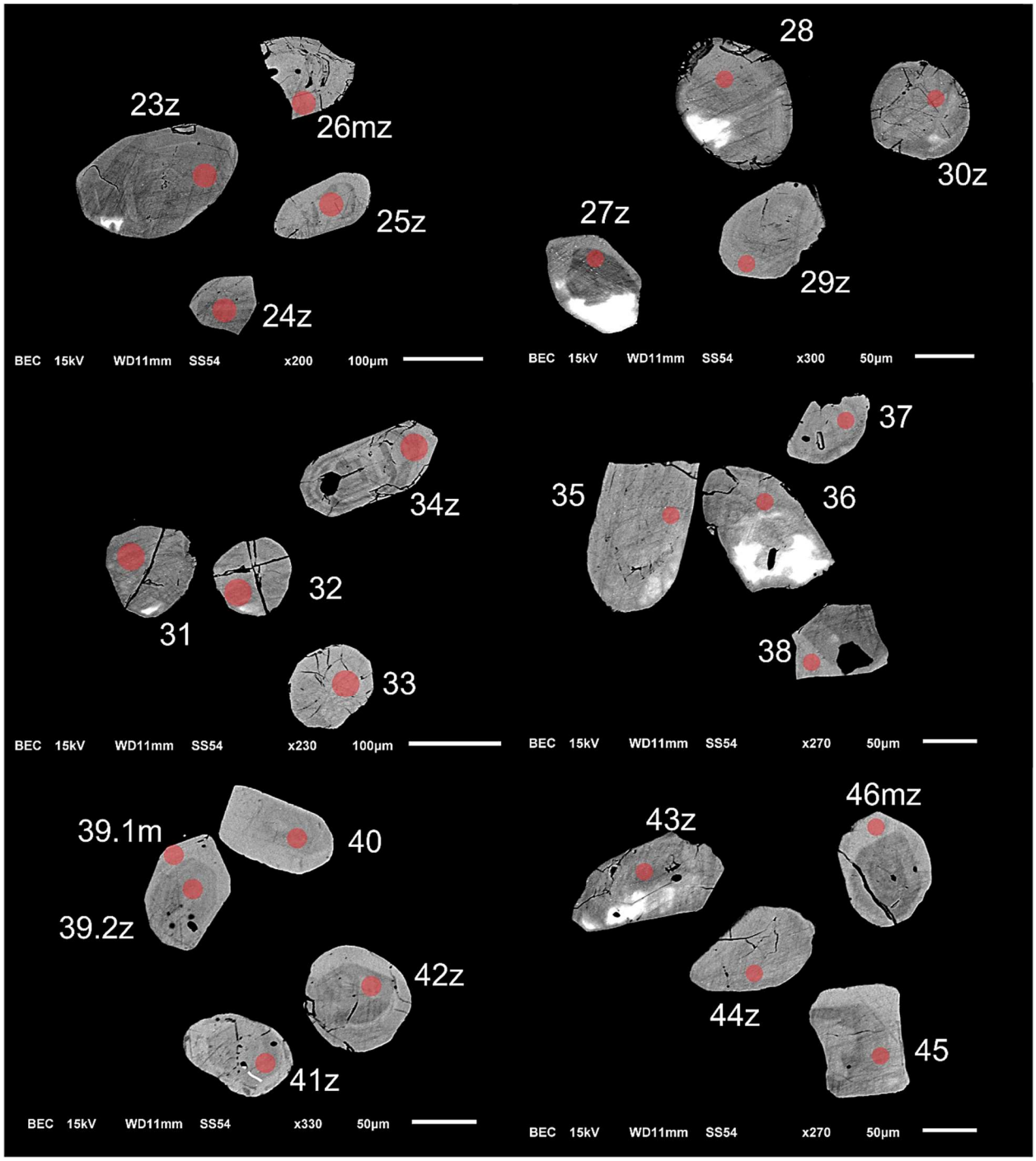

Figure 16-2-2. BSE images of selected grains from sample 24-TD-2179-A. The red circles represent the approximate locations of laser ablation spots.

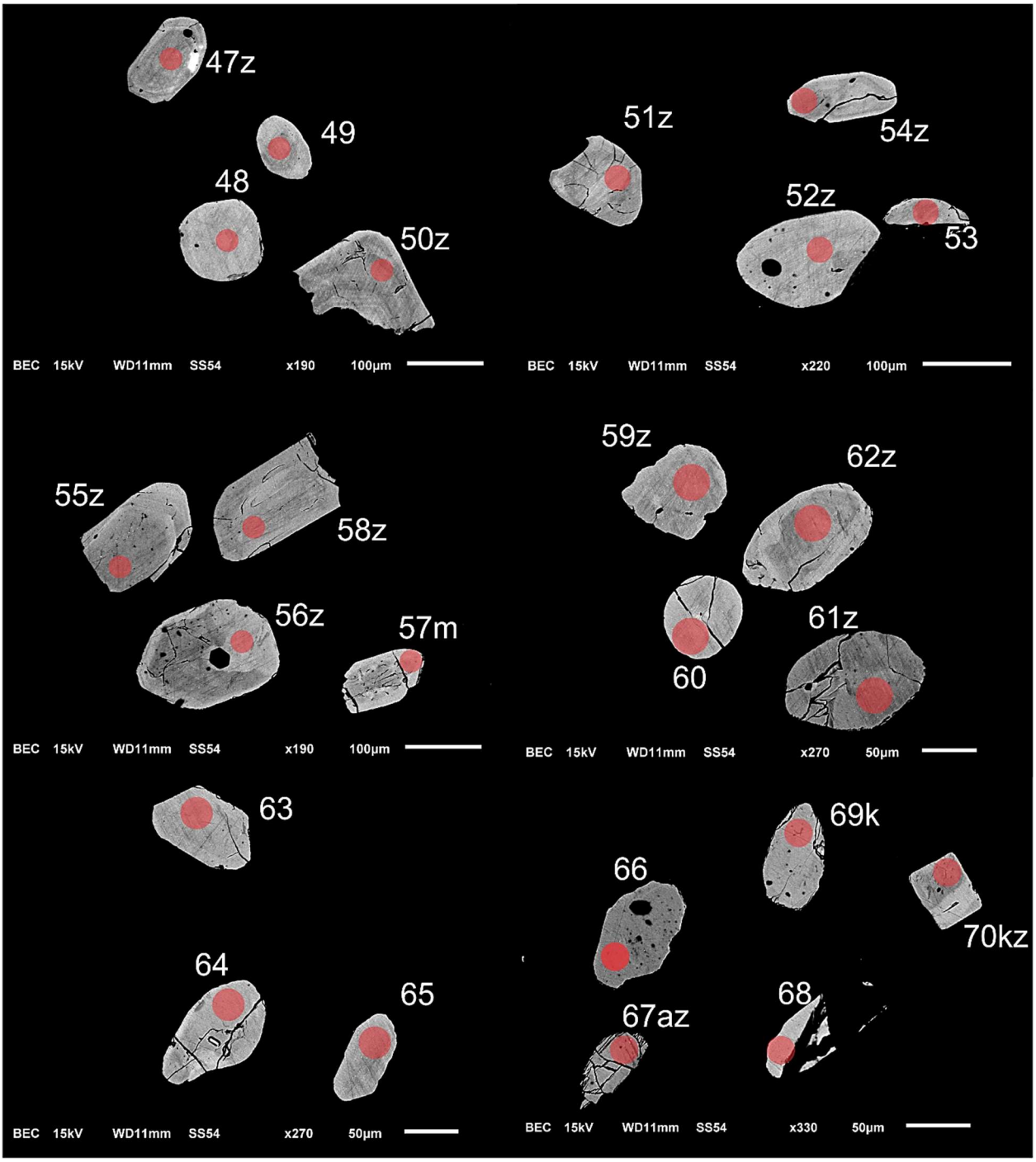

Figure 16-2-3. BSE images of selected grains from sample 24-TD-2179-A. The red circles represent the approximate locations of laser ablation spots.

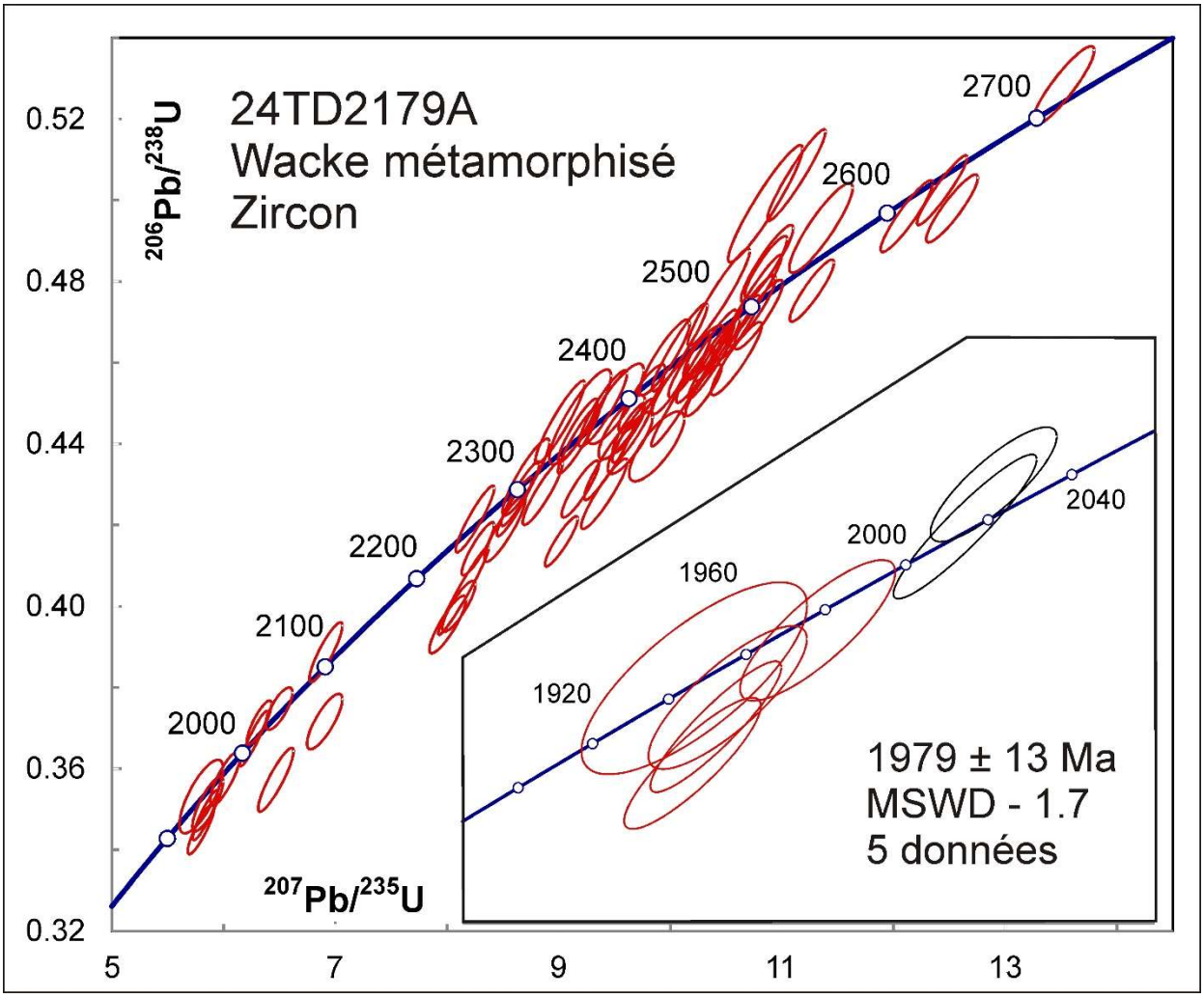

Figure 16-3. Concordia plot showing U-Pb isotopic data on zircon from meta-wacke sample 24-TD-2179-A. Ellipses in black are not included in the average.

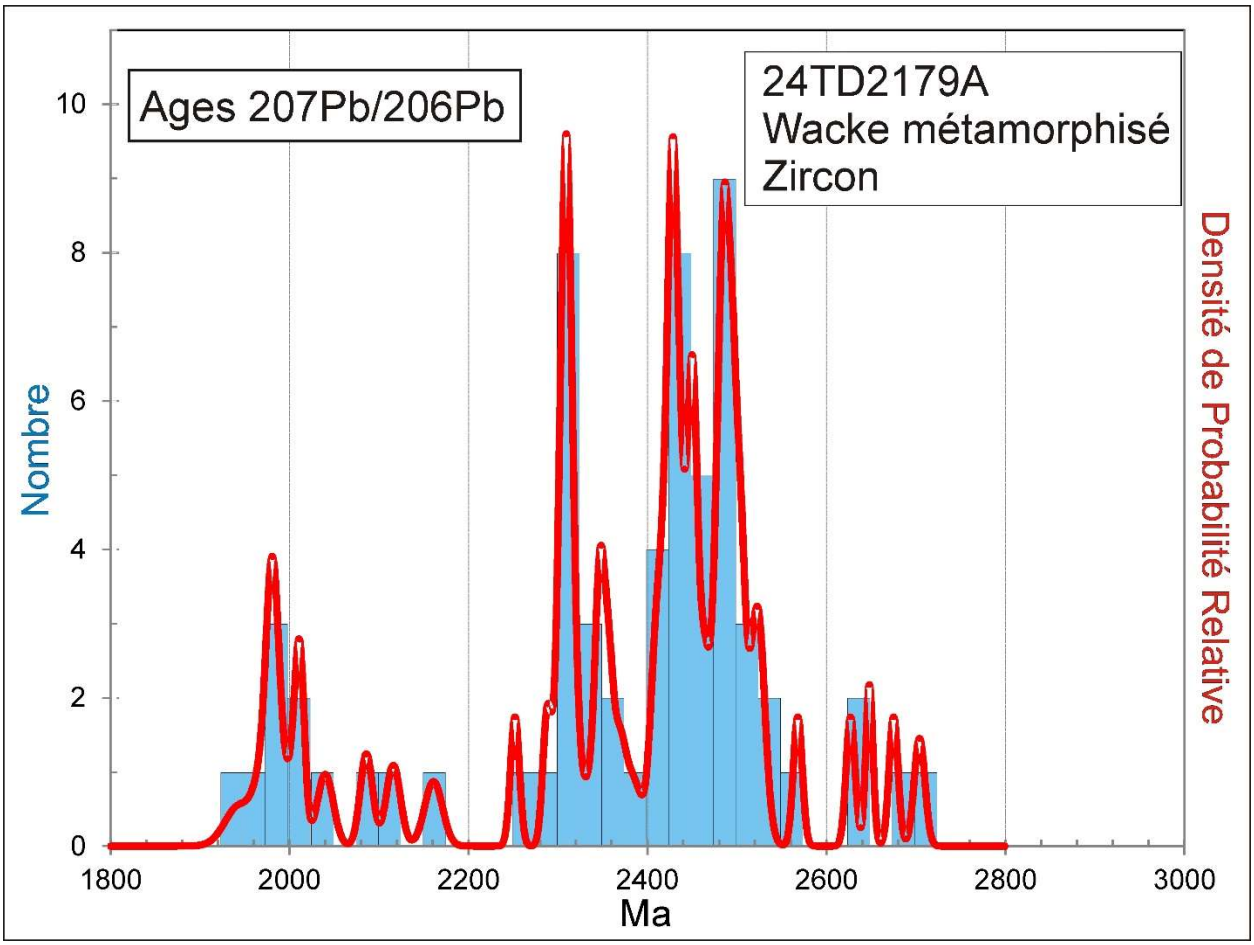

Figure 16-4. Combined age relative probability density plot and histogram showing the distribution of $^{207}Pb/^{206}Pb$ ages on zircon from meta-wacke sample 24-TD-2179-A.

17. 24-TD-2182-A
Paragneiss, Complexe de Qaaneq (pPqaa1)

This sample yielded a diverse population of zircon grains with morphologies varying from stubby multifaceted to long-prismatic (Fig. 17-1). BSE images show oscillatory zoning in some grains, but the most important feature is the presence of thin high-U (bright) overgrowths around some (e.g. grain 20, Fig. 17-2). U-Pb TRA profiles were relatively simple for most grains, which show Paleoproterozoic and late Neoarchean ages similar to wacke 24-TD-2179-A. Both show a major peak at 2310 Ma, which in this case is defined by 9 data with a mean of 2312 ± 4 Ma (MSWD – 0.6, Fig. 17-3 and Fig. 17-4), but the prominent earliest Paleoproterozoic peak seen in the wacke sample above at around 2430 Ma (Fig 17-4) is not evident here. Some analyses show increases in Th/U from <0.1 to magmatic values, confirming the presence of thin metamorphic rims. The youngest analysis from one of these rims (spot 20.2) gives a near-concordant datum with an age of 1861 ± 44 Ma. This is the best estimate for the age of the formation of the paragneiss, whereas the older analyses correspond to detrital zircon, which may or may not have been partially reset.

This sample also contains small grains of monazite, which are not easy to visually distinguish from zircon. Two small data sets were measured that include some detrital zircon but also an apparent metamorphic zircon rim phase with an age of 1887 ± 30 Ma. Together with the age on a similar phase from the zircon data set, this defines a mean age of 1879 ± 24 Ma for metamorphic zircon. The 10 monazite analyses define a spread of ages well outside of analytical error from 1876 ± 10 Ma to 1895 ± 12 Ma (Fig. 17-5), suggesting that monazite crystallization was a protracted process that may have occurred over a period of at least 20 Ma.

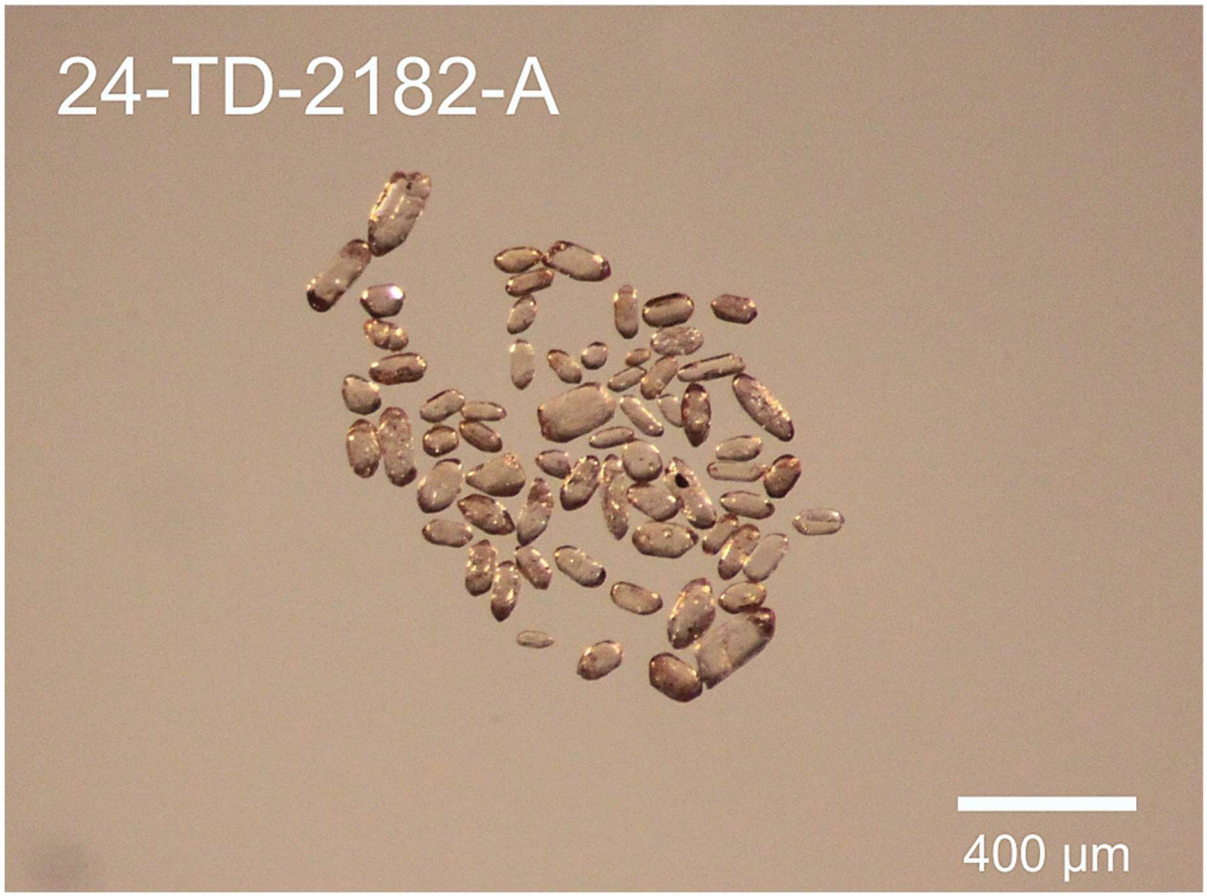

Figure 17-1. Picked zircon from paragneiss sample 24-TD-2182-A.

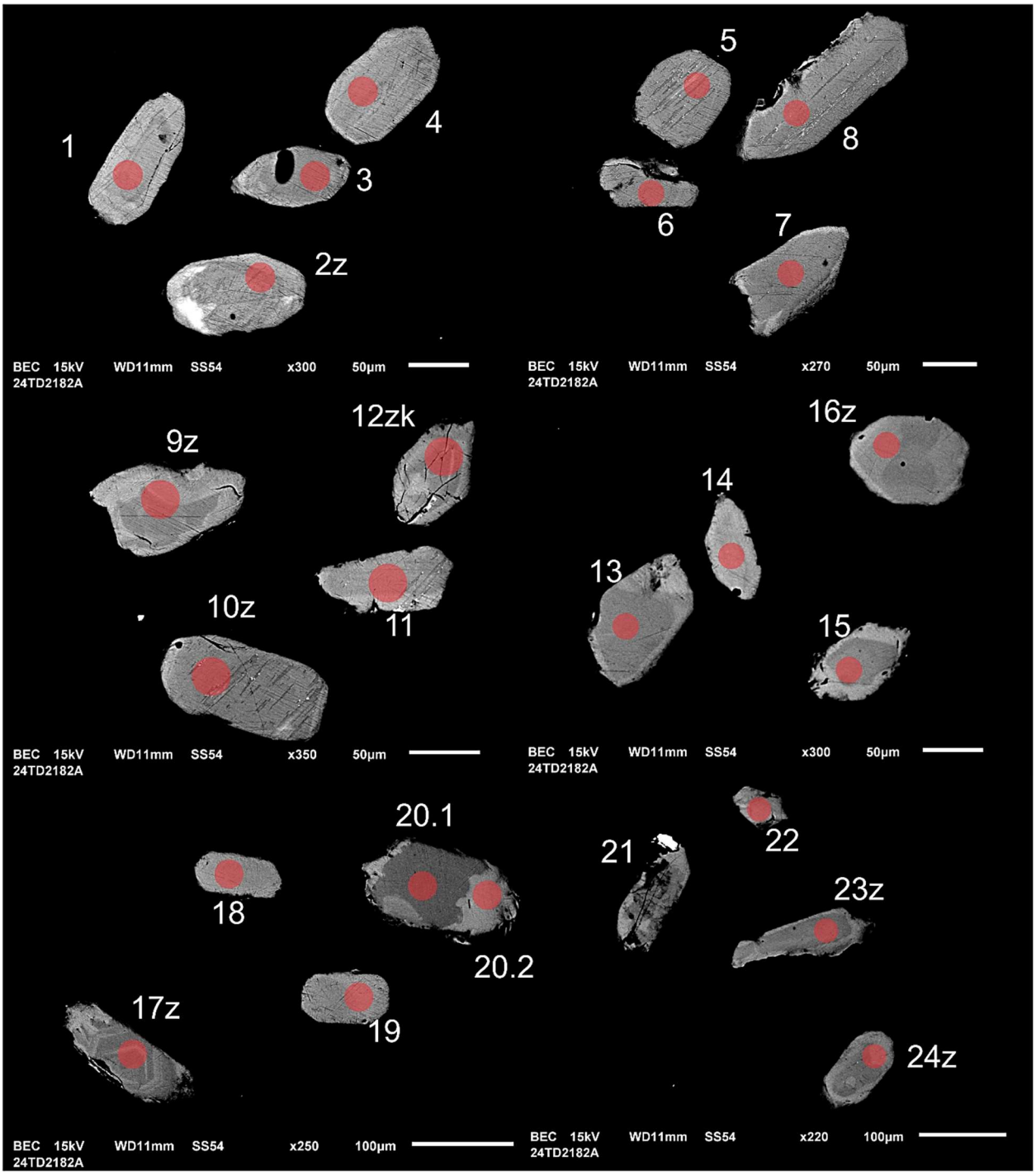

Figure 17-2-1. BSE images of selected grains from sample 24-TD-2182-A. The red circles represent the approximate locations of laser ablation spots.

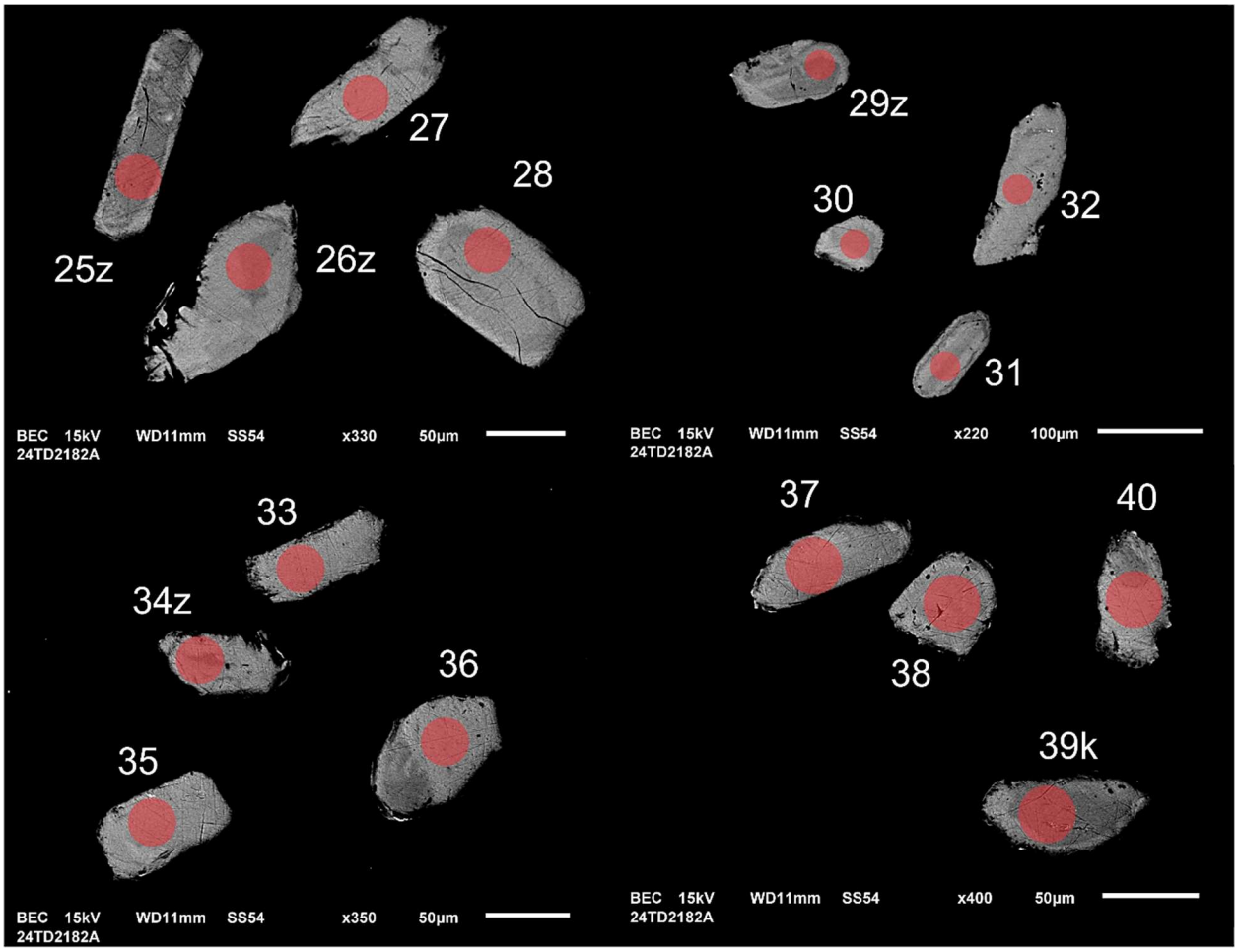

Figure 17-2-2. BSE images of selected grains from sample 24-TD-2182-A. The red circles represent the approximate locations of laser ablation spots.

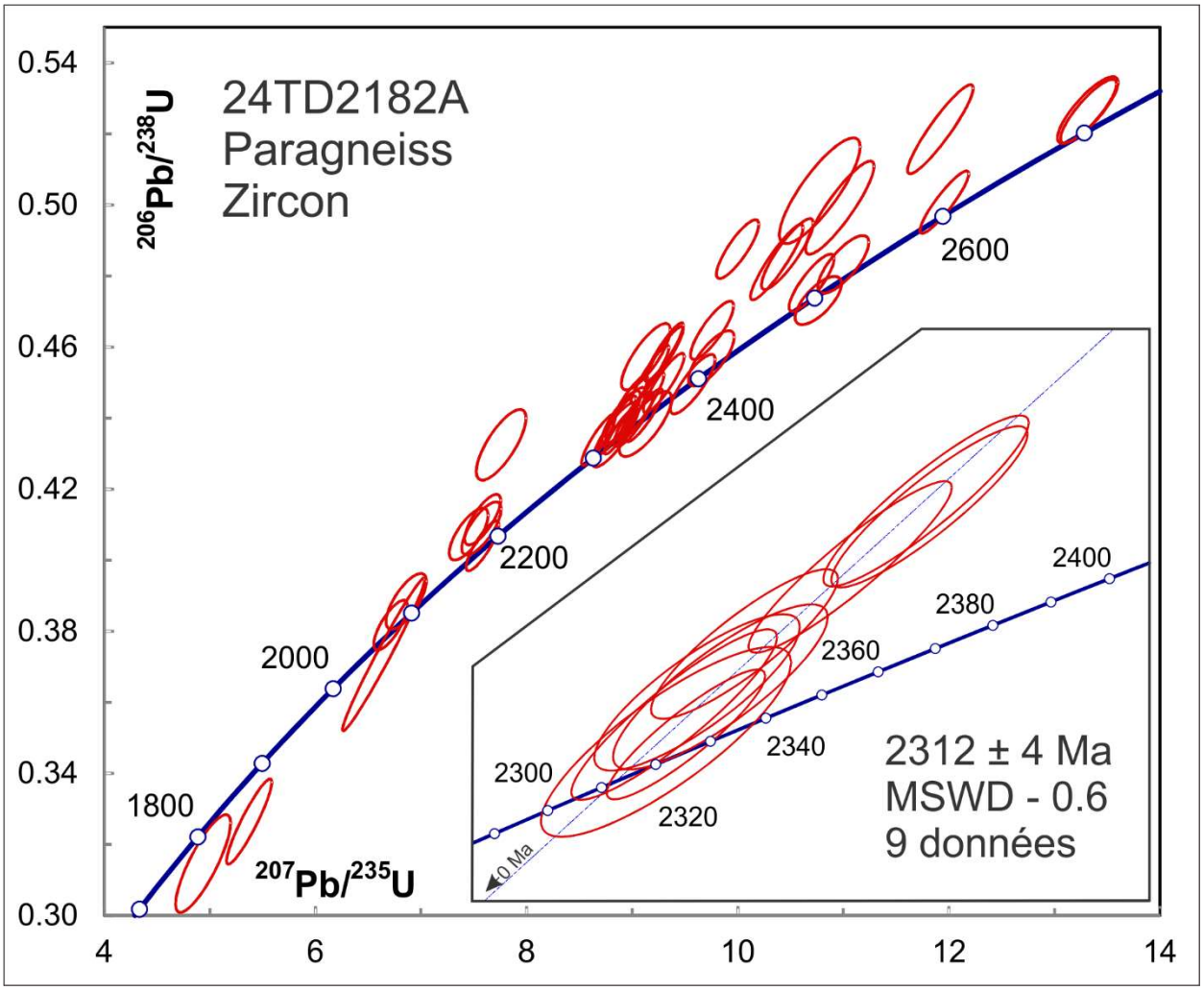

Figure 17-3. Concordia plot showing U-Pb isotopic data on zircon from sample 24-TD-2182-A. Insert is a blow-up of the Paleoproterozoic cluster.

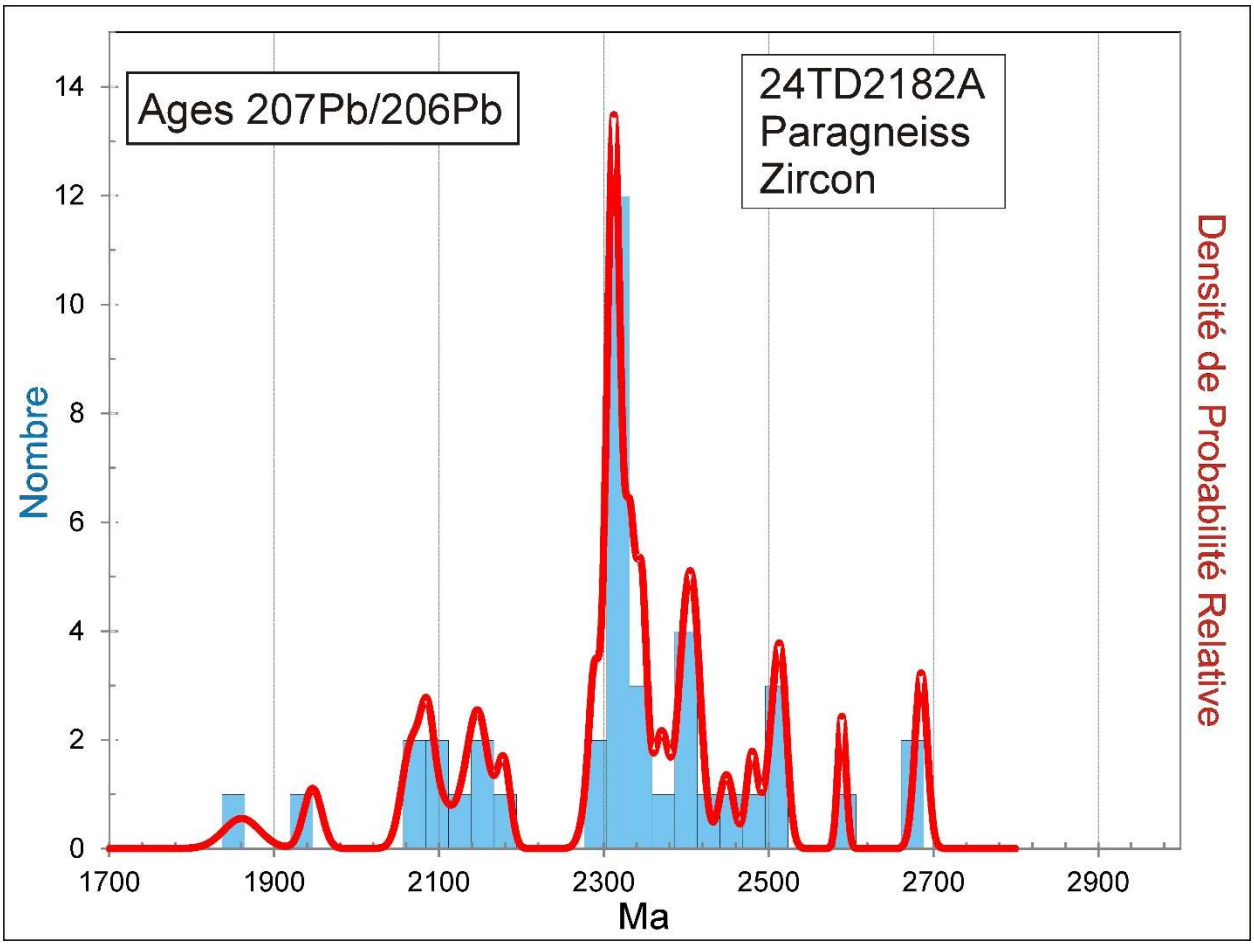

Figure 17-4. Combined age relative probability density plot and histogram showing the distribution of $^{207}Pb/^{206}Pb$ ages on zircon from sample 24-TD-2182-A.

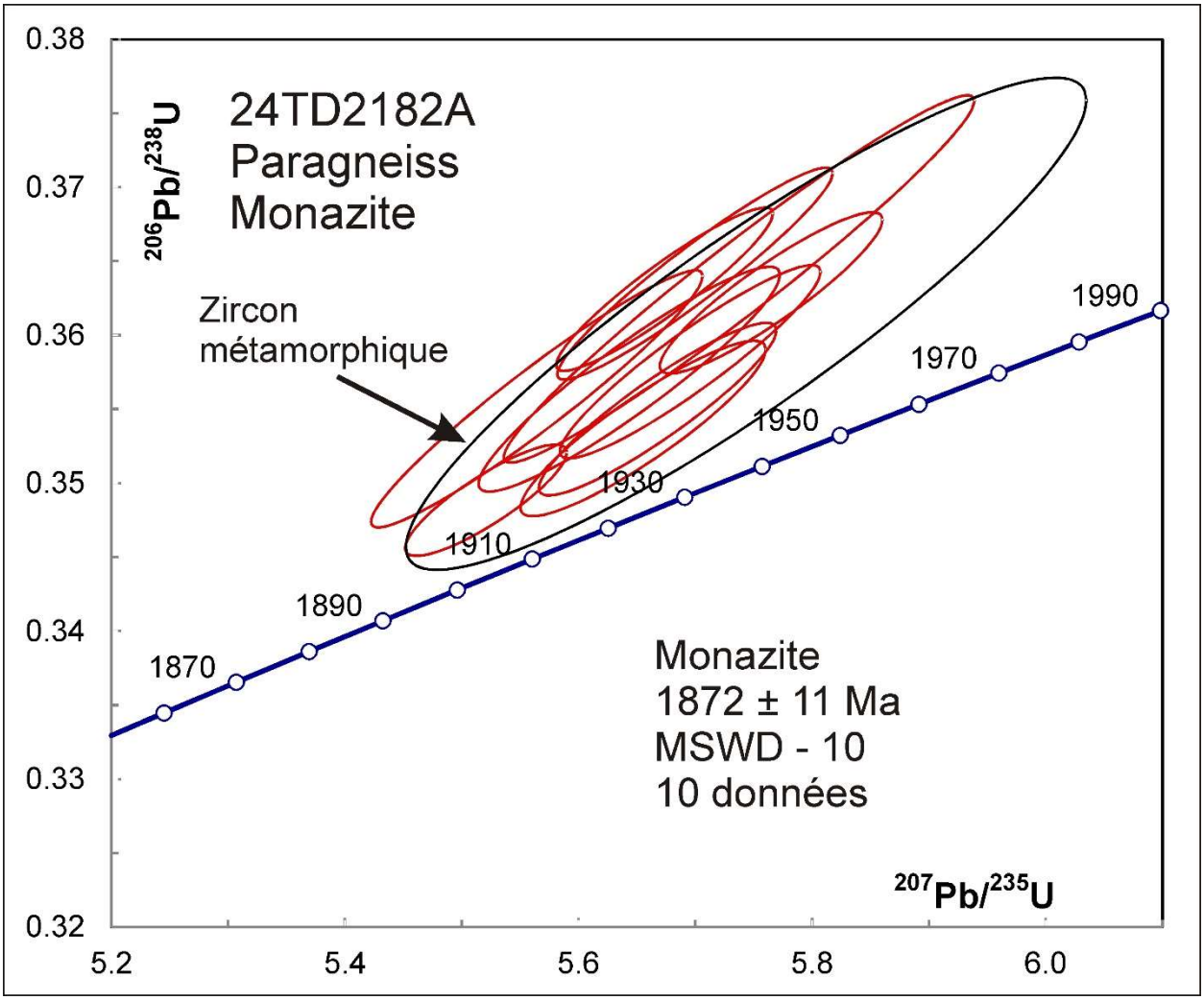

Figure 17-5. Concordia plot showing U-Pb isotopic data on monazite and one metamorphic zircon grain from sample 24-TD-2182-A.

18. 24-TD-2180-A
Tonalite, Pluton de Pingasulik (pPpig)

This sample yielded a diverse population of zircon grains with morphologies varying from stubby multi-facetted to long-prismatic (Fig. 18-1). BSE images show a variety of zoning patterns with some grains possibly having cores (Fig. 18-2). U-Pb analyses show a range of ages from about 1850 Ma to 2660 Ma but most magmatic grains cluster around an age of 1876 ± 4 Ma (MSWD – 2.5) although they scatter somewhat outside of error (Fig. 18-3). This is most likely the age of crystallization of the pluton. A single youngest analysis gives an age of 1854 ±12 Ma (spot 1) but this was measured on a uniform domain with Th/U < 0.1, which might represent a metamorphic phase. The presence of this grain suggests that the granodiorite may have crystallized at depth under metamorphic conditions. Older ages may be inherited from the protolith to the tonalite magma. Notably, these include a single Neoarchean grain and a cluster of 6 grains, 4 of which scatter within error of 2370 ± 7 Ma (MSWD – 0.5).

U-Pb analyses of titanite from this rock give slightly discordant data with $^{207}Pb/^{206}Pb$ ages that scatter over the approximate range 1880-2040 Ma (Fig. 18-4). This is most likely due to small amounts of common Pb, but it could also reflect Pb loss from much older titanite. The pluton might be a remobilized Archean body but this would require a large proportion of partial melting to explain the Paleoproterozoic magmatic zircon.

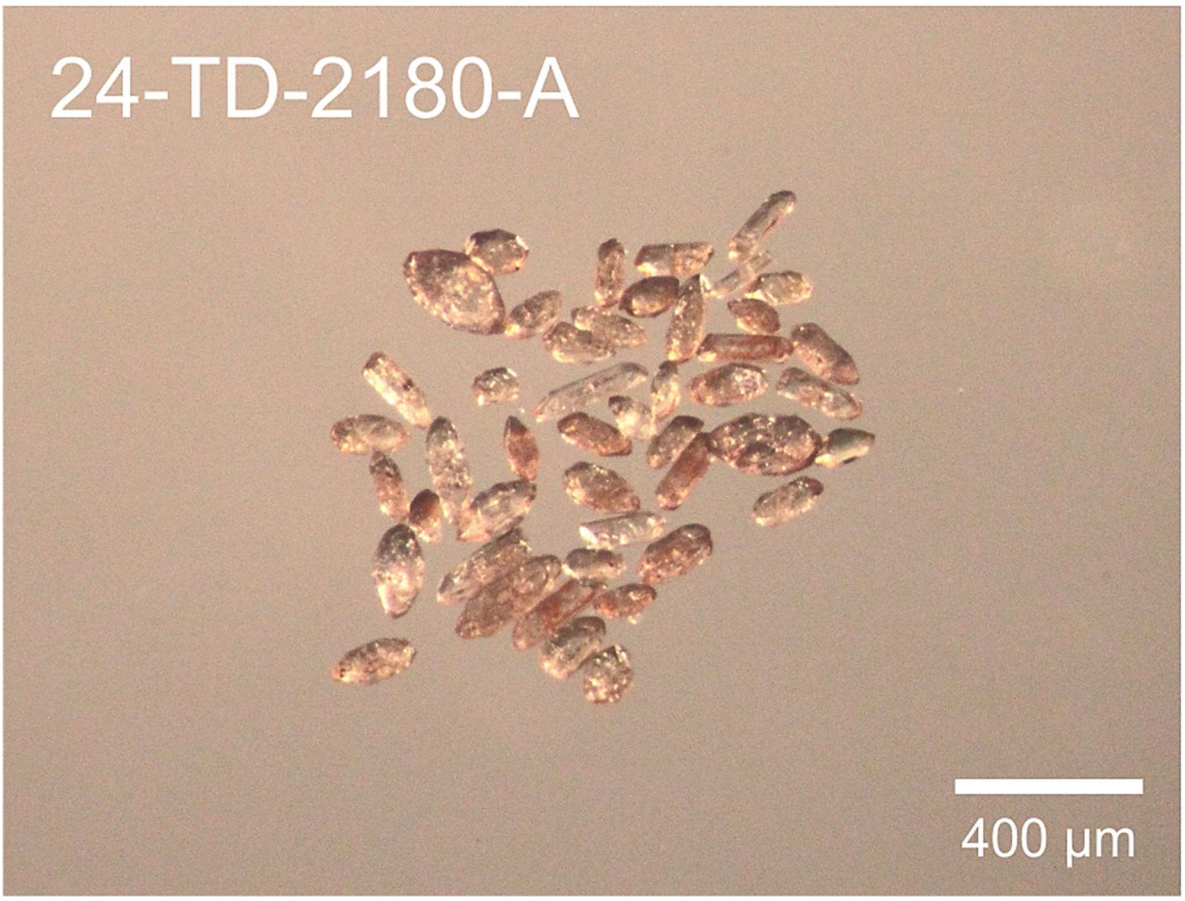

Figure 18-1. Picked zircon from tonalite sample 24-TD-2180-A.

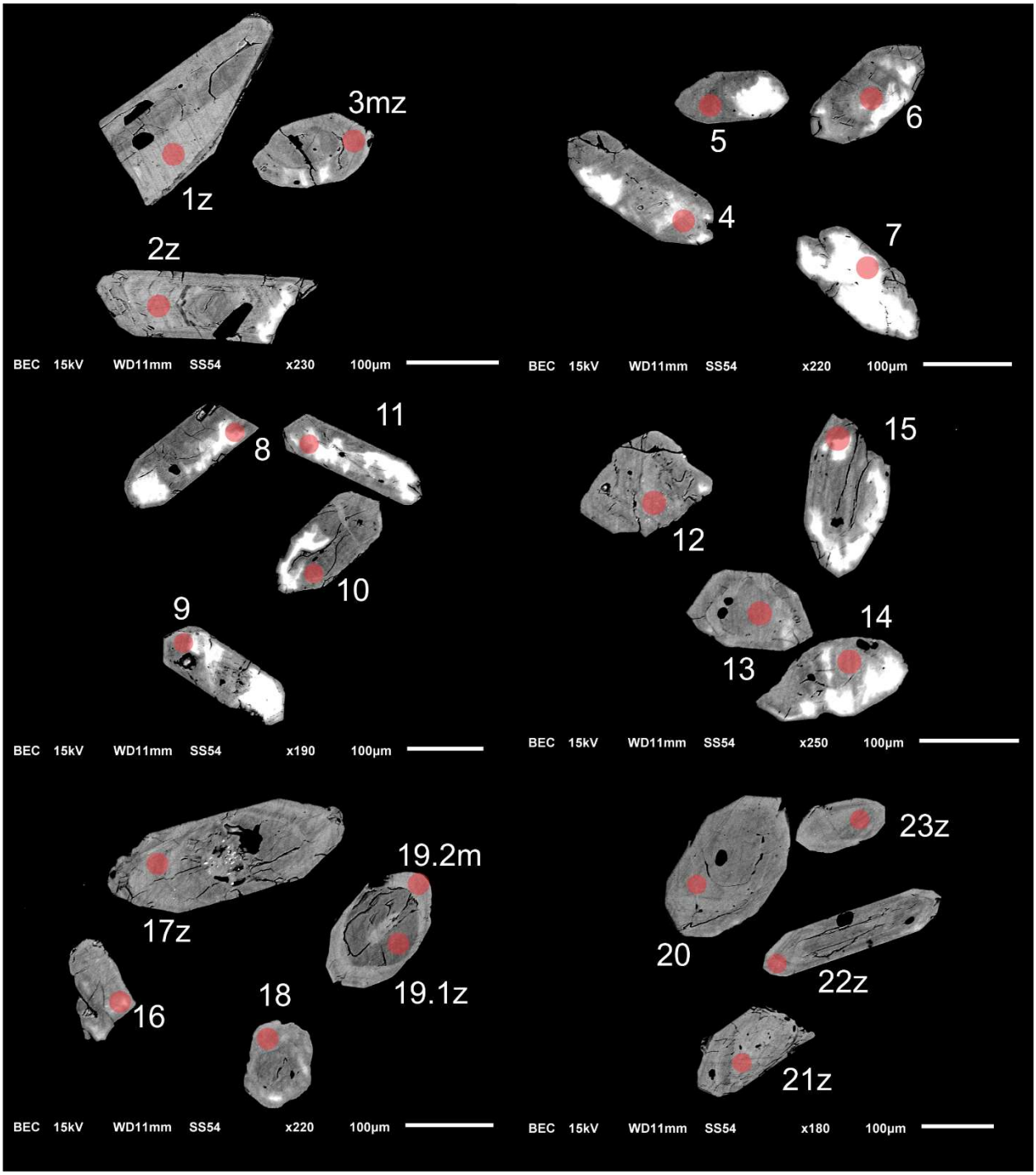

Figure 18-2-1. BSE images of selected grains from sample 24-TD-2180-A. The red circles represent the approximate locations of laser ablation spots.

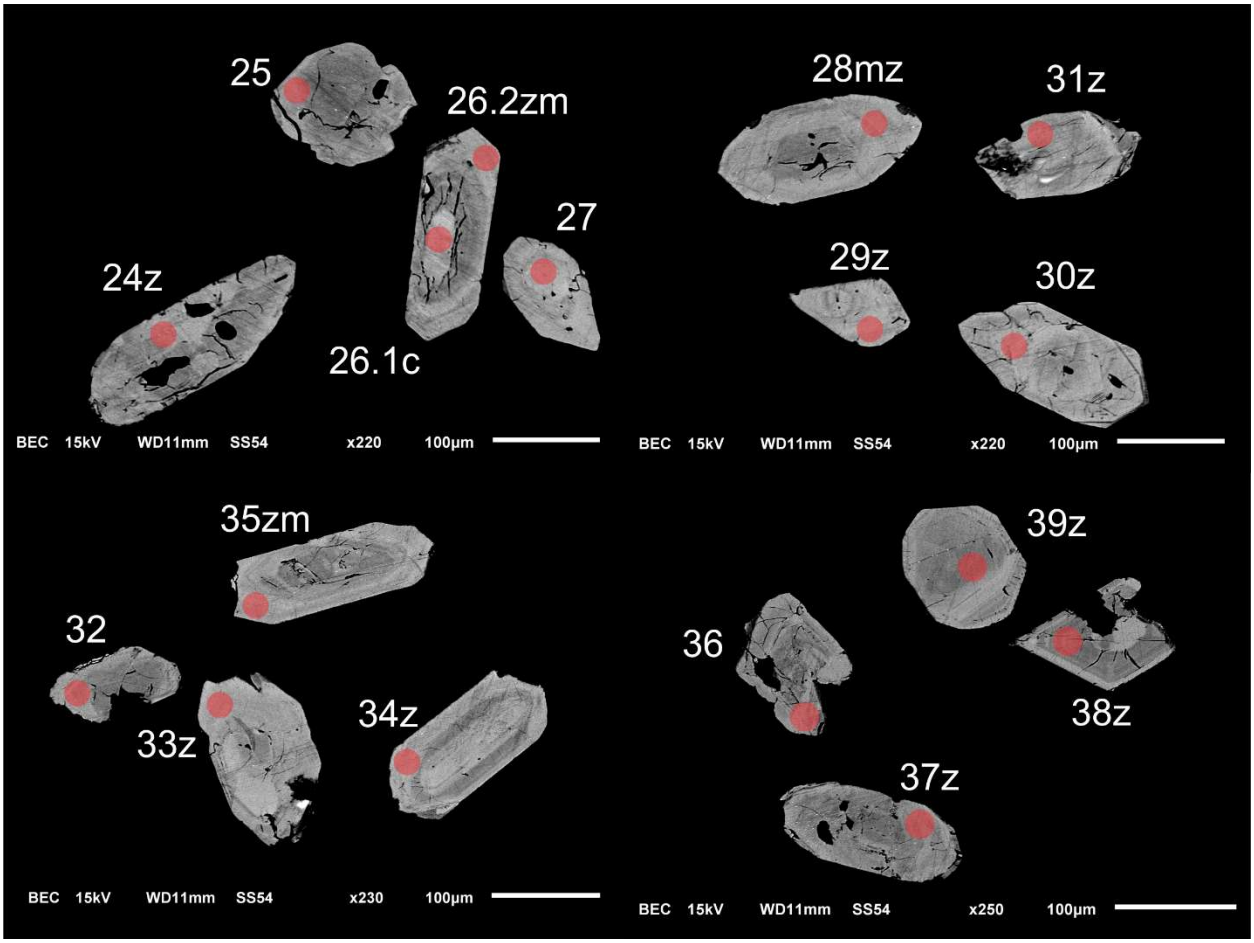

Figure 18-2-2. BSE images of selected grains from sample 24-TD-2180-A. The red circles represent the approximate locations of laser ablation spots.

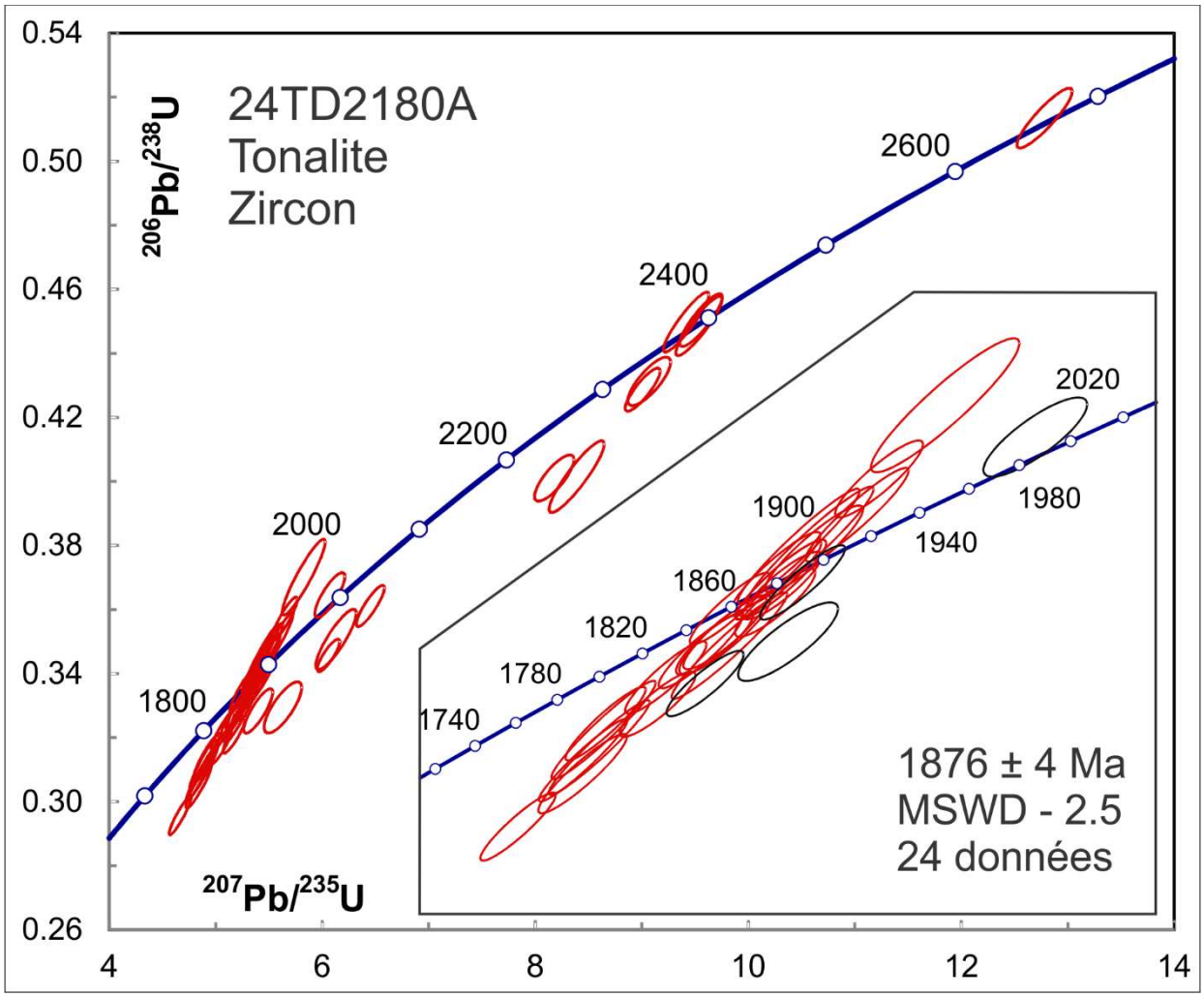

Figure 18-3. Concordia plot showing U-Pb isotopic data on zircon from sample 24-TD-2180-A. Black ellipses in the blow-up are omitted from the average.

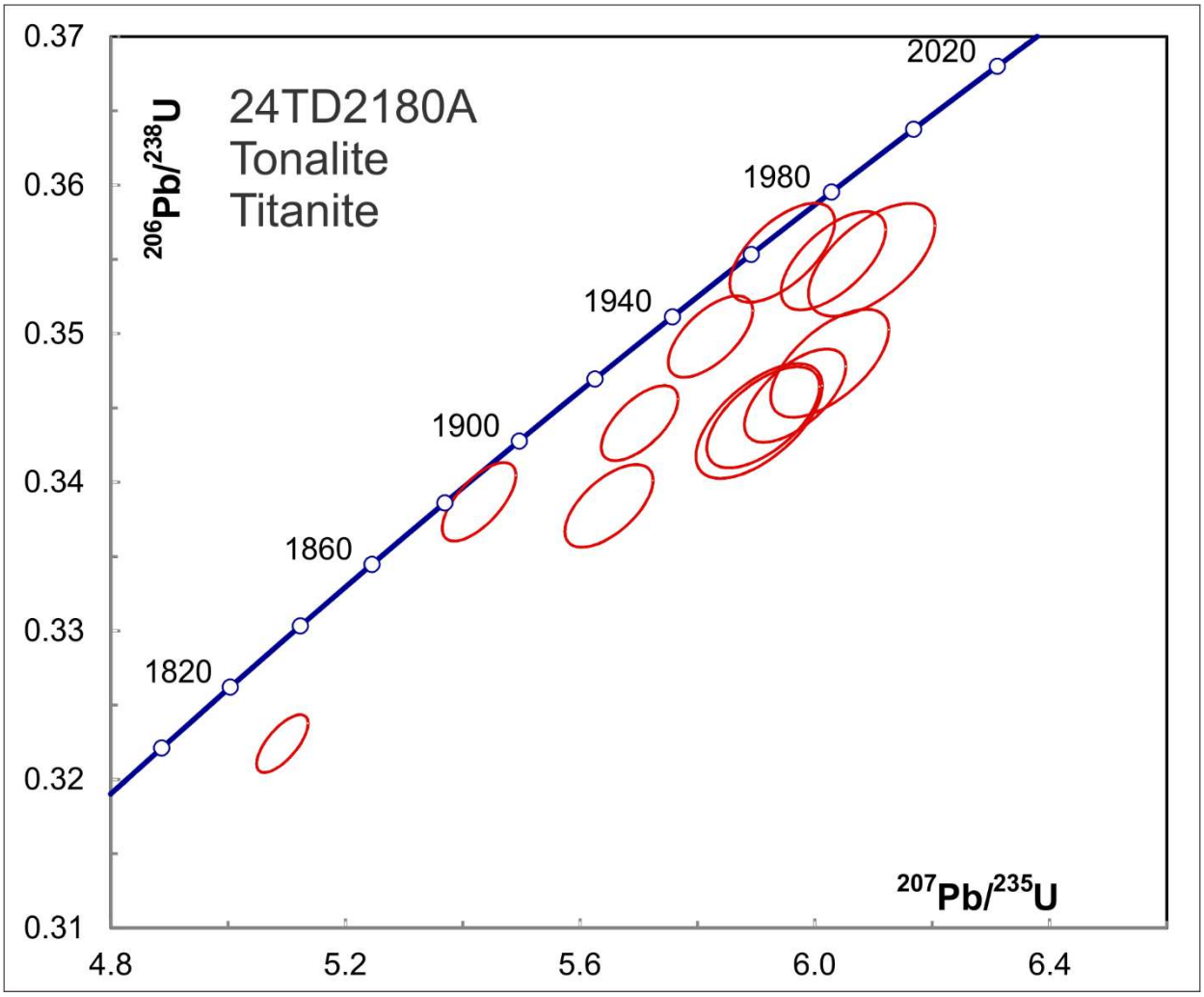

Figure 18-4. Concordia plot showing U-Pb isotopic data on titanite from sample 24-TD-2180A.

19. 24-MY-1140-A
Granodiorite, Pluton de Qimiujait (pPqmi)

This sample yielded abundant zircon as subhedral to rounded grains (Fig. 19-1). BSE images show a variety of zoning patterns with no clear evidence of cores although some grains show rims that are too thin to analyze (Fig. 19-2). U-Pb analyses show a single clearly inherited grain with an age of 2351 ± 12 Ma (Fig 19-3). Most other analyses cluster within error of 1885 ± 4 Ma (MSWD – 1.2), which is the best estimate for the age of crystallization of the granodiorite. A few spots give slightly older ages around 1950 Ma and may suggest protracted crystallization or inheritance from slightly older phases.

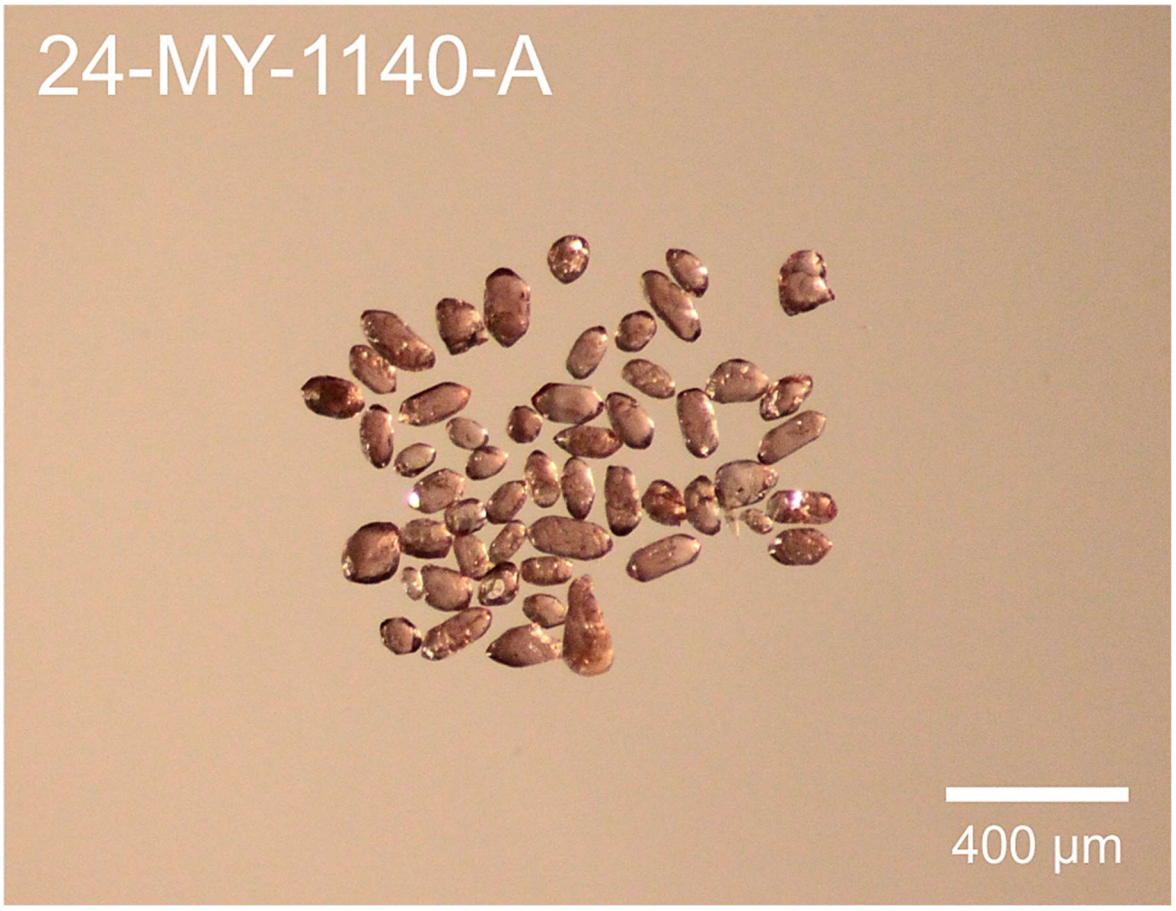

Figure 19-1. Picked zircon from granodiorite sample 24-MY-1140-A.

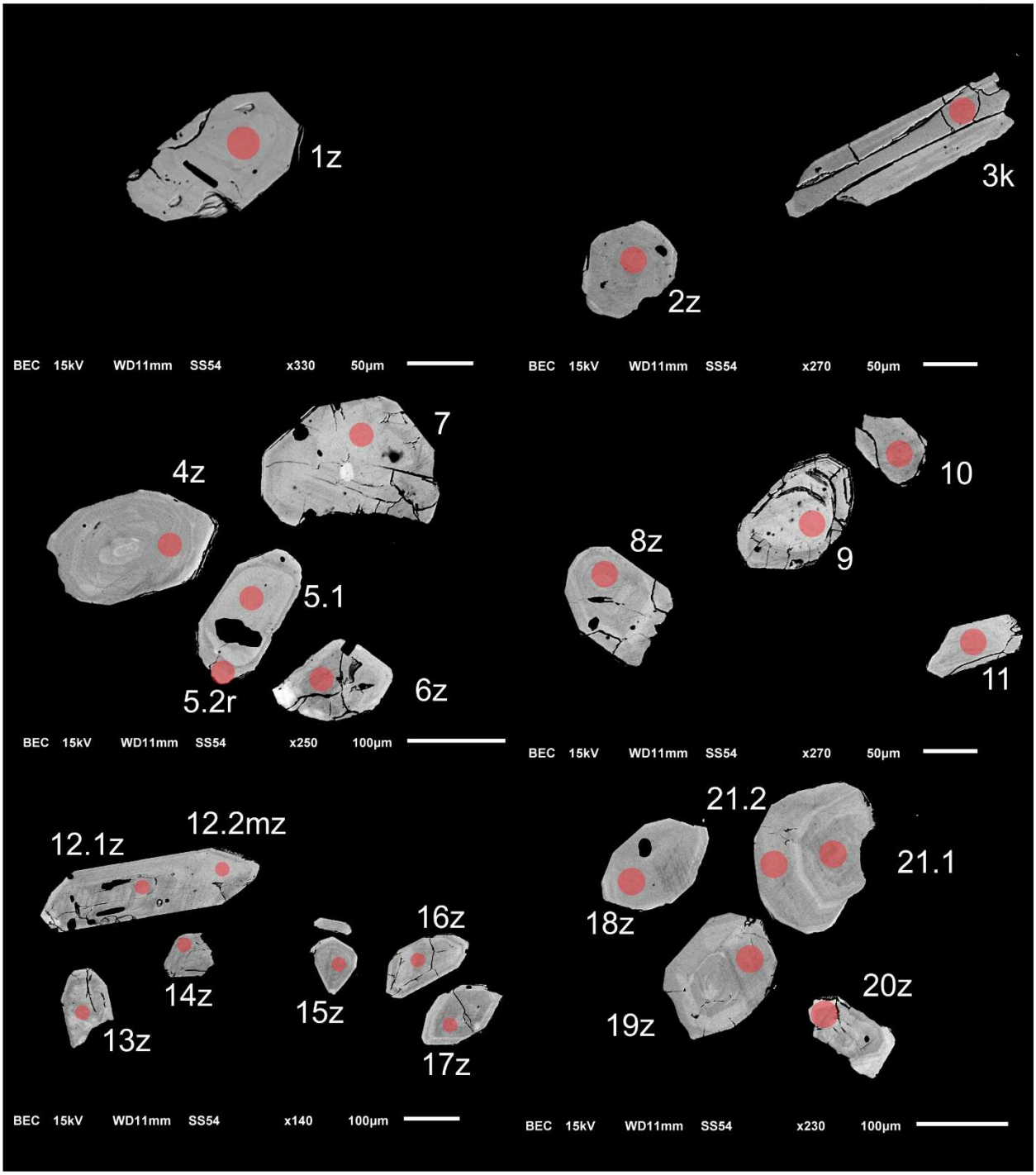

Figure 19-2-1. BSE images of selected grains from sample 24-MY-1140-A. The red circles represent the approximate locations of laser ablation spots.

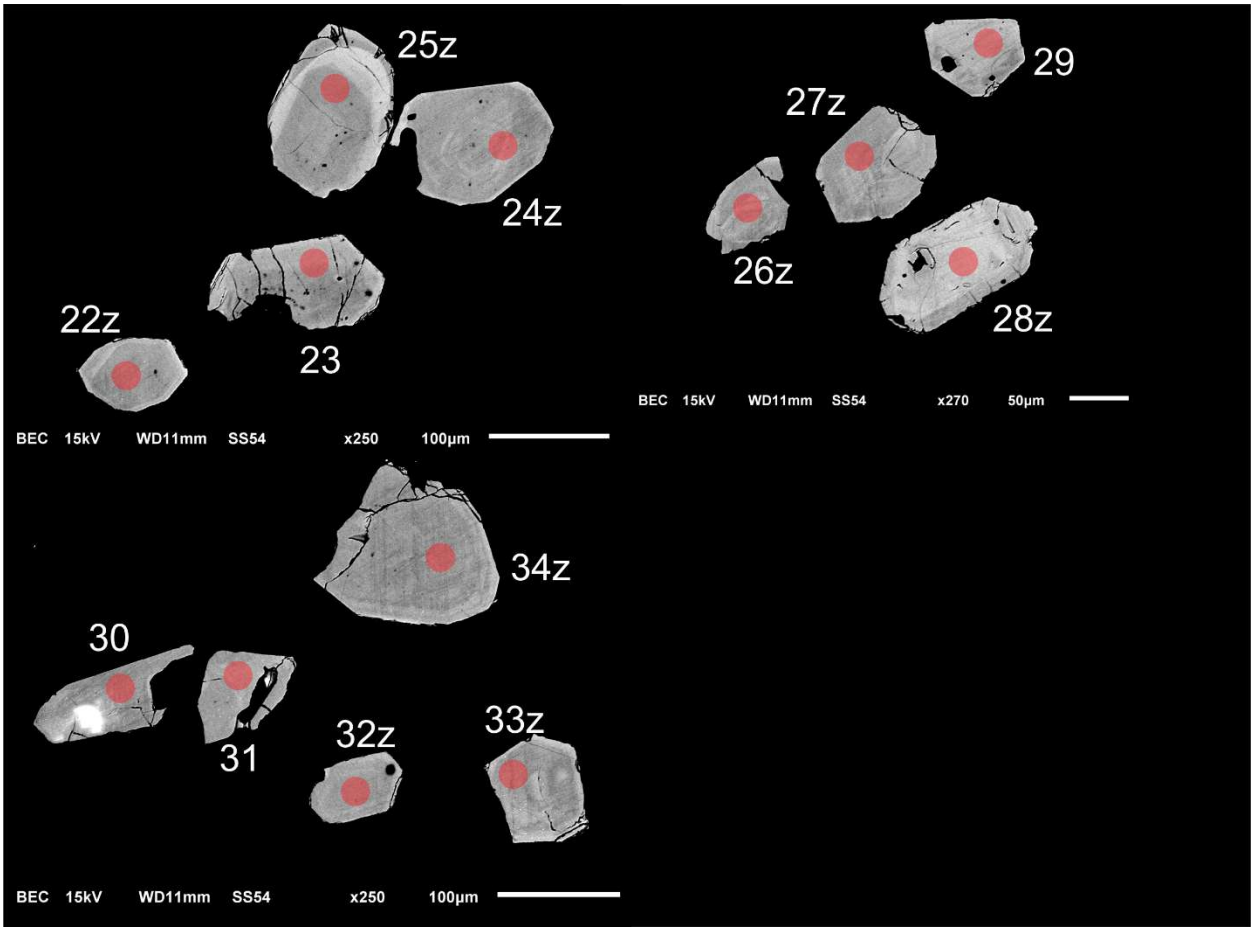

Figure 19-2-2. BSE images of selected grains from sample 24-MY-1140-A. The red circles represent the approximate locations of laser ablation spots.

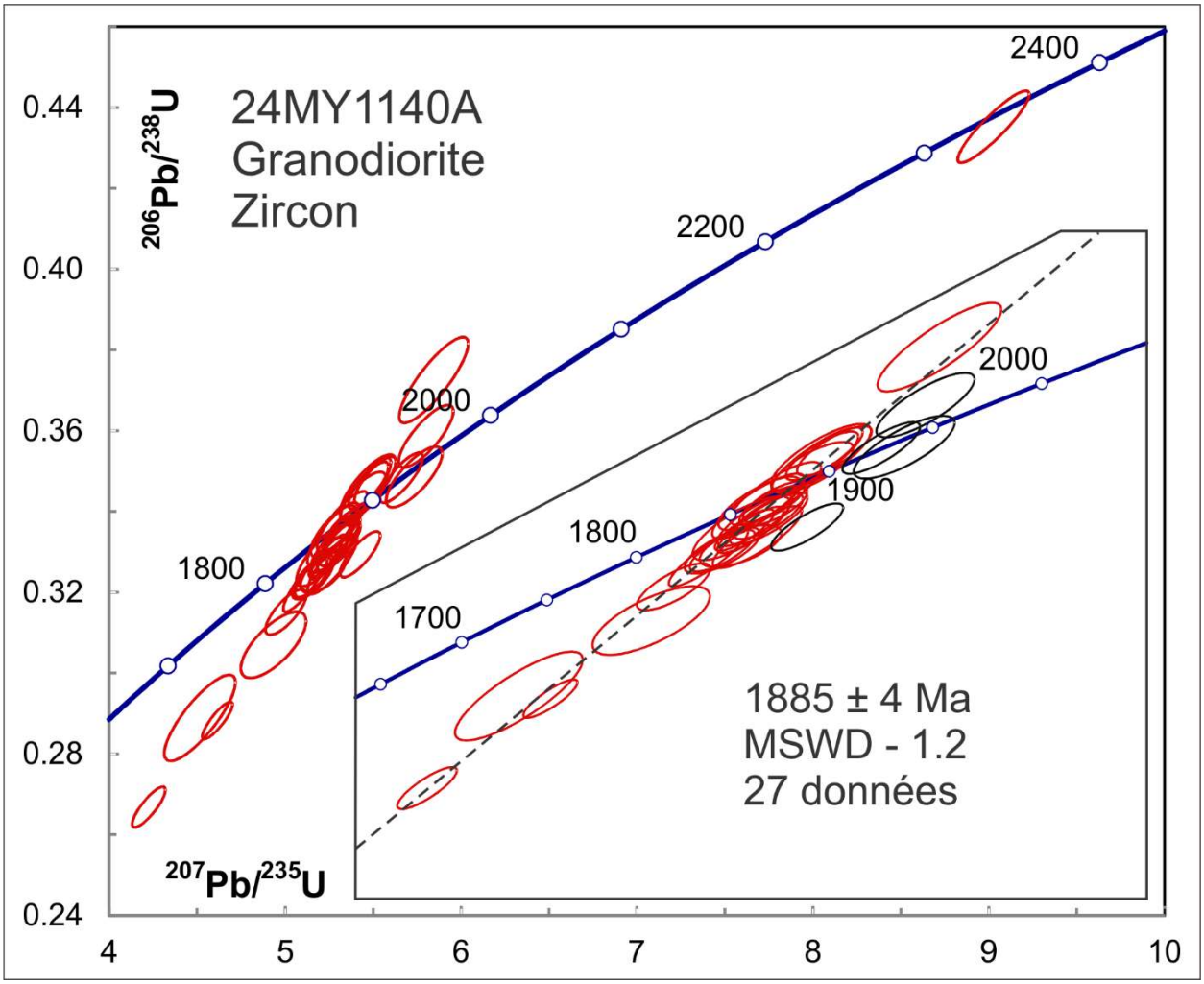

Figure 19-3. Concordia plot showing U-Pb isotopic data on zircon from sample 24-MY-1140-A.

20. 24-AO-4150-A
Diorite, Pluton d'Ulluvinaaluit (pPull)

This sample yielded a small amount of zircon consisting of fragments and short-prismatic rounded grains (Fig. 20-1). BSE images are generally uniform showing an absence of zoning without evidence of rims or cores (Fig. 20-2). U-Pb analyses show a unimodal distribution of ages (Figs. 20-3 and 20-4). $^{207}Pb/^{206}Pb$ ages cluster approximately within error with a mean age of 1856 ± 5 Ma (MSWD – 1.5) (Fig. 20-3). This is the best estimate for crystallization of the zircon which shows fairly uniform Th/U ratios of about 0.3. Metamorphic zircon crystallized under granulite conditions can have Th/U>0.1 so this may represent crystallization under high-grade conditions.

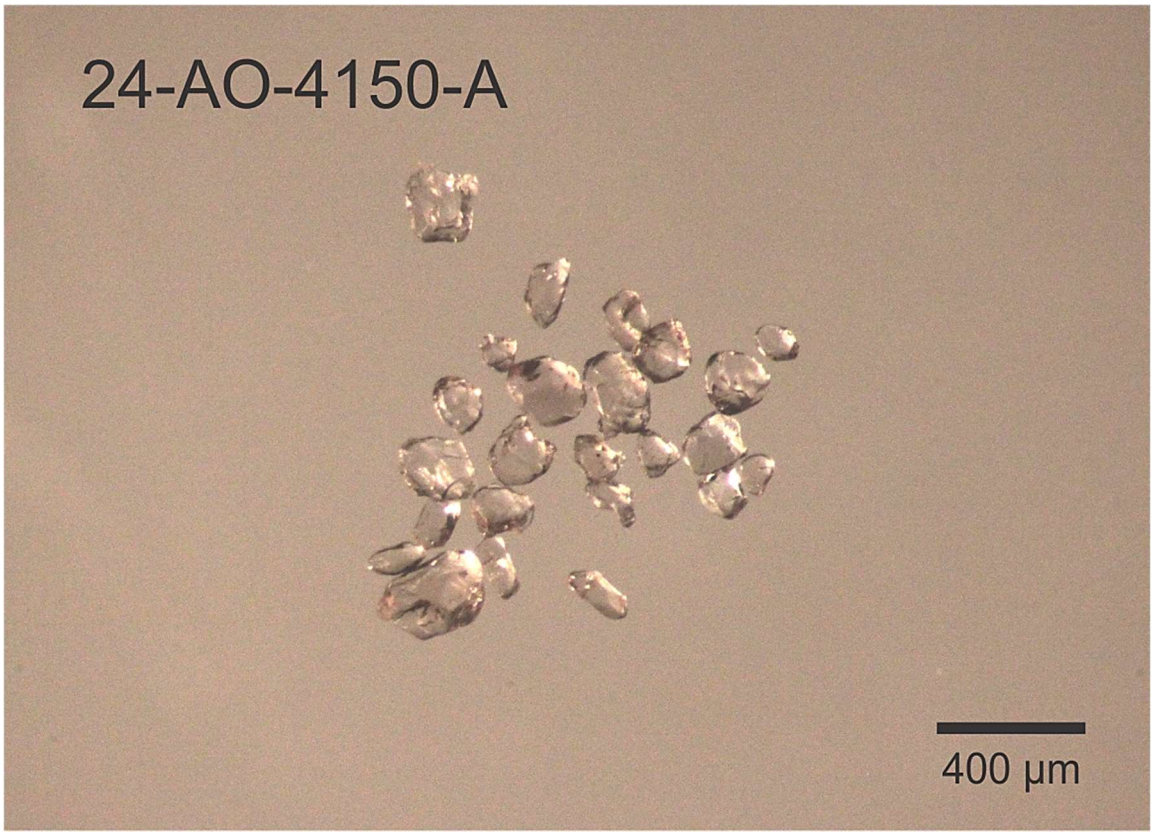

Figure 20-1. Picked zircon from diorite sample 24-AO-4150-A.

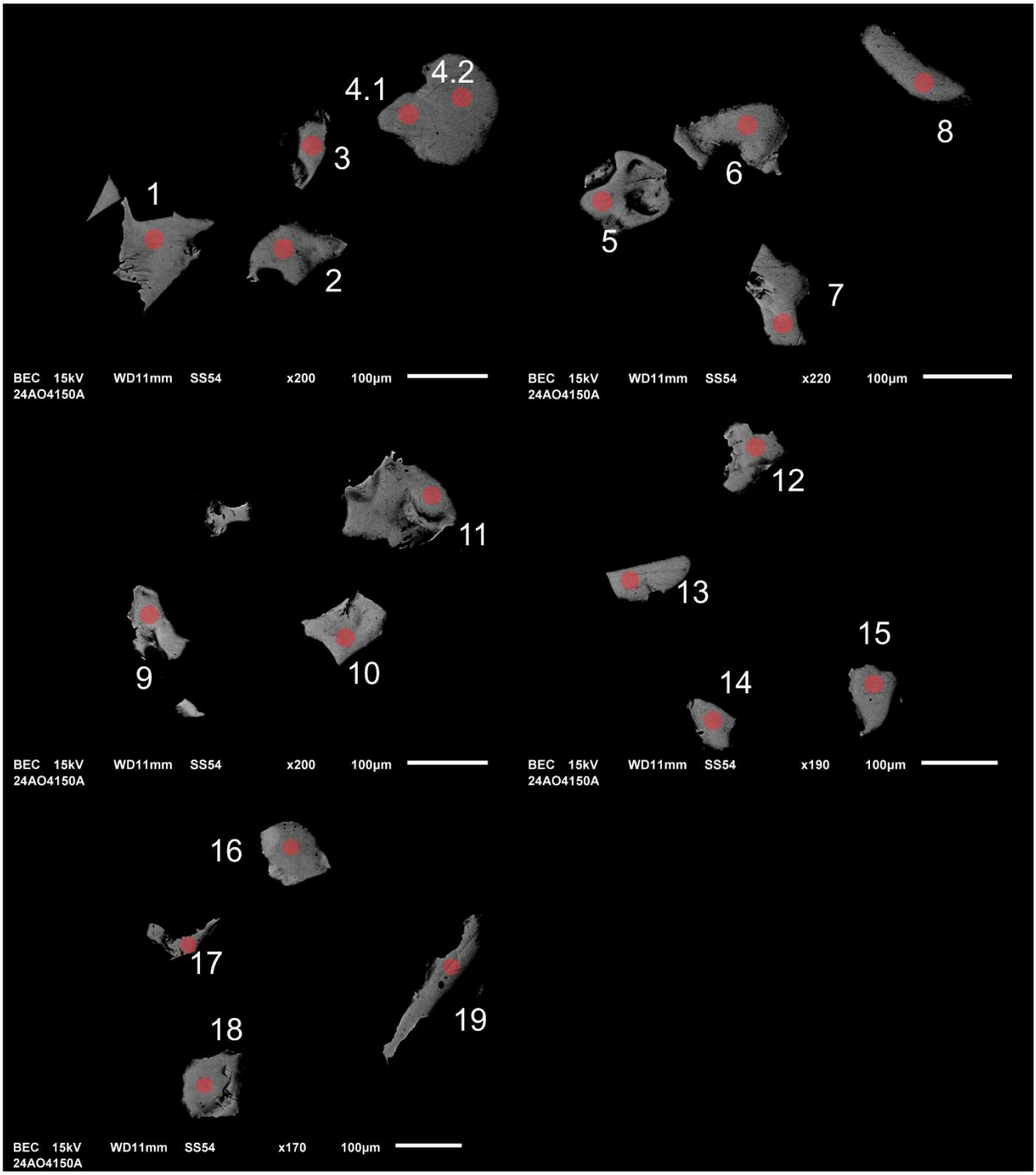

Figure 20-2-1. BSE images of selected grains from sample 24-AO-4150-A. The red circles represent the approximate locations of laser ablation spots.

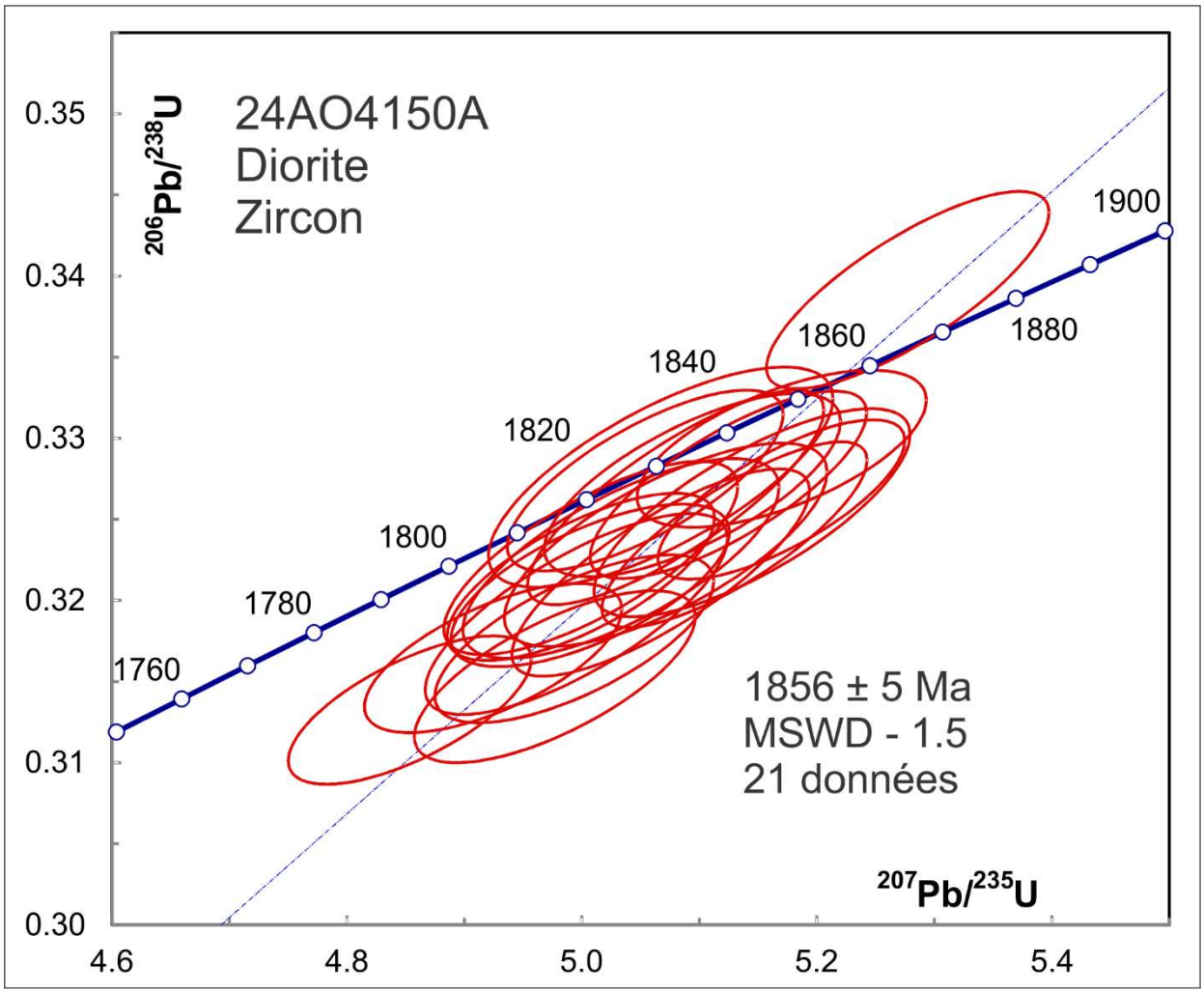

Figure 20-3. Concordia plot showing U-Pb isotopic data on zircon from sample 24-AO-4150-A.

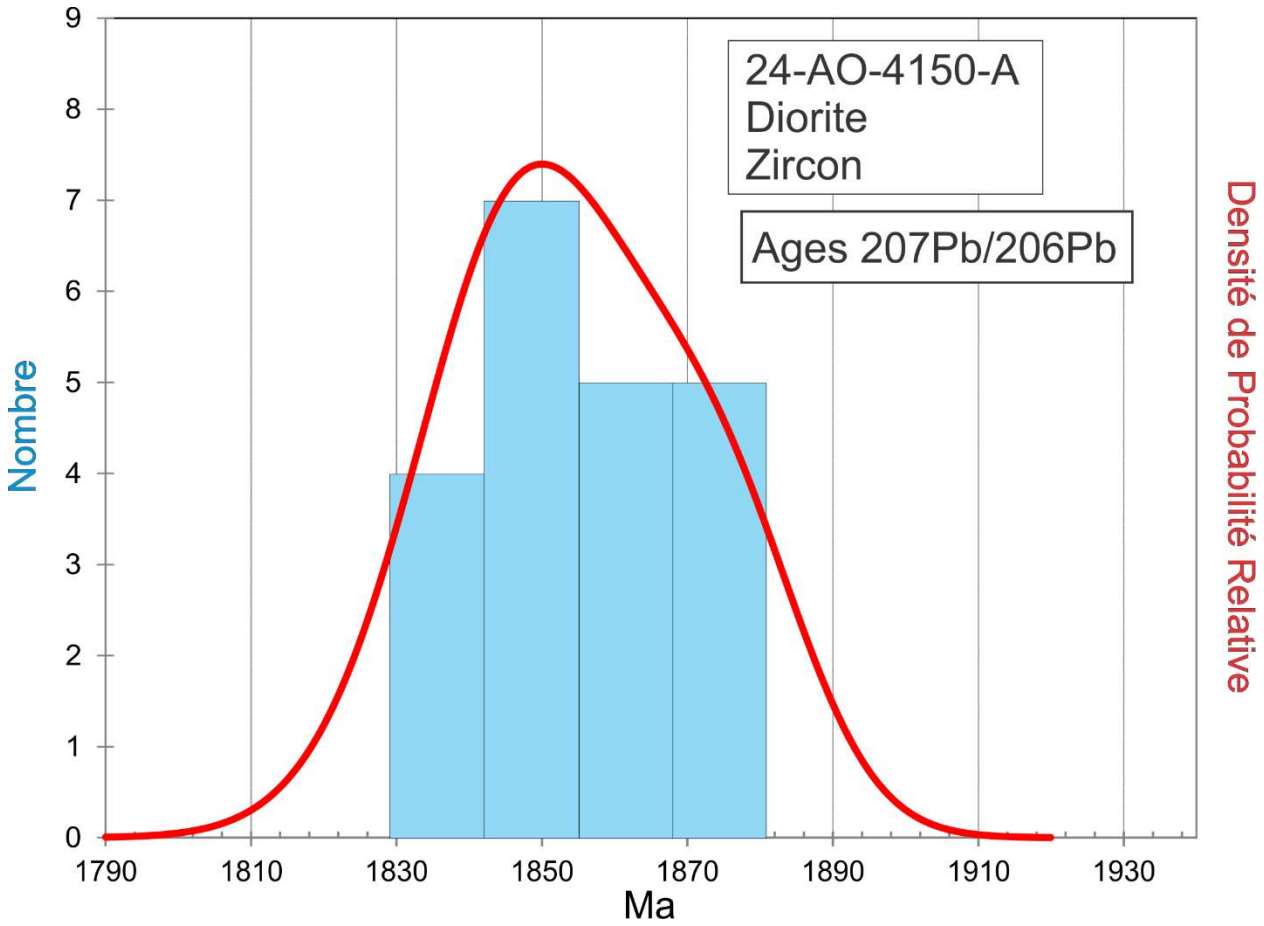

Figure 20-4. Combined probability density plot and histogram showing the distribution of 207Pb/206Pb ages on polished zircon from sample 24-AO-4150-A.

Nuvujjuaq

21. 24-AM-5039-A
Paragneiss, Suite métamorphique d'Argutialuk (Aarq2b)

This sample yielded a small amount of zircon consisting of subhedral to rounded grains (Fig. 21-1). BSE images show a variety of zoning patterns with high-U rims that are too thin to date (Fig. 21-2). U-Pb analyses give a wide range of Paleoproterozoic and Archean detrital ages ranging back to 3171 ± 30 Ma but most define a major peak at an age of 1870 Ma (Fig. 21-3 and Fig. 21-4). The youngest 12 ages cluster within error and define a mean of 1870 ± 6 Ma (MSWD – 1.1) which, if detrital, is an older age limit on deposition of the sedimentary protolith. For further discussion, see section 27. All analyses except one show Th/U > 0.1. The exception is a ca. 2700 Ma grain that is probably detrital and formed during a previous Archean metamorphism.

Analyses on monazite grains recovered from this sample are clustered but scatter outside of error with a mean age of 1808 ± 7 Ma (MSWD – 5.0; Fig. 21-5) and a spread from about 1790 Ma to about 1830 Ma. There is no apparent difference between monazite analyses in terms of U concentration or Th/U. They all show the characteristics of ‘magmatic’ monazite (high U, relatively low Th/U) as discussed above in sections 1 and 2 so may approximate the time of formation of the paragneiss, possibly over an extended time period of several tens of Ma. The monazite ages are about 60 Ma younger than the youngest zircon cluster in the same sample, supporting the assumption that all the dated zircon is detrital in origin.

Figure 21-1. Picked zircon from paragneiss sample 24-AM-5039-A.

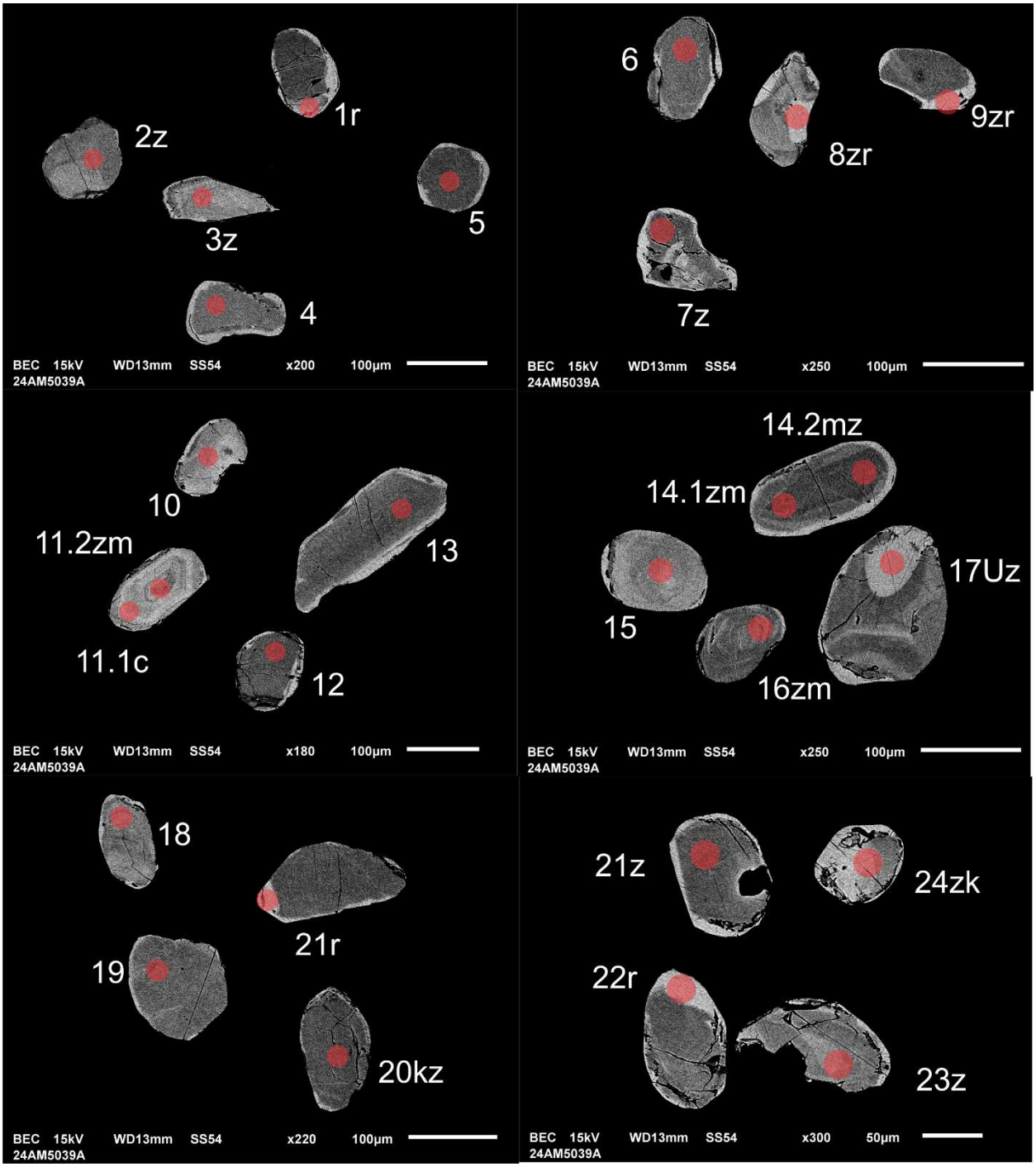

Figure 21-2-1. BSE images of selected grains from sample 24-AM-5039-A. The red circles represent the approximate locations of laser ablation spots.

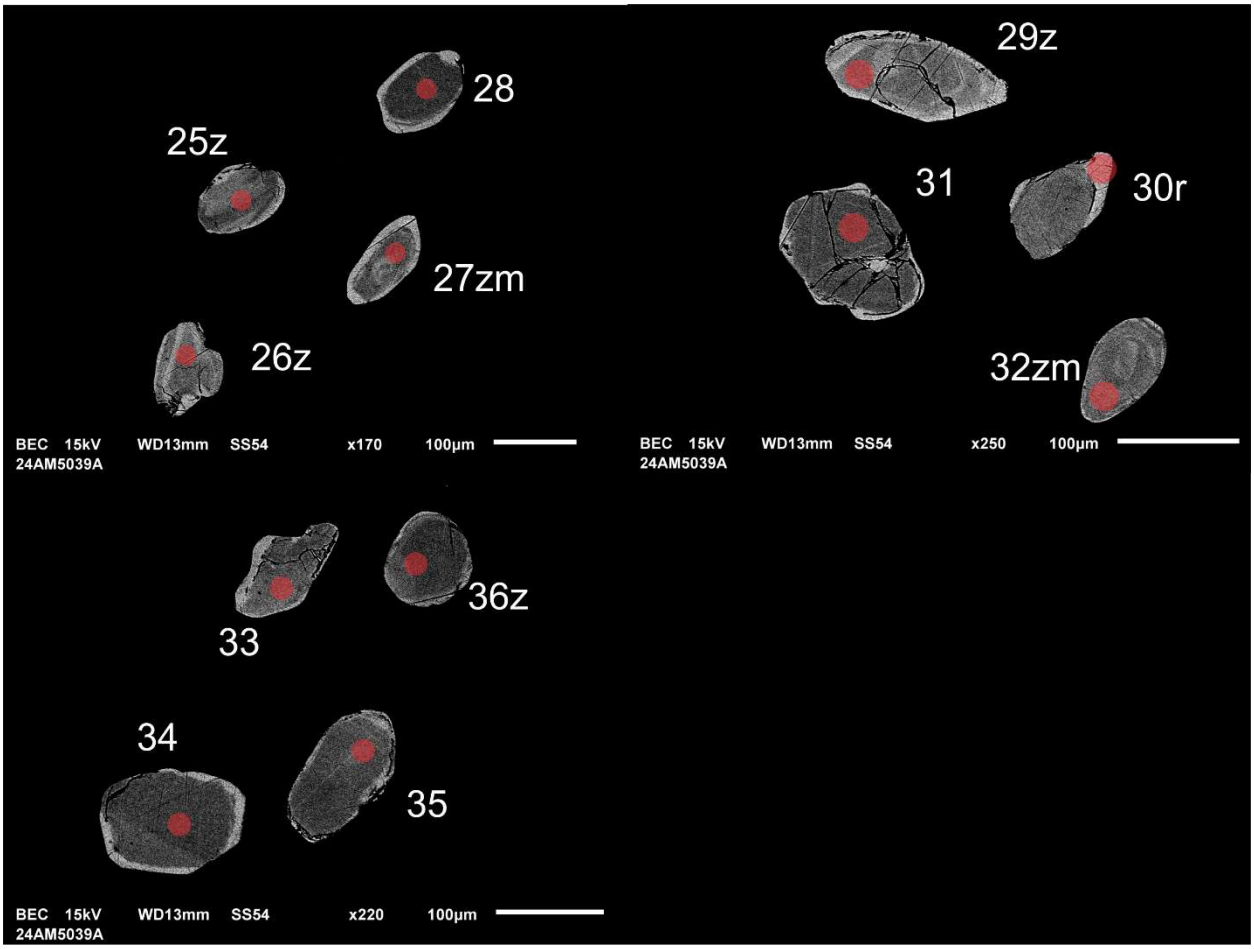

Figure 21-2-2. BSE images of selected grains from sample 24-AM-5039-A. The red circles represent the approximate locations of laser ablation spots.

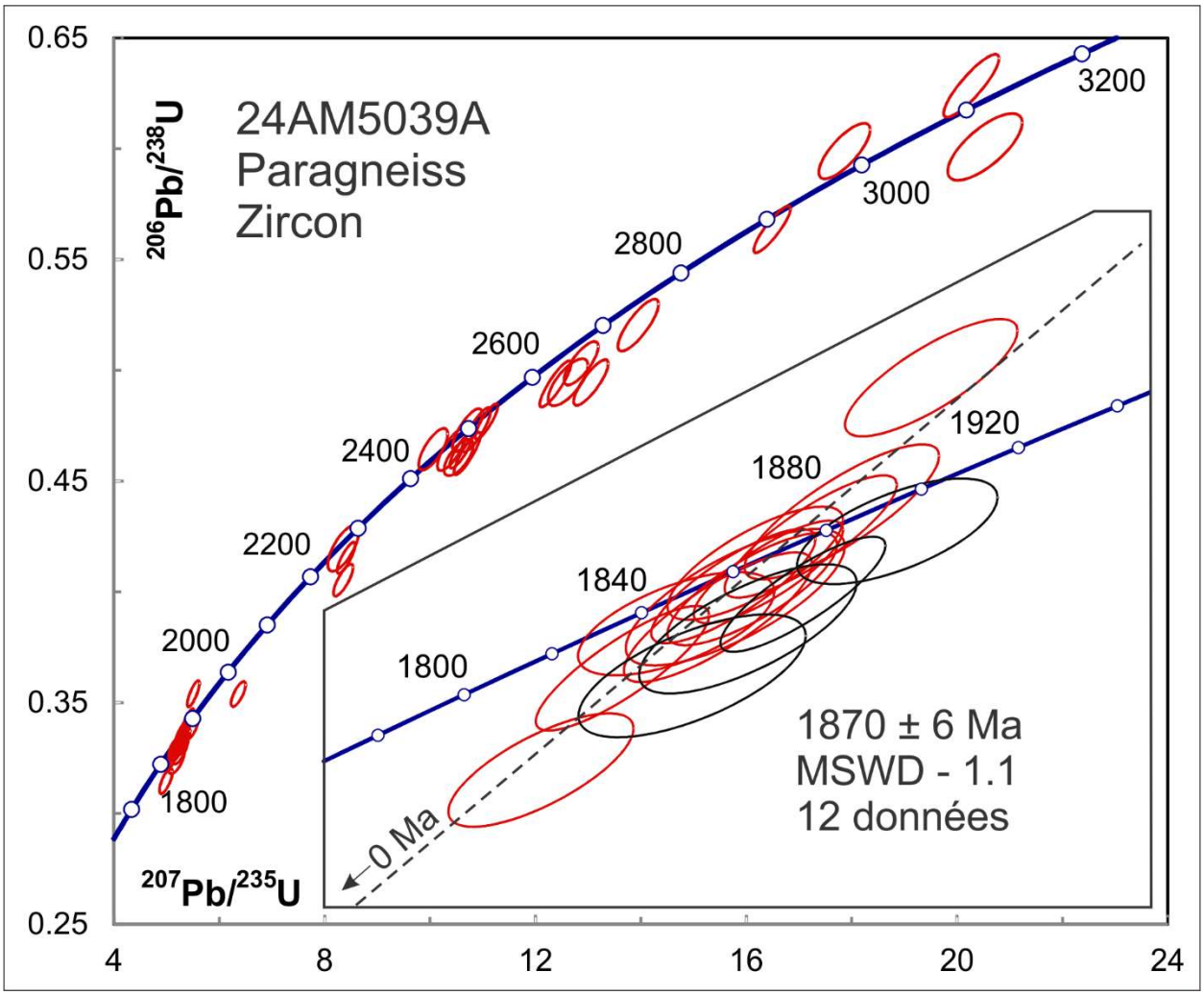

Figure 21-3. Concordia plot showing U-Pb isotopic data on zircon from sample 24-AM-5039-A. Black ellipses are not included in the average.

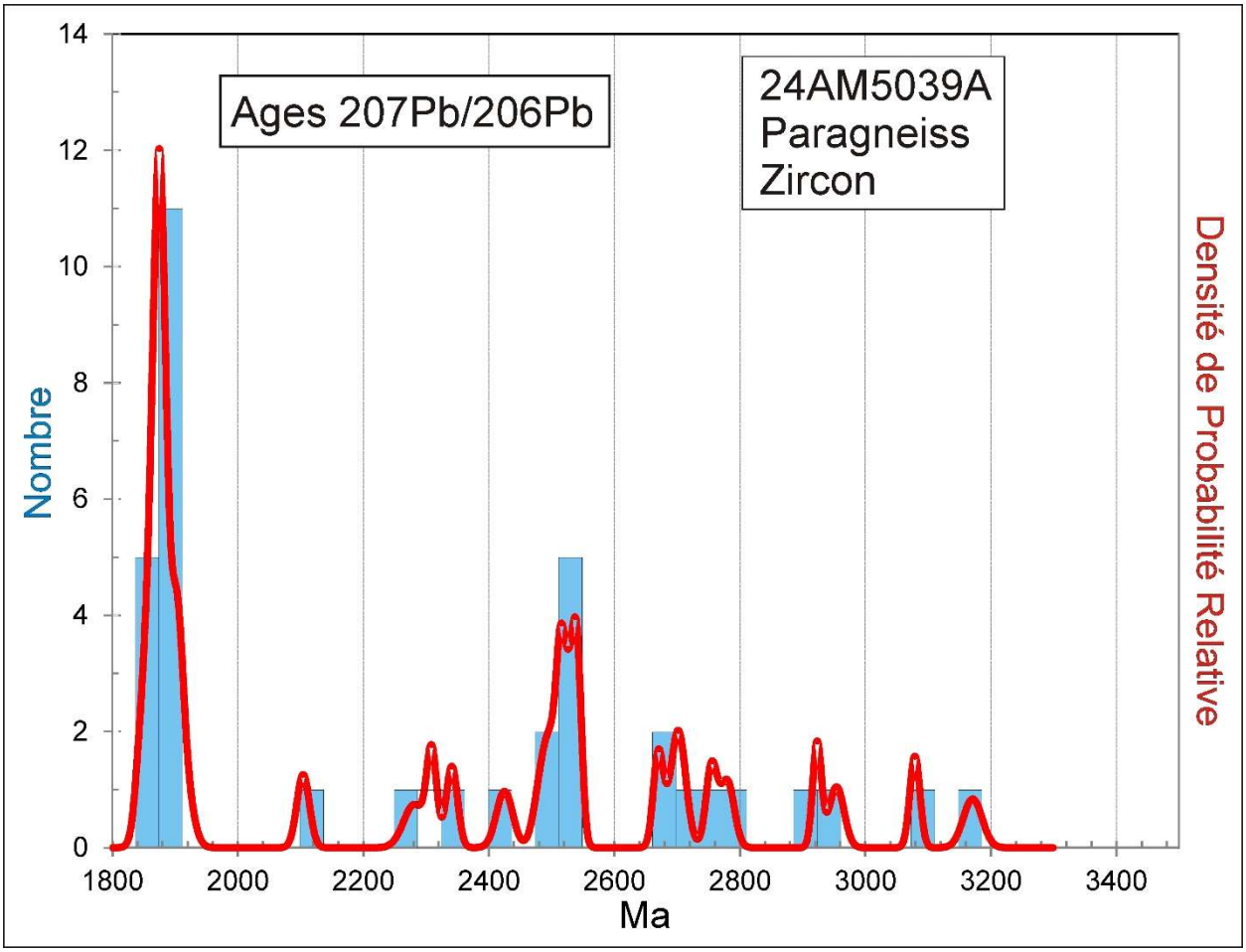

Figure 21-4. Combined age relative probability density plot and histogram showing the distribution of $^{207}Pb/^{206}Pb$ ages on zircon from sample 24-AM-5039-A.

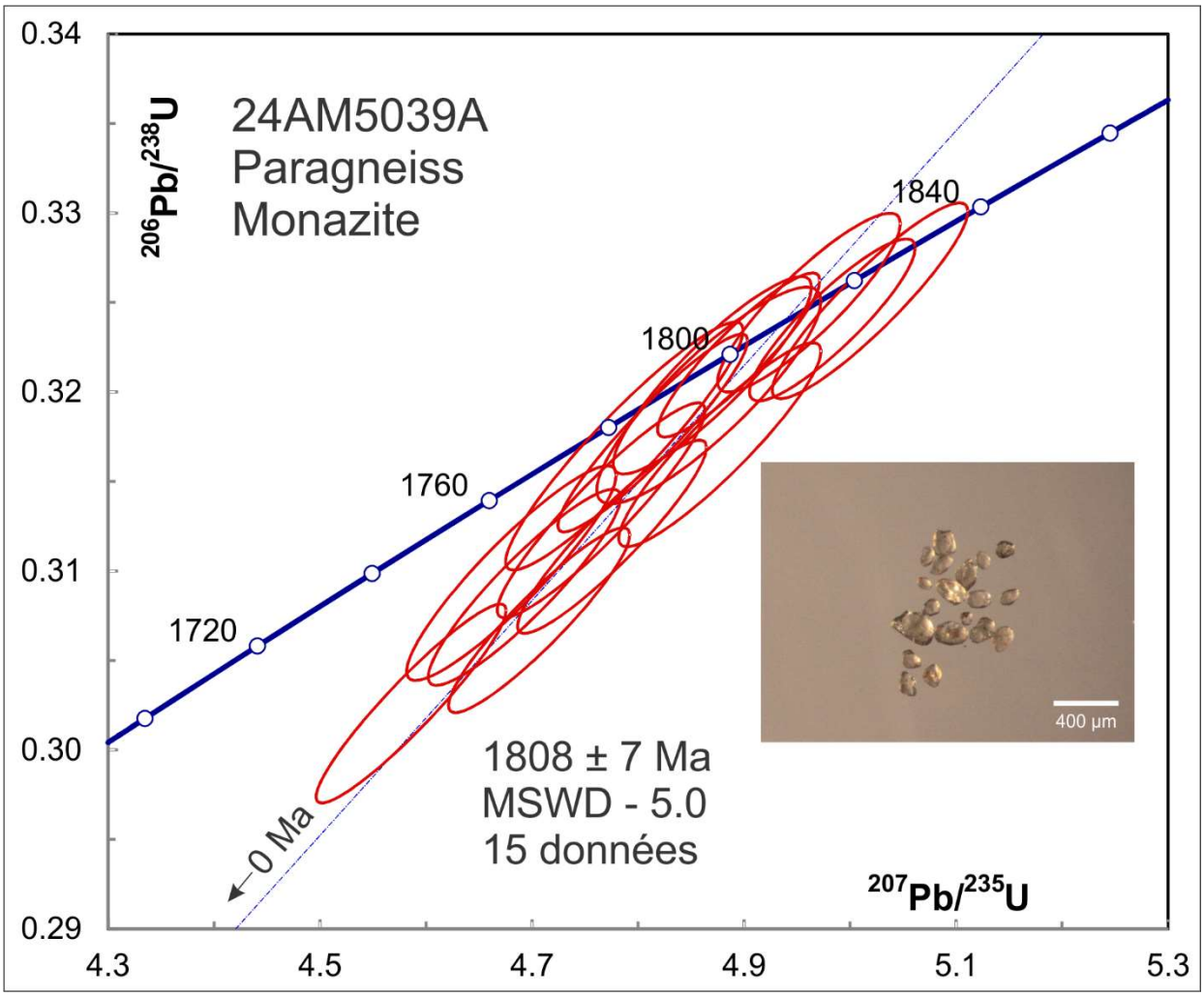

Figure 21-5. Concordia plot showing U-Pb isotopic data on monazite from sample 24-AM-5039-A.

22. 24-AM-5140-A
Paragneiss migmatitisé, Complexe de Déception (Adec5b)

This sample consists of small subhedral to well rounded stubby grains (Fig. 22-1). Because of the small size of grains, it was decided to mount them on double sided tape and ablate on natural (unpolished) surfaces. Most U-Pb TRA profiles show either uniform Th/U<0.1 or, more often, Th/U increasing with depth from metamorphic to magmatic values, due to the presence of metamorphic rims. Care was taken to average ratios over either the metamorphic or magmatic range, depending on which was best represented. Analyses that are >10% discordant are omitted, which includes many of those with the youngest ages. Of the remaining data set, 21 analyses from magmatic grains (Th/U > 0.1) span a range from about 2730 Ma to 2940 Ma with one grain at 3070 Ma (Figs. 22-2 and 22-3). Results from metamorphic phases (Th/U < 0.1) are the youngest with generally high U but scatter well outside of error over the range 2662-2726 Ma (Figs. 22-2 and 22-4). This again suggests an extended period of crystallization, or at high enough temperature for some diffusion of Pb.

An attempt was made to isolate and date small “monazite” crystals. Most were found to have low Th/U compared to typical monazite and are likely zircon. These generally show disparate ages over the range 2600-2700 Ma (Fig. 22-5) and are reversely discordant, partly because a monazite standard was used. This should not affect the accuracy of the $^{207}Pb/^{206}Pb$ ages, but these may have been partially reset due to the small size of the grains.

Three grains are likely monazite and give clustered analyses, although outside of error, with a mean age of 2808 ± 27 Ma. This suggests that the dated monazite is detrital in origin. In contrast to the previous sample, provenance as well as metamorphism appear to be Archean.

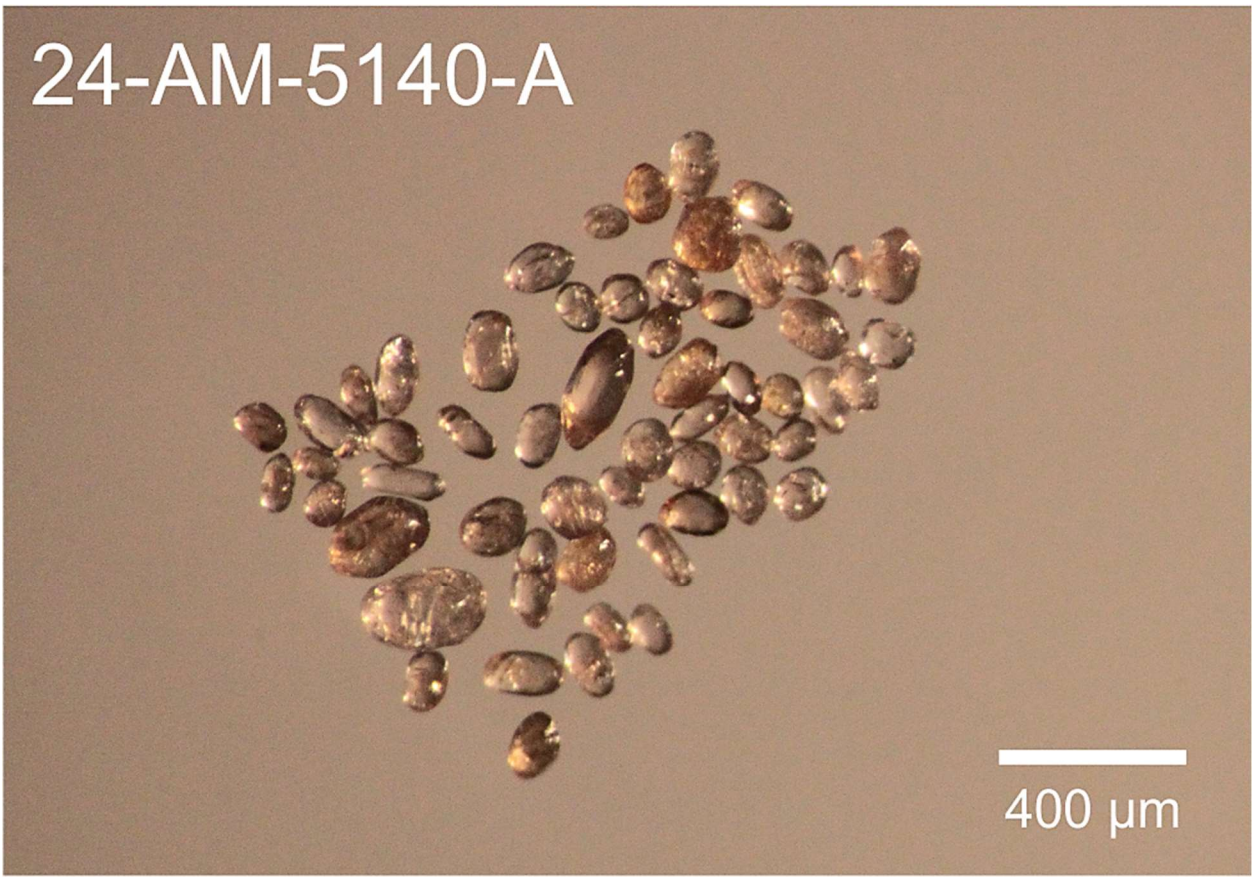

Figure 22-1. Picked zircon from paragneiss sample 24-AM-5140-A.

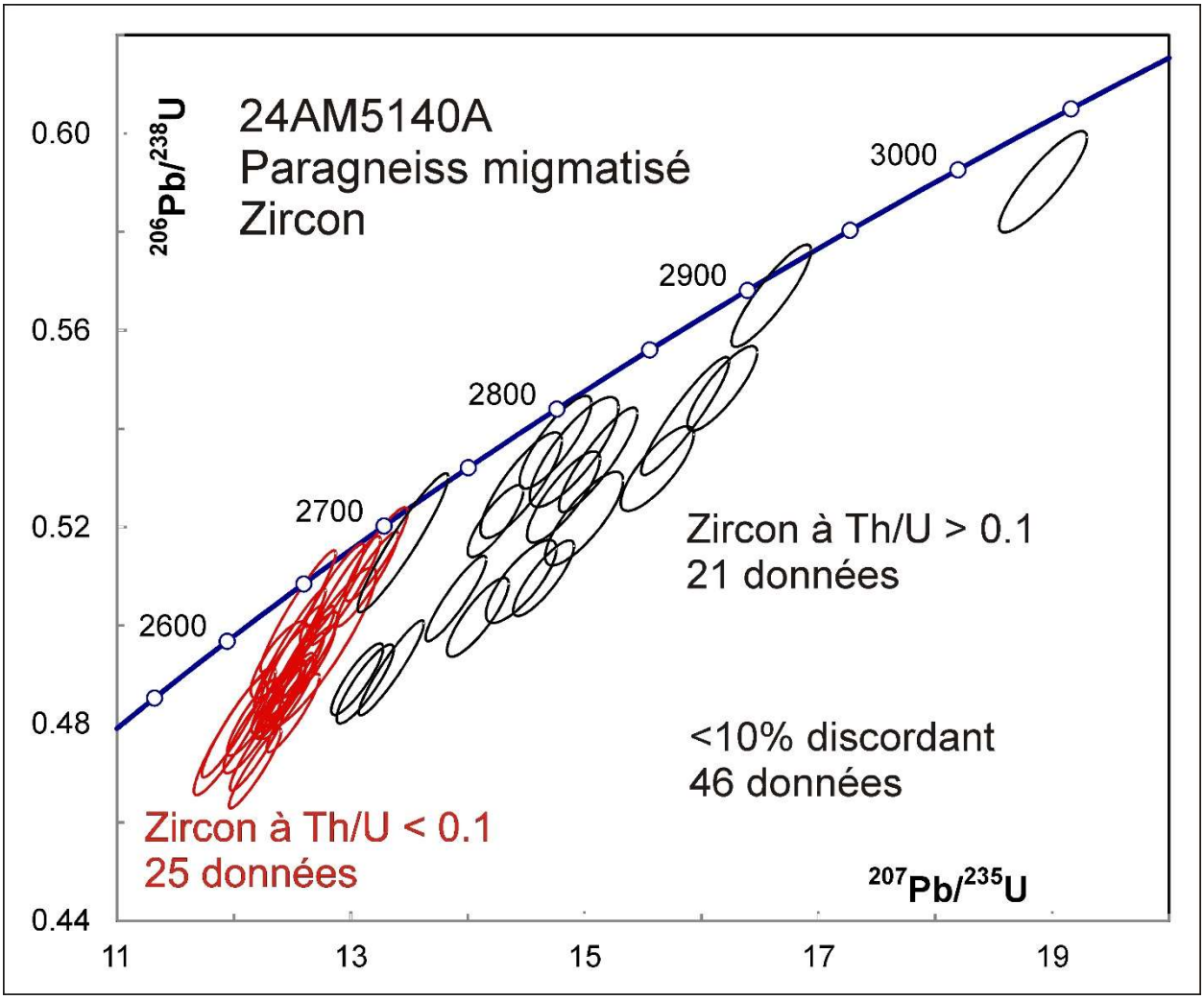

Figure 22-2. Concordia plot showing U-Pb isotopic data on zircon from sample 24-AM-5140-A.

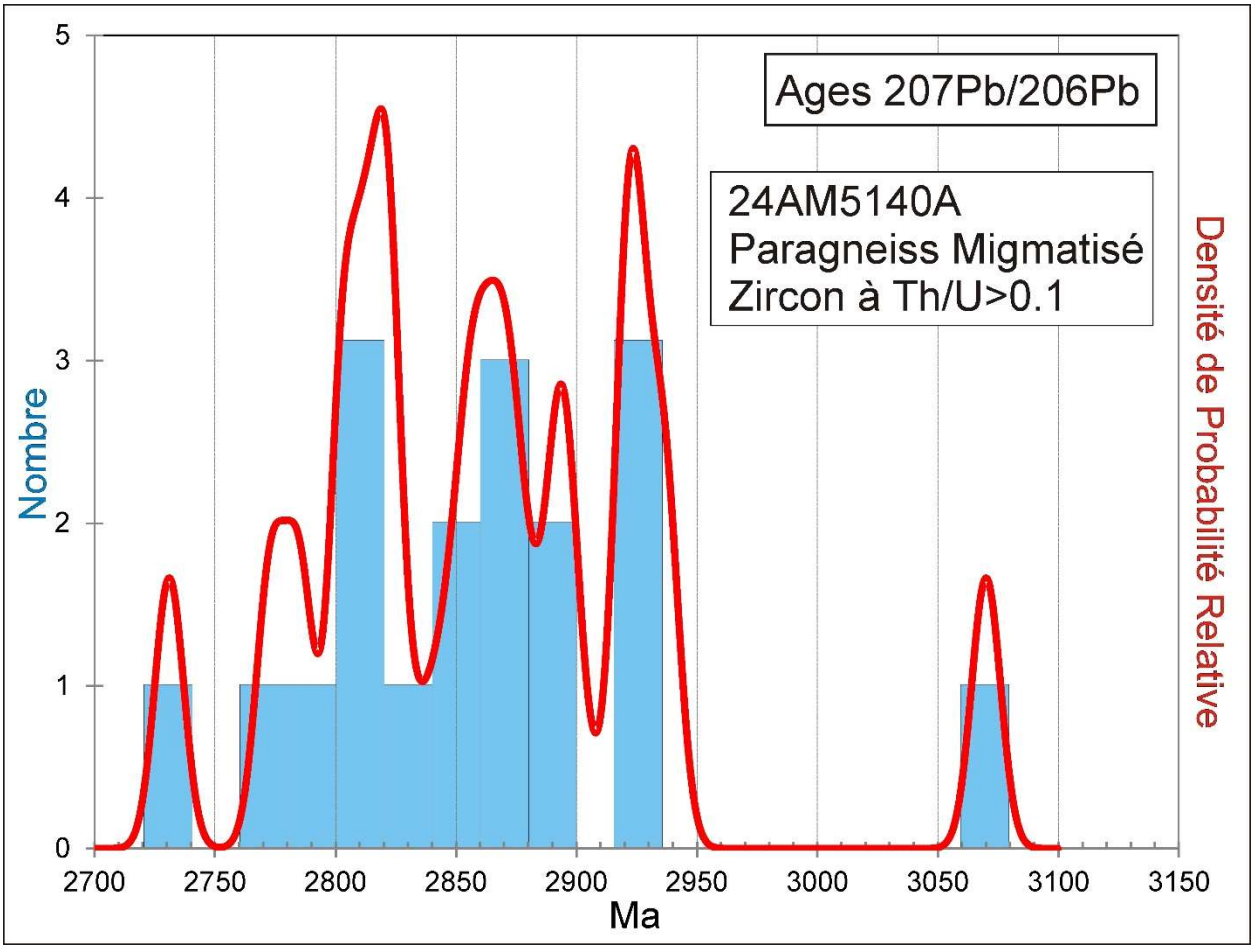

Figure 22-3. Combined age relative probability density plot and histogram showing the distribution of $^{207}Pb/^{206}Pb$ ages on magmatic zircon from sample 24-AM-5140-A.

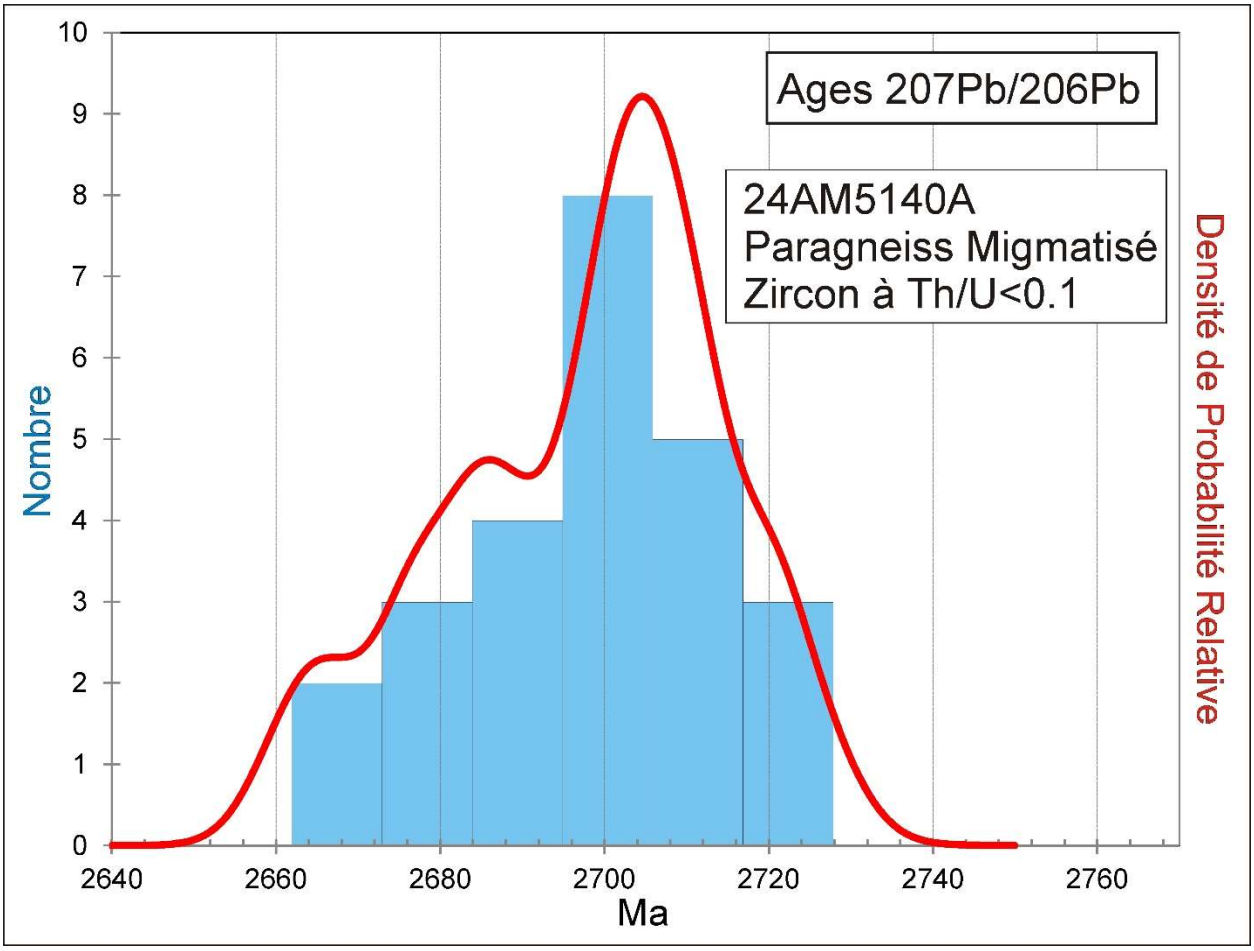

Figure 22-4. Combined age relative probability density plot and histogram showing the distribution of $^{207}Pb/^{206}Pb$ ages on metamorphic zircon from sample 24-AM-5140-A.

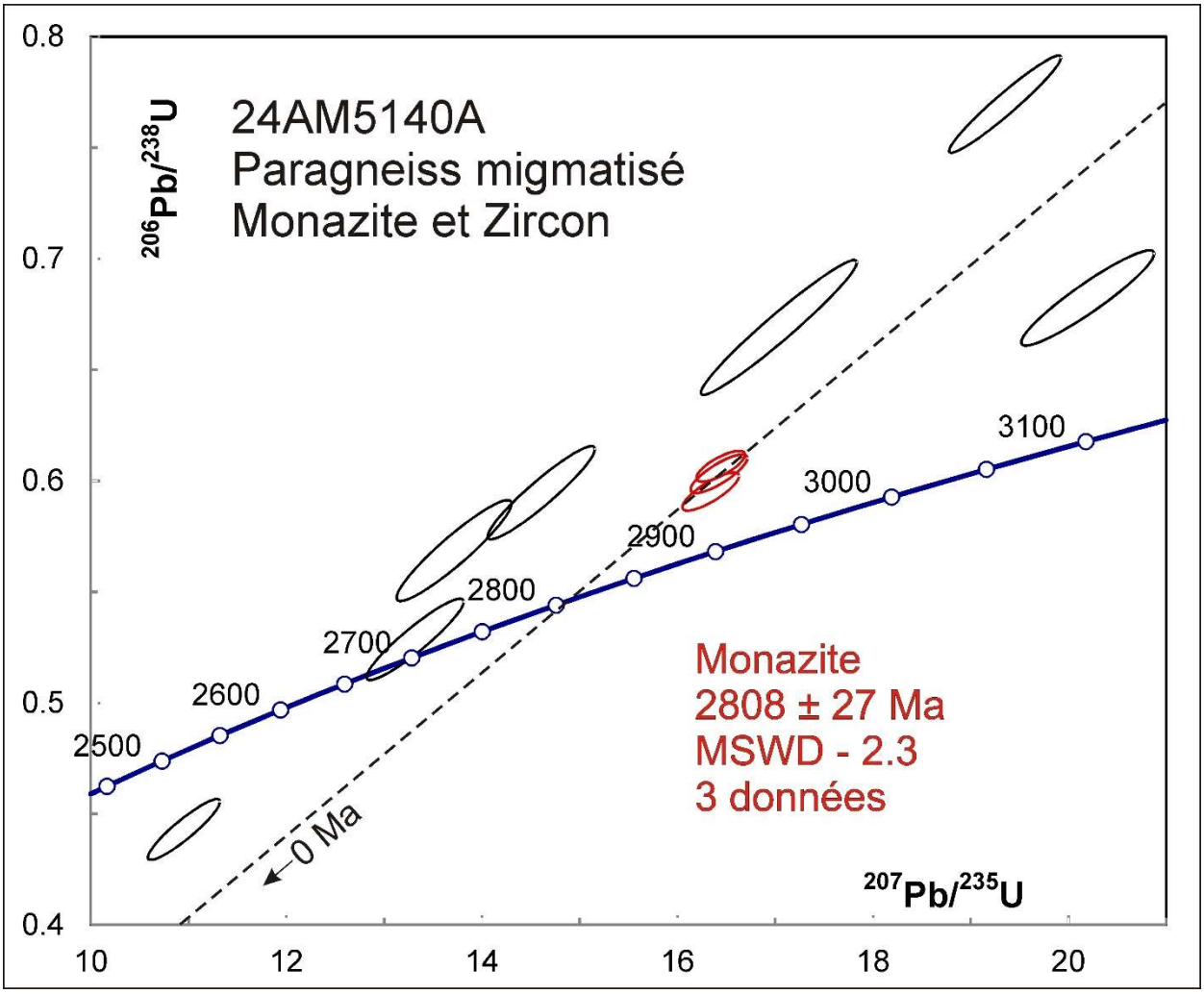

Figure 22-5. Concordia plot showing U-Pb isotopic data on small monazite and zircon grains from sample 24-AM-5140-A. Black ellipses represent zircon and are not included in the average.

23. 24-CB-2063-A
Gneiss granulitique de composition tonalitique, Complexe d'Akimmiup (A/pPakm1)

This sample yielded a large amount of zircon consisting of euhedral-subhedral to rounded grains (Fig. 23-1). Some of the grains were very thin so, it was decided to mount them on double sided tape and ablate on natural (unpolished) surfaces. U-Pb analyses show a wide range of U concentrations from a few ppm to about 350 ppm. These show a rough proportionality to Th/U ratios down to <0.1 for the two lowest U grains. As mentioned above, zircon formed under granulite conditions does not show the consistently low Th/U ratios seen under amphibolite conditions.

U-Pb analyses are clustered and remarkably concordant compared to most other samples (Fig. 23-2 and Fig. 23-3). However, ages scatter outside of error with a mean of 1839 ± 5 Ma (MSWD – 2.9). The probability density plot suggests the possibility of two groups. Applying ‘Unmix’ with the assumption of 2 modes gives ages of 1844 ± 3 Ma (74%) and 1820 ± 7 Ma (26%). This may be evidence for crystallization over an extended time period in the deep crust or for some degree of resetting during a later period of granulite metamorphism. The clustering around 1844 Ma suggests that this is close to the age of emplacement.

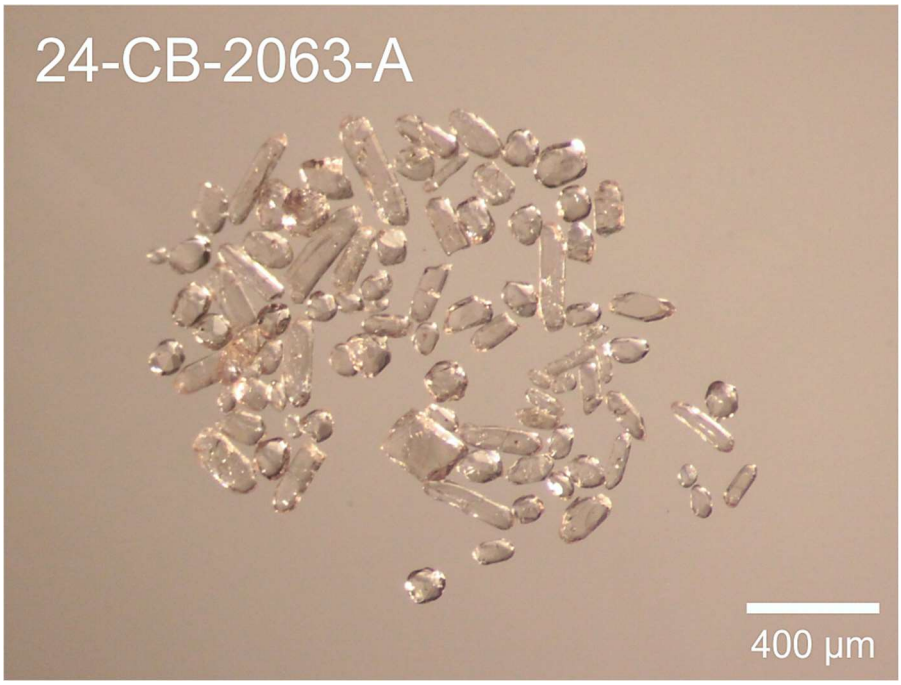

Figure 23-1. Picked zircon from gneiss sample 24-CB-2063-A.

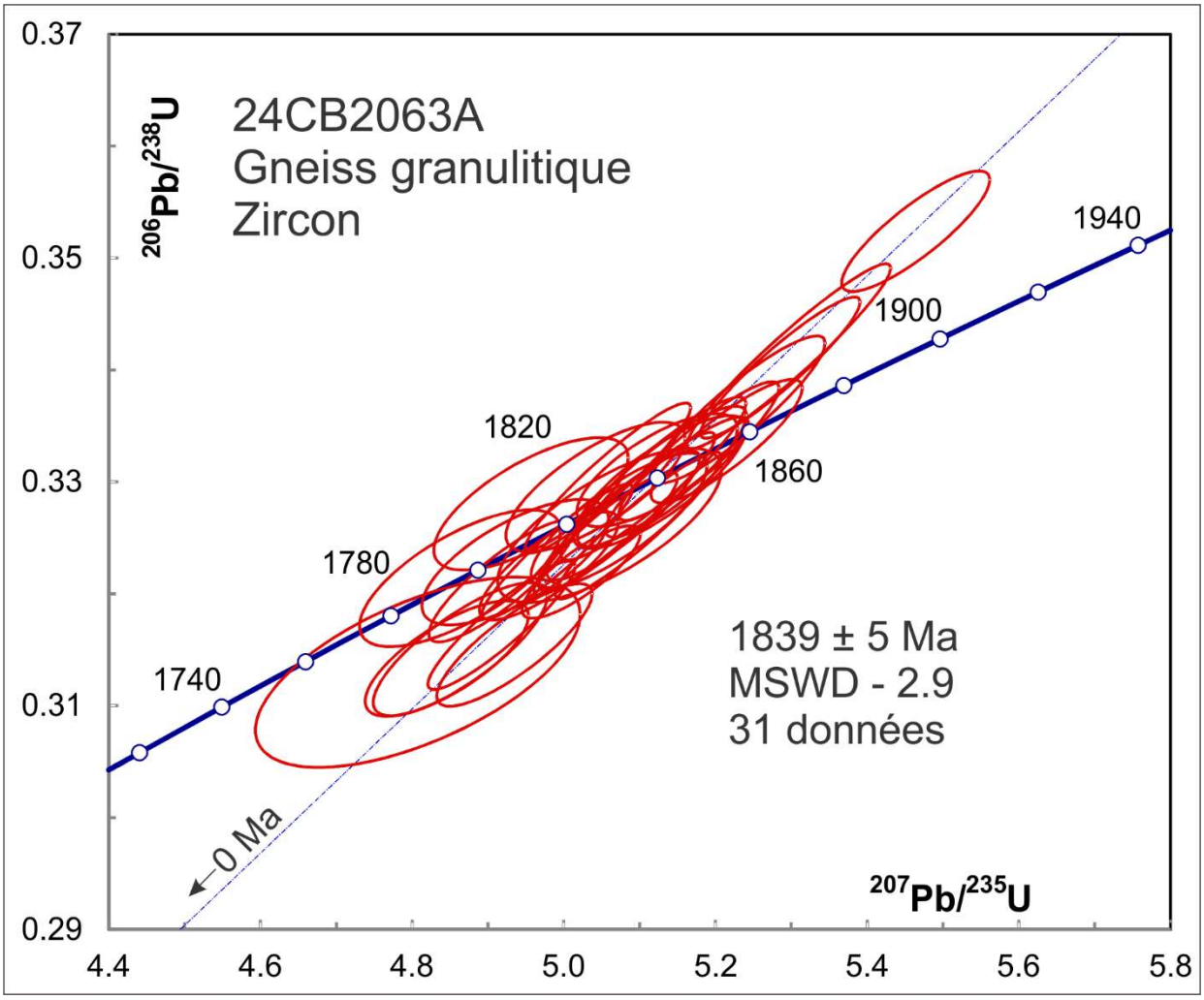

Figure 23-2. Concordia plot showing U-Pb isotopic data on zircon from sample 24-CB-2063-A.

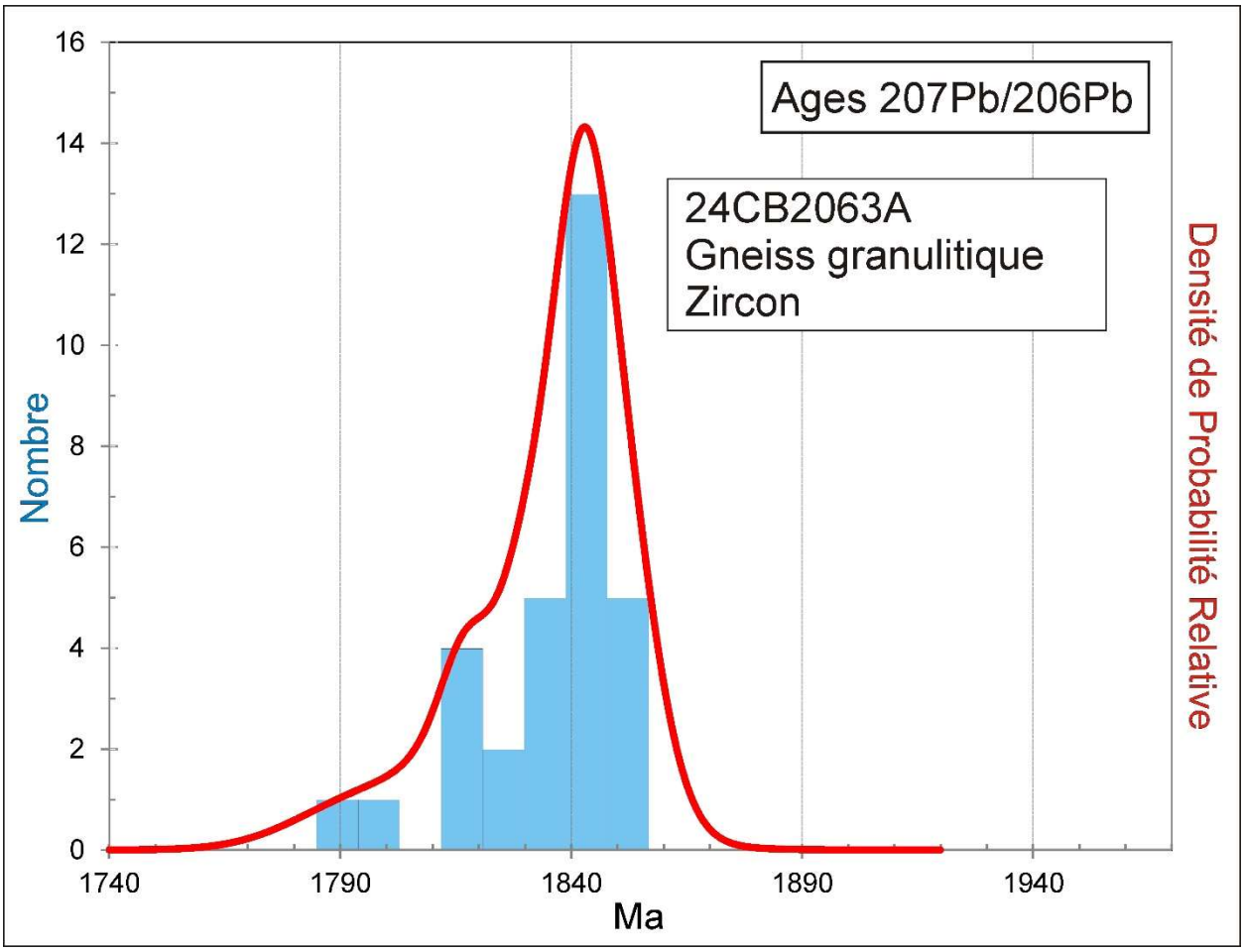

Figure 23-3. Combined age relative probability density plot and histogram showing the distribution of $^{207}Pb/^{206}Pb$ ages on zircon from sample 24-CB-2063-A.

24. 24-AM-5096-A
Granite, Complexe de Déception (Adec1a)

This sample yielded zircon consisting of subhedral to well rounded grains (Fig. 24-1). BSE images show little evidence for zoning but many grains have thin, relatively bright, overgrowths under BSE (Fig. 24-2). TRA profiles through many grains show regions with Paleoproterozoic ages and Th/U < 0.1 as well as regions with Archean ages and magmatic values for Th/U, which may correspond to rims and cores, respectively. Care was taken not to mix information between these phases when averaging profiles. In addition, data show the presence of regions with both low Th/U and low U, which are therefore difficult to date without mixing domains with possibly different ages. All of the zircon with magmatic Th/U gives Archean ages with a cluster of 19 data giving an average age of 2817 ± 17 Ma (MSWD – 5.6, Fig. 24-3). Although the scatter is outside of error and there may be partial disturbance from Paleoproterozoic metamorphism, this is the best estimate for the primary emplacement age of the granite. All the analyses with low Th/U <0.1 give Paleoproterozoic ages. U concentrations range from low to very low. Some of the Proterozoic as well as a couple of Archean domains with Th/U > 0.1 show very low U concentrations (Table 3). The 'Archean' cases could represent Proterozoic phases to which older Pb was added from Archean cores during prolonged residence at high temperature. The youngest analyses are clustered, although scatter outside of error, with a mean age of 1817 ± 17 Ma (MSWD – 5.6, Fig. 24-3) on the youngest 19 spots. This is the best estimate for metamorphism of the granite. There is no obvious relationship between age and U concentration within this group.

Six tiny grains were picked as monazite. Three proved to be zircon, giving Archean and Paleoproterozoic ages. Three have high Th/U ratios so are probably monazite (Fig. 24-4). These gave overlapping $^{207}Pb/^{206}Pb$ ages with a mean of 2672 ± 7 Ma (MSWD – 1.2). They may represent monazite growth during an earlier Archean episode of metamorphism.

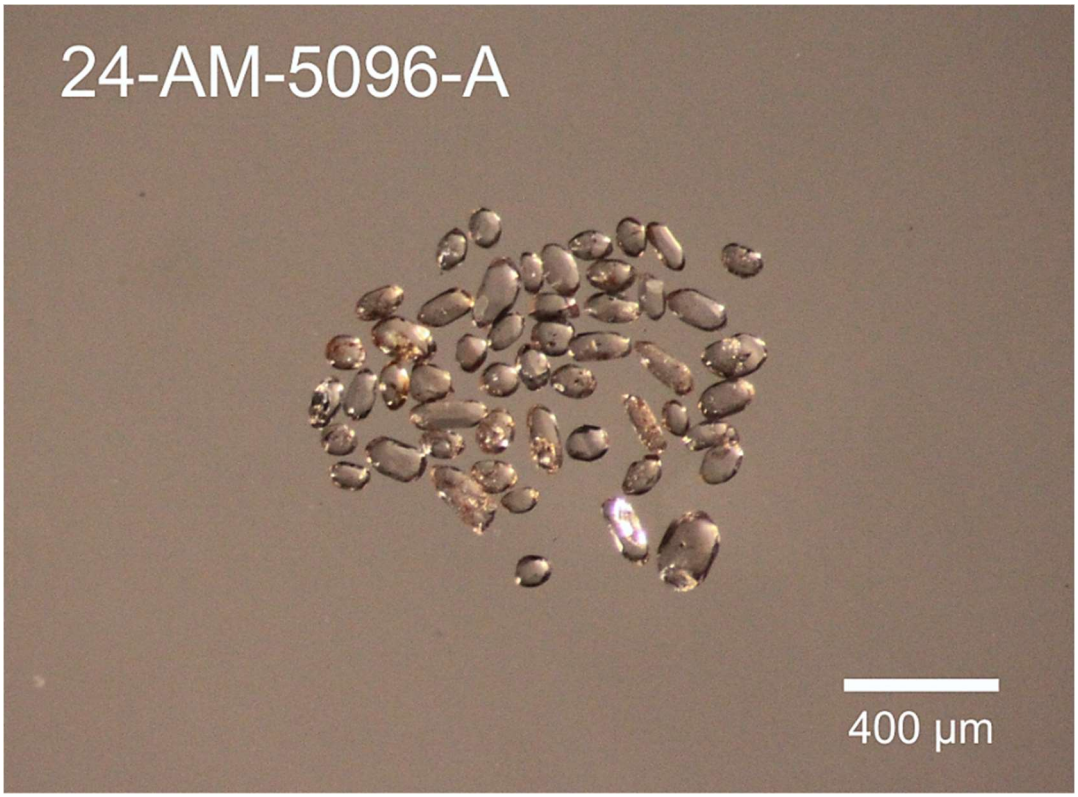

Figure 24-1. Picked zircon from granite sample 24-AM-5096-A.

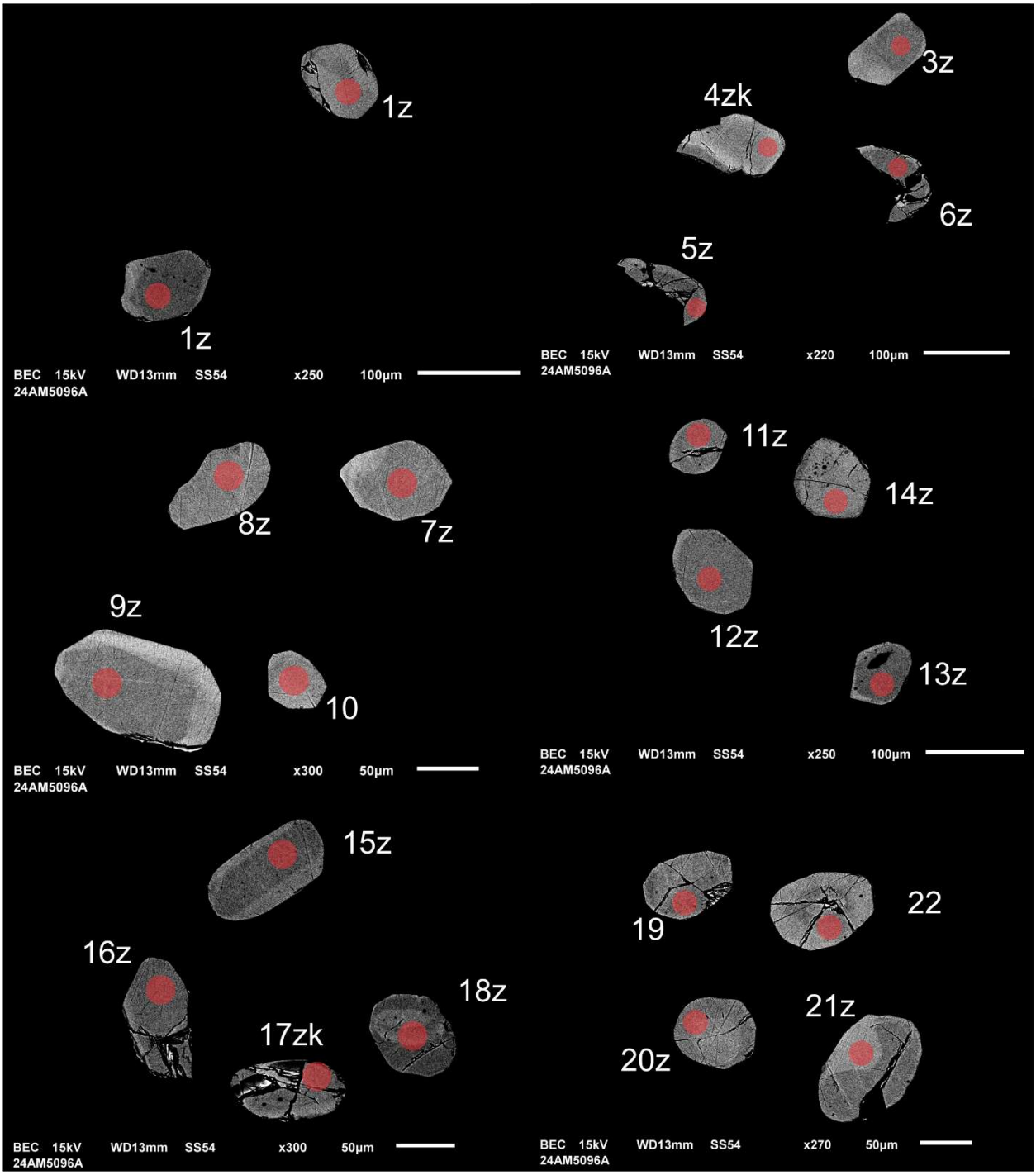

Figure 24-2-1. BSE images of selected grains from sample 24-AM-5096-A. The red circles represent the approximate locations of laser ablation spots.

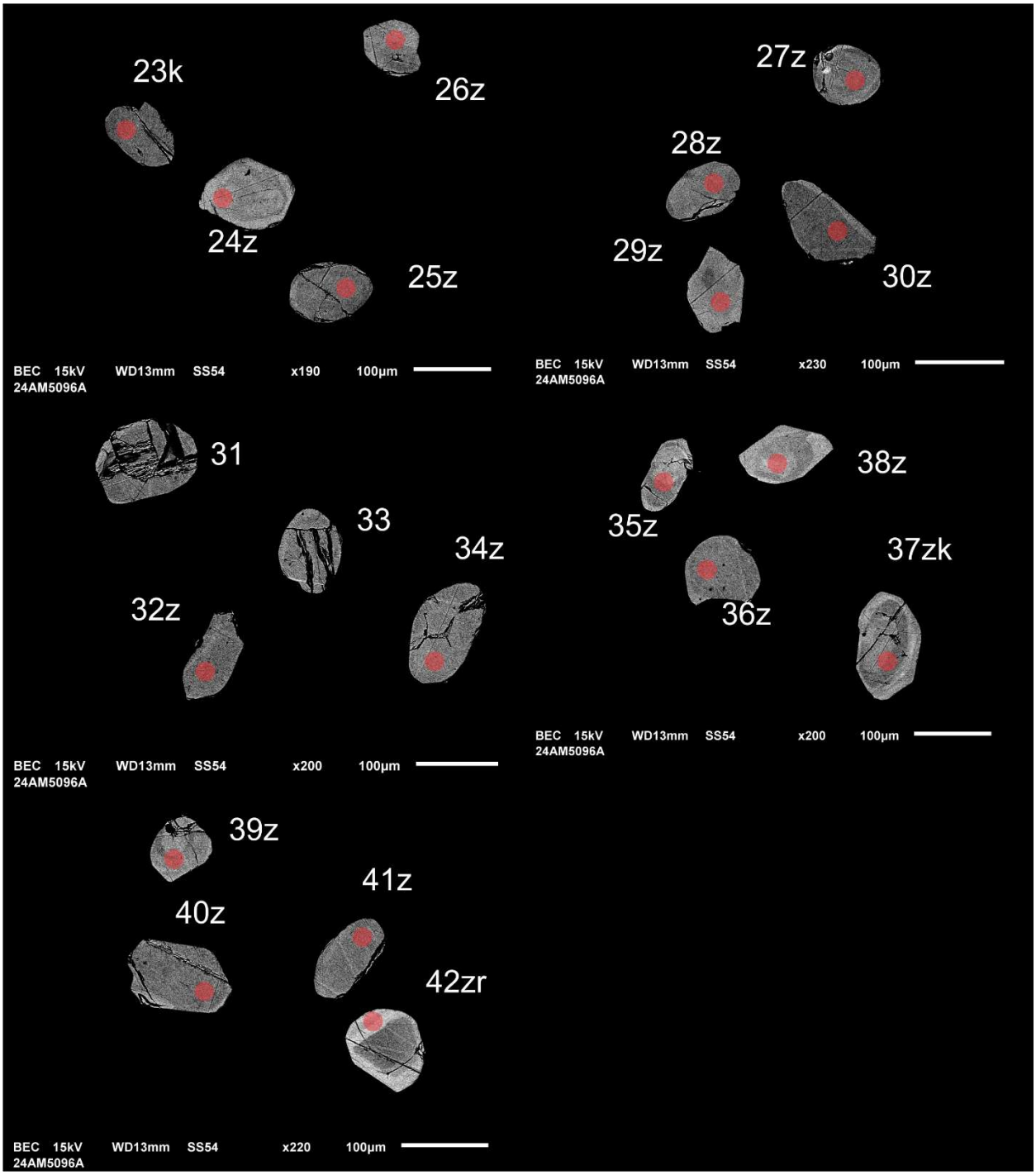

Figure 24-2-2. BSE images of selected grains from sample 24-AM-5096-A. The red circles represent the approximate locations of laser ablation spots.

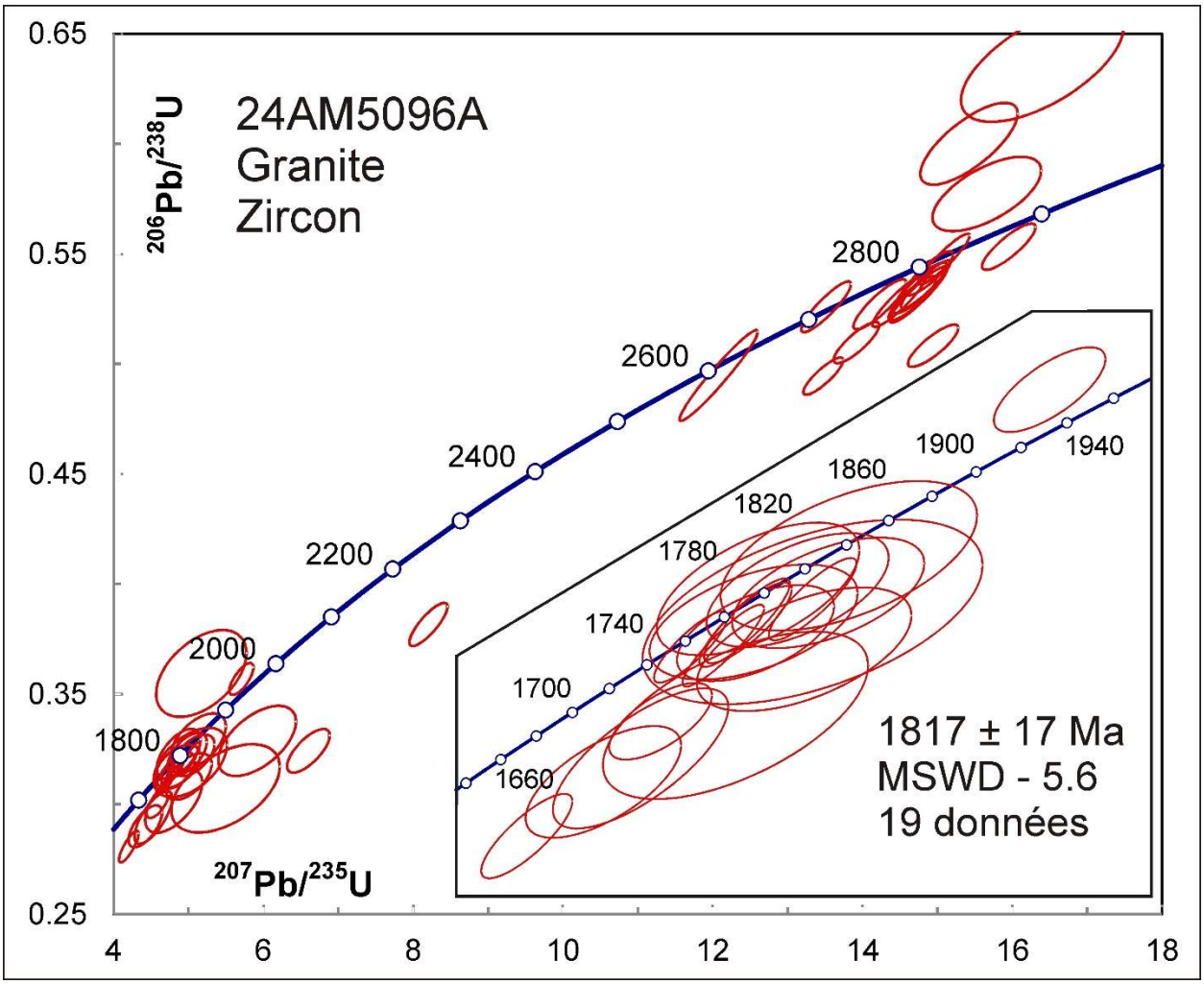

Figure 24-3. Concordia plot showing U-Pb isotopic data on zircon from sample 24-AM-5096-A.

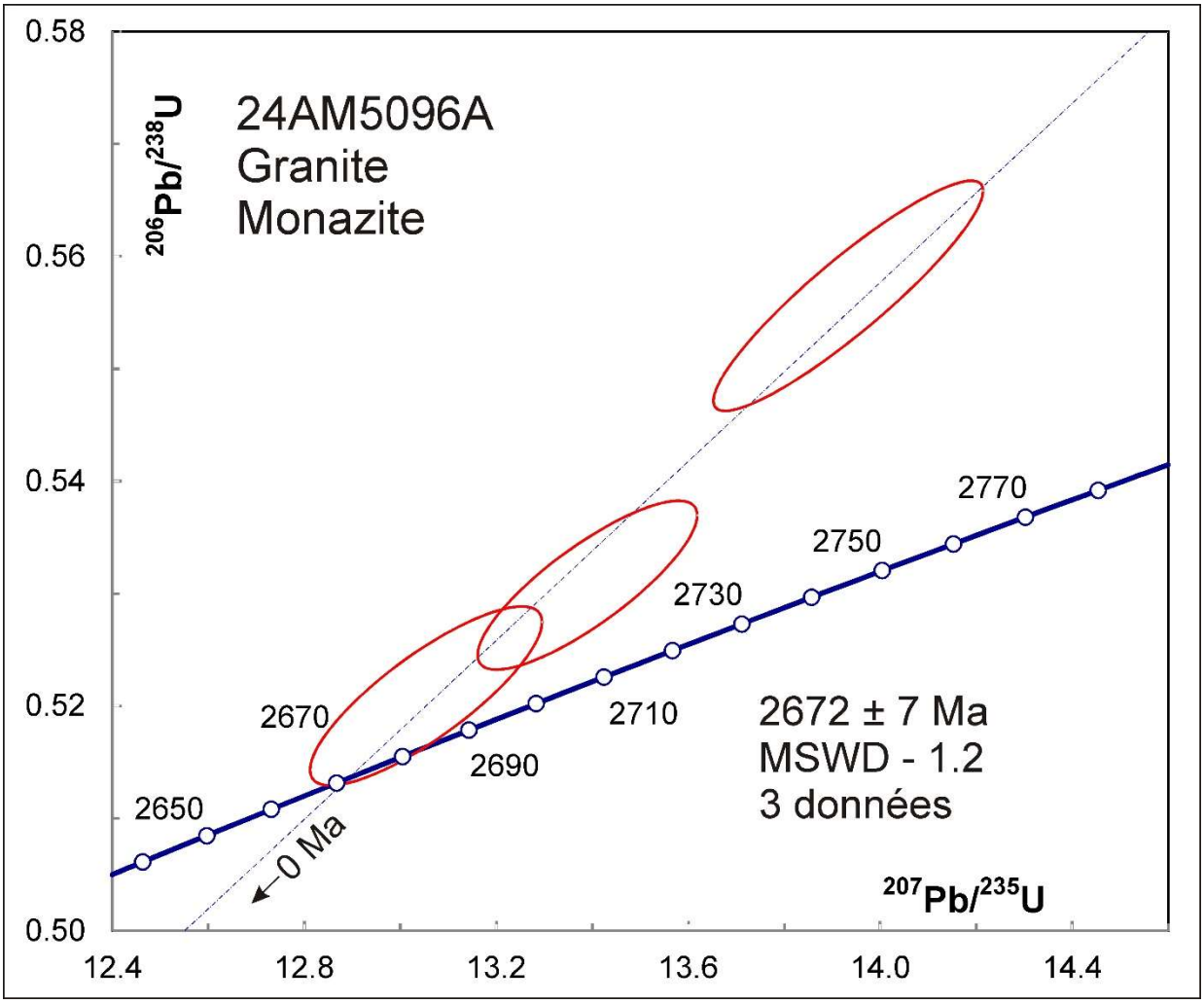

Figure 24-4. Concordia plot showing U-Pb isotopic data on monazite from sample 24-AM-5096-A.

25. 24-MV-1002-A
Granodiorite, Complexe de Déception (Adec2)

This sample yielded a small amount of zircon consisting of euhedral to rounded grains (Fig. 25-1). The zircon grains were analyzed on natural (unpolished) surfaces. U-Pb analyses are almost all near-concordant and cluster, although the scatter is outside of analytical error. Omitting the two oldest and two youngest gives a mean age of 2722 ± 6 Ma (MSWD – 3.6, Fig. 25-2). The probability density plot suggests the presence of 2 modes (Fig. 25-3), which are calculated by 'Unmix' to have ages of 2709 ± 5 Ma (48%) and 2733 ±4 Ma (52%). The grains show a wide range of U concentrations from moderate to high (3000 ppm), as well as a considerable range in Th/U ratios, all of which are >0.1 and therefore indicate a magmatic origin, but there is no obvious correlation with age. The most straightforward interpretation would be that the older age represents inheritance while the younger one is the best estimate for emplacement of the tonalite. There is no good evidence for a Paleoproterozoic overprint.

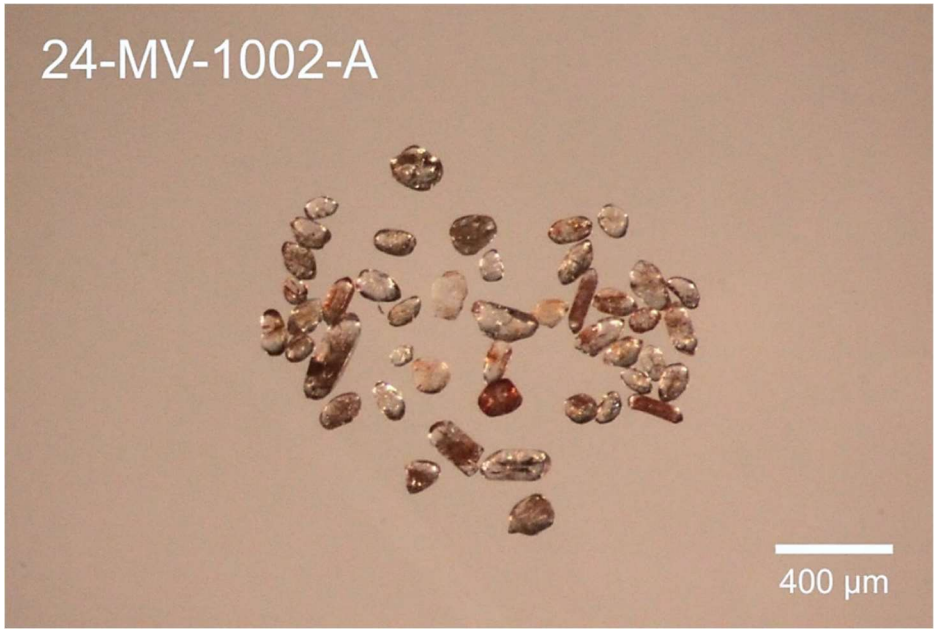

Figure 25-1. Picked zircon from granodiorite sample 24-MV-1002-A.

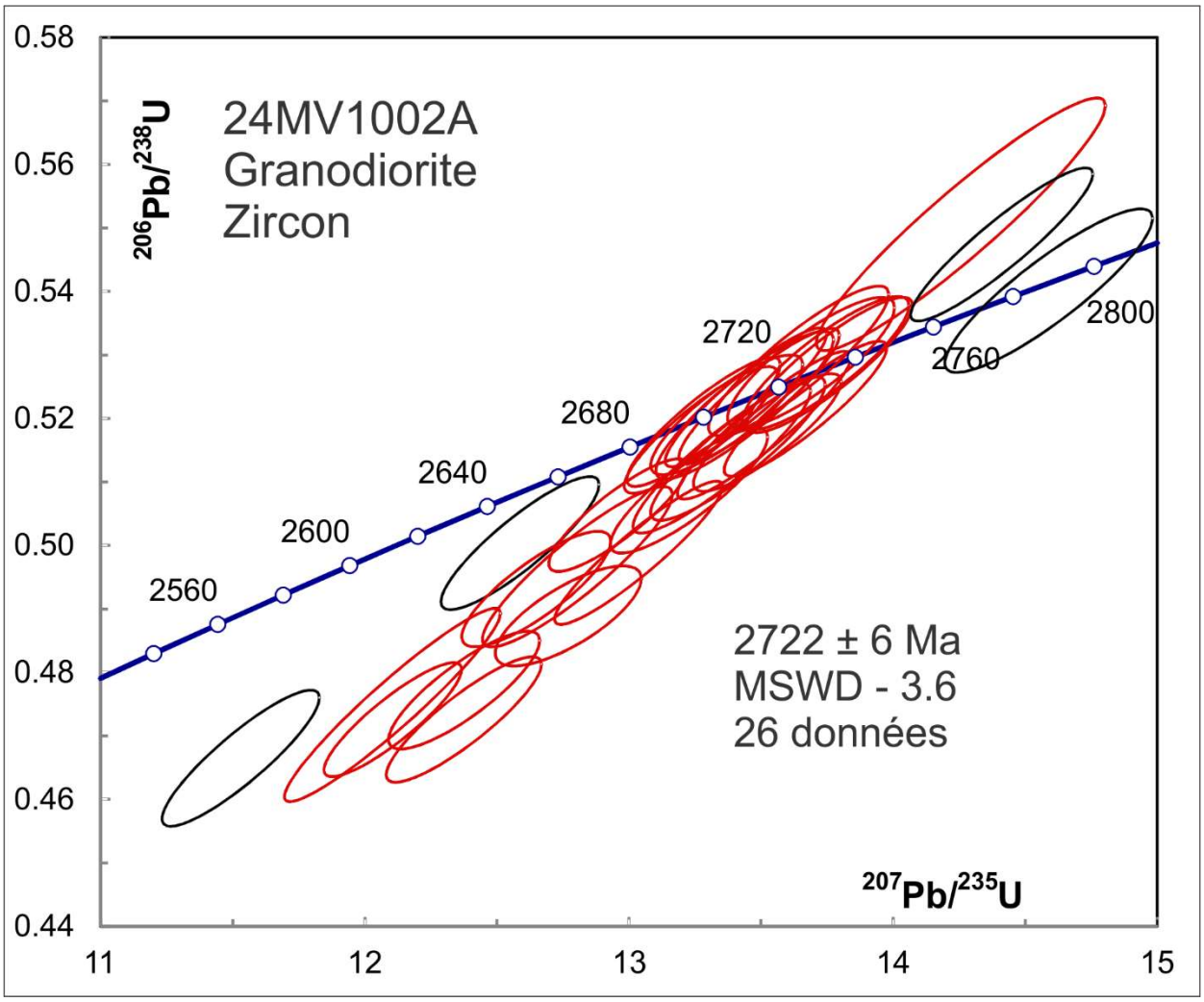

Figure 25-2. Concordia plot showing U-Pb isotopic data on zircon from sample 24-MV-1002-A. Black ellipses are omitted from the average.

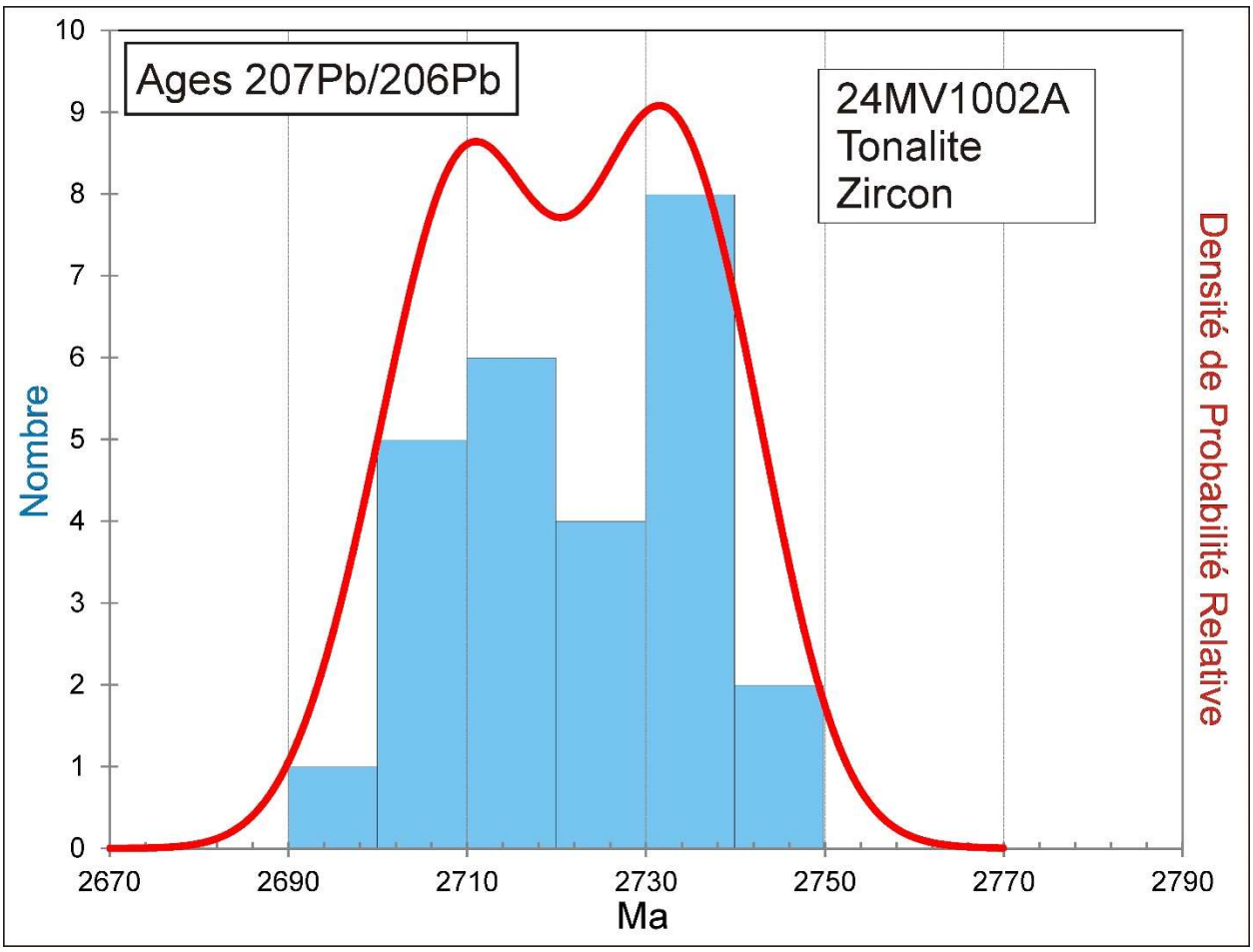

Figure 25-3. Combined age relative probability density plot and histogram showing the distribution of $^{207}Pb/^{206}Pb$ ages on zircon from sample 24-MV-1002-A.

26. 24-MV-1024-A
Tonalite, Complexe de Déception (Adec1)

This sample yielded zircon consisting of subhedral to well rounded grains (Fig. 26-1). BSE images show cracks, alteration zones, oscillatory zoning, and possible rims (Fig. 26-2). Most U-Pb analyses are near-concordant and cluster around either Paleoproterozoic or Mesoarchean ages (Fig. 26-3). The scatter in Mesoarchean ages exceeds errors. Omitting the oldest grain, the next oldest 15 grains give a mean age of 2905 ± 5 Ma (MSWD – 1.9). The probability density distribution of Archean grains (Fig. 25-4) shows a principal peak with a pronounced leftward tail, which suggests that the grains may have undergone small amounts of resetting. Applying the 'Unmix' program gives 2910 ± 4 Ma for the major component. This is the best estimate for the original age of magmatic emplacement of the tonalite. Three analyses with Th/U < 0.1 and relatively low U concentrations give overlapping near-concordant data with a mean age of 1791 ±18 Ma (MSWD – 0.7; Fig 26-5), which should be an age of metamorphism. This zircon has relatively low U concentrations (Table 3) as well as low Th/U, suggesting a late depleted melt phase. Some of the zircon with Archean ages also shows exceptionally low U (10 ppm). This may represent Proterozoic zircon rims that had Archean Pb diffuse into them from higher U magmatic cores.

The sample also yielded reddish rutile crystals (Fig. 26-6) which were analyzed on natural (unpolished) surfaces. Rutile can form from metamorphic or hydrothermal reactions. It usually contains low U concentrations (a few ppm) but has a much lower partition coefficient for Pb so that Precambrian rutile usually contains predominantly radiogenic Pb. Its closure temperature to Pb diffusion is estimated to be 400-450°C (Flowers et al., 2005). It can therefore be used to constrain the cooling history. U-Pb isotopic analyses on 6 rutile crystals give an age of 1774 ± 29 Ma (MSWD – 0.67, Fig. 26-6). Although imprecise, this age overlaps with that of the metamorphic zircon but is still compatible with a cooling history spanning tens of Ma.

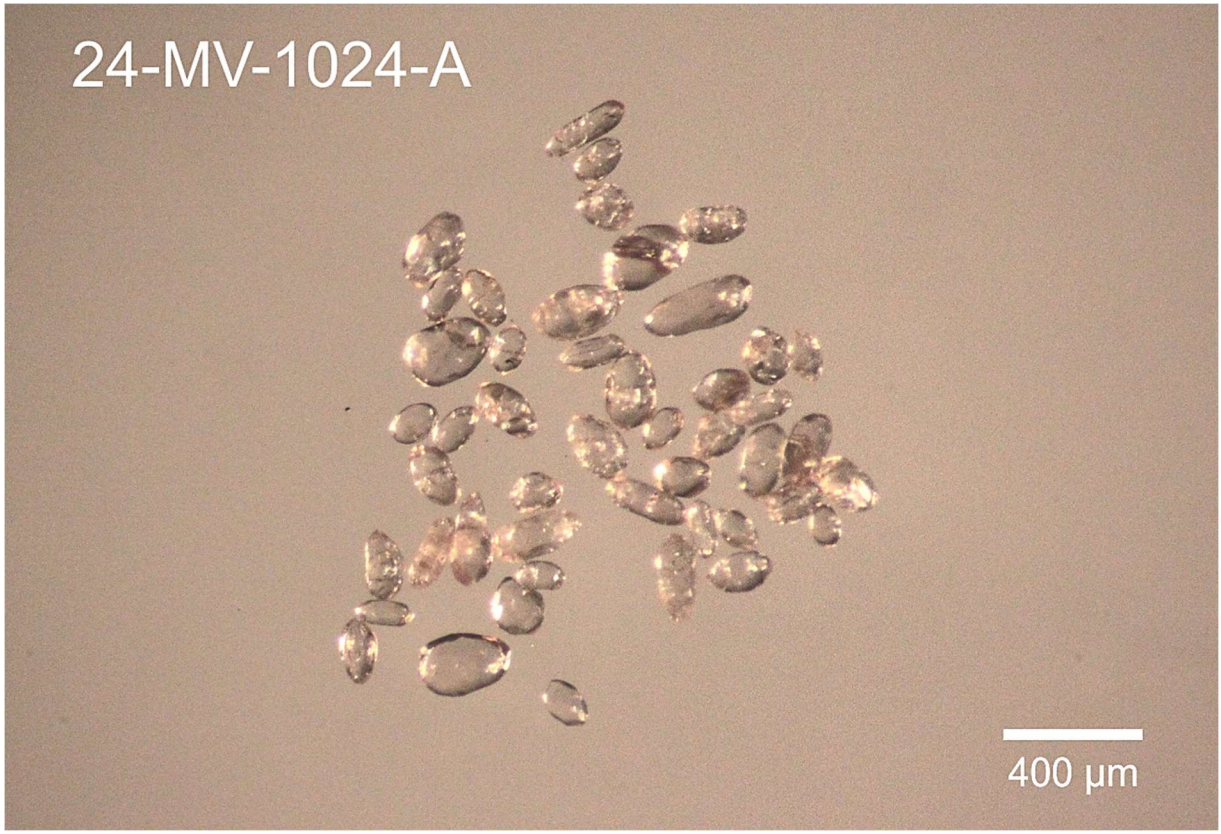

Figure 26-1. Picked zircon from tonalite sample 24-MV-1024-A.

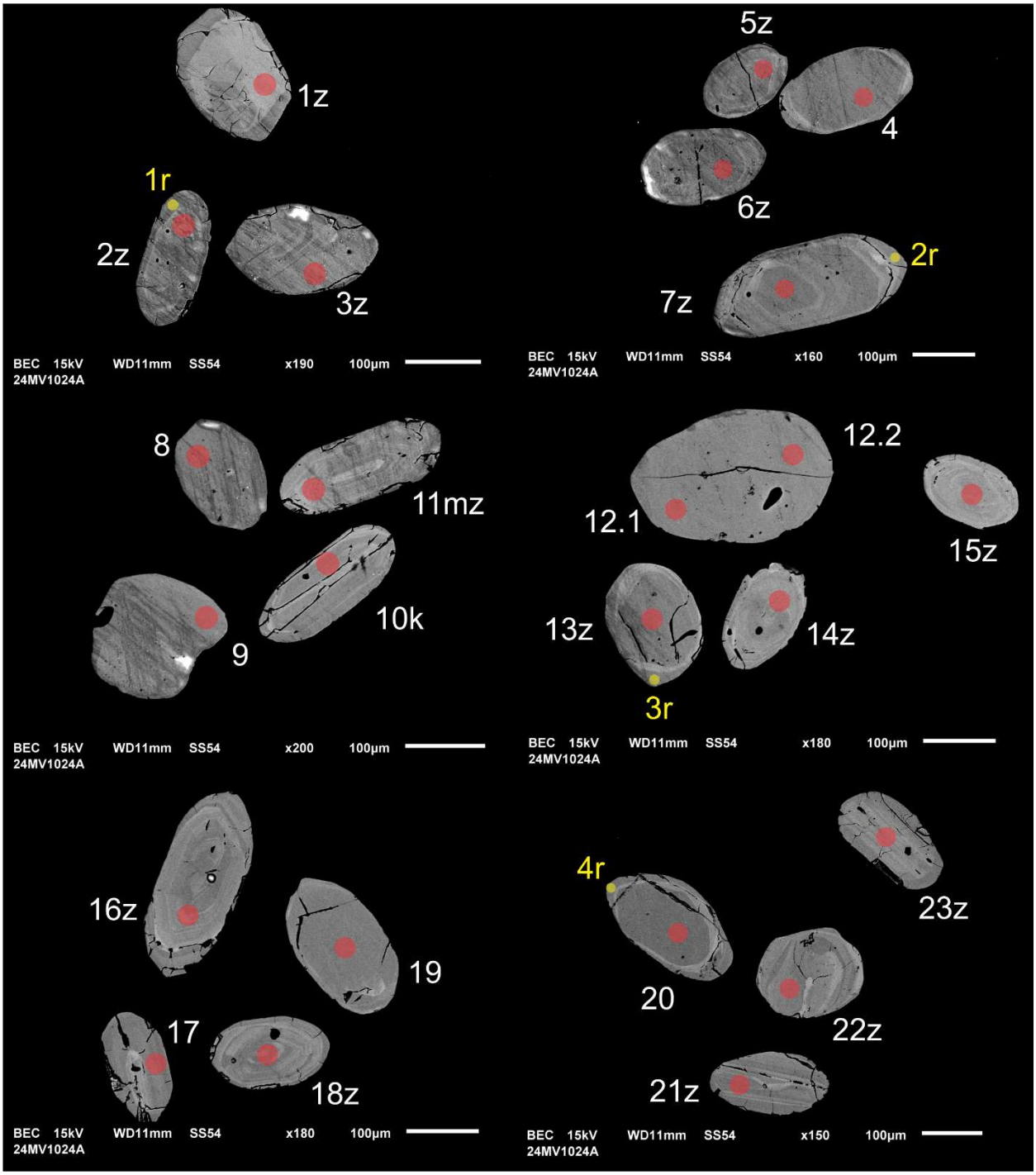

Figure 26-2-1. BSE images of selected grains from sample 24-MV-1024-A. The red and yellow circles, zircon and rims respectively, represent the approximate locations of laser ablation spots.

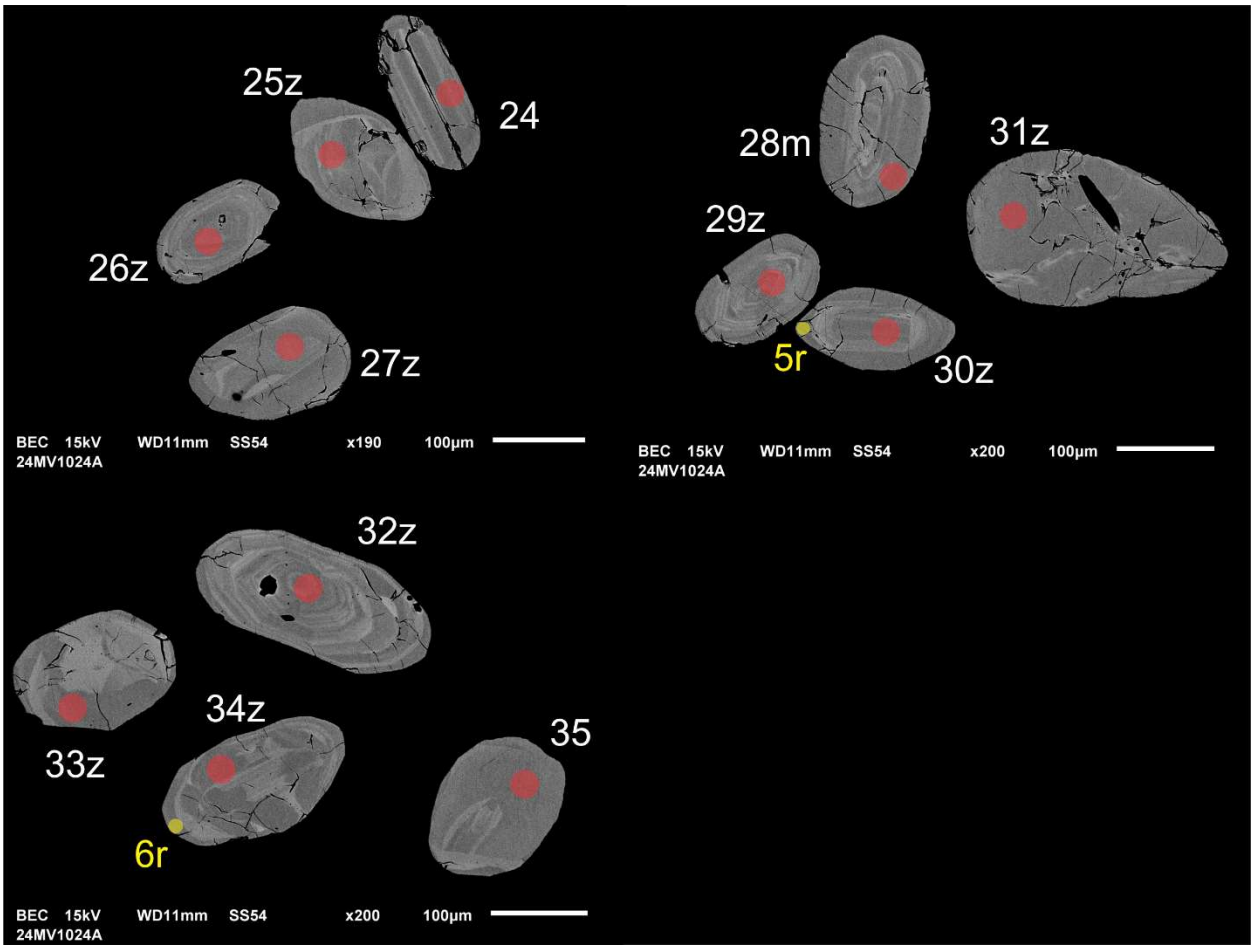

Figure 26-2-2. BSE images of selected grains from sample 24-MV-1024-A. The red and yellow circles, zircon and rims respectively, represent the approximate locations of laser ablation spots.

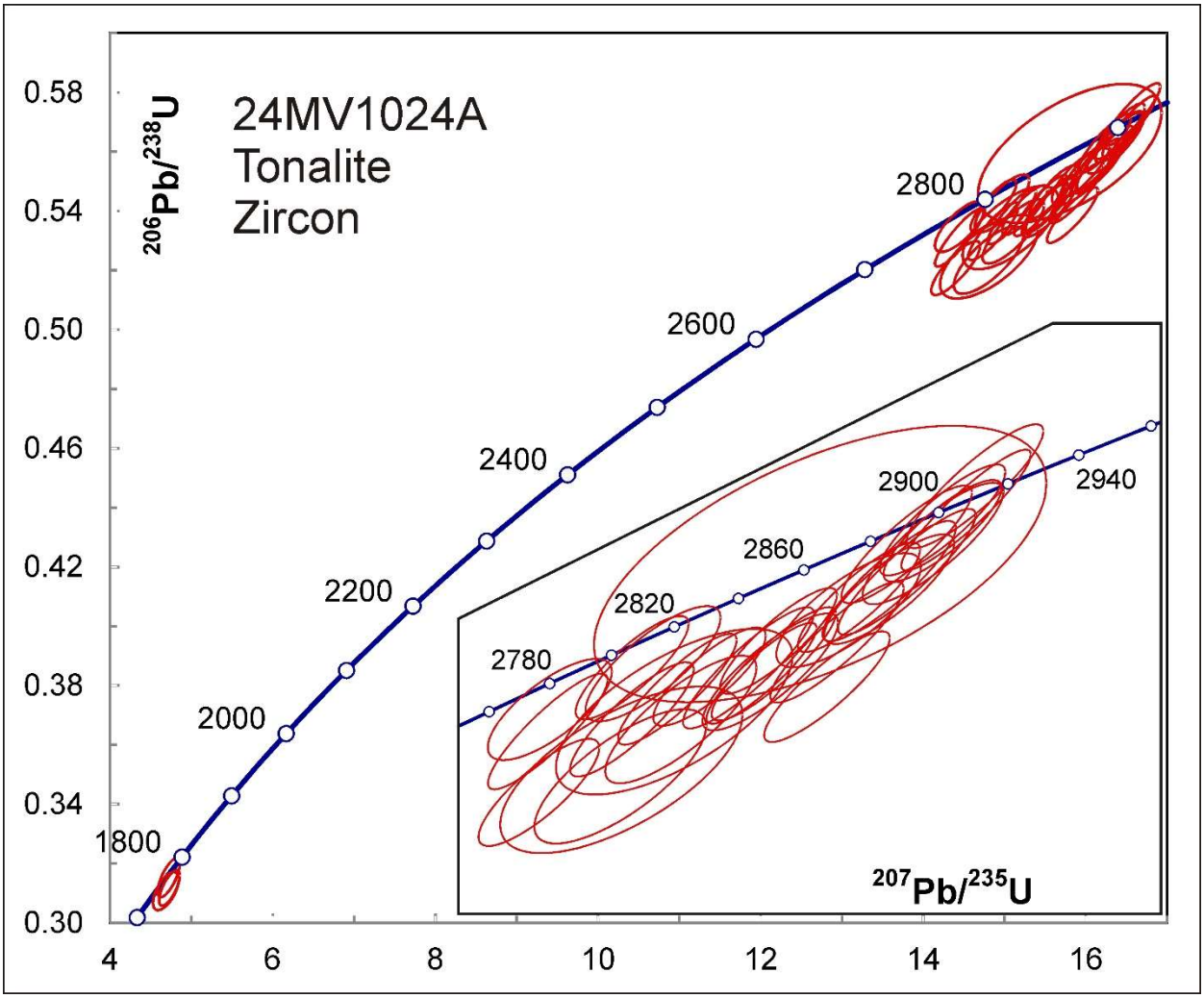

Figure 26-3. Concordia plot showing U-Pb isotopic data on zircon from tonalite sample 24-MV-1024-A.

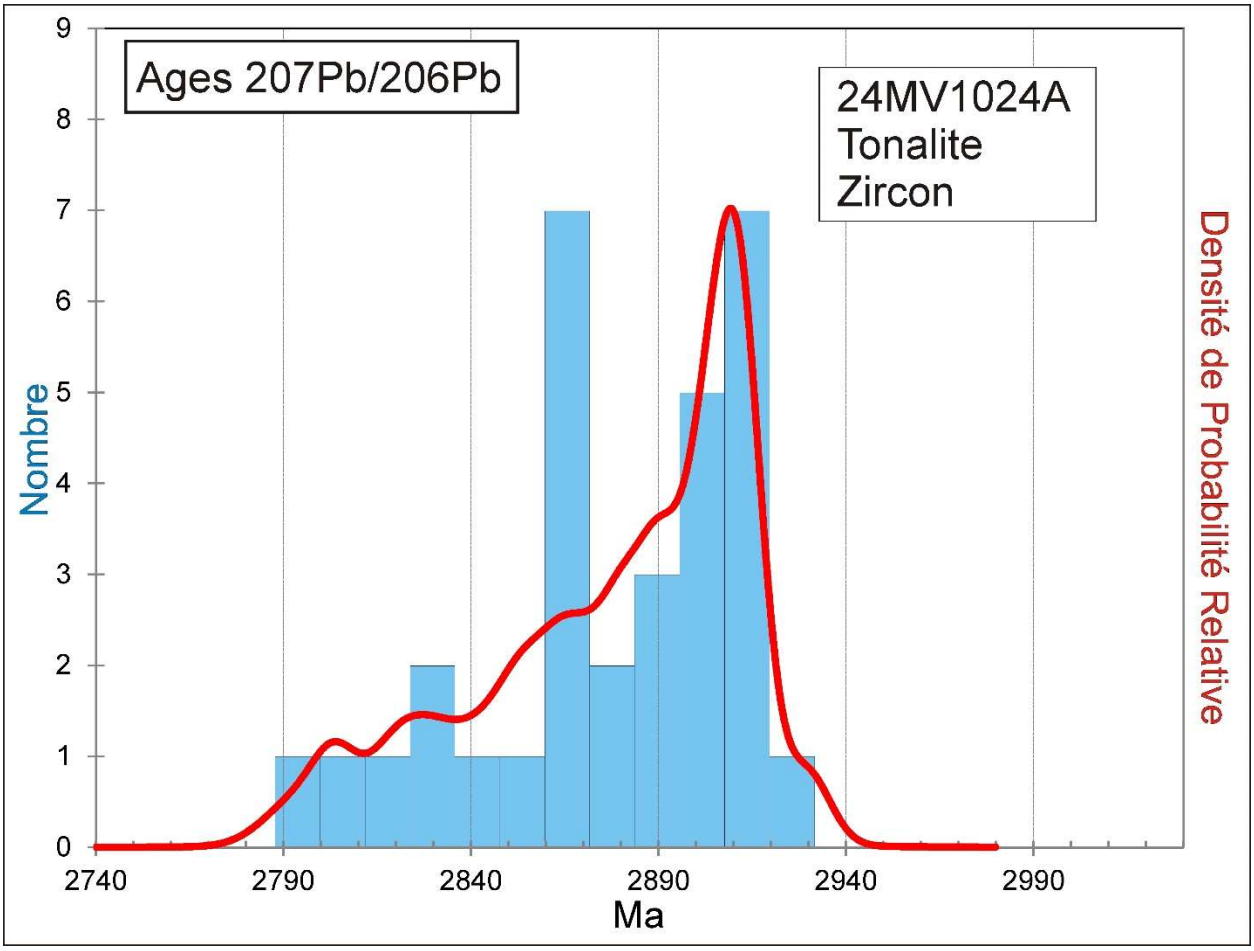

Figure 26-4. Combined age relative probability density plot and histogram showing the distribution of $^{207}Pb/^{206}Pb$ ages on Archean zircon from sample 24-MV-1024-A.

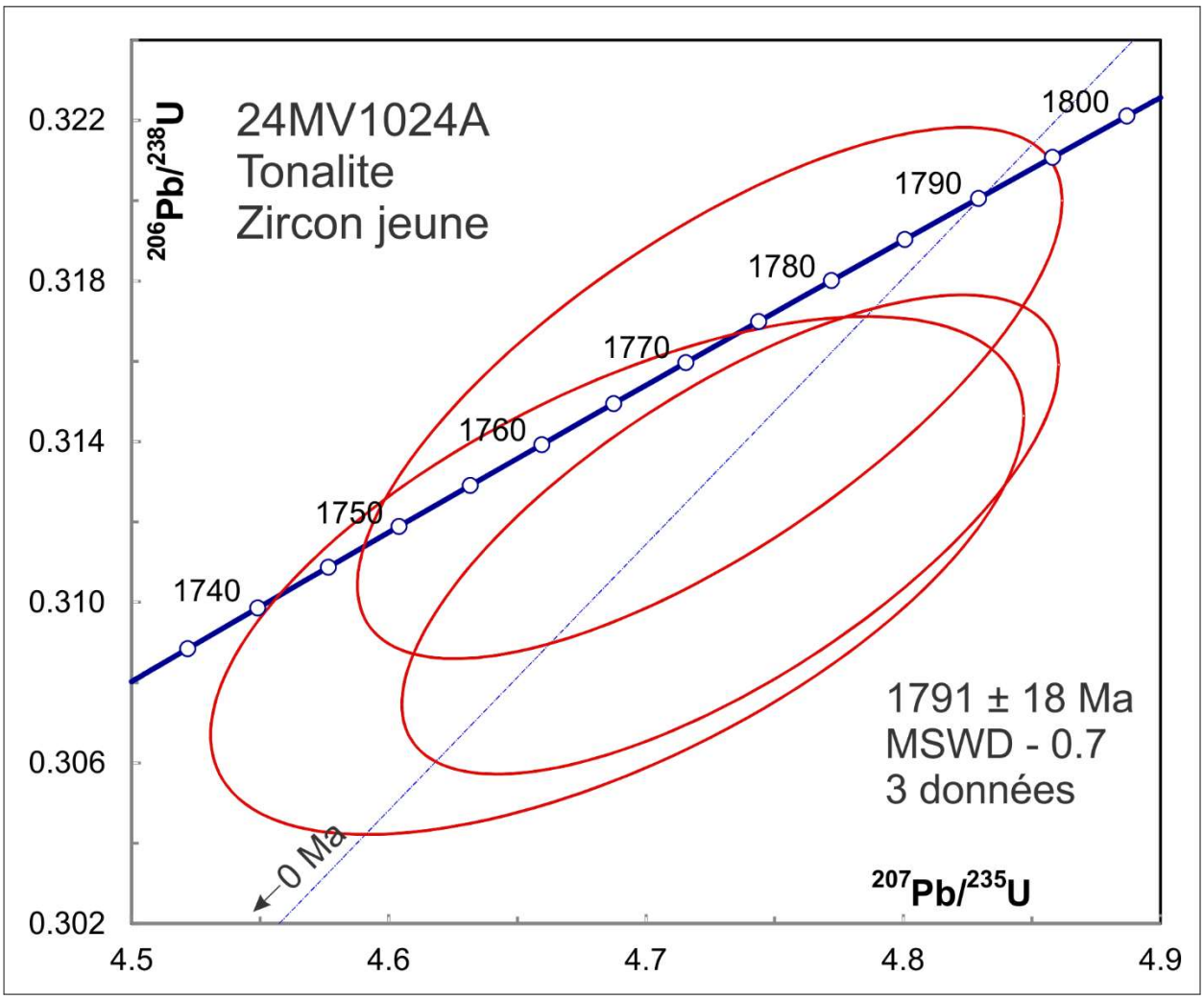

Figure 26-5. Concordia plot showing U-Pb isotopic data on metamorphic zircon (Th/U<0.1) from tonalite sample 24-MV-1024-A.

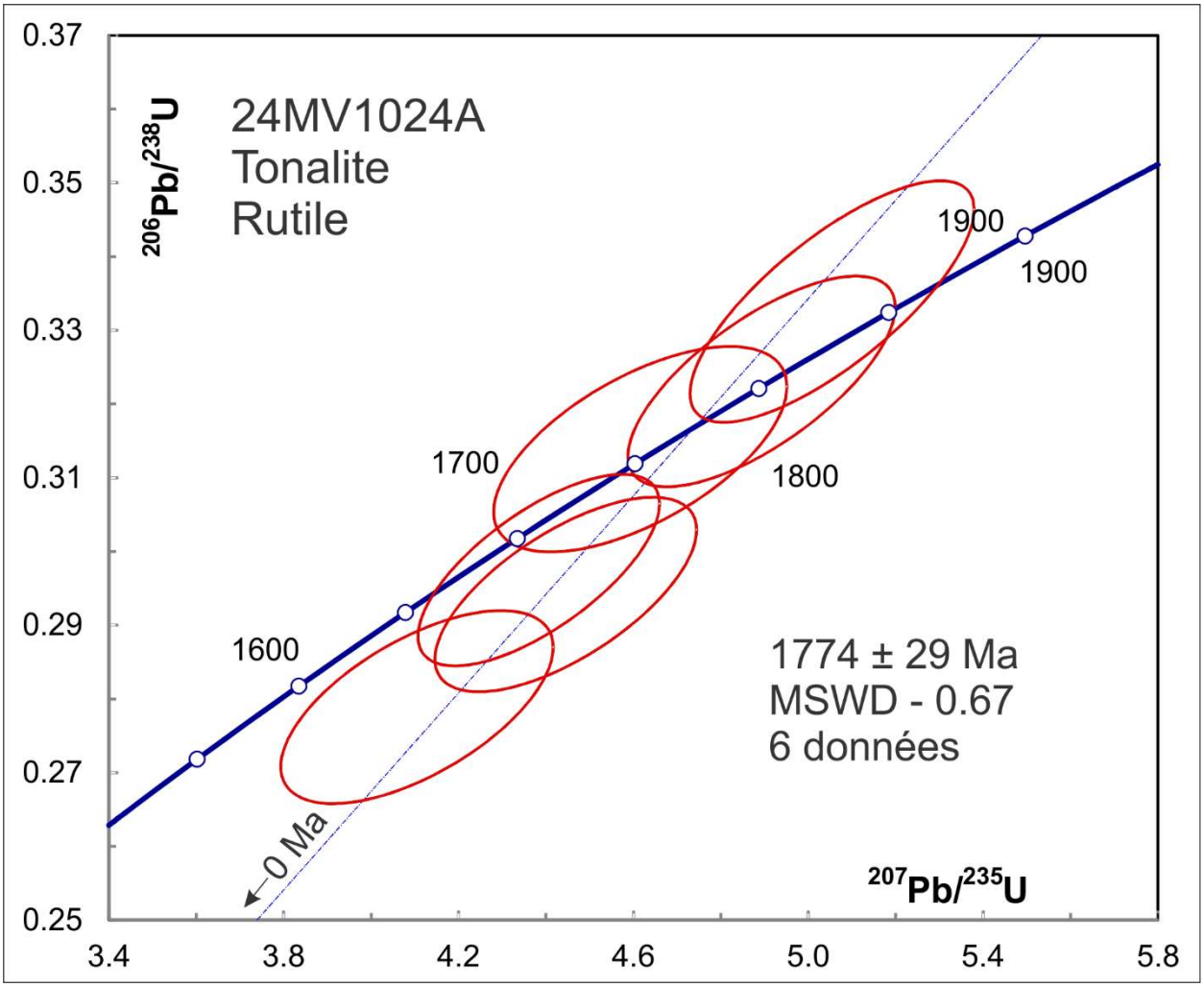

Figure 26-6. Concordia plot showing U-Pb isotopic data on rutile from sample 24-MV-1024-A.

27. 24-MV-1044-A
Monzogranite, Suite de Poly (nAply)

This sample yielded zircon as euhedral, short to long prismatic grains grains (Fig. 27-1). BSE images show a pattern of broad zoning with fractures, inclusions, and some evidence for thin brighter rims (Fig. 27-2).

U-Pb analyses are all near-concordant and scatter around a possible mixing line with intercept ages of 1816 ± 50 Ma and 2527 ± 53 Ma (MSWD – 6.4, Fig. 27-3). The high MSWD is largely the result of analytical variability in discordance. A more precise idea of the younger end point is given by averaging data from the low Th/U phases, which gives 1817 ± 11 Ma (MSWD – 2.0; Fig. 27-4) and should be an age of metamorphism. The best estimate for the emplacement age of the pluton is given by the mean age of the oldest ten data which is 2521 ± 12 Ma (MSWD – 1.2). These grains have relatively low U concentrations (Table 3), which may have limited their Pb diffusivity because of relatively low radiation damage. This interpretation conflicts with field evidence that the syenite body crosscuts paragneiss sample 24-AM-5039-A (section 21). The interpretation of its data suggests that its sedimentary protolith was deposited after 1870 ± 6 Ma and that metamorphism occurred at about 1810 Ma. While the geochronological interpretation is not definitive, the nature of contact relationships in a deformed area (whether intrusive or unconformable) needs also to be carefully considered.

Titanite analyses from this sample are clustered but notably discordant, most likely because they contain significant common Pb. Assuming that the common Pb has the isotopic composition predicted by the Stacey and Kramers (1975) crustal Pb model at the age of the oldest zircon data, extending the mixing line through the titanite data cluster to concordia gives an average model age of about 1770 Ma (Fig. 27-5). Although there are significant uncertainties due to variable discordance and the use of a model, this is the best estimate for cooling of the titanite through about 700^{o}C.

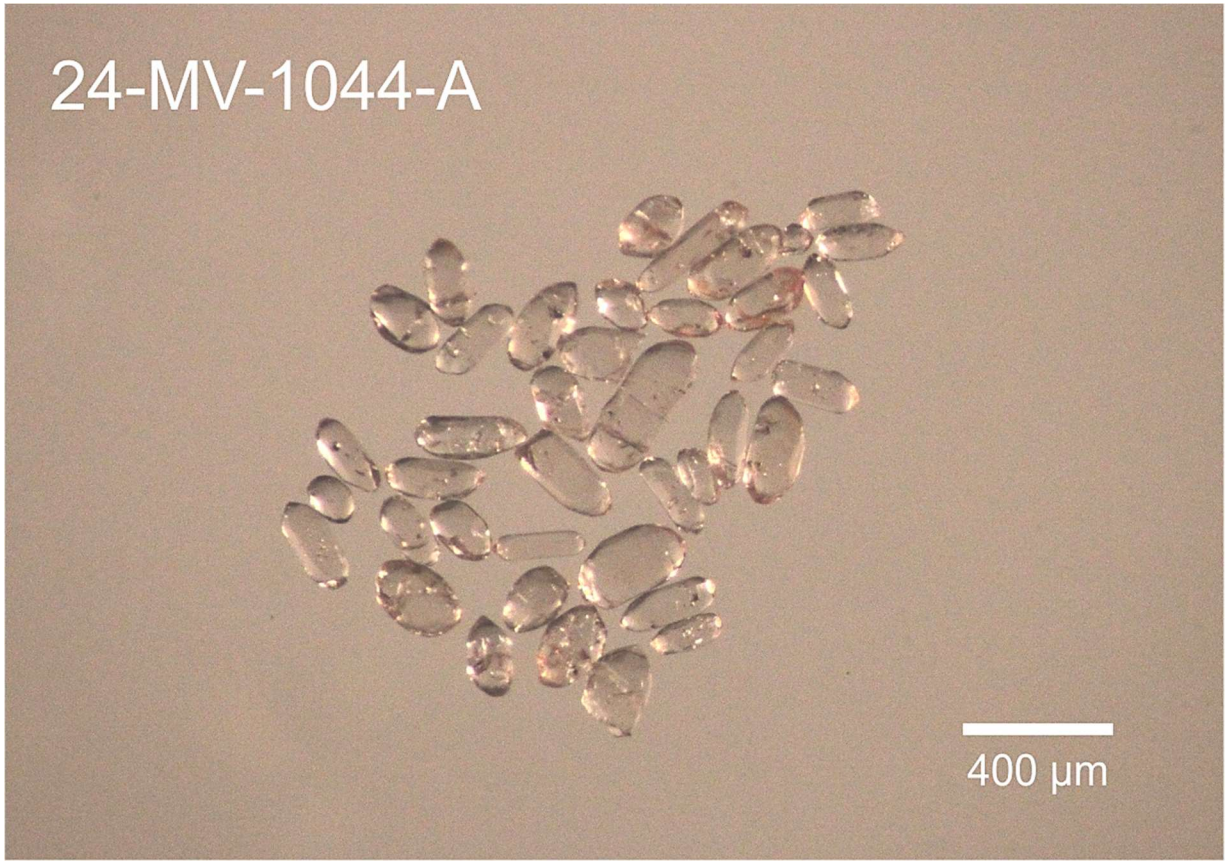

Figure 27-1. Picked zircon from monzogranite sample 24-MV-1044-A.

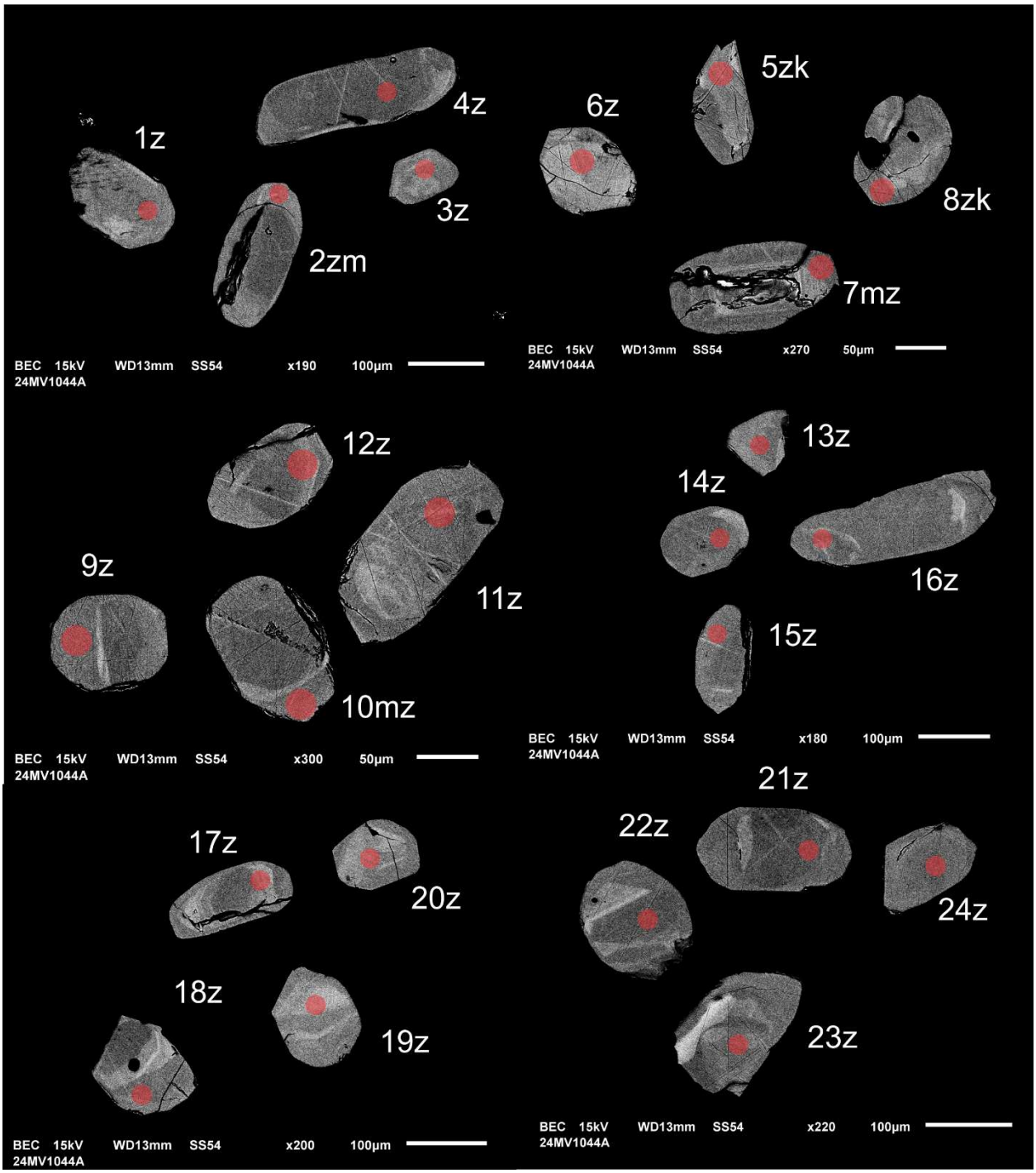

Figure 27-2-1. BSE images of selected grains from sample 24-MV-1044-A. The red circles represent the approximate locations of laser ablation spots.

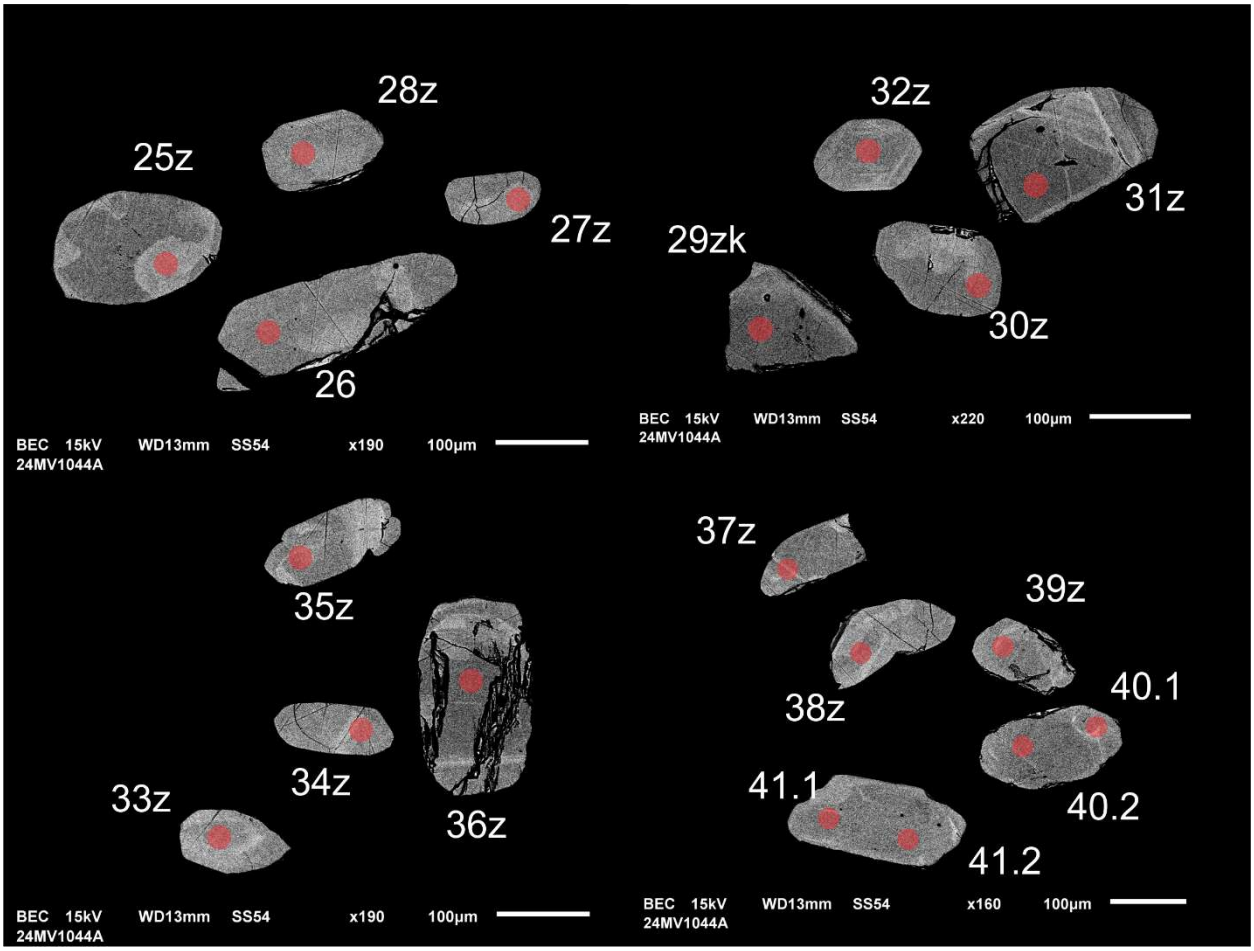

Figure 27-2-2. BSE images of selected grains from sample 24-MV-1044-A. The red circles represent the approximate locations of laser ablation spots.

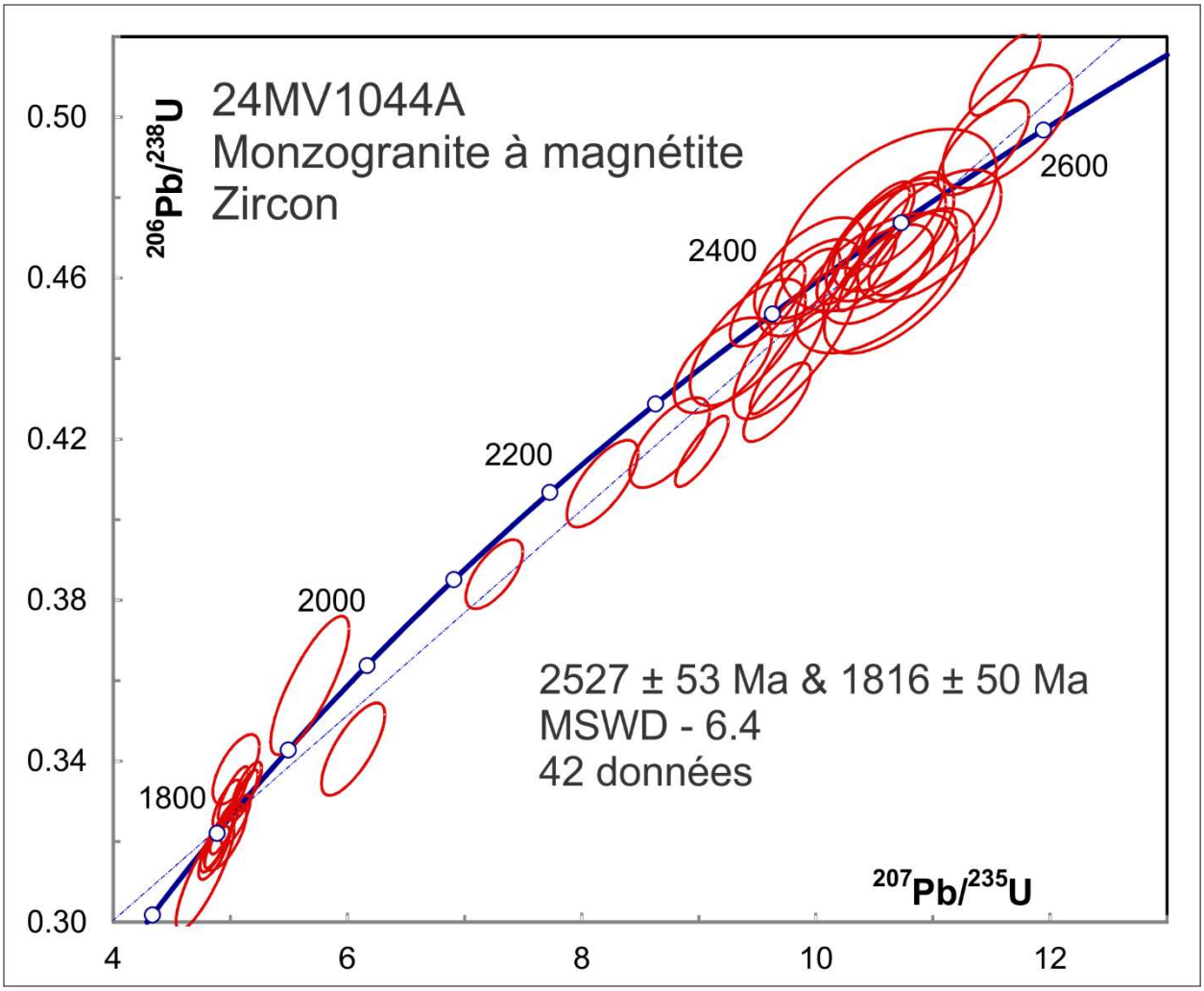

Figure 27-3. Concordia plot showing U-Pb isotopic data on zircon from sample 24-MV-1044-A. The line is a regression to all of the data and may approximate a Pb diffusion pattern.

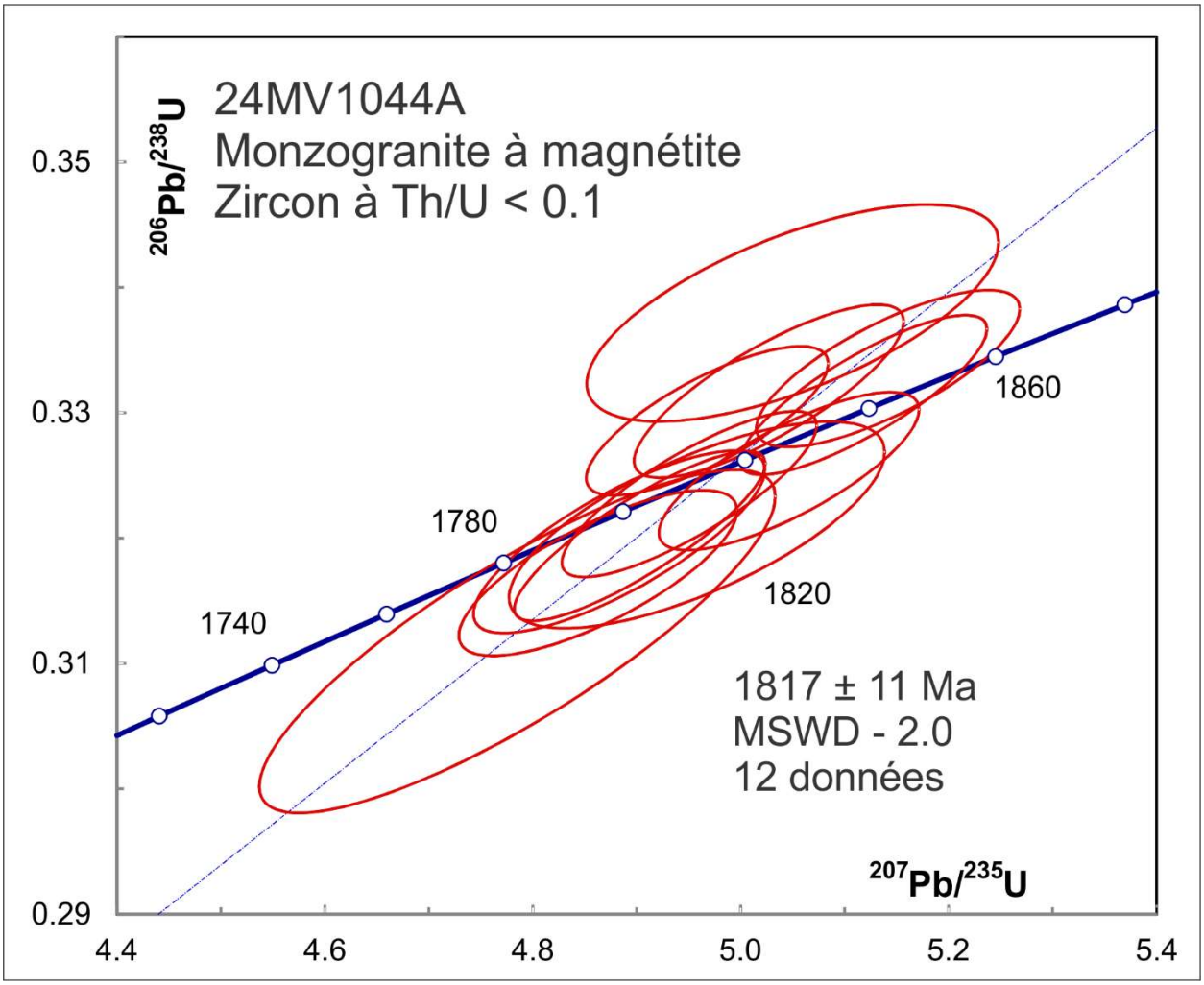

Figure 27-4. Concordia plot showing U-Pb isotopic data on metamorphic zircon (Th/U < 0.1) from sample 24-MV-1044-A.

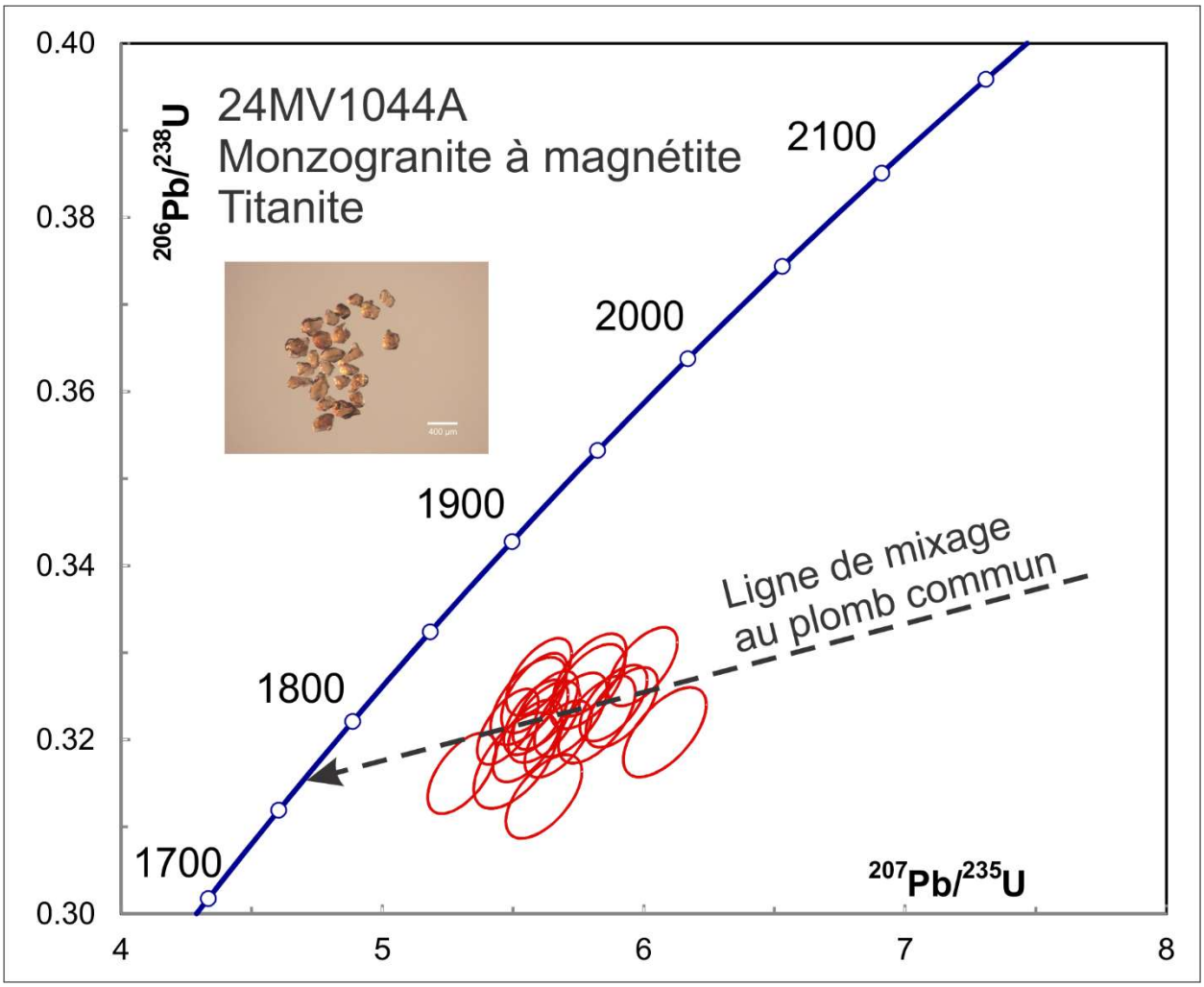

Figure 27-5. Concordia plot showing U-Pb isotopic data on titanite from sample 24-MV-1044-A. The line shows the effect of adding common Pb with a $^{207}Pb/^{206}Pb$ composition predicted for Pb derived from 2530 Ma old crust The intersection of this line with concordia should give the closure age of the titanite after cooling to about 700°C.

REFERENCES

Bingen, B., Austerheim, H. and Whitehouse, M. (2001) Ilmenite as a source of zirconium during high-grade metamorphism? Textural evidence from the Caledonides of western Norway and implications for zircon geochronology, Journal of Petrology, 42(2), 355-375.

Flowers, R.M.; Bowring, S.A.; Tulloch, A.J.; Klepeis, K.A. (2005). Tempo of burial and exhumation within the deep roots of a magmatic arc, Fiordland, New Zealand, Geology. 33 (1), doi:10.1130/G21010.1.

Jaffey, A.H., Flynn, K.F., Glendenin, L.E., Bentley, W.C. and Essling, A.M. (1971). Precision measurement of half-lives and specific activities of 235U and 238U. Physical Review 4: 1889-1906.

Ludwig, K.R. (2003). User's manual for Isoplot 3.00 a geochronological toolkit for Excel. Berkeley Geochronological Center Special Publication 4, 71 p.

Moser, A. C., Hacker, B. R., Gehrels, Seward, G. G. E., Kylander‐Clark, A. R. C., Garber, J. M. (2022) Linking titanite U–Pb dates to coupled deformation and dissolution–reprecipitation. Contributions to Mineralogy and Petrology 177:42, 27 p. doi.org/10.1007/s00410-022-01906-9.

Sambridge, M.S. and Compston, W. 1994. Mixture modeling of multi-component data sets with application to ion-probe zircon ages. Earth and Planetary Science Letters, v. 128, p. 373-390.

Stacey, J.S., and Kramers, J.D., 1975, Approximation of terrestrial lead isotope evolution by two stage model. Earth and Planetary Science Letters, v. 26, p. 207–221.